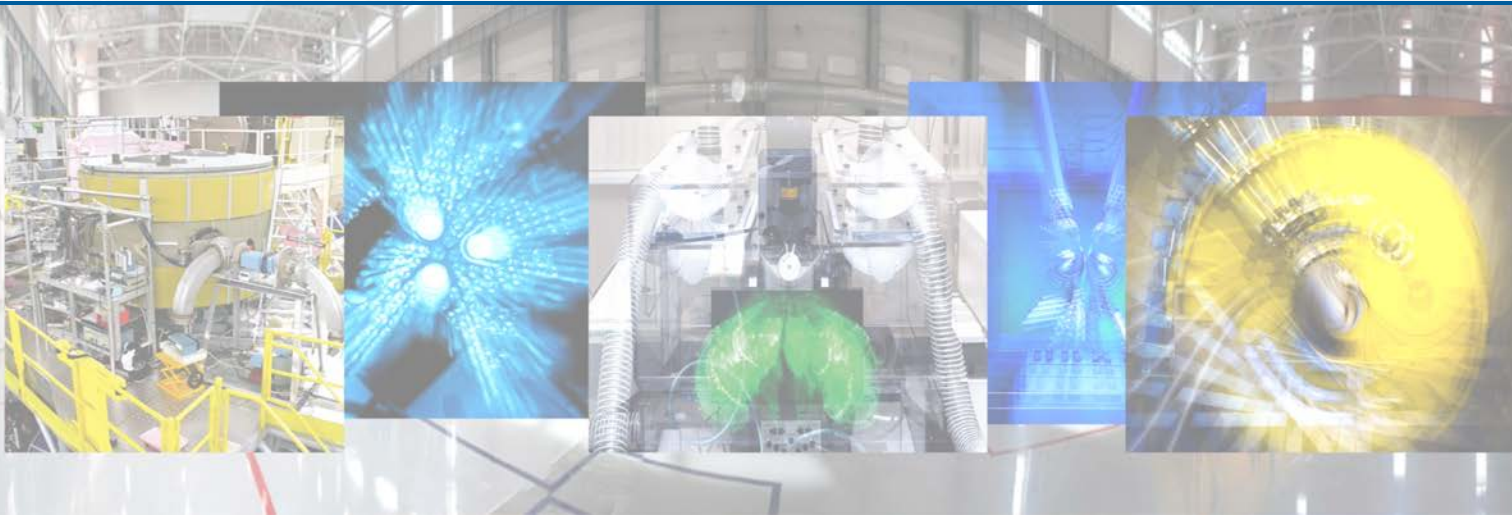




KONSTANTINOV PETERSBURG NUCLEAR PHYSICS INSTITUTE
OF NATIONAL RESEARCH CENTER
“KURCHATOV INSTITUTE”



PNPI Scientific Highlights 2016

Gatchina • 2017

Chief-editors:

Victor L. Aksenov
Svetlana V. Sarantseva
Vladimir V. Voronin

Editors:

Georgy D. Alkhazov
Stanislav A. Artamonov
Alexey A. Vorobyov
Sergey I. Vorobyov
Andrey L. Konevega
Geliy F. Mikheev
Victor Yu. Petrov
Sergey R. Friedmann
Yury P. Chernenkov

Proofreaders:

Alena M. Arkhipova
Elena Yu. Orobets
Nadezhda V. Silinskaya
Anastasia I. Zaitseva (translation)

Technical editing and design:

Tatiana A. Parfeeva

Layout composition:

Elena V. Veselovskaya
Anastasiya B. Kudryavtseva

PNPI Scientific Highlights 2016. – Gatchina, Leningradskaya obl.:
NRC “Kurchatov Institute” – PNPI Publishing, 2017. – ??? pages.

The publication is a compilation of abstracts of the most significant results of scientific research at NRC “Kurchatov Institute” – PNPI in 2016. In addition to an abstract, each scientific result in the volume features references to the full articles of leading domestic and foreign publications, where the study is described in detail and where one can get acquainted with its full content.

Printed on Konica Minolta bizhub PRO C1060L

ISBN 978-5-86763-???-?

Copyright © 2017 NRC “Kurchatov Institute” – PNPI

Table of contents

5	Preface
9	Research Divisions
25	Theoretical and Mathematical Physics
39	Research Based on the Use of Neutrons, Photons and Muons
59	Research Based on the Use of Protons and Ions. Neutrino Physics
83	Molecular and Radiation Biophysics
93	Nuclear Medicine (Isotope Production, Beam Therapy, Nano- and Biotechnologies for Medical Purposes)
101	Nuclear Reactor and Accelerator Physics
109	Applied Research and Developments
117	Basic Installations
121	Management and Research



СЕРГЕЙ МИХАЙЛОВИЧ
КОСЕНТИНОВ

Preface

Konstantinov Petersburg Nuclear Physics Institute of National Research Center “Kurchatov Institute” (NRC “Kurchatov Institute” – PNPI) is a multidisciplinary research center. It conducts fundamental and applied research in particle and high-energy physics, nuclear physics, condensed matter physics, molecular and radiation biophysics. In 2016, the Institute celebrated its 45th anniversary.

The scientific works of researchers of the Institute have been awarded the Lenin and State prizes, the prizes of the Government of the Russian Federation and the Academic prizes. Three employees of NRC “Kurchatov Institute” – PNPI were elected full members and eight employees – the corresponding members of the Russian Academy of Sciences. NRC “Kurchatov Institute” – PNPI currently employs 1906 people including 581 researchers, 69 Doctors of Sciences and 254 Candidates of Sciences. At the moment, one of its employees is a full member and three are the corresponding members of the Russian Academy of Sciences.

NRC “Kurchatov Institute” – PNPI consists of five research divisions sharing a common infrastructure:

- Theoretical Physics Division;
- Neutron Research Division;
- High Energy Physics Division;
- Molecular and Radiation Biophysics Division;
- Knowledge Transfer Division.

The long-term and short-term research programs of the Institute can be found in two documents, which are the program concerning the collaborative activity of the NRC “Kurchatov Institute” and the Research and Development program of the Institute in accordance with the State assignment.

Just like other institutes within the National Research Center “Kurchatov Institute”, NRC “Kurchatov Institute” – PNPI takes an active part in various international projects and collaborates with

the largest international research centers within its main research areas.

There is a number of operating installations as well as designs new set-ups for the physical research at the Institute. The WWR-M nuclear reactor (built in 1959) was brought to the state of a long-term shutdown on 31 December 2015 owing to the end of its operating license. In 2016, the proton synchrocyclotron SC-1000 built in 1970 performed 3225 operating hours. For the first time an isochronous cyclotron C-80 accelerating negative hydrogen ions was brought to its designed parameters. The cyclotron creates the proton beam with the energy ranging 40–80 MeV. The implementation of investment projects on modernization and renovation of engineering and technical systems of the PIK neutron research facility was in progress in 2016.

The year 2016 was an important phase in the creation of the PIK neutron research facility. The budgetary funds of the Russian Federation were allocated to ensure the implementation of modernization of engineering and technical supporting systems and to ensure the renovation of a laboratory complex of the PIK neutron research facility in order to facilitate the power start-up of the PIK reactor in 2018. To implement these projects, NRC “Kurchatov Institute” created the Operational office for the PIK power start-up preparation. The Office is comprised of keynote head officers of NRC “Kurchatov Institute”, NRC “Kurchatov Institute” – PNPI, the chief design manager, the general design engineer as well as primary contracting organizations. The Office has been given ample authorities in terms of project management. The director of the Institute Denis Yu. Minkin has been appointed the head of the Operational office.

The year 2016 was rich in the events of scientific and social life. The holiday “Russian Science Day” was celebrated at the Institute on 7-8 February. The program organized by the Committee



of young researchers and specialists included the lessons for schoolchildren and a celebratory meeting of the Scientific council. At the meeting young scientists of the Institute were awarded with the scholarships in honor of outstanding scientists, who worked in the Institute a short time ago: V.N. Gribov scholarship for achievements in the field of theoretical physics, G.M. Drabkin scholarship for achievements in the field of condensed state physics, V.M. Lobashev scholarship for achievements in the field of nuclear physics, S.E. Bresler scholarship for achievements in the field of biology. The celebration ended with a winter ball.

The 50th anniversary NRC “Kurchatov Institute” – PNPI Winter Scientific School was convened in early March. Winter School featured lectures by renowned scholars, seminars and presentations of the School attendees in all key areas: nuclear physics and elementary particle physics, physics and technology of reactors, theoretical physics, condensed matter physics, and, after a long break – biophysics and molecular biology. The 50th Winter School was attended by more than 500 scientists and researchers from our Institute and other leading scientific centers of Russia and abroad. Furthermore, in 2016 the Institute organized 13 scientific conferences. Special attention should be given to the events, which were organized by young staff members

of the Institute: a large-scale social event of the Institute – business game “PNPI-2020”, the PIK reactor school for young scientists, and “Open Science 2016” – III annual conference for young scientists and specialists, which was held in the format of a youth scientific forum. The forum was held in the building of the PIK neutron research facility that will become the basis for the International Center for Neutron Research.

This publication is a compilation of brief descriptions of the most significant results of scientific research conducted at the Institute in 2016. The description is prefaced with the overviews made by heads of the Divisions within the main lines of activity. The structure of Divisions is also provided. The abstracts of those papers are presented, which had been discussed and recommended by the scientists of Divisions' councils. In addition to the abstract, each result in the collection of articles contains links to the articles in leading Russian and foreign journals in which the paper is described in detail, and where one can get acquainted with its full content.

The scientific achievements of the Institute employees have been published in 569 articles in the leading Russian and international reviewed journals and presented at 130 national and international conferences.

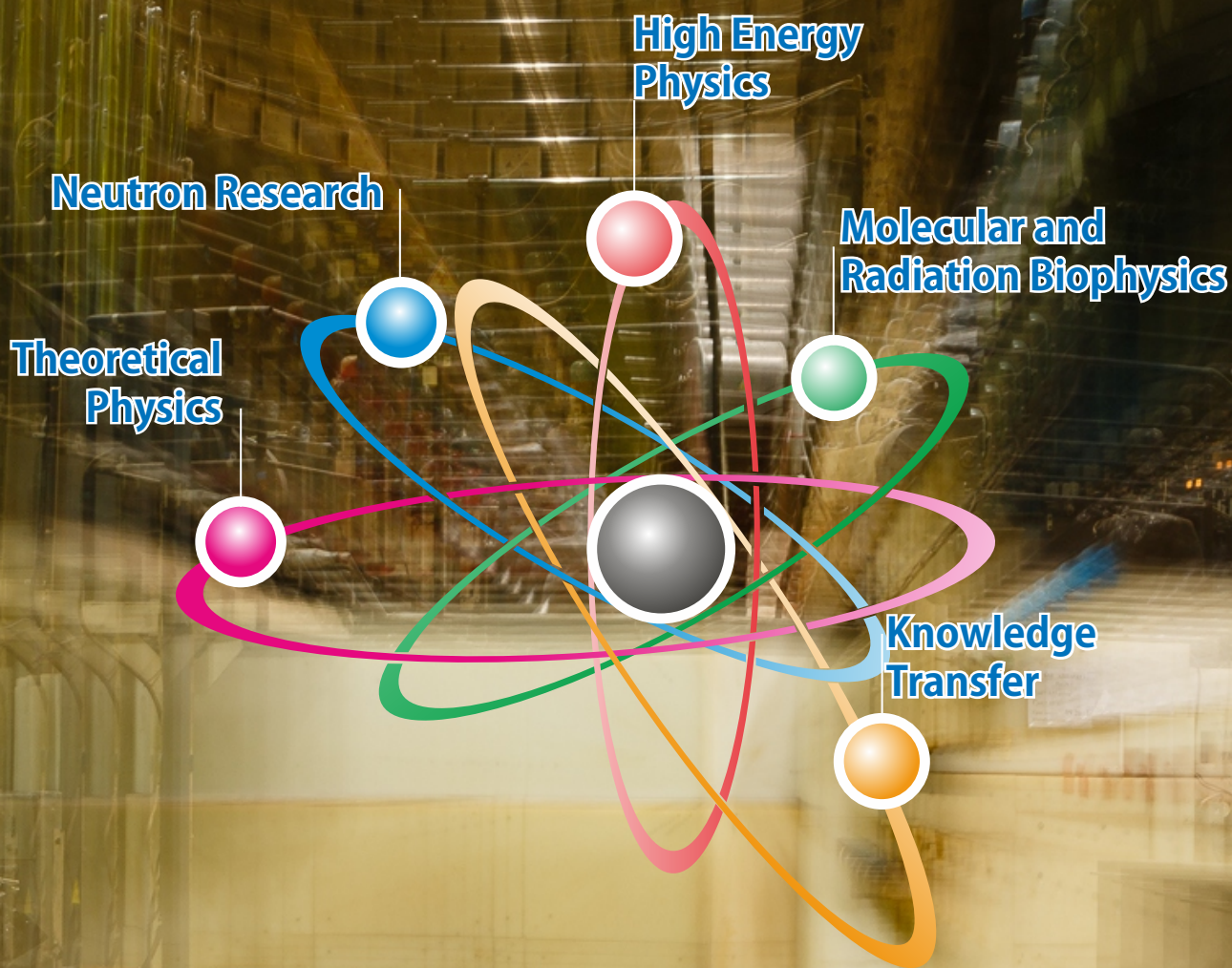
The general information about the Institute is given in the conclusive part of the document.



Director of NRC “Kurchatov
Institute” – PNPI
Professor D.Yu. Minkin



Science Director of NRC “Kurchatov Institute” –
PNPI Corresponding member of the Russian
Academy of Sciences V.L. Aksenov



Research Divisions

- 10** Theoretical Physics Division
- 13** Neutron Research Division
- 17** High Energy Physics Division
- 20** Molecular and Radiation Biophysics Division
- 23** Knowledge Transfer Division

Theoretical Physics Division

Theoretical Physics Division (TPD) headed by Lev N. Lipatov (member of the Russian Academy of Sciences) consists of seven departments:

- **Theory of Electroweak Interactions** (headed by Dr. Gennady S. Danilov);
 - **Theory of Strong Interactions** (headed by Dr. Victor Yu. Petrov);
 - **Quantum Field Theory** (headed by Dr. Vyacheslav A. Kudryavtsev);
 - **High Energy Theory** (headed by Dr. Victor Yu. Petrov);
 - **Condensed Matter Theory** (headed by Dr. Saul L. Ginzburg);
 - **Nuclear Theory** (headed by Dr. Mikhail G. Ryskin);
 - **Atomic Theory** (headed by Dr. Alexander I. Mikhailov)
- and a **Group of Physics of Nuclear Reactors** (headed by Dr. Mikhail S. Onegin).

TPD employs 69 research staff members (28 Doctors of Sciences and 32 Candidates of Sciences).



Lev N. Lipatov
Head of TPD
academician
of the Russian Academy
of Sciences

TPD research covers most of the branches of modern theoretical physics: from elementary particle physics and quantum field

theory to physics of nuclear reactors.

Scattering at high energies is a traditional area of TPD research. It can be said that for a long time the activity of TPD researchers has determined the frontier in this field. In 2016 L.N. Lipatov *et al.* continued with the investigation of BFKL (Balitsky, Fadin, Kuraev, Lipatov) equation determining the asymptotics of the scattering amplitude at high energies. In particular, the BFKL pomeron was considered in the Higgs model with the running coupling constant. The spectrum of pomerons in the j -plane was calculated. This allows the determination of the asymptotics of the scattering amplitudes at high energies. This theory is a prototype of the Standard model (SM).

TPD is also one of the world leaders in the field of the so-called AdS/CFT duality (anti-de Sitter/conformal field theory). The duality means that non-

trivial field theory ($N = 4$ supersymmetric Yang–Mills theory) in $d = 4$ space-time is equivalent to some string theory in the anti-de Sitter space and both are exactly solvable. Duality implies that anomalous dimensions of the operators in the SUSY theory are related to the string spectrum in the string theory. Recently, N.A. Gromov suggested a rather general method of calculation of dimensions of arbitrary operators. This method is based on the so-called “algebraic curve” method. Using this method in the paper of V.N. Velizhanin anomalous dimensions of SUSY theory were calculated with 7-loop accuracy. This accuracy is a kind of a record in the field theory. Calculations lead to the rather large systems of the Diophant equations which were solved.

Quark confinement is the most interesting and still unclear phenomenon in quantum chromodynamics (QCD). It is still impossible to study it directly, and for that reason, simpler (more symmetrical) supersymmetrical (SUSY) theories are used to clarify its mechanism. A.V. Yung has studied these theories for many years. Now this mechanism is almost completely clear. Perhaps, it is not exactly what we need to explain confinement in QCD, however, a number of very interesting non-perturbative phenomena were revealed. In the paper presented in this volume, the strings appearing in the $d = 4$ SUSY theories are investigated. It appears that under definite conditions

these non-Abelian strings have properties very close to those required in nature. The constructed string theory remains critical (i.e. this theory has no ultraviolet divergences) in the $d = 4$ time-space.

In 2015 LHCb collaboration declared observation of two pentaquark resonances. In the paper of M.I. Eides, V.Yu. Petrov and M.V. Polyakov these resonances are interpreted as a bound state of an excited state of charmonium and proton. Another possible interpretation of pentaquarks is the loosely bound state of two hadrons with open charm. In the paper of 2016 both alternatives are analyzed and properties of pentaquarks in either of scenarios are calculated. Also a number of new pentaquarks are predicted. It is shown that measurements of the ratio of pentaquark decay probabilities to open and hidden charm states can give the answer to the question which scenario is realized in nature.

The paper of M.G. Ryskin with collaborators is devoted to the exclusive production of J/ψ -mesons at LHC energies. Some time ago it was proposed to use this process to measure the proton gluon structure function with high accuracy at very small x . Unfortunately, it appears that previous calculations did not take into account a number of corrections, both power and double-logarithmic, which appear to be rather large. In the paper of 2016, presented below, these corrections are calculated. A new method to extract the precise gluon structure function from the data is developed.

The ideas concerning the origin of hierarchy of quark masses and the Kobayashi–Maskawa matrix continue to attract attention of theoreticians. One of the popular extensions of the Standard model in this relation is the idea of “mirror” symmetry. In the paper of I.T. Dyatlov presented here it is shown how this idea can explain, on the one hand the absence of hierarchy in the neutrino spectrum and on the other – the observed hierarchy of lepton and quark masses. One needs for this the so-called “inverse” order in the neutrino spectrum and the mass of the lightest neutrino around 0.1 eV.

One of the most discussed processes beyond the SM is the process of doubled beta-decay.

It can be discovered experimentally. The paper of E.G. Drukarev discusses the influence of the electron shells on this process. It appears that the interaction with atom electrons shifts the energy of electrons produced in the decay to smaller energies. This shift was calculated for atoms of germanium and xenon and appeared to be several hundred eV.

Three papers below can be related to the condensed state physics. The paper of A.V. Syromiatnikov and A.V. Sizanov deals with the Bose-glass phase. Such a phase can appear in the system of interacting bosons. The theory of this phase was suggested by Fisher *et al.* However, this theory contradicts the experiments performed recently. The paper presented here generalizes the Fisher's scenario. It is shown that the last scenario can be realized only in the region very close to the critical point. This region was not reached by the present experiments. Then Bose glass system proceeds to the percolation scenario which is also universal but critical powers are different from Fisher's scenario. The proposed theory is able to explain all experimental data.

The paper of N.E. Savitskaya is devoted to the theory of avalanches which are phenomena specific for the dynamics of the complex systems. The paper considers the methods of avalanche stabilization, i.e. methods to reduce their size and frequency. It is shown that avalanches developing on the dynamic lattices are, in general, more stable than on the static lattices.

During the last years, V.V. Shaginyan with co-authors have been developing the theory of a new phase of matter related to the phenomenon of the so-called “fermion condensation”. A hypothesis of fermion condensation helps to explain a large number of unusual properties of different materials discovered in recent experiments. The paper below summarizes the results of these investigations.

The physical theory of hurricanes is investigated in the paper of V.G. Gorshkov, A.M. Makarieva, and A.V. Nefiodov. The source of the rainfall in the area of a few hundred kilometers around the hurricane is discussed. It is shown that summary rainfall is immediately related to the speed of hurricane movement.

Reactor physics is represented by the paper of M.S. Onegin. His paper demonstrates the abilities of the program complex MURE in neutron calculations of the PIK reactor. The complete fuel cycle of PIK reactor is calculated both with standard and modified fuel elements.

The following statistics demonstrate the results obtained by TPD employees during the year 2016:

- 109 research papers published in reviewed journals (88 papers published in foreign editions);
- One monograph published;
- 35 research reports presented at international and Russian events;
- Two dissertations (Candidate of Sciences) defended.

Neutron Research Division

Neutron Research Division (NRD) headed by Dr. Alexander I. Kurbakov consists of two research and four scientific and technological departments:

Neutron Physics Department (headed Corresponding member of the Russian Academy of Sciences Prof. Anatoly P. Serebrov) **consists of four laboratories:**

- **Neutron Physics** (headed by Prof. Anatoly P. Serebrov);
- **Nuclear Spectroscopy** (headed by Dr. Ivan A. Mitropolsky);
- **Molecular and Atomic Beams** (headed by Dr. Victor F. Ezhov);
- **X- and γ -Ray Spectroscopy** (headed by Prof. Valery V. Fedorov)

and two groups:

- **Weak Interaction Research** (headed by Dr. Alexander N. Pirozhkov);
- **Nuclear Fission Physics** (headed by Dr. Alexander S. Vorobyov).

Condensed State Research Department (headed by Dr. Sergey V. Grigoryev) **consists of four laboratories:**

- **Disordered State Physics** (headed by Dr. Vladimir V. Runov);
- **Neutron Physical and Chemical Research** (headed by Dr. Vasily T. Lebedev);
- **Crystal Physics** (headed by Dr. Yury P. Chernenkov);
- **Materials Research** (headed by Dr. Alexander I. Kurbakov)

and two groups:

- **Condensed Matter Electrodynamics** (headed by Dr. Oleg V. Gerashchenko);
- **Solid State Radiation Physics** (headed by Dr. Sergey P. Belyev).

There are four scientific and technological departments:

- **Engineering and Technological Support of Experiments at Reactors** (headed by Alexey P. Bulkin);
- **Automation of Experiments on Reactors** (headed by Dr. Valery A. Solovey);
- **Semiconductor Nuclear Detectors** (headed by Dr. Alexander V. Derbin);
- **Operation of Neutron Stations at the PIK Reactor** (headed by Dr. Evgeny V. Moskvina).

NRD employs 165 research staff members (16 Doctors of Sciences and 63 Candidates of Sciences).



Dr. Alexander I. Kurbakov
Head of NRD

Main directions of NRD research are fundamental and applied fundamental physics. Most of employees of scientific departments and practically all staff of scientific

and technological departments are involved in the creation of the PIK neutron research facility. In recent years, another important line of activity has emerged: the teaching activity in universities of Saint Petersburg, whose main goal is the training

of young scientists who in several years will become the scientific staff members of the PIK-based International Center for Neutron Research.

In the field of scientific research NRD is generally focused on carrying out activities in the area of Nuclear Physics, Particle Physics and Condensed Matter Physics.

In 2016, just like in recent years, great success was achieved in the field of neutrino physics. The Borexino collaboration, in which employees from NRD participate, analyzed correlations of Borexino detector data collected in the period from December 2007 to November 2015 with 2350 Gamma-ray bursts (GRB). No statistically significant correlations have been found. The most stringent upper limits on the fluence in neutrinos and antineutrinos associated with

a GRB have been obtained for energies below 7-8 MeV.

NRC “Kurchatov Institute” – PNPI and NRC “Kurchatov Institute” participate in the collaboration DarkSide since its inception in 2010. DarkSide-50 is a two-phase liquid-argon detector with the mass of 46 kg. In 2016, an underground argon with the content of radioactive ^{39}Ar isotope contamination 1400 times less than that of the atmospheric argon was used in the detector for the very first time ever. As a result of the new 71-day measurement, the most stringent limits on the spin-independent cross-sections and masses of weakly interacting massive particles have been obtained.

In June 2016 in the Neutrino laboratory of NRC “Kurchatov Institute” – PNPI – Research Institute of Atomic Reactors the detector of a cellular type with 16 sections was installed at the SM-3 reactor (Dimitrovgrad, Russia) to search for neutrino oscillations in a sterile state. The measurements of the antineutrino flux depending on distance (R) from a center of the reactor core have been done. Measurements of the antineutrino flux from the reactor at small distances of 6–12 m by means of the moveable detector were carried out for the first time. In the frame of the available statistical accuracy it is not revealed if there are reliable deviations of antineutrino flux distance dependence from the law $1/R^2$. The results in the range 10–12 m require the measurements in this region to be repeated with more accuracy.

Measurement of the lifetime of a free neutron by the method of storage of ultracold neutrons in a cryogenic material trap with gravitational locking has to shed light on a problem of a difference in neutron lifetime measured both by the “beam” method and the “storage” method. The result of 2016 can be considered the value of the neutron lifetime: $(880.3 \pm 0.8_{\text{stat}} \pm 0.8_{\text{sys}})$ s. For the final result, a systematic error should be evaluated.

Crystal-diffraction studies of the fundamental properties and interactions of a neutron continue. Currently we are preparing an experiment to verify the equivalence of inertial and gravitational mass of a neutron by a new method based on the use of effects arising from neutron diffraction in large perfect crystals. The main feature

of the proposed method is the direct compensation of the gravitational force acting on the neutron by the inertia force acting on the neutron in a non-inertial coordinate system connected with the Earth. During 2016, the study of the experiment spatial resolution for Bragg angles $(74\text{--}82)^\circ$ was carried out. A decrease in the spatial resolution at Bragg angles more than 78° was observed.

The study of the dynamics of nuclear fission by neutrons was continued. In 2016, a detailed study of the TRI and ROT effects measured in the ILL reactor (Grenoble, France) in threefold ternary fission for the four fissile nuclei ^{233}U , ^{235}U and ^{239}Pu , ^{241}Pu was carried out. It is established that the specified effects take place for all investigated nuclei, but they differ considerably both in the sign and in absolute value.

Investigations of the mechanism of emission of “instantaneous” neutrons in nuclear fission within the framework of the CORA experiment were continued. As a result of the analysis of the data obtained at the first stage of experimental studies, it was possible to receive an estimation of the anisotropy coefficient of instantaneous neutron emission in ^{252}Cf fission in the system of the center of mass of the fission fragment.

In 2016, the work carried out within the framework of the IAEA CRP project “Prompt fission neutron spectra of actinide nuclei” was completed. Measurements of the integral spectra of prompt neutrons in the fission of ^{235}U , ^{233}U and ^{239}Pu both by thermal neutrons and at spontaneous fission of ^{252}Cf were conducted. Their joint estimation with the data of other experiments was performed. The recommendations on the use of the estimated spectra to design new power installations and to perform model simulations were given.

In the field of atomic physics NRD developed a computer package to calculate atomic properties taking into account electron correlations and relativistic effects to find most perspective systems of ultra-cold highly charged ions and molecules. In 2016, new programs were added to this package to account for quantum electrodynamics corrections and effective three-electron interactions. New methods for cooling and trap-

ping of such ions for high precision experiments with them are being developed as well.

The study of functional materials and new physical phenomena in them takes is a prominent line of the scientific activity of NRD.

A series of the works address a fundamental scientific problem: the experimental establishment of the ground quantum states in low-dimensional magnetic materials. The physics of low-dimensional magnetism is a rather new and one of the most interesting and rapidly developing areas of modern science, because the quantum essence of matter in low-dimensional magnetic materials is the most pronounced and it becomes possible to observe experimentally as well as to apply in the future, a lot of non-classical quantum cooperative effects. In NRD, multilateral systematic study of the static and dynamic magnetic characteristics of a wide class of quasi-two-dimensional magnetic materials with various geometry of the exchange bonds and identifications of nontrivial types of a ground state of such systems are conducted. Currently, compounds both with a triangular magnetic sublattice and cationic sublattice of a “honeycomb” type in a layer are studied. In 2016, the study of complex oxides $\text{Li}_3\text{Ni}_2\text{SbO}_6$ and $\text{Na}_3\text{Co}_2\text{SbO}_6$ was finished. Non-trivial antiferromagnetic zigzag-type quantum ground state, namely zig-zag ferromagnetic chains coupled with each other antiferromagnetically in *ab*-plane were experimentally established.

The research into single crystals of quasi-two-dimensional magnetic materials $\text{La}_{1.4}\text{Sr}_{1.6}(\text{Mn}_{1-x}\text{Co}_x)_2\text{O}_7$ was conducted. In such two-layer manganites, a giant magnetoresistance anisotropy is observed, which is associated with the layered structure of these compounds that leads to a spin-dependent tunneling of carriers between manganese-oxygen planes. During the research, the abnormal growth of resistance and decrease in magnetization at low temperatures were observed.

The morphology, magnetic properties and longitudinal electric resistance in multilayered nanocomposites $[(\text{Co}_{40}\text{Fe}_{40}\text{B}_{20})_{34}(\text{SiO}_2)_{66}/\text{C}]_{47}$ containing 47 amorphous metal-dielectric/carbon bilayers produced by ion-beam evaporation and different

in the thickness of the carbon layer were investigated. Superparamagnetic properties of granules were confirmed by the results of SQUID magnetometry. The thickness of the layers, the characteristic sizes of metal granules and the distances between them were determined by the GISAXS method. It was revealed that the thermoactivated conductivity of such multilayered structures is described by the universal law “1/2”, and the characteristic temperature decreases linearly with the increase of the carbon layer thickness.

In the last few years in NRD the research of various unique nanostructural materials was carried out extensively. Neutron scattering data analysis in direct and reciprocal space has allowed the decoding of the structure of diamond hydrogels with the sizes from ones to tens of nanometers. The hydrogels were synthesized for the first time. It has been established that a formation of short range order in such a system is realized sequentially through bonding of charged particles (diameter ~ 5 nm) within the first coordination sphere, association of these fragments in the chain aggregates and connection of the chains into the network (scale ~ 40 nm). A key role of an electrostatic attraction of non-spherical diamond crystals, which stabilizes the gel structure strongly, has also been confirmed in neutron experiments.

The creation of new nanomaterials such as wound bandages, synthetic cartilage, precursor of bone tissue is an urgent problem in modern medicine. The complex analysis of experimental data obtained in the study of the morphology of the structure of cellulose *Gluconacetobacter xylinus* and organo-inorganic composite materials on its basis showed that the initial gel film represents a porous system with a complex three-level fractal organization of the structure. It was found that both the composition and the aggregate state of the alloying additives used in the synthesis (ZrO_2 nanoparticles, Tb^3 ions in the form of the low-molecular TbCl_3 salt and in the metal-polymer complex $[\text{Tb}(\text{PolyLig})](\text{III})$) have a significant effect on structural characteristics of organo-inorganic composites.

Instrumental and radiochemical neutron activation techniques were developed for the analysis

of samples from quartz-adularia lodes of the Milogradovsky gold-silver deposit. The optimal conditions of the Pt, Au, Ir, Re and Ag separation from base metals were assigned. The principal result of the study is confirmation of the platinum mineralization in the quartz-adularia veins.

Quite a considerable part of NRD employees takes part in the creation of the experimental stations for PIK neutron research facility.

In 2016 numerical simulation of individual units of the installations for condensed matter physics, namely the polarizer/analyzer for the SANS installations, calculation of the beam shaper for the NERO reflectometer, preliminary calculations of the three-axis cold-neutron spectrometer, preliminary calculations of the neutron guide system of a neutron guide hall were performed. Development and optimization of the neutron-optical lines of the reactor complex PIK in accordance with the requirements of the "Reconstruction" and "Creation of the instrument base of the RC PIK" projects were carried out. New mirror systems for the polarization and analysis of neutron polarization were developed. The creation of a neutron beam-defining device for the REFLEX reflectometer at the IBR-2 reactor was completed. It will be used as an alternative to continue the activities undertaken to enhance polarizing and not polarizing mirror optics in the absence of neutrons at NRC "Kurchatov Institute" – PNPI. Calculations and simulations of the first source of cold neutrons were completed. An outline design of the

cold neutrons source (CNS) and a neutron guide system for HEC-3 channel of the PIK reactor have been created.

The WWR-M reactor is planned to be equipped with a source of ultracold neutrons (UCN). The UCN density at the level of 10^4 cm^{-3} will be reached, which is two orders of magnitude greater than that at the sources currently existing around the world. This will make NRC "Kurchatov Institute" – PNPI the world center of fundamental research with ultracold neutrons. A full-scale model of the ultracold neutron source for the WWR-M reactor, where superfluid helium with a temperature of 1.3 K was obtained in November 2015 at the thermal load of 15 W, demonstrated a smooth operation during 2016. Experimental helium temperatures at a thermal load of up to 60 W were obtained. Helium remained in the superfluid state even at such a high load.

Following statistics demonstrates the results obtained by NRD employees during 2016:

- 105 research papers published in reviewed journals (including 68 papers indexed in the database Web of Science);
- Two monographs were published;
- 111 research reports presented at international and Russian conferences;
- Six patents and four certificates of state registration of specialized programs and databases obtained;
- Four theses (Candidate of Sciences) defended.

High Energy Physics Division

High Energy Physics Division (HEPD) headed by Prof. Alexey A. Vorobyov (corresponding member of the Russian Academy of Sciences) consists of 10 laboratories:

- **Elementary Particle Physics** (headed by Prof. Georgy D. Alkhazov);
- **Meson Physics of Condensed Matter** (headed by Dr. Sergey I. Vorobyov);
- **Relativistic Nuclear Physics** (headed by Prof. Vladimir M. Samsonov);
- **Short-Lived Nuclei** (headed by Dr. Vladimir N. Panteleev);
- **Meson Physics** (headed by Prof. Victorin V. Sumachev);
- **Few Body System** (headed by Prof. Stanislav L. Belostotski);
- **Crystal Optics of Charged Particles** (headed by Dr. Yuri M. Ivanov);
- **Hadron Physics** (headed by Dr. Oleg L. Fedin);
- **Physics of Exotic Nuclei** (headed by Prof. Yuri N. Novikov);
- **Cryogenic and Superconductive Techniques** (headed by Dr. Alexander A. Vasilyev)

and four technical departments:

- **Radio Electronics** (headed by Dr. Victor L. Golovtsov);
- **Track Detectors** (headed by Prof. Anatoly G. Krivshich);
- **Computing Systems** (headed by Andrey E. Shevel);
- **Muon Chambers** (headed by Vladimir S. Kozlov).

HEPD employs 134 research staff members (16 Doctors of Sciences and 69 Candidates of Sciences).



Prof. Alexey A. Vorobyov
Corresponding member
of the Russian Academy
of Sciences,
Head of HEPD

HEPD activity is mainly aimed at the experimental research in the field of elementary particle physics and nuclear physics.

Also, solid-state physics research with the use of the μ SR-method is being conducted. As in the previous years, research activities were carried out at facilities of NRC “Kurchatov Institute” – PNPI as well as at accelerators of the world’s leading nuclear centers.

In 2016, the following experiments were carried out

Experiments at NRC “Kurchatov Institute” – PNPI synchrotron:

- Production and studies of short-lived nuclei with the laser-mass spectrometer complex IRIS.

- Studies of polarization effects in proton quasi-elastic scattering of nuclei.
- Studies of η -meson production in the pion beam.
- Studies of magnetic properties of materials with the μ SR method.
- Investigations in the field of crystal-optics of high-energy protons.

Also, the 1 GeV proton beam was in use for testing various experimental equipment at a special test stand.

Experiments at the European Center for Nuclear Research (CERN):

- Participation in the experiments CMS, ATLAS, LHCb, and ALICE at the Large Hadron Collider (LHC).
- Production and studies of short-lived nuclei with the laser-mass spectrometer complex ISOLDE.
- Studies of possibilities to use crystal collimation of the LHC beams – experiment UA9.

Experiment at the Brookhaven National Laboratory (USA):

- Experiment PHENIX. Studies of the relativistic heavy ion collision physics.

Experiment at the Paul Scherrer Institute – Meson factory (Switzerland):

- Experiment MUSUN. High precision studies of muon capture on deuteron.

Experiments at the electron accelerators at Bonn and Mainz universities (Germany):

- Study of the nucleon structure by γ - p - and e - p -scattering.

The following experiments were completed, the data analysis being continued:

- Experiments HERMES and OLYMPUS at DESY, Germany (study of the spin structure and form factors of nucleons);
- Experiment D0 at the Fermi National Accelerator Laboratory, USA (physics of proton-antiproton collisions at the Tevatron);
- Experiment EPECURE at NRC “Kurchatov Institute” – ITEP, Moscow (search for narrow resonances in πp -scattering).

New projects:

- Experiment POLFUSION (NRC “Kurchatov Institute” – PNPI) (study of the nuclear dd -synthesis in polarized deuterons collisions);
- Experiments R3B, MATS, PANDA, and CBM (GSI, Germany) (preparation of experiments at the accelerator complex FAIR);
- Experiment PROTON at the accelerator MAMI (Mainz, Germany) (measurement of the proton charge radius);
- Experiment COMPTON at the accelerator MESA (Mainz, Germany) (studies of the nucleon polarizability);
- Project IRINA at the high-flux neutron reactor PIK (NRC “Kurchatov Institute” – PNPI) (production and studies of short-lived nuclei);
- Project RIC-80 at the cyclotron C-80 (NRC “Kurchatov Institute” – PNPI) (production of radioisotopes for medical application).

One of the main HEPD activities was the participation in the LHC experiments CMS, ATLAS, LHCb, and ALICE. NRC “Kurchatov Institute” – PNPI participated in these experiments from the initial phase of design and construction of the collider

detectors with essential contributions to the construction of various subsystems of these detectors. After the LHC start, HEPD physicists and engineers shared responsibilities in maintenance and operation of these detectors and took part in the analysis of the experimental data.

The analysis of the experimental data collected in Run I (2010–2012) yielded a great amount of new results crowned with the discovery of the Higgs boson. In Run II (2015–2016), the energy of the colliding protons at the LHC was increased from 4 TeV + 4 TeV up to 6.5 TeV + 6.5 TeV. The luminosity was also increased. The analysis of the new experimental data allowed obtaining more detailed information on the Higgs boson as well as getting more strict limitations on the possible appearance of new physics beyond the Standard Model. A number of other important results were obtained, in particular new baryon exotic states – pentaquarks – were observed and studied. More than 280 papers were published by the ATLAS, CMS, LHCb, and ALICE collaborations in 2016. The list of authors in these publications includes 35 scientists from the HEPD.

Physicists of NRC “Kurchatov Institute” – PNPI participate actively in the programs of modernization of the collider detectors. In particular, in the framework of the ATLAS upgrade, a special facility at NRC “Kurchatov Institute” – PNPI has been prepared, which is intended for assembling the thin-gap chambers (TGC) for the forward part of the ATLAS muon spectrometer. At present, the first chamber prototype is being assembled. In total, 36 quadruplets of TGC chambers should be manufactured at NRC “Kurchatov Institute” – PNPI.

An important result was obtained in the experiment UA9 (the laboratory headed by Yu.M. Ivanov). The channeling of 6.5 TeV protons in the curved crystals has been demonstrated for the first time. The experiment was performed directly inside the LHC ring using the halo of the circulating proton beam. Thus, a principle possibility of collimation of the proton beams in the LHC has been proven. It is noteworthy that the crystals fabricated at NRC “Kurchatov Institute” – PNPI were used in this experiment.

In the laboratory headed by A.A. Vasilyev, a unique experimental set-up has been built for investigation of the dd-synthesis of polarized deuterons, which has become a major step toward the experiment POLFUSION. It should be noted that physicists from Germany and Italy participate in this experiment.

The present volume contains some of the results published in 2016 obtained in LHC experiments, as well as in experiments performed at NRC “Kurchatov Institute” – PNPI and at other nu-

clear centers with the participation of HEPD physicists.

The following statistics demonstrates scientific activity of the HEPD in 2016:

- 361 research papers published in reviewed journals;
- 45 research reports presented at various international and Russian events;
- Three Candidate of Sciences theses and two Doctor of Sciences theses defended.

Molecular and Radiation Biophysics Division

Molecular and Radiation Biophysics Division (MRBD) headed by Dr. Andrey L. Konevega consists of 14 laboratories:

- **Biophysics of Macromolecules** (headed by Dr. Vladimir V. Isaev-Ivanov);
- **Genetics of Eukaryotes** (headed by Dr. Vladimir G. Korolev);
- **Protein Biosynthesis** (headed by Dr. Andrey L. Konevega);
- **Molecular Genetics** (headed by Dr. Valery N. Verbenko);
- **Biopolymers** (headed by Dr. Andrey L. Timkovsky);
- **Cell Biology** (headed by Dr. Mikhail V. Filatov);
- **Human Molecular Genetics** (headed by Dr. Alexander Schwartzman);
- **Enzymology** (headed by Dr. Anna A. Kulminskaya);
- **Experimental and Applied Genetics** (headed by Dr. Svetlana V. Sarantseva);
- **Medical Biophysics** (headed by Prof. Dr. Leonid A. Noskin);
- **Medical and Bioorganic Chemistry** (headed by Dr. Farid M. Ibatullin);
- **Proteomics** (headed by Dr. Stanislav N. Naryzhny);
- **Cryoastronomy** (headed by Dr. Sergey A. Bulat);
- **Molecular and Cellular Biophysics** (headed by Dr. Georgiy N. Rychkov);
- **Test Center of Radiopharmaceuticals and Other Medical Products** (headed by Dr. Alexander P. Trashkov);
- **Scientific-Technical Department of Bioelectronics** (headed by Dr. Alexander P. Roganov).

MRBD employs 121 research staff members (13 Doctors of Sciences and 64 Candidates of Sciences).



Dr. Andrey L. Konevega
Head of MRBD

The research at MRBD is focused on the most significant fundamental questions in the molecular biology, biophysics, molecular and medical genetics.

The studies of macromolecular complexes by methods of small-angle neutron and synchrotron scattering, atomic-force microscopy and molecular modeling are being actively conducted in MRBD (Laboratory of Biophysics of Macromolecules and Laboratory of Molecular and Cellular Biophysics).

In a paper of G.N. Rychkov *et al.* the full-atom models of partially assembled nucleosome structures – disome, tetrasome and hexasome – were developed for the first time in the world. The developed models provide a new interpretation of the experimental data at hand, characterizing

structural and dynamic properties of nucleosome particles obtained by means of atomic force microscopy, fluorescence resonance energy transfer and small-angle X-ray scattering. The existence of such structures regulates the access of protein factors to genetic information encoded in DNA and may accelerate the transcription process.

The studies of molecular mechanisms of chromatin remodulation are traditional for MRBD. A paper of A.Yu. Konev (Laboratory of Genetics of Eukaryotes) co-authored by foreign colleagues is dedicated to the study of the role of the ACF1 expression level during *Drosophila* oogenesis. ACF1 was found to be expressed in somatic and germline cells, with notable enrichment in germline stem cells and oocytes. It was shown that the asymmetrical localization of ACF1 in these cells depends on the transport of the *Acf1* mRNA by the Bicardal-D/Egalitarian complex. The new deletion mutant of the gene *Acf* was found, which represents a true null allele of the gene *Acf1*.

Also among the most prominent scientific achievements of MRBD a special place is given

to a study of the possible link between the Parkinson's disease (PD) and lysosomal storage diseases (LSDs) (Laboratory of Human Medical Genetics). In 2016, a study was conducted on the correlation between levels of oligomeric forms of an alpha-synuclein protein and the activity of a lysosome enzyme glucocerebrosidase (GBA) in Gaucher's disease (GD) patients. The presence of two mutant alleles in a *GBA* gene is the cause for the development of a rare genetic disorder – Gaucher's disease – classified as one of lysosomal storage diseases. The high risk of PD development in patients bearing mutations of the *GBA* gene is found in all populations of the world, including Russia, however, the molecular mechanism remains unknown. Measuring the level of plasma oligomeric alpha-synuclein and GBA activity it was demonstrated that mutation carriers had a more distinct decrease in GBA enzymatic activity and an increase in oligomeric alpha-synuclein levels compared to the carriers of polymorphous variants. This observation clarifies the mechanism of a high risk of PD development in GBA mutation carriers, as well as suggests using the GBA pharmacological chaperones (ambroxol, isofagomine) to treat GBA-associated PD as well as to come up to the treatment of one form of PD.

A large group of conformational diseases, called amyloidoses, is accompanied by the formation and accumulation in the body of aggregates (fibrillar and oligomeric) of amyloid proteins with toxic properties. However, it should be noted that the aggregates of amyloid proteins have a series of physiological functions and are not always associated with pathological processes. Brain proteins BASP1 and GAP-43 localized at the inner surface of the presynaptic membrane of neuron axon terminals are of critical importance for the life-sustaining activity of the body, they participate in axon directed growth, synaptic plasticity and neuroregeneration, are capable of forming oligomers in the presence of acidic phospholipid membranes. In a paper of O.S. Vituk and V.V. Zakharov (Laboratory of Biopolymers) in the course of the study of the structure of oligomers BASP1 and GAP-43 by applying different methods it was estimated that oligomers GAP-43 and BASP1 consist of 6-7 and 10–14 monomers respectively

as well as have a circular arrangement of monomers. On the basis of the obtained results a model of “electrostatic nucleus” was suggested, which describes the structure of oligomers BASP1 and GAP-43. According to this model, short positively charged (“effector”) domains while interacting with the molecules of phosphatidylinositol-4,5-bisphosphate or sodium dodecylsulfate form an alpha-spiral nucleus of a complex. At the same time, the main part of the protein chains remains in an unstructured form.

Research dedicated to homologous genome repair is traditional for MRBD. RecA protein is the central link of homologous recombination in bacteria, and it is one of the key components of recombination reparations. It is studied in detail in the Laboratory of Genetics of Eukaryotes. In a paper of D.M. Baitin it was shown that the suppression of the hyperrec phenotype results from mutations blocking the expression of RecA D112R protein, the recombinase function of RecA protein represents an evolutionary compromise between necessary levels of recombinational DNA repair and the deleterious consequences for bacterial growth.

The research concerning the structure-functional characteristics of enzymes has been carried out for many years in MRBD Laboratory of Enzymology. The paper of S.V. Shvetsova is dedicated to the studies of enzymatic properties of a novel α -L-fucosidase from *Fusarium proliferatum* LE1 (FpFucA). Detailed characterization of FpFucA provided the physicochemical data and kinetic parameters for the hydrolysis of the model substrate *n*-nitrophenyl- α -L-fucopyranoside (*p*NPFuc), synthetic α -L-fucobiosides with different types of linkages, and several fucosylated oligosaccharides. The ability of this enzyme to catalyze the transglycosylation reaction with different types of acceptors was determined and analyzed.

Activities on the creation of methods aimed at diagnosing various diseases, including malignant tumors – glioblastomas – are carried out in the Laboratory of Cell Biology. Proteomic search for biomarkers of glioblastomas could be one of approaches for the diagnosis creation. It is known that many proteins are marked by a large number of proteoforms and it is expected that

these forms could be a potential source of highly specific biomarkers of glioblastoma. In a paper of S.N. Naryzhny, the proteomic profiling of high-grade glioblastoma using virtual-experimental two-dimensional electrophoresis was generated. The use of an original method of gel sectionalization of 2D-electrophoresis in 96 gel sections with mass-spectrometry (ESI LC-MS/MS) helped to identify a bigger amount of proteoforms – 16 012 (coded by 4 050 genes) in comparison to 1 542 (coded by 600 genes) while using a conventional method.

In a paper by V.A. Ryzhov (Laboratory of Biophysics of Macromolecules) the use of an original method of measuring the second harmonic of non-linear response M_2 to a weak magnetic field in parallel to its steady field demonstrated the selective accumulation of magnetic particles Hsp70-SPION in the myocardium infarction zone. This opens up the possibility of targeted drug delivery to the affected area using Hsp70-SPION conjugate.

The study of the effects of low-dose radiation of a radioactive isotope ^{169}Yb on proliferation and death of human cells in culture, showed that the sources on the basis of isotope ^{169}Yb have a pronounced antiproliferative effect realized in the induction of apoptotic death of the progeny of irradiated cells. The obtained results can be of interest for clinical usage of brachytherapy with ytterbium sources.

The study of the lake water of the subglacial lake Vostok is conducted in MRBD. The possible

existence of microbial life in lake Vostok located under a four-kilometer ice shield in Antarctica is investigated in a paper of S.A. Bulat. We now have the results of molecular-microbiological analysis of available samples of lake water, which entered the bore-hole after the first two drilling sessions of the lake and which got frozen in it. The DNA analysis of lake water samples with various levels of drilling fluid contamination showed a non-identified and a non-classified bacteria w123-10 (less than 86% of similarity with the closest taxons), which demonstrated a remote relationship with a non-identified bacteria AF532061 (92% similarity with closest taxons) from the lake ice. These two bacterium can represent an unstudied microbial life that exists in the water layer underneath the ice of lake Vostok. However, this hypothesis requires further confirmation.

In 2016, a new scientific department was founded within the Division – the Test Center of Radiopharmaceuticals and Other Medical Products. The objectives of the test center include preclinical testing, development of biomodels of socially significant human diseases, as well as joining the efforts and competences of different departments of the Institute to conduct research in the field of biomedicine.

MRBD staff members published more than 60 scientific papers in peer-reviewed journals including 22 papers in foreign journals. The researchers of the Division presented more than 40 talks at international conferences.

Knowledge Transfer Division 2016

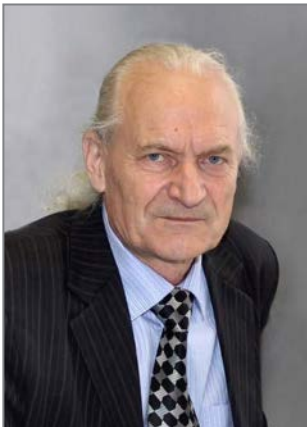
Knowledge Transfer Division (KTD) headed by Dr. Victor F. Ezhov consists of three laboratories:

- **Holographic Information and Measuring Systems (HIMSLab)** (headed by Dr. Boris G. Turukhano);
- **Radiative Physics** (headed by Dr. Nikolay A. Ivanov);
- **Quantum Chemistry** (headed by Dr. Anatoly V. Titov)

and two departments:

- **Accelerator Department** (headed by Dr. Evgeny M. Ivanov). **The department included the Laboratory of Accelerator Physics and Technology** (headed by Dr. Stanislav A. Artamonov);
- **Science and Technology – Information Technologies Department** (headed by Dr. Sergey B. Oleshko), which includes the **Laboratory of Information Computation Systems** (headed by Dr. Sergey B. Oleshko) and **Proton Therapy Group** (headed by Dr. Djan L. Karlin).

KTD employs 151 research staff members (3 Doctors of Sciences and 15 Candidates of Sciences).



Dr. Victor F. Ezhov
Head of KTD

Main accelerative facilities of the Institute are concentrated in Knowledge Transfer Division (KTD). First of all, it is the 1 000 MeV synchrocyclotron with unique features. A wide

range of scientific and applied studies in different areas from nuclear physics to medicine can be carried out at the synchrocyclotron. In 2016, a unique system was introduced at the synchrocyclotron of NRC “Kurchatov Institute” – PNPI. It resulted in a considerable expansion of the range of proton energies that are available for experiments.

A specialized center for radiation tests with proton energies from 60 to 1 000 MeV started to operate at this beam. The center includes the modern workplace with beam diagnostic systems, modern dosimetry devices, automated result processing system, and a modern user infrastructure. Also, the radiation physics laboratory developed the absolute monitors with the chamber diameters 10 and 20 cm to measure parameters of proton beams with a large cross-section and with energies in the range 50–1 000 MeV. These chambers

were used to measure proton beams with the energies ranging 64–1 000 MeV.

In 2016 in KTD the Accelerator Department of NRC “Kurchatov Institute” – PNPI in collaboration with JSC “NIIIEFA” performed a start of an isochronous cyclotron C-80. It is aimed at creating the proton beam with the energy ranging 40–80 MeV and the current up to 100 μA . The high energy of an accelerated beam combined with its high intensity allows the production of high-quality radioactive isotopes and radiopharmaceuticals that cannot be produced at commercial cyclotrons (for example, generator isotopes of ^{82}Sr and ^{68}Ge). The project provides the possibility of isotope separation by means of a magnetic separator.

The use of a mass-separator for electromagnetic separation of the produced radionuclides will ensure the production of a wide range of ultra-pure radionuclides (better than $1 \cdot 10^{-4}$) for the diagnostics and therapy.

The high energy of the proton beam will allow the creation of an ophthalmology center for radiation therapy of eye cancer disease. It will become the first center of this kind in Russia. Such technology of treatment of eye cancer diseases is highly effective, it is widely used abroad and it is in demand in the medical community.

At the present time, the standards and regulations of the leading countries require the electronic equipment used in space and aviation tech-

nologies to be tested for radiation resistance when exposed to a flux of neutrons with a spectrum similar to the atmospheric spectrum of neutrons and high-energy protons, which constitute the primary component of cosmic radiation. NRC “Kurchatov Institute” – PNPI has two universal centers of radiation resistance testing. Radiation tests of radio-electronic equipment can be carried out here using both the proton beam with the energy range from 100 to 1000 MeV, and a neutron beam, whose spectrum is similar to the spectrum of atmospheric neutrons. In 2016, 20% of the synchrotron's running time was used for the performance of these tests for Roscosmos State Corporation.

The Laboratory of Holographic Information and Measuring Systems (LHIMS) is one of the world leaders in the field of precision measuring in the range of nanometers. In order to conduct this type of studies, the LHIMS has a unique holographic underground vibration-free laboratory. The results of many years of research were published in 2016. The research findings substantiate the synthesis of the aperture of interference field in the optical range. The use of this method allows the creation of wide-aperture ultrahigh-precision linear diffraction gratings that are used for the creation of linear and angular sensors for measuring systems possessing the record precision.

Information Technologies and Automation Department (ITAD) of KTD provides support and development of the local computer network of the Institute, including the computing cluster and NRC “Kurchatov Institute” – PNPI site of Worldwide LHC computing Grid (WLCG) network. In 2016 one of the main activities of the department was the creation of a data center at the PIK reactor. When the center is commissioned in 2017, computational capabilities for employees of the Institute will increase significantly.

In 2016, ITAD staff members together with MRBD researchers designed and created a Micro-CHIP for biological studies (an AngioChip for the study of combinatorial effect of angiogenic factors on the process of the formation of a microcirculatory bloodstream *ex vivo*).

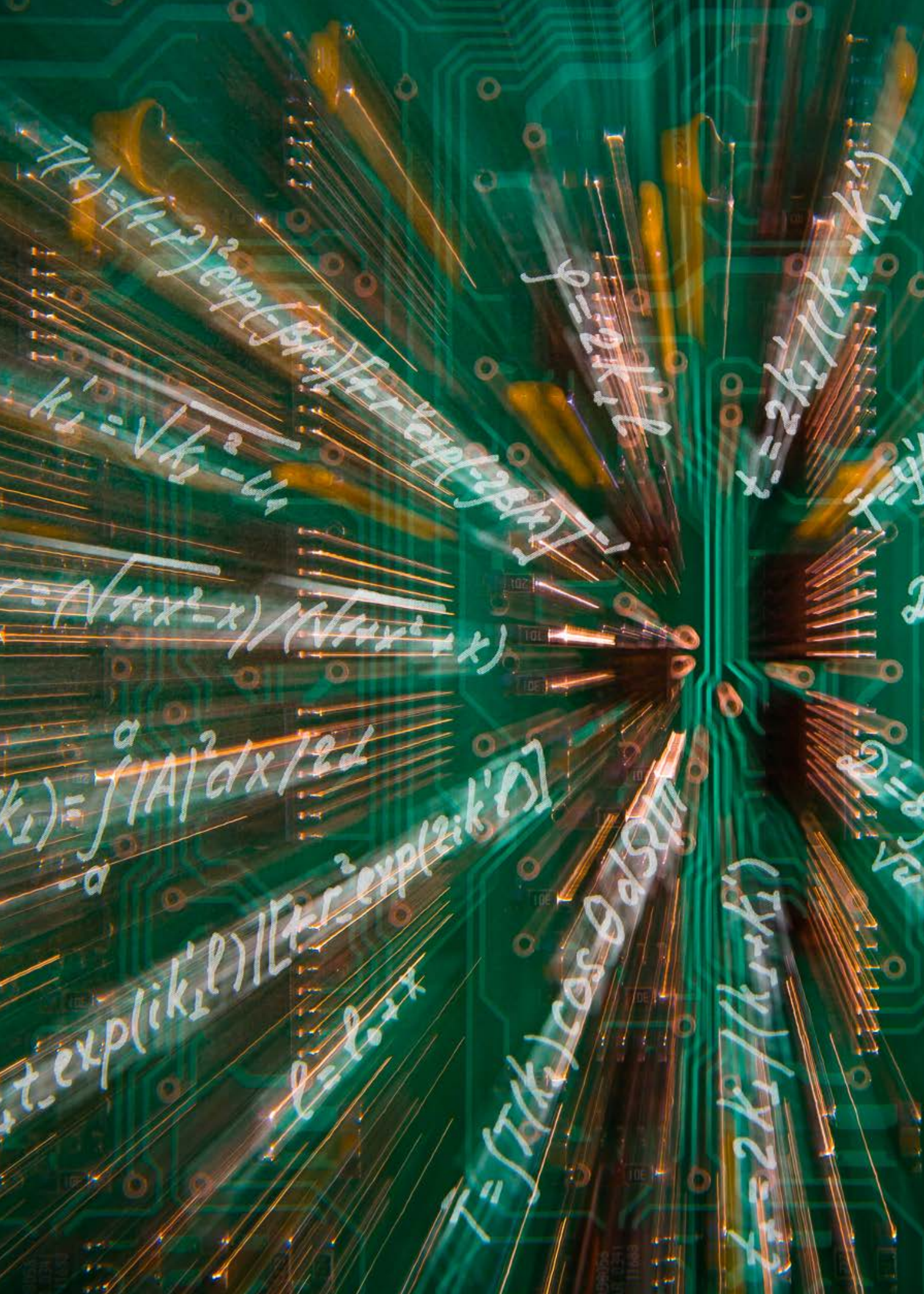
The discovery of the subglacial lake Vostok in Antarctica became the last geographic discovery of XX century. Its exploration will allow the provision of the unique data about the origin and evolution of different forms of life in ecosystems that are characterized by being highly oligotrophic (i.e. possessing the lowest concentration of nutrients) as well as by extreme conditions. NRC “Kurchatov Institute” – PNPI is the head organization in the research investigation of Vostok lake water. The scientists of KTD, MRBD and NRD take an active part in this research. The Institute faces an extremely challenging technical task of developing a technology of penetrating the lake water environment without polluting the lake with the bore liquid. In 2016 NRC “Kurchatov Institute” – PNPI manufactured and delivered to Vostok station the equipment, whose purpose is to collect water samples from the subglacial lake, to perform a shooting in the bore hole and to measure the oxygen content in the water.

The main line of activity of the Laboratory of Quantum Chemistry of KTD is the development of the calculation technique which can be applied to the electronic structure of molecules containing heavy elements. This activity was initiated in 1980's because of the necessity to calculate the *P*- and *CP*-odd effects in heavy diatomic molecules. A two-step method developed by the laboratory became the basis of calculations. The method allowed the subdivision of computation structure of such molecules into two consequent computations in valence and core regions. The presently achieved accuracy of these computations is the best in the world. The computation data of the gain of the nEDM value have been used in the experiment for the search of the electron EDM with the molecule ThO, which is considered to be the best to date.

Сотрудниками ОПР в 2016 г. опубликовано 35 работ (и более 100 в соавторстве с учеными коллаборации ATLAS), сделано 33 доклада на российских и международных научных конференциях, проведено 2 международных конференции, получены 4 гранта, защищены 2 кандидатские диссертации.



On November 2016, an ejected proton beam with designed parameters was obtained at the isochronous cyclotron C-80 of NRC “Kurchatov Institute” – PNPI. The start of this set-up at the Institute opens up new tasks connected with its practical application



$$\psi(x) = (1-x^2)^2 \exp(-\beta|x|) \exp(i k_1 x)$$
$$k_1 = \sqrt{k_0^2 - \beta^2}$$

$$\phi = 2k_1 l$$

$$x = 2k_1 / (k_1 + k_0)$$

$$r = (\sqrt{1+x^2} - x) / (\sqrt{1+x^2} + x)$$

$$k_1) = \int_{-a}^a |A|^2 dx / 2L$$

$$t \exp(ik_1 l) / [k_1 r^2 \exp(2ik_1 l)]$$
$$e = 2 \cos \phi$$

$$T = \int T(k) \cos \theta d\theta$$

$$t = 2k_1 / (k_1 + k_0)$$

Theoretical and Mathematical Physics

- 28 BFKL Pomeron in the Higgs model with the running coupling constant
- 29 LHCb pentaquarks: deuteron analogue or hadro-charmonium
- 30 Structures of neutrino mass spectrum and lepton mixing as results of violated mirror symmetry
- 31 Exclusive J/ψ process tamed to probe the low x gluon
- 32 Strongly correlated Fermi systems as a new state of matter
- 33 Non-Abelian strings in SUSY theories
- 34 Percolation scenario near transition from the ordered (“superfluid”) phase to the Bose-glass phase
- 35 Integrability and AdS/CFT correspondence
- 36 Stabilization of the avalanche-like processes on dynamical networks
- 37 Role of electron shell in double beta decay
- 38 Adaptation of MURE code to the neutronic calculations of the reactor PIK
- 39 Quantum chemical modelling of electronic structure of superheavy element compounds
- 41 Laser cooling and high-precision spectroscopy of radium compounds for “new physics” search
- 42 Search for new physics with atoms and molecules
- 43 Rainfall and hurricane propagation velocity

BFKL Pomeron in the Higgs model with the running coupling constant

L.N. Lipatov

Theoretical Physics Division of NRC "Kurchatov Institute" – PNPI

In the paper the stationary equation of Balitskii–Fadin–Kuraev–Lipatov (BFKL) is solved to find the Pomeron spectrum ω in the j -plane for the field theories with the gauge group $SU(N_c)$:

$$\omega \psi_\omega(k) = \int \frac{d^2 k'}{2\pi} \alpha_s(k, k') K(k, k') \psi_\omega(k'), \quad \omega = j - 1,$$

beyond frameworks of the leading logarithmic approximation $\alpha_s \ln s \sim 1$, when effects of the running coupling constant $\alpha_s(k, k')$ are taken into account. Instead of the usual dimensional transmutation in the region of small transverse momenta $|k| \sim \Lambda_c \approx 200$ MeV an effective gluon mass $m \approx 0.54$ GeV is generated through the Higgs phenomenon in an agreement with the lattice computations. In the paper various forms of the parametrization of α_s are used, including the so-called "triumvirat" of coupling constants

$$\alpha_s(k, k') = \frac{\alpha_s(k') \alpha_s(k - k')}{\alpha_s(k)}, \quad \alpha_s(k) = \frac{1}{\beta \ln \frac{k^2}{\Lambda_c^2}},$$

where $\beta = \frac{11}{12} N_c - \frac{1}{6} n_f$ is the first coefficient of

the Callan–Simanzik function. The Pomeron spectrum ω_n in the complex plane of the t -channel angular momentum j is calculated approximately using the discreet modification of the BFKL equation and semi-classically by matching two solutions in the region $|k| \geq m$. The first solution corresponds to large k , where one can neglect the gluon mass, another one can be obtained from the equation by freezing the coupling constant α_s at $|k| \sim m$. Their matching leads

to the discreet Pomeron spectrum at the vanishing momentum transfer $\sqrt{-t} = 0$ in the form

$$\omega_n = \frac{0.4085}{n - \frac{1}{4}}, \quad n = 1, 2, \dots$$

For large n the quasi-classical approach is supported by the direct calculations of the eigenvalues of the integral kernel of the BFKL equation. However, the position of the leading Regge pole ω_n with $n = 1$ depends strongly on details of matching of solutions in the confinement region $|k| \sim m \sim \Lambda_c$ (in particular, from the choice of the k -dependence of α_s). At the same time the direct calculations of ω_1 are in a good agreement with the results obtained with the variational principle. These calculations are also important for the investigation of the continuous spectrum of Pomerons at $\omega < 0$, which gives a significant contribution to the completeness relation for the eigenfunctions of the BFKL kernel. In the paper it is shown that in the Higgs model the density of the eigenvalues has a discontinuity at a negative value of ω , corresponding to the possible Pomeron decay to the constituent gluons. Such rapid change of the Pomeron density due to their deconfinement could have place in the real Quantum Chromodynamics (QCD), but for its investigation one should go beyond frameworks of perturbation theory. A possible modification of QCD at small distances due to a new physics (for example, the supersymmetry) also has some influence on the Pomeron spectrum, but the position of the leading Regge pole ω_1 does not depend practically on various generalizations of the Standard Model of elementary particles.

LHCb pentaquarks: deuteron analogue or hadro-charmonium

M.I. Eides, V.Yu. Petrov, M.V. Polyakov
 Theoretical Physics Division of NRC “Kurchatov Institute” – PNPI

The main question in the interpretation of pentaquarks discovered recently in LHCb is related to the distance between heavy quarks. The interaction between heavy quarks in the pentaquark looks approximately as on the Figure. It is seen that this interaction has two minima which correspond to two possible interpretations of pentaquark.

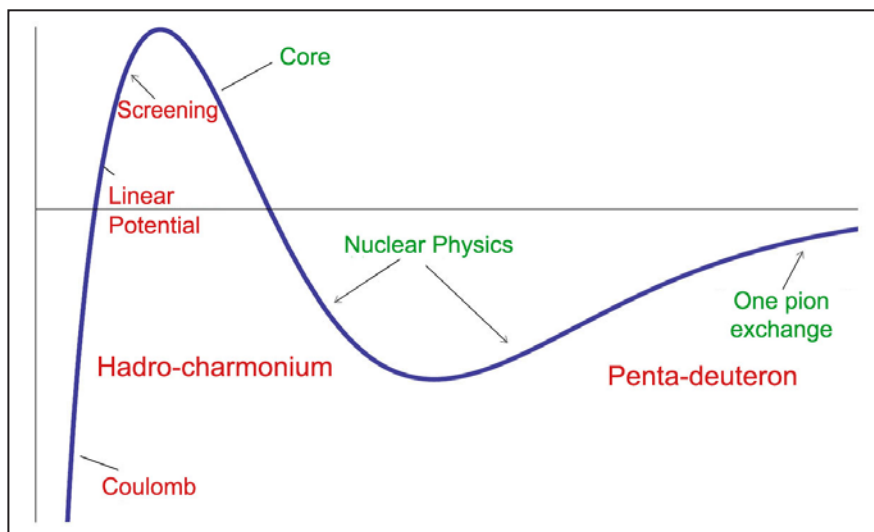
If the distance between heavy quarks is large (~ 1.5 fm), we have to consider pentaquark as a loosely bound state of two hadrons with open charm. An adequate description in this case is based on the “nuclear physics” of Σ_c -hyperons and *D*-mesons. Properties of the pentaquark appear to be rather close to the properties of deuteron.

In the opposite case when the distance is small (~ 0.3 fm) one can describe pentaquark as an excited charmonium $\Psi(2s)$ located in the center of the proton. Such a state is usually called

hadro-charmonium. The binding of two hadrons ($\Psi(2s)$ and proton) is due to non-perturbative two gluon exchange.

In our paper we have considered both possibilities and calculated pentaquark properties in either of approaches. Both interpretations predict additional pentaquark states and we have calculated their masses. Also new states appear if light quarks are substituted by strange quarks or when instead of *c*-quarks we consider more heavy *b*-quarks.

A crucial experiment, which allows to judge which picture of pentaquark is correct is the measurement of the ratio of pentaquark decays into open charm and hidden charm hadrons. If this ratio is large, pentaquark is definitely the hadro-charmonium. As we know that LHCb pentaquark was discovered exactly in this type of decays, we consider this hypothesis as more probable.



Potential interaction energy between infinitely heavy quarks (“quark term”) as a function of distance between *c*-quarks

Structures of neutrino mass spectrum and lepton mixing as results of violated mirror symmetry

I.T. Dyatlov

Theoretical Physics Division of NRC “Kurchatov Institute” – PNPI

The observed neutrino mass spectrum, with two states 1, 2 very close in mass and one state 3 located away from the first two, is different from the strict hierarchy of spectra of all other fermions in the Standard Model (SM), i. e., quarks and charged leptons. The weak mixing matrix (WMM) for leptons is also completely different from the WMM for quarks – that is, the Cabibbo–Kobayashi–Maskawa (CKM) matrix.

Both differences can be explained by a model in which fermion masses of SM are formed as a result of the spontaneous violation of initial mirror symmetry, i. e., in SM supplemented by heavy analogs with opposite (left-right) weak properties. With the observed mass hierarchy for quarks, such system reproduces all qualitative properties of the CKM matrix. The large mass of mirror particles is a necessary condition of the reproduction.

For leptons, the mirror model introduces factors that are indicative of the exceptional smallness of SM neutrino masses, the inverse order of these masses (the two states located close to each other are heavier), and their Dirac nature.

The absence of any visible hierarchy in the neutrino mass spectrum is a consequence of two independent spectra of neutral mirror masses – Dirac and Majorana – being jointly involved in the formation of the mass matrices. Separately, however, each of these spectra demonstrates the “normal” mass hierarchy, similar to the spectra of all other fermions in SM.

Therefore, mass hierarchy is a common property of all spectra involved in the formation of masses

of any fermion generations, including neutrinos. We are dealing here with a universal mechanism that has not yet been explained.

The mirror scenario can also furnish an explanation for the different form of the lepton WMM. The observed neutrino mass spectrum, its inverse order and hierarchy of charged lepton masses produce a WMM – the PMNS matrix – with properties that differ essentially from those of the CKM matrix. An important condition is also the smallness of the mass of the lightest (in the case of inversion) neutrino $m_3 \ll m_1, m_2$. Experimentally obtained properties of the PMNS matrix are reproduced qualitatively.

The smallness of the Daya–Bay angle θ_{13} – the major characteristic of the PMNS matrix – is defined by the orthogonality (in generation space) of wavefunctions of the electron and remote neutrino 3. The value of θ_{13} is defined precisely by these small ratios, mainly, probably, by the neutrino mass ratios $m_3/m_1, m_3/m_2$.

The inverse order of the spectrum and required smallness of m_3 permit evaluation of the absolute values of neutrino masses. The observed value $\sin\theta_{13} = 0.14\text{--}0.16$ corresponds to the unknown mass of the light neutrino 3 less than 0.01 eV. “Large” masses m_1, m_2 under the given conditions are equal to approximately 0.05 eV. No further conditions on the model constants (except those that are imposed by mass hierarchy) are required for reproduction of the qualitative picture.

1. Dyatlov I.T. // *Yad. Fiz.* 2015. V. 78. P. 1015: arXiv:1509.07280 [hep-ph].

2. Dyatlov I.T. // *Yad. Fiz.* 2017. No. 1. P. 80: arXiv:1611.05635 [hep-ph].

3. Dyatlov I.T. Структуры спектра масс нейтрино и смешивания лептонов. Результат нарушенной зеркальной симметрии // *Yad. Fiz.* 2017. Готовится к печати.

Exclusive J/ψ process tamed to probe the low x gluon

M.G. Ryskin

Theoretical Physics Division of NRC “Kurchatov Institute” – PNPI

The cross section of diffractive J/ψ meson photoproduction is proportional to the gluon density squared:

$$\frac{d\sigma}{dt}(\gamma^* p \rightarrow J/\psi p)|_{t=0} = \frac{\Gamma_{ee} M_\psi^3 \pi^3}{3\alpha^{\text{QED}}} \left[\frac{4\alpha_s}{(Q^2 + M_\psi^2)^2} xg(x, \mu_F^2) \right]^2 \left(1 + \frac{Q^2}{M_\psi^2} \right).$$

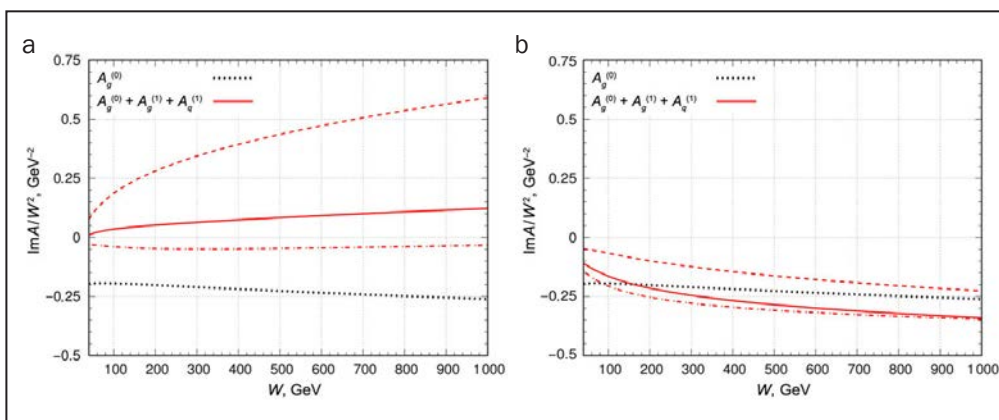
In principle, this allows the measurement at the Large Hadron Collider (LHC) of the gluon distribution down to a very small $x \sim 3 \cdot 10^{-6}$ at the scales $\mu_F \sim 1\text{--}2$ GeV. This is just the region which controls the high energy cross section behavior. It turns out, unfortunately, that the NLO corrections to the leading logarithmic (LO) formula are quite large. Thus, one can doubt the accuracy of the gluon densities, $xg(x, \mu_F^2)$, obtained this way.

The corrections are large for two reasons: (a) there are double logarithmic (DL) terms enhanced by a large value of $\ln(1/x)$; (b) next are the power corrections of Q_0^2/μ_F^2 type coming from the region of $q < Q_0$, which were accounted for twice –

first, in the input condition for the Dokshitzer–Gribov–Lipatov–Altarelli–Parisi (DGLAP) parton evolution and then – calculating the NLO coefficient functions. These power corrections are negligible in hard processes with a large $\mu_F \gg Q_0$. However, for the J/ψ production, where the input scale of evolution Q_0 is of the order of charm quark mass, its contribution is important.

We proved that it is possible to remove all the DL (enhanced by a large $\ln(1/x)$) terms. Taking the factorization scale $\mu_F = M_\psi/2$ one moves all these DL terms to the incoming parton distribution where they will be resummed by DGLAP equation. Besides this, to avoid the double counting we subtracted from the NLO coefficient functions all the low $q < Q_0$ contributions.

This way we get a stable result allowing in the future to use the LHC data on ultraperipheral J/ψ meson production to constrain the gluons at extremely small x and at a low factorization scale, that is in the region where the uncertainties of the present global parton analysis are quite large.



J/ψ meson photoproduction amplitude in the leading logarithmic (black curve) approach and accounting for the NLO corrections (red curves). The dependence of the results under the factorization scale variations from $\mu_F^2 = 1.7$ to 4.8 GeV² is shown by the dashed curves

1. Jones S.P. ..., Ryskin M.G. et al. // J. Phys. G. 2016. V. 43. P. 035002.
 2. Jones S.P. ..., Ryskin M.G. et al. // Eur. Phys. J. C. 2016. V. 76. P. 633.

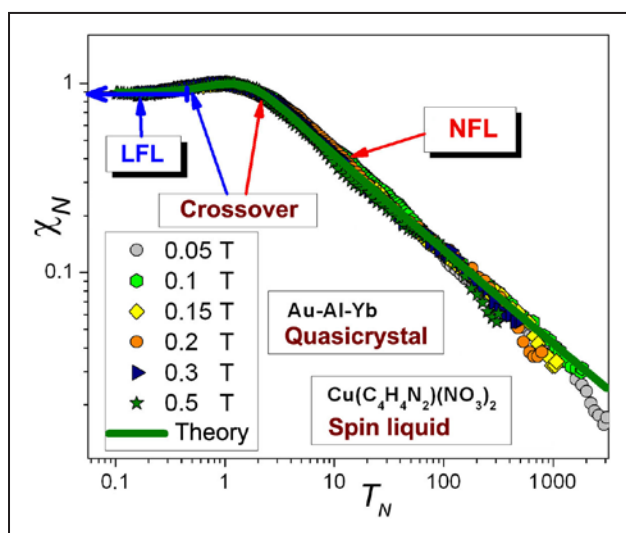
Strongly correlated Fermi systems as a new state of matter

V.R. Shaginyan

Theoretical Physics Division of NRC “Kurchatov Institute” – PNPI

In many correlated Fermi systems and compounds at zero temperature a phase transition occurs that leads to a specific state called fermion condensation that forms a new state of matter. As a signal of the topological fermion condensation quantum phase transition (FCQPT) serves unlimited increase of the effective mass of quasiparticles that determines the excitation spectrum and creates flat bands. We have theoretically carried out a systematic study of the phase diagrams of strongly correlated Fermi systems, including heavy-fermion (HF) metals, high temperature superconductors, insulators with strongly correlated quantum spin liquid, quasicrystals, and two dimensional Fermi systems (like ^3He), one-dimensional spin liquids, and have demonstrated that these diagrams have universal features. We name these various systems HF compounds, since they exhibit the behavior typical of HF metals. In HF compounds at zero temperature the unique phase transition, FCQPT, can occur; it is this FCQPT that

creates flat bands and in turn leads to the specific state, known as the fermion condensate. Our analysis of numerous salient experimental data within the framework of FCQPT resolves the mystery of the new state of matter, taking place in HF compounds. The obtained results are in good agreement with experimental facts. We have shown both analytically and using arguments based entirely on the experimental grounds that data collected on these very different heavy-fermion compounds have a universal scaling behavior, and these materials with strongly correlated fermions can unexpectedly have a uniform behavior in spite of their microscopic diversity. Thus, the quantum critical physics of different Fermi systems is universal, defined by the topological fermion condensation quantum phase transition, emerges regardless of the underlying microscopic details of compounds, and forms the new state of matter.



The universal scaling behavior of the magnetic response of quite different compounds: 1D spin liquid of $\text{Cu}(\text{C}_4\text{H}_4\text{N}_2)(\text{NO}_3)_2$ and the quasicrystal Au-Al-Yb. The Fermi liquid behavior, non-Fermi one and the crossover are shown

1. Amusia M.Ya. ..., Shaginyan V.R. et al. Theory of Heavy-Fermion Compounds: Theory of Strongly Correlated Fermi-Systems. Berlin: Springer, 2015. V. 182. 359 p.
2. Shaginyan V.R. et al. // Front. Phys. 2016. V. 11. P. 117103.

Non-Abelian strings in SUSY theories

A.V. Yung

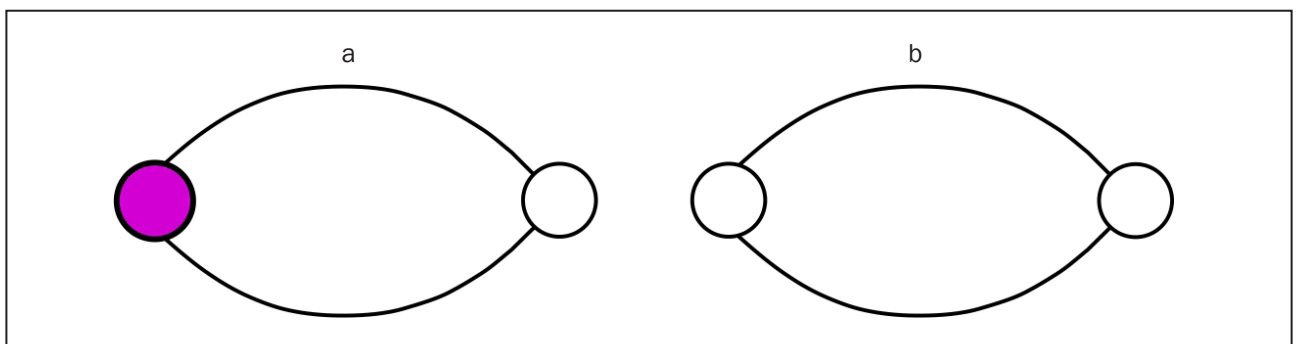
Theoretical Physics Division of NRC “Kurchatov Institute” – PNPI

Non-Abelian vortex strings supported in a certain four-dimensional $N = 2$ supersymmetric Yang–Mills theory with fundamental matter at strong coupling were shown to become critical superstrings. In addition to translational moduli non-Abelian string under consideration carries orientational and size moduli. Their dynamics is described by two-dimensional sigma model whose target space is a tautological bundle over the complex projective space. For the $N = 2$ Quantum ChromoDynamics (QCD) with the $U(2)$ gauge group and four fundamental hypermultiplets there are six orientational and size moduli. After combining with four translational moduli they form a ten-dimensional target space required for a superstring to be critical. For the theory in question the target space of the sigma model

is a product of the flat four dimensional (4D) space and a six dimensional non-compact Calabi–Yau manifold, the conifold.

We study closed string states which emerge in four dimensions and identify them with hadrons of the 4D bulk $N = 2$ supersymmetric QCD. It turns out that most of the states arising from the ten-dimensional graviton are non-dynamical in 4D. In particular, there is no 4D graviton, because its wave function is non-normalizable over the conifold.

We find a single dynamical massless hypermultiplet associated with the deformation of the complex structure of the conifold. We interpret this degree of freedom as a stringy monopole-monopole baryon of the 4D QCD (at strong coupling), see Fig.



Monopole-antimonopole stringy meson (a). Monopole-monopole stringy baryon (b). Open and closed circles denote monopole and antimonopole respectively

1. Koroteev P. ..., Yung A. // Phys. Rev. D. 2016. V. 94. P. 065002: arXiv:1605.08433[hep-th].
2. Koroteev P. ..., Yung A. // Phys. Lett. B. 2016. V. 759. P. 154–158: arXiv:1605.01472[hep-th].

Percolation scenario near transition from the ordered (“superfluid”) phase to the Bose-glass phase

A.V. Sizanov, A.V. Syromyatnikov

Theoretical Physics Division of NRC “Kurchatov Institute” – PNPI

Quantum phase transition in the system of interacting Bose-particles between Mott insulator (MI) and superfluid (SF) phases is equivalent to transition in Heisenberg antiferromagnet (HAF) in magnetic field between fully polarized (“MI”) and antiferromagnetically ordered (“SF”) phases (order parameter is the component of the mean staggered magnetization orthogonal to the magnetic field). Disorder of the system leads to the appearance of an intermediate non-SF phase called Bose-glass (BG) characterized by localized single-particle excitations. In terms of HAF the BG phase is represented by a set of isolated finite volume islands of unsaturated magnetization surrounded by saturated regions. When the field decreases, these islands grow, merge, and it is the moment of transition to the ordered phase (SF) when a large island appears, whose volume is of the order of the system volume.

The theory of SF to BG transition was built by M.P. Fisher *et al.* on the basis of simple scaling ansatz for the free energy. But in recent years a large amount of experimental and numerical data appeared, which contradict Fisher’s theory. Particularly the latest theory shows $\varphi > 2$ for critical temperature exponent φ of BG to SF transition. But corresponding experiments and numerical calculations on different compounds and models give $\varphi > 1.1$. That is, in recent works the universal behavior was found, which is different from that predicted by Fisher. A convincing explanation of this contradiction was not proposed.

In our paper we build the theory of an ordered phase near transition to BG phase based on hydrodynamic description of long wavelength excitations. Our results are in agreement with Fisher’s theory but are more general and can describe a crossover from critical behavior predicted by Fisher to another universal behavior. We obtained formulae, which describe recent experimental and numerical results well (particularly $\varphi > 1.1$ contradicting Fisher’s theory) if percolation critical behavior not very close to critical point is assumed. Thus, we propose the following picture: in the vicinity of critical point the critical behavior predicted by Fisher’s works, but when moving away from this point there is a crossover to percolation critical regime (also universal), which violates Fisher’s ansatz. Seemingly, in recent works only percolation regime was explored and the crossover to Fisher’s critical regime was not reached due to small system sizes in numerical investigations and the temperature in experiments being too high. It serves the important confirmation of our crossover hypothesis that value of correlation length critical exponent is the same in percolation and Fisher’s regime.

In addition, we supplemented Fisher’s theory with a number of new results. One of the most important is the “superuniversal” behavior for density of states (DOS) of localized, relatively high-energy excitations (i. e. independence of DOS not only from lattice type and model details (usual universality) but also from space dimensionality (“superuniversality”).

Integrability and AdS/CFT correspondence

V.N. Velizhanin

Theoretical Physics Division of NRC "Kurchatov Institute" – PNPI

In recent years, great interest is demonstrated in the investigation of different aspects of AdS/CFT-correspondence – the correspondence between gravity theory in anti-de Sitter space and conformal field theory (maximally extended $N = 4$ supersymmetric Yang–Mills theory). One of the objects of intensive research in this model is the composite operators, whose anomalous dimensions correspond to the energy spectrum of the strings. It was found some time ago that the results for the anomalous dimensions can be found with the help of integrability. Recently, a new very powerful and general method for the computations of the anomalous dimensions for any operators with arbitrary coupling constant was suggested, which is based on the usage of the so-called Quantum Spectral Curve (QSC) approach. Using the computer realization of this method we calculated several (more than 100) first even values for the seven-loop anomalous dimension for twist-2 operators in this model. Based on the assumption about the functions, which can enter into the desired result (generalized harmonic sums) and applying the methods

of the number theory, which allow solving the system of Diophantine equations, that is the system of equations in the integer numbers in which the number of unknowns is greater than the number of equations, we reconstructed a general expression for this anomalous dimension (for the arbitrary Lorentz spin of the operator). It ought to be noted that the system of equations, which we solved with the help of the number theory, consisted of more than 100 equations for more than 1000 variables, that is to say the number of variables was an order greater than the number of equations, nevertheless, the LLL-algorithm and the usage of the modular arithmetic for the subdivision of basis of the harmonic sums allow solving such a system in the integer numbers. The obtained result after the analytical continuation provided a lot of new information about analytical properties of the anomalous dimensions of twist-2 operators in this model, in particular, about the structure of the corrections to the BFKL (Balitskii–Fadin–Kuraev–Lipatov) and the generalized double-logarithmic equations.

Stabilization of the avalanche-like processes on dynamical networks

N.E. Savitskaya

Theoretical Physics Division of NRC "Kurchatov Institute" – PNPI

The avalanches caused by external perturbations are a widespread type of dynamics of complex systems consisting of a large number of the interacting threshold elements (magnetic flux dynamics in discrete superconductors, earthquakes, financial markets dynamics and many other things). The avalanches arising in a system can be both small and large, covering the whole system. The latter is typically considered as the catastrophic one. Therefore, when studying such systems, the problem of stabilization of the avalanche process is very important.

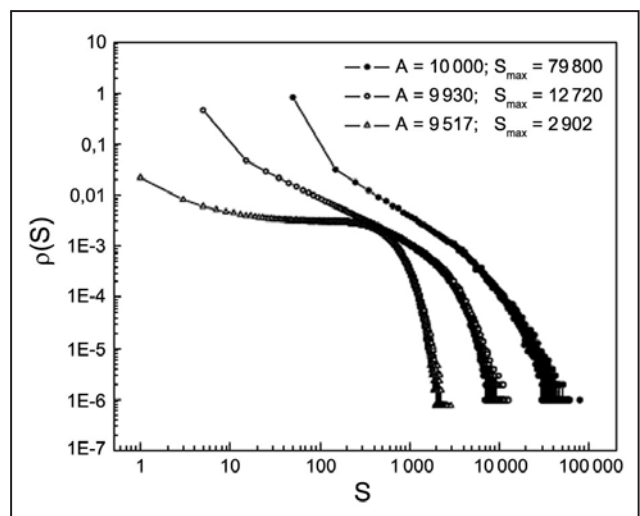
In this paper, the problem of stabilization of avalanche processes developing on a temporal network is considered for the first time. A temporal or time-varying network is a network whose structure changes in time owing to the presence of the individual "activity" of each site. This characteristic determines the probability for a site to connect with other sites per unit time. We consider the case when the structure of links in a network is stable during the time of the avalanche. Such a case is of practical interest as it is quite often realized in social systems, for example, the spreading of contact diseases or information propagation in a social network.

To study such processes, a mathematical model of the system with avalanche dynamics is constructed including changes in the structure of the network on which avalanches are developed.

As a result, we showed that the avalanche-like processes developing on a dynamic lattice are

more stable than similar processes on the static lattice with respect to the appearance of catastrophic events. In particular, this effect manifested itself in the decrease of the maximum size of an avalanche with the decrease of mean value of active sites per unit time A . It means that the sizes of avalanches on the dynamical lattice can be controlled by varying the distribution function of "activities" of its sites.

This remarkable result is illustrated in Figure, where the probability density of avalanche sizes is presented. We can see that the maximum size of an avalanche decreases the volume considerably with the decrease of value of A .



Плотность вероятности размеров лавин для динамической решетки размером $N = 10\,000$ с различным количеством активных узлов A в каждый момент времени

Role of electron shell in double beta decay

E.G. Drukarev

Theoretical Physics Division of NRC "Kurchatov Institute" – PNPI

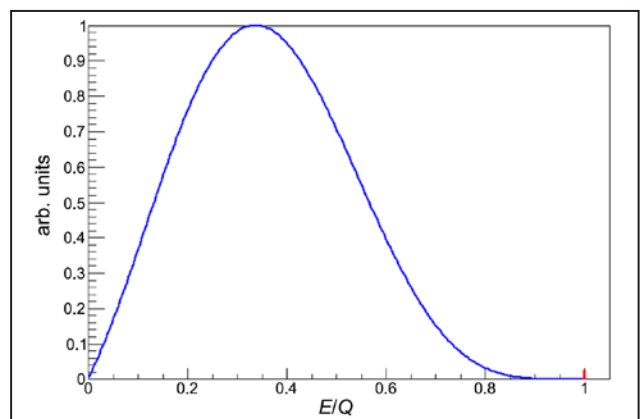
In the double beta decay two neutrons of the nucleus convert into protons with the emission of two electrons and two electron antineutrinos. This second order process in weak interactions has been observed for eleven nuclei. This process involves the intermediate nuclear state, thus being of interest for nuclear physics. The hypothetical double beta decay without neutrino emission is still more interesting. It cannot take place in the framework of the Standard Model of electroweak interactions since it requires the violation of the lepton quantum number.

The process becomes possible if the electron neutrino is a Majorana particle which coincides with its own antiparticle, having also a nonzero mass. It was understood recently that the neutrinos do have a finite mass. This increased interest in the neutrinoless decay. If there are the massive Majorana neutrinos, its mechanism is quite simple. Two W -mesons are produced by two successive beta decays. They interact by the neutrino exchange, producing two electrons. Several groups tried to detect the neutrinoless decay and several projects are in progress. The neutrinoless process has not been observed yet.

The sum of the electron energies E does not exceed the mass difference of the decaying and the daughter atoms Q . The distribution over E in the double beta decay exhibits a smooth curve tending to zero at $E = Q$ due to the vanishing antineutrino phase volume. In the neutrinoless decay the electrons are always ejected with $E = Q$. Thus, we expect a monochromatic peak at this value of the energy carried by the electrons (it is marked by red in the Figure).

The value of Q can be measured with good accuracy if the masses of both the decaying and the daughter atoms are in the ground states. However, electron shell can suffer inelastic transitions. The energy available for the ejected electrons becomes smaller. This leads to the shift of the value of Q to $Q' < Q$. Determination of the shift $Q' - Q < 0$ becomes increasingly important for the current experiments and for those in preparation because of the high level of the electron energy resolution.

We calculated the shift for the decays studied nowadays using the shake off approximation employing the Hartree-Fock wave functions for description of the bound electrons. We found it to be -350 eV for germanium and -400 eV for xenon. Corrections to the shake off value caused by the final state interactions between the beta electrons and the bound ones increase the value of $|Q' - Q|$ by several eV.



Распределение по суммарной энергии электронов в двухнейтринном двойном бета-распаде (синяя линия) и в безнейтринном распаде (красный пик)

Adaptation of MURE code to the neutronic calculations of the reactor PIK

M.S. Onegin

Theoretical Physics Division of NRC "Kurchatov Institute" – PNPI

The selection of the appropriate code for neutronic calculations of the burn up company of the reactor PIK is considered to be an important task at the present time. The potential of MURE code for doing such calculations is demonstrated in this work. For the PIK core with standard fuel assemblies (FA) the calculations that are important for the reactor safety have been done: the temperature coefficients of reactivity; the heat release pattern of the core and the influence of the burnable absorption rods on this pattern were calculated. The operation company of the reactor PIK with standard FAs has been calculated and the influence of the improved FAs with burnable poison pins on the reactor operational cycle has been investigated. Fur-

thermore, the radiation properties of the PIK spent fuel were obtained.

The change of the reactor reactivity with fuel temperature in general appeared to follow the theoretical law (Fig. 1):

$$\Delta\rho(T) = 0.19(1/\sqrt{T} - 1/\sqrt{T_0}). \quad (1)$$

At the same time, the change of the reactor reactivity with the increase of the water temperature in the core is according to the law:

$$\Delta\rho = -0.397(|\Delta c_{\text{H}_2\text{O}}|)^{1.4}, \quad (2)$$

where $\Delta c_{\text{H}_2\text{O}}$ is the difference in the water density (g/cm^3) in the range from 20 °C up to the current temperature. The approximation of the MURE results with the law (2) is presented in Fig. 2.

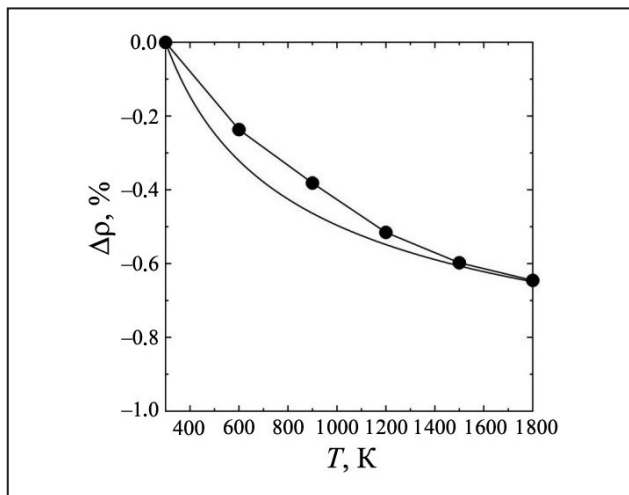


Fig. 1. Influence of the fuel temperature on the reactivity of PIK reactor. Circles – MURE code results; the curve – theory approximation

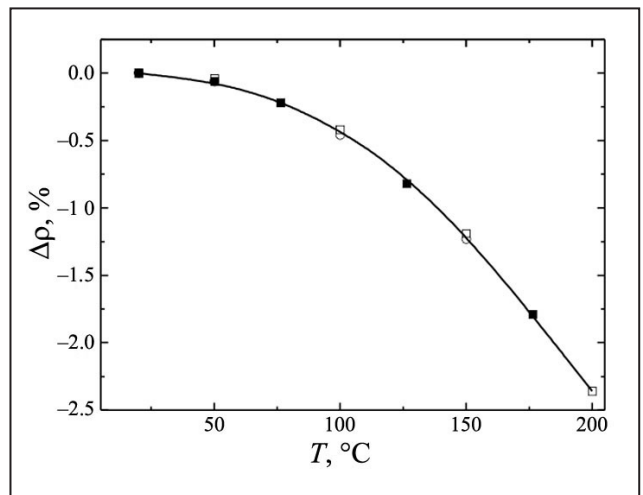


Fig. 2. Changing of the reactor reactivity with the temperature of the light water in the core: ○ – MURE results with thermal library JEF-2.2; □ – the same using library JEFF-3.1; ■ – using library ENDF/B-VII; — – approximation (2)

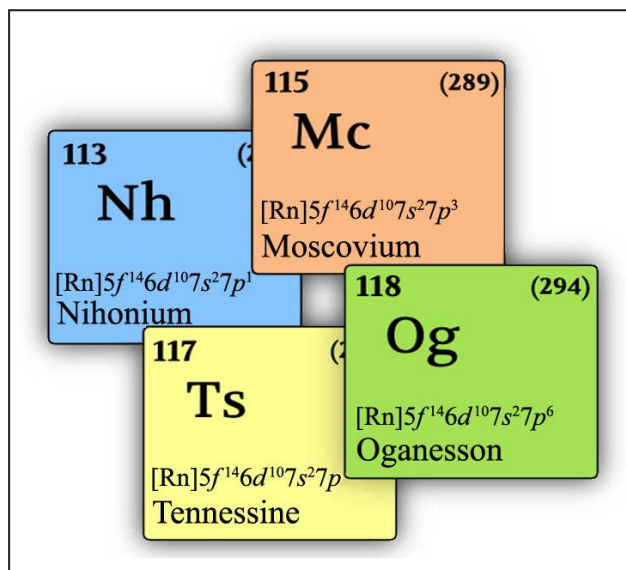
Quantum chemical modelling of electronic structure of superheavy element compounds

Yu.A. Demidov, A.V. Zaitsevskii

Knowledge Transfer Division of NRC "Kurchatov Institute" – PNPI

The discovery of long-lived isotopes of superheavy elements (SHEs) in nuclear fusion reactions of ^{48}Ca with actinide targets signifies a close approach to the island of particularly shell-stabilized nuclei. While the emergence of the new elements is a fantastic discovery itself, the longevity of certain isotopes is thought-provoking for chemical investigations, both experimental and theoretical. Successful chemical identification of copernicium (element 112, Cn) and flerovium (element 114, Fl) has been recently followed by the recognition of the discovery of nihonium (element 113, Nh) confirmed at the fourth IUPAC/IUPAP Joint Working Party. Although preliminary experimental results have been recently obtained in FLNR JINR (Dubna), the chemical properties of nihonium remain of top interest. From the theoretical standpoint, investigations of the SHE chemistry are especially challenging as they require an understanding of the electronic structure in the presence of strong fields of heavy nuclei and thus governed by relativistic effects.

Our research is focused on the quantum-chemical modeling of compounds containing atoms of heavy and superheavy elements (Fig.). To simulate the electronic structure of such systems, we combine accurate shape-consistent relativistic pseudopotentials (RPPs) and non-collinear two-component relativistic density functional theory (2c-RDFT). The exceptional feature of the RPP model consists in the replacement of the intricate problem of the relativistic interacting electron gas in the field of nuclei by a much simpler problem of the state of the formally non-relativistic electron gas in the external field, though at the expense of a rather complex structure of the latter. This replacement is accompanied by a sharp reduction of the number of variables (the wave functions



Элементы, включенные в таблицу Менделеева в 2016 г.

or electron densities depend only on the coordinates of the valence electrons) and elimination of the difficult to approximate oscillations of the wave function in the vicinity of the atomic nuclei. This model also accounts for a finite nuclear size, incorporates quantum electrodynamic effects (including the bulk of Breit interactions), and enables explicit correlation of both valence and subvalence electrons, thus providing a good foundation for attaining an optimal accuracy/cost ratio in the cases of large and strongly interfering relativistic and correlation effects characteristic for the SHE compounds.

Gas thermochromatography on gold is a unique method of chemical detection of SHEs. The corresponding experiments, however, are extremely sophisticated and expensive and produce very scarce data on the chemical properties of SHEs. Moreover, the correct and detailed interpretation of the available experimental data cannot be

performed without preliminary theoretical modeling. The main effort of our research is focused on the description of the SHEs atoms adsorption on a gold surface from first principles – a key component for quantitative theoretical predictions. The adsorption energies of SHEs on a gold surface are estimated using the cluster model. Monitoring charge distributions in the vicinity of the adsorption site and taking into account the effects of relaxation of the cluster surface are essential to maintain its reliability. As an important result of such modeling, we recommend new estimates of the elements 113 and 120 adsorption energies on gold – 110 and 250 kJ/mol, respectively.

Strong relativistic effects suggest dramatic dissimilarities in the chemical behavior of SHEs and their formal lighter homologues. The experimentally measured desorption enthalpy of single atoms of nihonium from a gold surface substantially differs from that of such nearest homologue – thallium. This casts doubt on the usefulness of the experiments with Nh formal homologues for understanding its chemistry. Despite manifest deviations of the chemical properties of the SHEs from the trends observed in their lighter formal homologues in the respective groups of the periodic table, finding chemical pseudo-homologues appears a practically meaningful issue. Further development of the SHE chemical identification techniques may benefit from having a broader view of their chemical properties. A part of our research is focused on systematic relativistic calculations of the molecular structures and energetics of presumably stable binary compounds of SHEs with the most common light elements. The results for SHEs, along with the similar data for their lighter

homologues, are visualized using the “chemical graphs” which reflect the main trends in gas-phase chemical properties of the elements in a given group of the periodic table and demonstrate the specificity of SHEs. It has been shown experimentally that the desorption temperatures and energies of Cn and Fl atoms from a gold surface are close to each other and lower than those for their immediate homologues – Hg and Pb, respectively. This confirms theoretical predictions concerning the electronic structure of Cn and Fl atoms: strong relativistic stabilization of s and $p_{1/2}$ shells in both Cn ($6d^{10}7s^2$) and Fl ($6d^{10}7s^27p_{1/2}^2$) results in a closed-shell character of the ground states of these atoms. Due to this unique feature of the 7th row of the periodic table, the electronic structure of a Nh atom can be interpreted as a hole in the closed $7p$ subshell of a Fl atom. This observation allows us to view astatine as a pseudo-homologue of Nh. Similarities in the chemical behavior of Nh and At in reactions with strong oxidizers are discussed in a comparative study of their hydroxide molecules. The resulting energy of the hydroxyl group elimination at 0 K is found to be 188 kJ/mol for NhOH, and the corresponding values for TlOH and AtOH are 319 kJ/mol and 174 kJ/mol, respectively. These estimates reveal At as a closer chemical “relative” of Nh than the formal homologue At and suggest At as a plausible lighter candidate in a search of the optimal experimental conditions for further explorations of the Nh chemistry. The presented results are crucial both for the detailed interpretation of the available experimental data and planning future benchmark experiments in superheavy element chemistry.

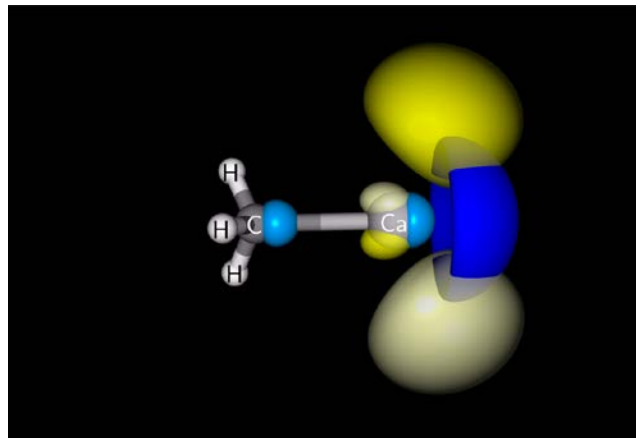
Laser cooling and high-precision spectroscopy of radium compounds for “new physics” search

T.A. Isaev

Neutron Research Division of NRC “Kurchatov Institute” – PNPI

Recently the method of molecular doppler cooling (MDC) has gained considerable popularity. Trapping the molecules in magneto-optical traps with the help of such a method allows to reach the unprecedented level of control over trapped molecules. It is very likely to lead to considerable progress in the investigations of effects outside of Standard Model, search for axionic-like dark matter, etc. The molecules with highly diagonal Frank–Condon matrix for a transition between the working levels (typically the ground and the first excited electronic states) are required for an efficient realization of the MCD scheme. As we displayed in 2010 the number of candidate molecules is very high, and in 2016 we demonstrated the existence of the highly-closed cooling loops also in polyatomic molecules. The heavy-atom compounds present considerable interest for the search for permanent electric dipole moments (EDMs) of elementary particles (like neutron, proton and electron) due to strong dependence of the EDM enhancement in molecules on the nuclear charge. In [3] we have

considered the triatomic molecule of radium monohydroxyl (RaOH) as a candidate molecule for search of the effects of nuclear spin-dependent space-parity non-conservation on laser-coolable molecules.



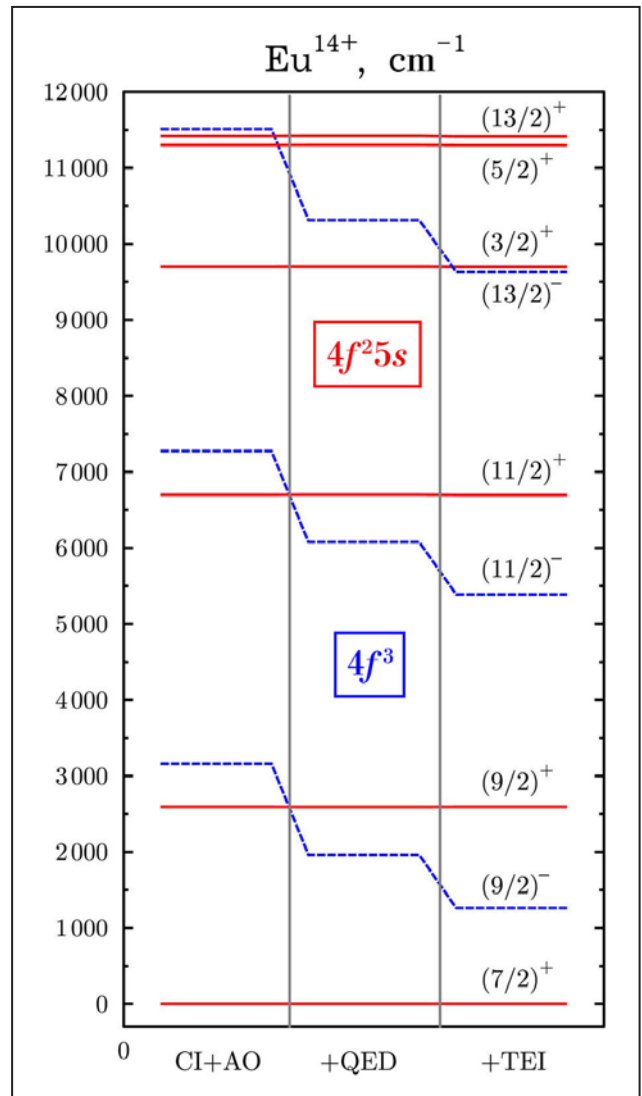
The isosurfaces of the valence electron wavefunction in the ground (blue) and first excited (yellow) electronic states are provided as a typical example of the electronic structure of laser-coolable molecules for CaCH_3 . One can see that the main part of the electronic density in both cases is shifted away from the bonding region, which indicates the non-bonding character of the valence electron

1. Isaev T.A. et al. // Phys. Rev. Lett. 2016. V. 116. P. 063006.
2. Isaev T.A., Zaitsevskii A.V. et al. 2016. arXiv:1610.08243.

Search for new physics with atoms and molecules

M.G. Kozlov – Neutron Research Division
S.G. Porsev – Theoretical Physics Division
NRC “Kurchatov Institute” – PNPI

Experimental techniques in atomic physics are developing rapidly. On the one hand, it leads to an increase of sensitivity of atomic experiments to “new physics” beyond Standard Model. On the other hand, new systems, such as ultra-cold highly charged ions and molecules are now being used for precision experiments. Atomic theory is necessary to find the most perspective systems and calculate the contribution of new physics to the spectra of atoms and molecules. We developed a computer package to calculate atomic properties taking into account electron correlations and relativistic effects. In 2016, we added new programs to this package to account for quantum electrodynamics (QED) corrections and effective three-electron interactions (TEI). Both types of corrections are important, for example, for highly charged ions with filling $4f$ shell. In particular, the ion Eu^{14+} is interesting for building a new optical clock and has high sensitivity to the variation of the fine-structure constant α . Therefore, it can be used to search for α -variation, which is predicted by certain extensions of the Standard Model. The Figure demonstrates our results for the spectrum of Eu^{14+} ion. The left panel presents results of the calculation within Dirac-Coulomb-Breit approximation. In the central panel we include QED corrections, while TEI corrections are added in the right panel. One can see that these corrections not only affect transition frequencies, but also change the order of levels. Note that new methods for cooling and trapping of such ions are currently being developed for high precision experiments with them.



Results of the calculations of the spectrum of Eu^{14+}

1. Kozlov M.G., Porsev S.G. et al. // Comput. Phys. Commun. 2015. V. 195. P. 199.
2. Tupitsyn I.I., Kozlov M.G. et al. // Phys. Rev. Lett. 2016. V. 117. P. 253001.
3. Kozlov M.G. ..., Porsev S.G. et al. // Phys. Rev. A. 2016. V. 94. P. 032512.

Rainfall and hurricane propagation velocity

V.G. Gorshkov, A.M. Makarieva, A.V. Nefiodov
 Theoretical Physics Division of NRC “Kurchatov Institute” – PNPI

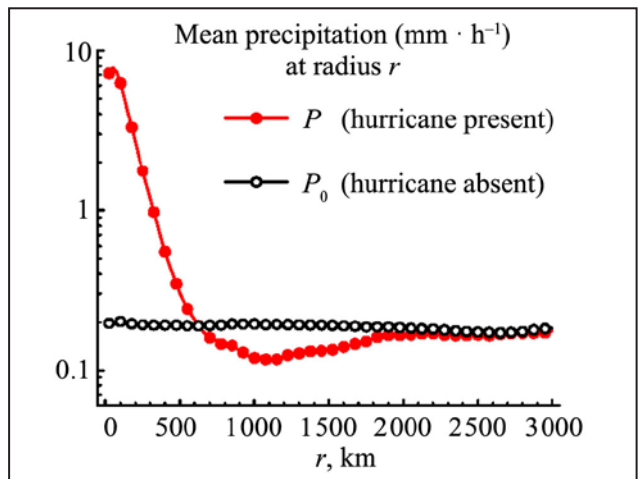
Despite the dangers associated with tropical cyclones and their rainfall, the origin of the moisture in these storms, which include destructive hurricanes and typhoons, remains surprisingly uncertain. Existing studies have focused on the region 40–400 km from the cyclone center. It is known that the rainfall within this area cannot be explained by local processes alone but requires imported moisture. Nonetheless, the dynamics of this imported moisture appears unknown.

Considering a region up to three thousand kilometers from the cyclone center, we have analyzed precipitation, atmospheric moisture and movement velocities for severe tropical cyclones – North Atlantic hurricanes. We use global atmospheric datasets monitoring rainfall (TRMM, Tropical Rainfall Measurement Mission) and atmospheric moisture (MERRA, NASA’s Modern-Era Retrospective Analysis for Research and Applications). Our findings indicate that even over such large areas a hurricane’s rainfall cannot be accounted for by concurrent evaporation. We propose instead that a hurricane consumes pre-existing atmospheric water vapor as it moves. The propagation velocity of the cyclone, i. e. the difference between its movement velocity and the mean velocity of the surrounding air (steering flow), determines the water vapor budget. Water vapor available to the hurricane through its movement makes the hurricane self-

sufficient at about 700 km from the hurricane center obviating the need to concentrate moisture from greater distances.

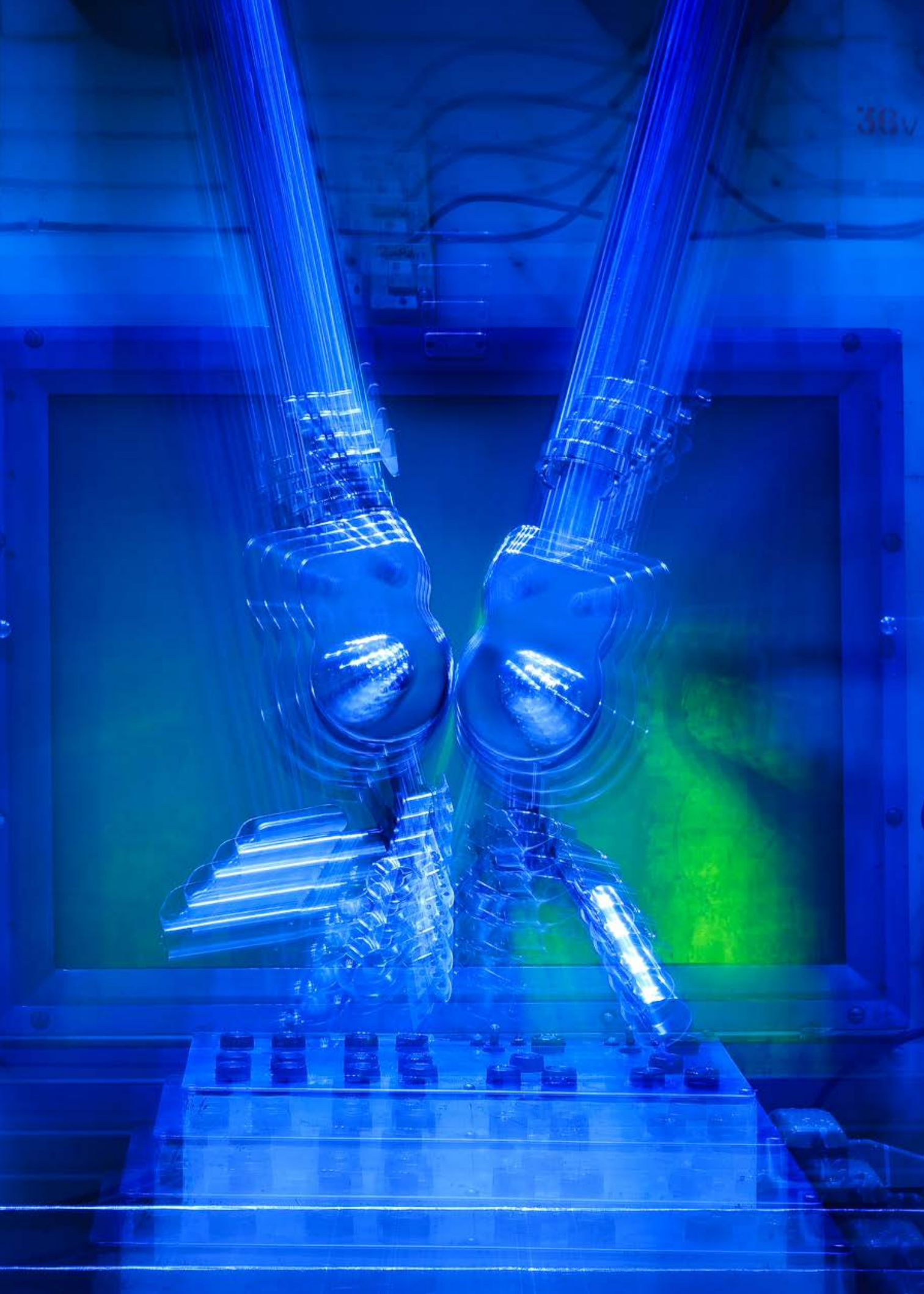
Such hurricanes leave a dry wake, whereby rainfall is suppressed by up to 40% compared to its long-term mean (see Fig). The inner radius of this dry footprint approximately coincides with the hurricane’s radius of water self-sufficiency.

We discuss how Carnot efficiency considerations do not constrain the power of such open systems. Our findings emphasize the incompletely understood role and importance of atmospheric moisture stocks and dynamics in the behavior of severe tropical cyclones.



Hurricane’s dry footprint: $P(r) < P_0(r)$, $r_d \approx 600$ km

1. Makarieva A.M., Gorshkov V.G., Nefiodov A.V. // Phys. Lett. A. 2015. V. 379. P. 2396–2398.
 2. Makarieva A.M., Gorshkov V.G., Nefiodov A.V. et al. // Atmos. Res. 2017. V. 193. P. 216–230.



Research Based on the Use of Neutrons, Photons and Muons

- 46 Neutron lifetime measurement with the big gravitational trap
- 48 Experiment Neutrino-4 search for sterile neutrino
- 50 Ultracold neutron source with superfluid helium at WWR-M reactor
- 52 Ultra-cold neutron detector for the spectrometer of the neutron lifetime measurement
- 53 Angular distributions and anisotropy of fission fragments of ^{233}U and ^{209}Bi induced by neutrons with the energy 1–200 MeV
- 54 Particular features of ternary fission induced by polarized neutrons in $^{233, 235}\text{U}$ and $^{239, 241}\text{Pu}$
- 56 Temporal characteristics of delayed neutrons from 1 GeV proton-induced fission of ^{238}U
- 57 Analysis of the resolution of an experiment for verification of the equivalence principle for the neutron by diffraction method
- 58 Effect of two-crystal focusing
- 59 Luminosity class of neutron reflectometers
- 60 Instrumental and radiochemical neutron activation analysis of the quartz adularia veins from the deposit Milogradovka
- 62 Spin structure of quasi- two-dimensional frustrated magnet $\text{Li}_3\text{Ni}_2\text{SbO}_6$ with a magnetic “honeycomb”-type lattice
- 63 Magnetic phase diagram of $\text{Y}_{1-x}\text{Tb}_x\text{Mn}_6\text{Sn}_6$ ($x = 0; 0.175; 0.2; 0.225; 0.25$) compounds
- 64 Multilevel structure of diamond hydrogels by neutron scattering
- 65 μSR study of $\text{Eu}_{0.8}\text{Ce}_{0.2}\text{Mn}_2\text{O}_5$ and EuMn_2O_5 multiferroics

Neutron lifetime measurement with the big gravitational trap

*M.E. Chaikovsky, A.V. Chechkin, A.K. Fomin, A.G. Kharitonov, E.A. Kolomensky,
I.A. Krasnoshekhova, A.O. Polyushkin, A.P. Serebrov, I.V. Shoka, V.E. Varlamov, A.V. Vasilev –
Neutron Research Division of NRC “Kurchatov Institute” – PNPI
P. Geltenbort, T. Jenke, O. Zimmer – Institute Laue-Langevin
M. van der Grinten, M. Tucker – Rutherford Appleton Laboratory*

The neutron lifetime measurement experiment falls within the domain of fundamental physics and aims to test the predictions of the Standard Model of elementary particles in the field of electro-weak interactions and models of nucleosynthesis in the early universe. At the moment, it is important to shed light on the problem of difference in neutron lifetime measured by the “beam” method and the neutron lifetime measured by the “storage” method.

In 2016, we carried out our experiment on the apparatus “Gravitrap-2”, located in the hall of the research reactor complex of Institute Laue-Langevin (ILL), Grenoble, France (Fig. 1). Two full reactor cycles (100 days in total) were allocated to carry out the experiment.

The experiment aims to measure the free neutron lifetime by storing ultracold neutrons (UCN) in a cryogenic material trap with the gravitational locking. The inner walls of the trap are covered with the polymer Fomblin Grease UT-18, having a low neutron capture cross section. UCN losses are strongly suppressed, if the trap is maintained at low temperature (80–100 K). UCN storage time without decay but due to losses on the walls equals $4 \cdot 10^4$ s. An additional surface (an insert), also polymer-coated, is positioned into the volume of the trap, thereby increasing the surface area inside the trap and hence increasing the frequency of neutron collisions with the surface. As a result, we measure two different UCN storage times (τ_1, τ_2) corresponding to two collision frequencies (γ_1, γ_2).

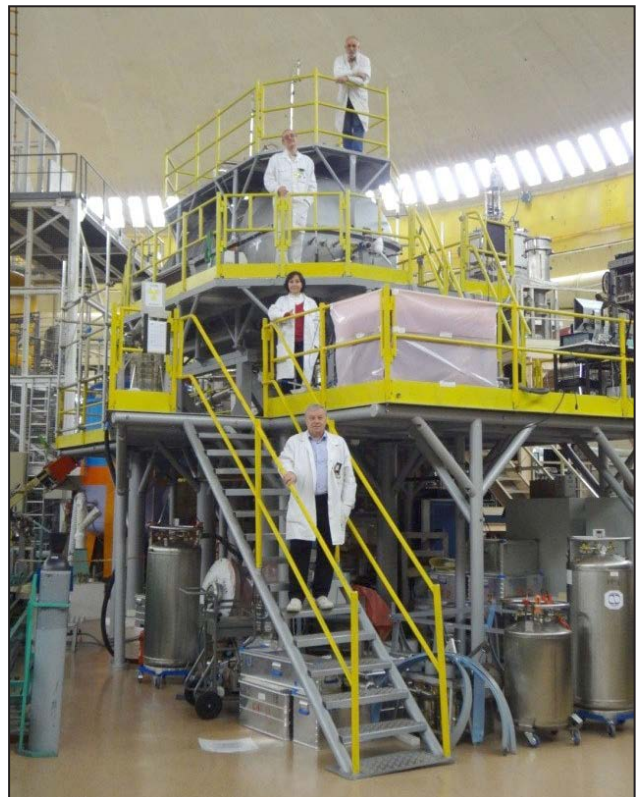


Fig. 1. Experimental apparatus of NRC “Kurchatov Institute” – PNPI for measuring neutron lifetime at reactor ILL (Grenoble, France)

The neutron lifetime is determined by extrapolation to an infinite trap with zero collision frequency. UCN loss probability for a single collision (η) is determined experimentally, but the frequency of collisions has to be calculated using Monte Carlo simulation. Results of measurements of the neutron lifetime obtained in reactor cycles 178 and 179 (2016) are shown in Fig. 2.

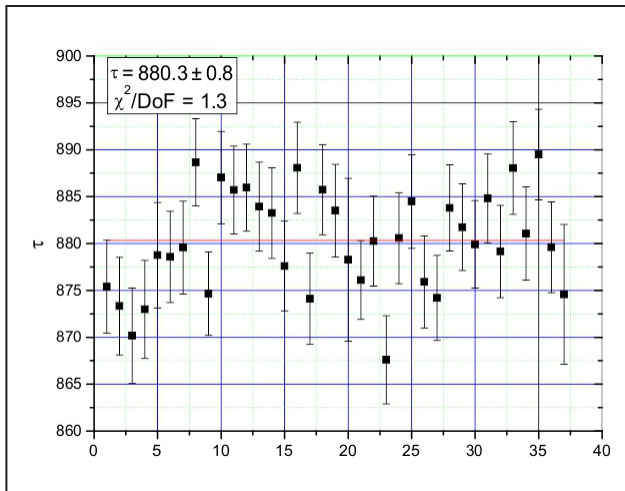


Fig 2. Neutron lifetime measured in cycles 178 and 179

The value of the neutron lifetime: $(880.3 \pm 0.8_{\text{stat}})$ s can be considered as the result of 2016. For the final result, a systematic error should be evaluated. We believe that there are two main sources of this error. The first source is associated with inequality of the uncoated surface of the trap and the insert.

The second one is related to the inaccuracy of the measurement of geometrical sizes of the trap and the insert.

We estimate the systematic error to be 0.8 s. However, our new measurement result of the neutron lifetime $(880.3 \pm 0.8_{\text{stat}} \pm 0.8_{\text{sys}})$ s differs from our result obtained in 2005 $(878.5 \pm 0.7_{\text{stat}} \pm 0.3_{\text{sys}})$ s by 1.8 s, so measurements should be continued and improved in accuracy.

Further improvement in accuracy is possible with experimental setup modifications, which will reduce the difference between the storage time with the insert and without the insert, i.e. when the storage time gets closer to the neutron lifetime. This is possible if we reduce the magnitude of losses in the collisions with the walls, for example, by the transition to temperature $\approx 10\text{K}$.

At the moment, the statistical error has been lowered to the size of the systematic error, and the result is in good agreement with the conventional neutron lifetime presented in the Particle Data Group review. The discrepancy between the results of our experiment and the “beam” experiment $(888.0 \pm 2.1 \text{ s})$ is greater than 3 standard deviations and for the further study of the source of this discrepancy, data obtained by the “beam” method need to be updated, i.e. the NIST experiment requires repetition (National Institute of Standards and Technology, USA).

Experiment Neutrino-4 search for sterile neutrino

*M.E. Chaikovskii, A.V. Chernyj, A.K. Fomin, V.G. Ivochkin, A.O. Polyushkin, R.M. Samoilo, A.P. Serebrov, M.E. Zaytsev, O.M. Zherebtsov, V.G. Zinoviev – Neutron Research Division
V.L. Golovtsov, P.V. Neustroev – High Energy Physics Division
NRC “Kurchatov Institute” – PNPI*

V.I. Aleshin, V.P. Martemyanov, V.G. Tarasenkov – NRC “Kurchatov Institute”

*V.V. Afanasiev, M.O. Gromov, A.L. Izhutov, A.L. Petelin, S.A. Sazontov, A.A. Tuzov – JSC “SSC RIAR”
D.K. Ryazanov, M.E. Zaytsev – Dimitrovgrad Engineering and Technological Institute
of NRNU MEPhI*

To search for neutrino oscillation in sterile state one has to observe the deviation of reactor anti-neutrino flux from $1/L^2$ law, there L is the distance from reactor core. If such a process exists, it can be described by the following oscillation equation:

$$P(\tilde{\nu}_e \rightarrow \tilde{\nu}_e) = 1 - \sin^2 2\theta_{14} \sin^2 \left(1.27 \frac{\Delta m_{14}^2 L}{E_{\tilde{\nu}}} \right),$$

where $E_{\tilde{\nu}}$ is antineutrino energy, eV; Δm_{14}^2 [eV] and $\sin^2 2\theta_{14}$ are the unknown oscillation parameters.

In order to carry out research in the field of possible existence of a sterile neutrino the laboratory based on SM-3 reactor (Dimitrovgrad, Russia) was created to search for oscillations of reactor anti-neutrino. Results of measurements of difference in counting rate of neutrino-like events for model and full-scale detectors are shown in Fig. 1 as dependence of antineutrino flux on distance from the reactor center.

Measurements of antineutrino flux from the reactor at small distances of 6–12 m by means of the moveable detector are carried out for the first time. In the frame of the available statistical accuracy it is not revealed if there are reliable deviations of antineutrino flux distance dependence from the law $1/L^2$. The results in the range 10–12 m require the measurements in this region to be repeated with more accuracy.

To combine our data with the measurement at longer distances, the analysis with the assump-

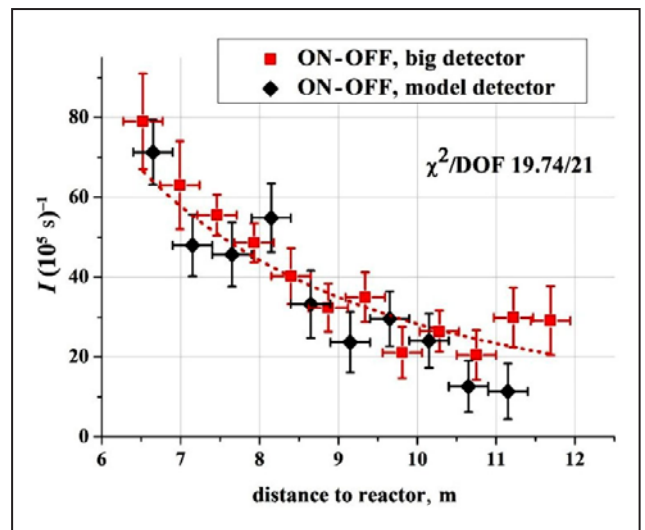


Fig. 1. Reactor antineutrino flux distance dependence for model and full-scale detectors, point graph is the fit for dependence $1/L^2$

tion of possible existence of a sterile neutrino is required, because some experiments at long distances show the deficiency of reactor antineutrino flux in comparison with the calculated flux. For this reason, at the end of the article we present results of our measurements in the range of 6–12 m from the center of an active core of the reactor together with results of widely known measurements up to 1000 m. Since the efficiency of antineutrino registration with our multi-sectional detector cannot be calculated with adequate accuracy, in our data we normalize the mean value to the standard ratio 0.936, i.e. to the ratio of the measured reactor antineutrino flux to the calculated flux. In our

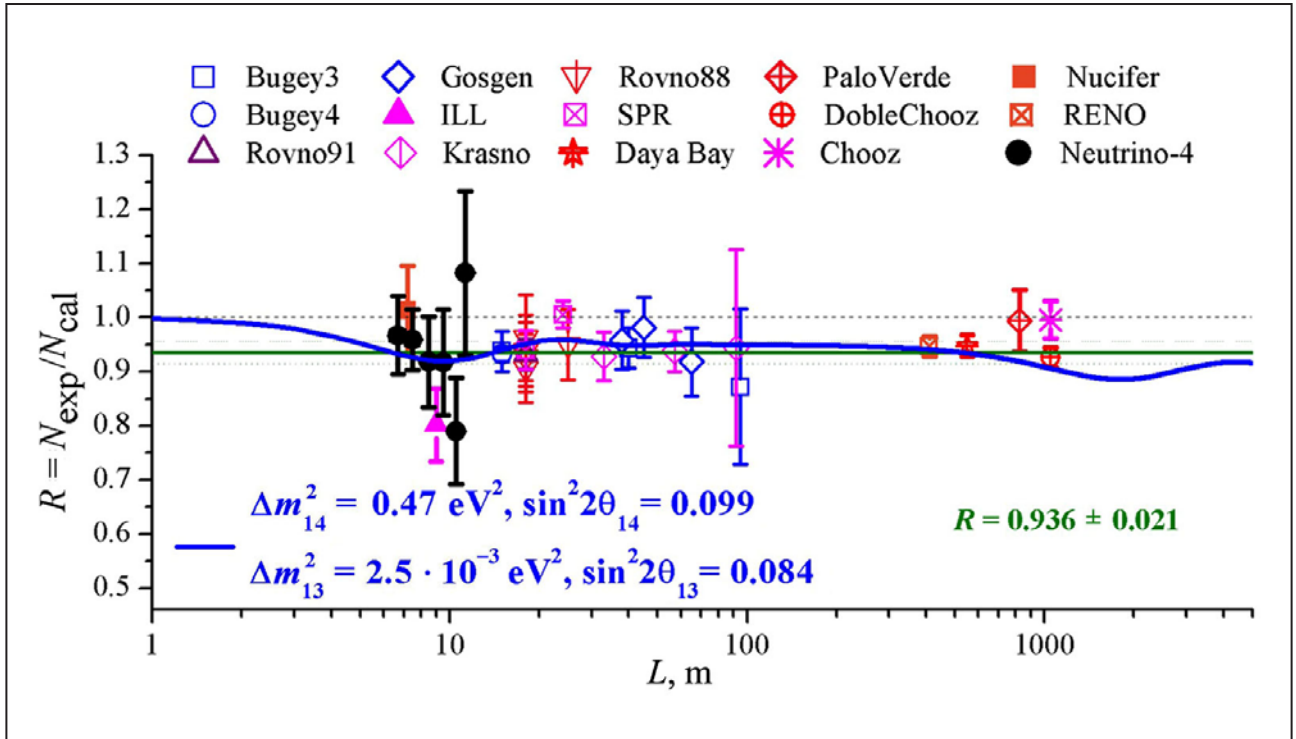


Fig. 2. The results of our measurements in distance range 6–12 m from the reactor core together with results obtained in well-known measurements up to 1 000 m and the curvature of oscillations with parameters $\Delta m_{14}^2 = 0.47 \text{ eV}^2$ and $\sin^2 2\theta_{14} = 0.099$, $\Delta m_{13}^2 = 0.0025 \text{ eV}^2$ and $\sin^2 2\theta_{13} = 0.084$

experiment with moveable detector we perform relative measurements in order to find deviations from $1/L^2$ law and distortions of spectrum form due to oscillations into sterile state. Unfortunately, current statistical accuracy of our measurements is not sufficient to observe the assumed processes with high precision. In order to further improve precision of the experiment we need to continue measurements to obtain better statistical accuracy and also use additional methods of background suppression. However, at the moment, we can provide the analysis of parameters for one sterile neutrino model using data presented in Fig. 2.

In conclusion, we should point out that at the moment it would be premature to present the re-

sults of this analysis as an observation of a sterile neutrino with parameters $\Delta m_{14}^2 = 0.47 \text{ eV}^2$ and $\sin^2 2\theta_{14} = 0.099$. Measurements with higher statistical accuracy in distances up to 15 m from the reactor core are required. Measurements at 15 m distance will allow us to compare our results of relative measurements with the results obtained at 15 m with absolute measurements of neutrino flux method.

Finally, one should take into consideration that the problem of a reactor antineutrino is associated with calculations of antineutrino flux from the reactor. However, the reliability and accuracy of these calculations are not guaranteed yet.

Ultracold neutron source with superfluid helium at WWR-M reactor

*A.K. Fomin, A.S. Kanin, V.A. Lyamkin, D.V. Prudnikov, O.Yu. Samodurov, A.P. Serebrov
Neutron Research Division of NRC “Kurchatov Institute” – PNPI*

Reactor WWR-M at NRC “Kurchatov Institute” – PNPI is going to be equipped with a high density ultracold neutron (UCN) source. The method of obtaining UCN is based on the accumulation of UCN in superfluid helium due to the peculiarities of this quantum liquid. The aim is to achieve the UCN density of 10^4 cm^{-3} in the experimental trap, which is two orders of magnitude greater than the density in existing UCN sources worldwide. Increasing the UCN density will lead to one order of magnitude improvement in the accuracy of measurement of the neutron electric dipole moment, which is extremely important for solving the problem of *CP*-violation. The source with the highest UCN density will allow NRC “Kurchatov Institute” – PNPI to become a center of fundamental research with ultracold neutrons.

Successful tests at a full-scale UCNS model showed the capability of keeping the helium in the superfluid state with the incoming heat load of 60 W (the calculated heat load is expected to be 20 W). After the tests, the designing of the technological complex in the reactor hall of WWR-M reactor has been started. By now, the project of placing the vacuum and cryogenic equipment in the reactor hall of the WWR-M reactor is completed (Fig. 1).

We already have all technological equipment shown in Fig. 1. However, cryogenic equipment (refrigerator and liquefier) and helium vacuum pumping system are located in the compressor room (right side of the figure) for performing tests at a full-scale model of the UCN source. To implement the project, the following problems have to be handled: 1) moving and assembling the cryoge-

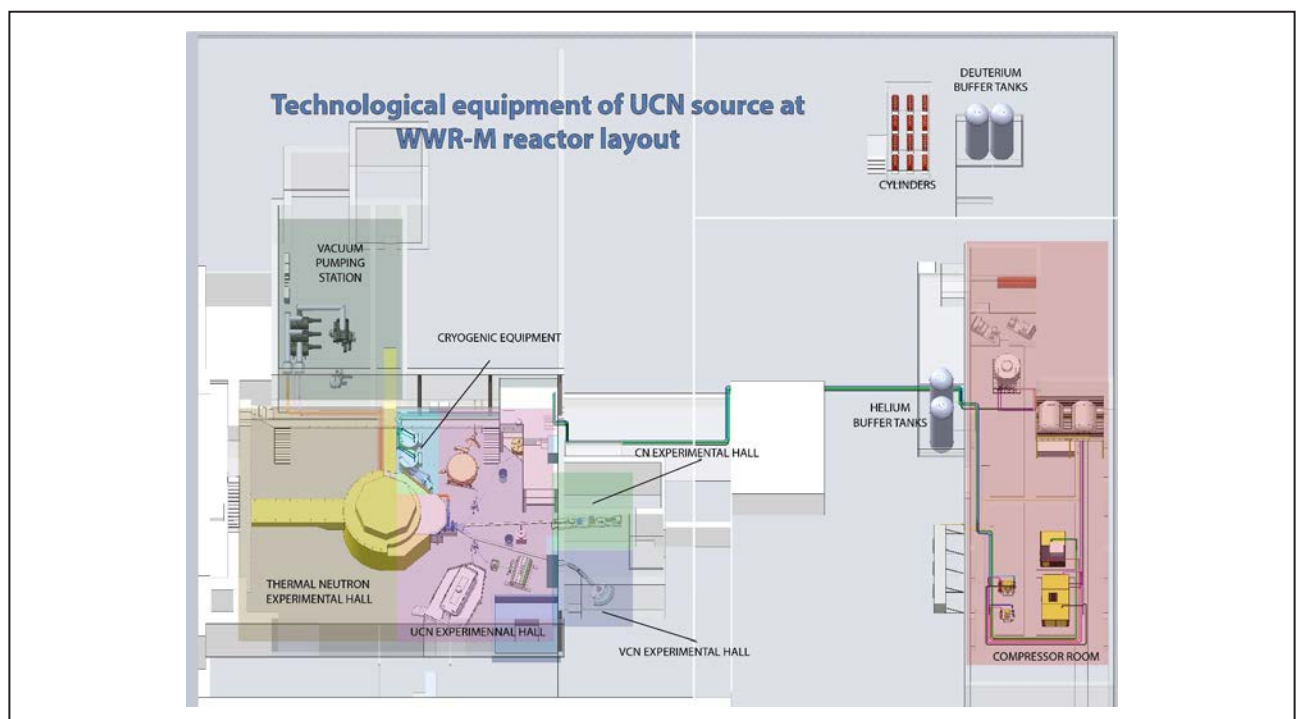


Fig. 1. Technological equipment of UCN source at WWR-M reactor layout

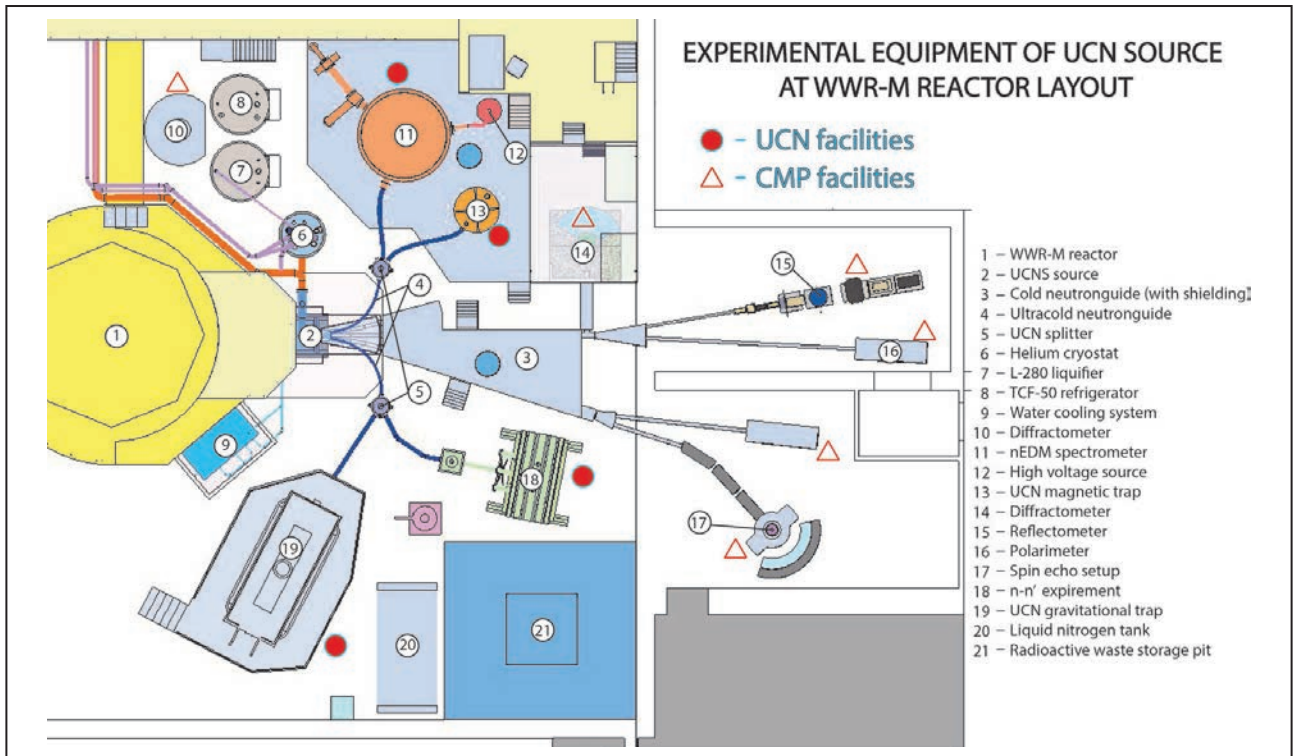


Fig. 2. Experimental equipment of UCN source at WWR-M reactor layout: ● - physics of fundamental interactions research facilities; △ - condensed matter physics research facilities

nic equipment at the reactor hall of the WWR-M reactor; 2) moving and assembling the pumping equipment at a special vacuum section of the WWR-M building; 3) assembling communications between the individual elements of the overall system; 4) replacing deuterium steel receivers with stainless steel receivers. Finally, the most important task is the manufacturing of the intra-canal part of UCN source.

The preparation of the northern part of the WWR-M reactor hall has already started. The dismantling of platforms and experimental facilities around the thermal column of the reactor was completed. Manufacturing of the intra-canal part of UCN source is conducted at NRC “Kurchatov Institute” – PNPI workshop.

We have developed the experimental equipment layout plan, which is shown in Fig. 2.

All experimental setups shown in Fig. 2 are either available or in varying stages of completion.

In particular, the NRC “Kurchatov Institute” – PNPI setup of searching for the electric dipole moment of the neutron and the measurement of the neutron lifetime are now being tested at the Institute Laue-Langevin (ILL) reactor and will be returned to NRC “Kurchatov Institute” – PNPI when the high-intensity UCN source is launched. Finally, it should be noted that the neutron guide system for cold and very cold neutrons with the Ni^{58} isotope coating is also available, although it requires some modifications in the wiring bundle system. UCN neutron guide manufacturing technology based on high-quality mirror replicas of Ni^{58} isotope coating was developed and tested at the ILL reactor.

The work was carried out at Konstantinov Petersburg Nuclear Physics Institute of National Research Center “Kurchatov Institute” and supported by the Russian Science Foundation (RSF) (Project No. 14-22-00105).

Ultra-cold neutron detector for the spectrometer of the neutron lifetime measurement

V.A. Andreev, D.S. Ilyin, E.A. Ivanov, A.G. Krivshich – High Energy Physics Division
A.P. Serebrov, A.V. Vasiliev – Neutron Research Division
NRC “Kurchatov Institute” – PNPI

A gas-discharge detector has been designed for a spectrometer measuring the neutron lifetime by storing ultracold neutrons (UCN) in a large gravitation trap. It counts the number of UCN in spectrometric measurements taken at the reactor at Institute Laue-Langevin (ILL, Grenoble, France).

The detector consists of six independent proportional counters. Anodes are gold-plated tungsten wires with the diameter of 25 μm . The lengths of the counters are optimized to cover the maximum detection area (see Fig.). The entrance window with the diameter of 290 mm is made of thin aluminum foil with the thickness 100 μm . The force acting on the foil at working conditions is about 660 kg. To support foil from the neutron guide side (vacuum), the special stainless-steel grid has been placed in front of it.

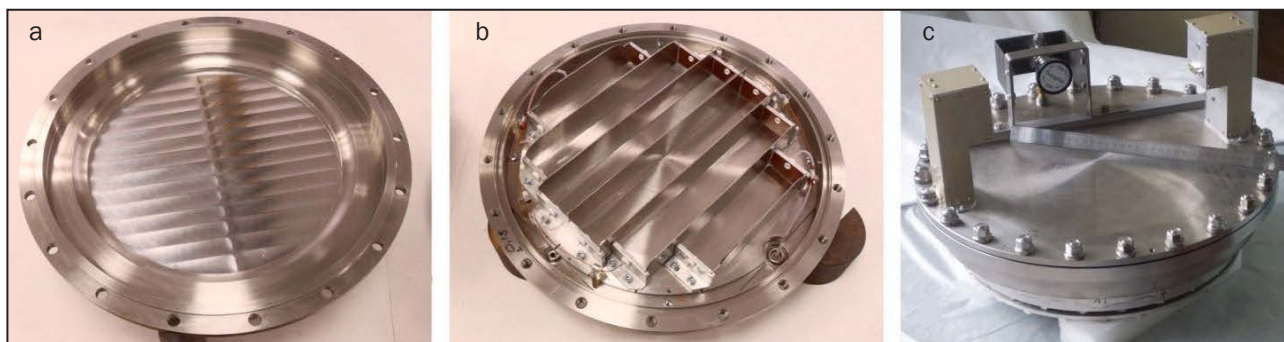
The electric field structure in each proportional counter was optimized to be nearly symmetric, thereby decreasing the maximal collection time of

ions created in a gas avalanche by more than eight times and minimizing the cross-talk between neighboring cells caused by a single proton-triton track due to the nuclear reaction ${}^3\text{He}(n, p)T$.

It has been shown that when processing the energy spectra of UCN, one should take into account the “wall” effect, as a result of which some useful events may fall into the range of small amplitudes and the observed energy spectrum becomes distorted. The “wall” effect is a key factor for ensuring the effective suppression of background and for providing maximum UCN detection efficiency.

The UCN detector has been tested in a laboratory of NRC “Kurchatov Institute” – PNPI and installed at a neutron lifetime measurement instrument at the reactor of Institute Laue-Langevin (ILL).

The work was performed with the support of the Russian Science Foundation, project No. 14-22-00105.



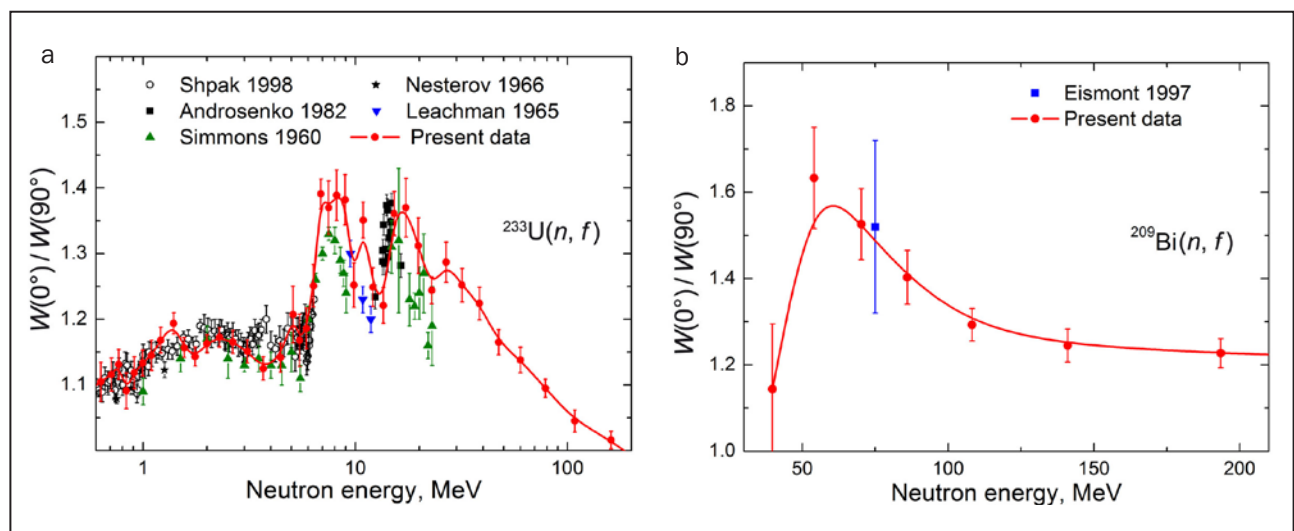
UCN detector parts: the upper part of the detector with entrance window. A relief on the foil support grid is visible after the application of pressure (a); the bottom part of the detector with a six proportional counters (b); assembled UCN detector is shown from back side. One can see two preamplifiers and gas valve (c)

Angular distributions and anisotropy of fission fragments of ^{233}U and ^{209}Bi induced by neutrons with the energy 1–200 MeV

A.S. Vorobyev, A.M. Gagarski, O.A. Shcherbakov – Neutron Research Division
 L.A. Vaishnene – High Energy Physics Division
 NRC “Kurchatov Institute” – PNPI
 A.L. Barabanov – NRC “Kurchatov Institute”

In 2016, the measurements of the angular distributions $W(\theta)$ of fission fragments of ^{233}U and ^{209}Bi induced by neutrons with the energy of 1–200 MeV were completed at the neutron time-of-flight spectrometer GNEIS (Fig.). From the experimental data obtained by means of the position-sensitive multiwire counters used as fission fragments, the value of anisotropy $W(0^\circ)/W(90^\circ)$ was estimated. This value is a parameter used for theoretical description of the fission fragment angular distributions. The uniqueness of the obtained results consists in the fact that there is practically no other experimental data available for ^{233}U – in the neutron energy range above 20 MeV, and for ^{209}Bi – in the whole investigated energy range.

The complexity of measurements for ^{209}Bi nucleus is caused by a very small value of the fission reaction cross section, from a few mb near the reaction threshold (~ 40 MeV) to ~ 70 mb at 200 MeV, which is 1-2 orders of magnitude lower than the fission cross sections of actinide nuclei. The high intensity of the neutron source of the GNEIS spectrometer in the intermediate energy range above 10 MeV allows handling the problem of measuring the fission reaction product characteristics at the value of fission cross section 1–100 mb. Lead is the next object of our research. There is no data on its anisotropy of fission fragments in intermediate neutron energy range.



Anisotropy of fission fragments for ^{233}U and ^{209}Bi by neutrons with the energy 1–200 MeV (см. русский сборник)

1. Vorobyev A.S., Gagarski A.M., Shcherbakov O.A., Vaishnene L.A. et al. // Book of Abstracts of the XXIV Int. Seminar on Interaction of Neutrons with Nuclei. JINR. 2015. P. 84.
2. Vorobyev A.S., Gagarski A.M., Shcherbakov O.A., Vaishnene L.A. et al. // JETP Lett. 2016. V. 104. Iss. 6. P. 365.

Particular features of ternary fission induced by polarized neutrons in $^{233, 235}\text{U}$ and $^{239, 241}\text{Pu}$

A.M. Gagarski, I.S. Guseva, G.A. Petrov, T.A. Zavarukhina –
 Neutron Research Division of NRC “Kurchatov Institute” – PNPI
 Yu.N. Kopatch – Joint Institute for Nuclear Research
 T.E. Kuzmina, G.P. Tiourine – Khlopin Radium Institute
 F. Gönnerwein, P. Jesinger – Physikalisches Institut, Universität Tübingen
 E. Lelièvre-Berna, V. Nesvizhevsky, T. Soldner – Institut Laue-Langevin
 M. Mutterer – Institut für Kernphysik, Technische Universität Darmstadt
 W.H. Trzaska – Department of Physics, University of Jyväskylä

Light charged particles (LCP) in nuclear ternary fission are mainly emitted at the rupture moment from the neck region between two fission fragments. Coulomb forces focus their angular distribution, therefore the most probable emission angle of α -particles, which comprise more than 90% of all LCPs yield, is equal to $\sim 82^\circ$ relative to momentum of the light fission fragment \mathbf{p}_{LF} .

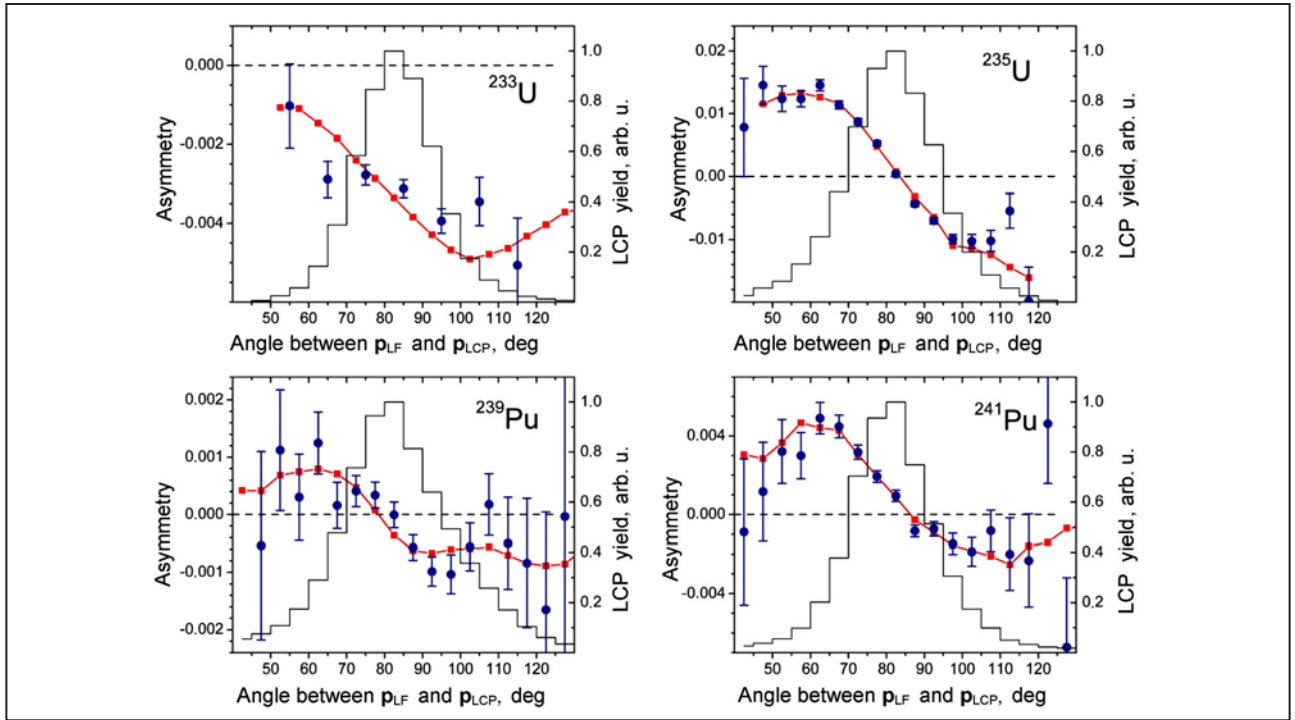
It was discovered that in ternary fission induced by polarized neutrons, the symmetry of LCP angular distribution around the fission axis appeared to be violated. Small shift of the LCP angular distribution ($\sim 0.1^\circ$) relative to the fission axis occurs while flipping the neutron spin σ_n , which is directed perpendicular to the momentum of light fission fragment \mathbf{p}_{LF} and LCP momentum \mathbf{p}_{LCP} (ROT effect). Besides this, the total probabilities of the LCP ejection upward and downward relative to the oriented plane defined by the light fission fragment momentum \mathbf{p}_{LF} and the neutron spin σ_n differ by $\sim 0.1\%$ (TRI effect).

These small effects were investigated by measuring of the angular dependence of asymmetry coefficient (A) in fission fragments – LCP coincidence count rates ($N_{\uparrow\downarrow}$) with periodic flipping of the neutron spin: $A = (N_{\uparrow} - N_{\downarrow}) / (N_{\uparrow} + N_{\downarrow})$. It is easy to understand that “pure” ROT effect yields the change of A sign from the left to the right relative to maximum of the angular distribution, while TRI effect gives constant asymmetry A over all range of the angular distribution.

Detailed studies of these effects for fission of $^{233, 235}\text{U}$ and $^{239, 241}\text{Pu}$ revealed that ROT and TRI effects are present simultaneously in all these

reactions, but their magnitudes and signs vary greatly. Experimental dependences of the asymmetry coefficient A on the angle between \mathbf{p}_{LCP} and \mathbf{p}_{LF} are shown in the Figure together with the result of their fitting by sum of expressions for TRI and ROT effects. The experimental values of the ROT shift between two opposite spin directions – 2Δ and the TRI asymmetry coefficient – D , obtained as a result of minimization of χ^2 are shown in the table for all studied nuclei.

In a proposed semiclassical model the TRI and ROT effects are explained by collective rotation and transversal vibrations of the fissioning nucleus before rupture. These motions are determined by the quantum numbers of the transition states above the fission barrier (J, K) (spin of the compound nucleus and its projection on the fission axis). ROT effect arises when LCP is moving in a rotating electric field of two fission fragments flying apart after scission, and the effect is an indicator of the nucleus rotation speed at the moment of rupture. (The fission axis continues to turn after the rupture with a rapidly decreasing angular velocity, in accordance with the law of conservation of angular momentum.) TRI effect is a result of influence of the collective rotation of a fissioning nucleus before rupture onto transverse motion of emerging LCPs in the region of the fissioning nuclear neck (Coriolis force). The rotation leads to a deviation from axial symmetry of the forces acting on the nascent LCPs that causes the asymmetry of their ejection relative to the plane defined by σ_n and \mathbf{p}_{LF} .



Angular dependence of the asymmetry A for the four studied reactions. Blue dots are experimental ones. Red dots are description of the experimental data in the framework of proposed model of TRI and ROT effects. Histograms with scale to the right are experimental angular distributions of LCPs

Table. Experimental values of ROT shift parameter 2Δ , coefficient of TRI asymmetry D for four investigated nuclei and quantum numbers (J, K) of dominant transition states above fission barrier, obtained in joint evaluation of the experimental data in the framework of proposed model. (Explanation in the text.)

Nucleus	^{233}U	^{235}U	^{239}Pu	^{241}Pu
Spin-parity, I^π	$5/2^+$	$7/2^-$	$1/2^+$	$5/2^-$
ROT, 2Δ	$0.021(4)^\circ$	$0.215(5)^\circ$	$0.020(3)^\circ$	$0.047(4)^\circ$
TRI, $D \cdot 10^3$	$-3.90(12)$	$1.7(2)$	$-0.23(9)$	$1.30(15)$
σ_{f+}/σ_{f-}	1.27	1.76	0.48	0.64
(J_+, K_+)	(3.2)	(4.0)	(1.1)	(3.0)
(J_-, K_-)	(2.0)	(3.2)	(0.0)	(2.1)

By using this model with almost unambiguous choice of dominant (J, K) for transition states, we managed to describe together the experimental signs and values of TRI and ROT effects in each of the four studied nuclei. The high sensitivity of the effects to the values of (J, K) was shown. Quantum numbers (J_\pm, K_\pm) of dominant transition states over fission barrier obtained by concerted description of the experimental data in the framework of the proposed model are presented in the table. The “ \pm ” signs correspond to neutron

capture into compound nucleus states with spins $J_\pm = I \pm 1/2$, where I is a spin of mother nucleus. Ratios of fission cross sections by cold neutrons from the compound states with spins J_\pm σ_{f+}/σ_{f-} , which were used for the analysis are given in the table.

Thus, the study of TRI and ROT effects in angular distributions of products in polarized neutron induced ternary fission is a new method for spectroscopy of the transition states (J, K) near fission.

Temporal characteristics of delayed neutrons from 1 GeV proton-induced fission of ^{238}U

O.A. Shcherbakov, A.S. Vorobyev – Neutron Research Division

F.V. Moroz, L.A. Vaishnene – High Energy Physics Division

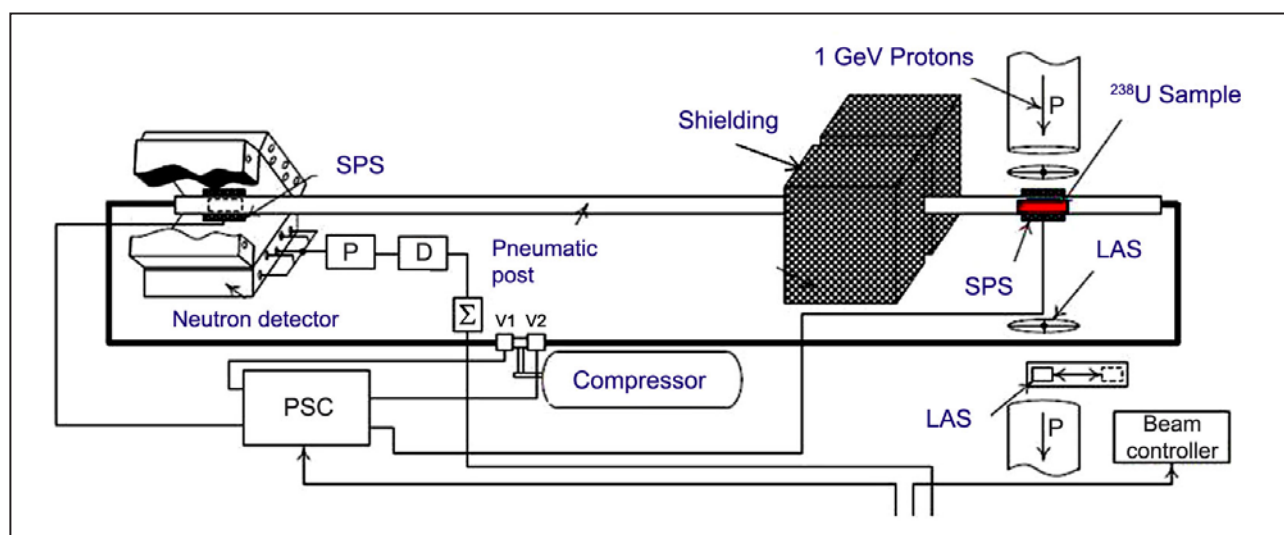
NRC “Kurchatov Institute” – PNPI

A.S. Egorov, D.E. Gremyachkin, K.V. Mitrofanov, V.F. Mitrofanov, V.M. Piksaikin, B.F. Samylin –

A.I. Leypunsky Institute for Physics and Power Engineering

The purpose of the present work is the measurement of relative yields of the delayed neutrons and half-lives of their precursor nuclei from an interaction of relativistic 1 GeV protons with ^{238}U . The experiment was carried out at the proton beam of the SC-1000 synchrocyclotron using the experimental set-up consisting of a neutron detector, a pneumatic “rabbit” (post) and an electronic measuring system. A comparison of the average half-life period $\langle T \rangle$ of the precursor nuclei emitting delayed neutrons in beta-decay chains measured in the present work with the results of other authors has shown that the data are consistent within experimental limits of error. It was also shown that the emitting of delayed neutrons in $^{238}\text{U}(n, f)$ -reaction took place in the asymmet-

ric fission channel, where the compound-nucleus $^{234}\text{U}^*$ is the main fissioning nucleus. At the same time, it was shown that the value of average half-life of the delayed neutron precursor nuclei measured in the present work ($\langle T \rangle = 7.13 \pm 0.12$ s) differs significantly from the value of $\langle T \rangle = 12.38 \pm 0.37$ s obtained from the low-energy fission of ^{233}U by fast neutrons, in spite of the fact that in both these cases the fissioning compound nucleus is the same. An explanation of such a discrepancy, as well as the measurements with ^{232}Th , ^{235}U and Pb nuclei is a purpose of further studies, which are planned at 1 GeV proton synchrocyclotron of NRC “Kurchatov Institute” – PNPI (Fig.).



Scheme of the experimental setup: SPS – sample position sensors; LAS – laser adjustment system; PSC – pneumatic system controller; P – preamplifier; D – discriminator; Σ – pulse sum; V1 and V2 – electromagnetic valves

1. Egorov A.S. ..., Vaishnene L.A., Moroz F.V., Vorobyev A.S., Shcherbakov O.A. // Probl. Atomic Sci. Technol. Ser.: Nucl. Reactor Const. 2016. Iss. 2. P. 5.
2. Egorov A.S. ..., Vaishnene L.A., Moroz F.V., Vorobyev A.S., Shcherbakov O.A. // Progr. Nucl. Energy. 2017. V. 97. P. 106.

Analysis of the resolution of an experiment for verification of the equivalence principle for the neutron by diffraction method

Yu.P. Braginets, V.V. Fedorov, I.A. Kuznetsov, M.V. Lasitsa, S.Yu. Semenikhin, V.V. Voronin – Neutron Research Division of NRC “Kurchatov Institute” – PNPI
 Ya.A. Berdnikov, A.Ya. Berdnikov – Peter the Great Saint Petersburg Polytechnic University

Currently we are preparing an experiment to verify the equivalence of inertial and gravitational mass of a neutron by a new method based on the use of effects arising from neutron diffraction in large perfect crystals. The main feature of the proposed method is the direct compensation of the gravitational force acting on the neutron, the inertia force acting on the neutron in a non-inertial coordinate system connected with the Earth. Essentially, the experiment is analogous to the classical experiments of Eotvos or Braginskii. During 2016 the study of the experiment spatial resolution for Bragg angles $74-82^\circ$ was carried out. A decrease in the spatial resolution at Bragg angles more than 78° was observed. The scheme of the experiment is shown in Fig. 1.

The experimental results are shown in Fig. 2, 3. It is evident that increasing Bragg angle leads to a decrease in contrast (Fig. 3). The research will

be continued at the ILL reactor (Grenoble, France) to answer the question about the reasons for reducing the contrast.

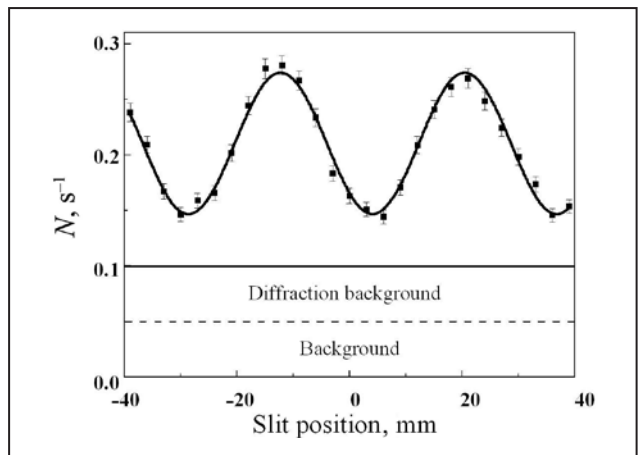


Fig. 2. Dependence of the intensity on the position of the output slit for the angle of diffraction 76°

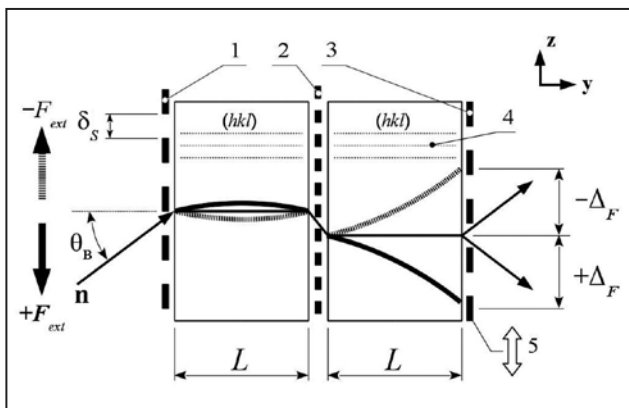


Fig. 1. Experimental setup: 1, 2, 3 – the input, intermediate and output slits, respectively; 4 – the crystallographic plane; 5 – the direction in which the output slit (3) is moving

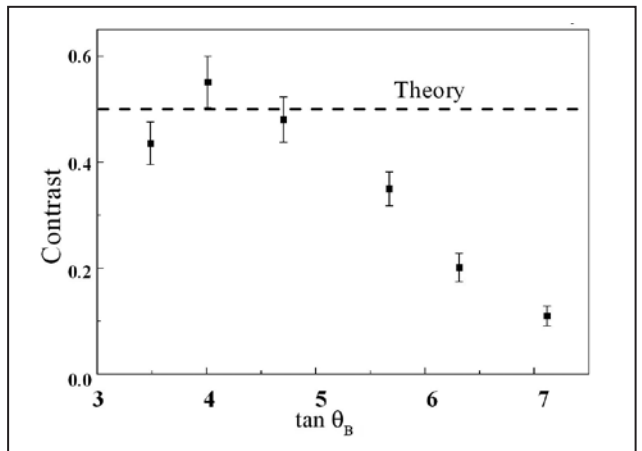


Fig. 3. The dependence of the contrast (see. Fig. 2) on the diffraction angle

Effect of two-crystal focusing

Yu.V. Borisov, Yu.P. Braginets, V.V. Fedorov, I.A. Kuznetsov, M.V. Lasitsa, S.Yu. Semenikhin, V.V. Voronin – Neutron Research Division of NRC “Kurchatov Institute” – PNPI
A.Ya. Berdnikov, Ya.A. Berdnikov, M.L. Ivanova – Peter the Great Saint Petersburg Polytechnic University

The effect of two-crystal focusing of neutrons for Laue diffraction by the large perfect silicon crystals has been studied. The experiment was performed with the thermal neutron beam from the WWR-M reactor (NRC “Kurchatov Institute” – PNPI, Gatchina, Russia). We analyzed Laue diffraction by two $110 \times 110 \times 100 \text{ mm}^3$ silicon crystals with the (220) reflection planes. The layout of the experiment is shown in Fig. 1. Crystals were made by cutting a slit in the whole single crystal. Thus, the distance between the crystals was fixed and could not be changed. As a result, two focus spots (lines) from the direct and reflected beams propagating between crystals appear on the exit surface of the second crystal (Fig. 2).

A combination of two-crystal focusing with a well-known diffraction enhancement effect (when a small change in the direction of the incident beam results in a significant deviation of the neutron trajectory inside the crystal that leads to the

shift of a neutron beam position at the exit face of the crystal) allows proposing a new ultra-precision neutron-spectrometry method to study the fundamental neutron properties and its interaction with the matter.

The linewidth shown in Fig. 2 corresponds to the angular deviation of the neutron beam between the crystals about $1.5 \cdot 10^{-7} = 0.03''$ that allows, for instance, reaching the sensitivity to neutron electric charge about $1,5 \cdot 10^{-21} e$ for the beam flux of the PIK reactor under construction in Gatchina, Russia.

A further improvement of the sensitivity by approximately two orders of magnitude is possible because the inherent spatial resolution of such a scheme of the experiment is much higher than the measured value. To analyze the experimentally achievable sensitivity of the method, more detailed experimental studies using high flux cold neutron beams are necessary.

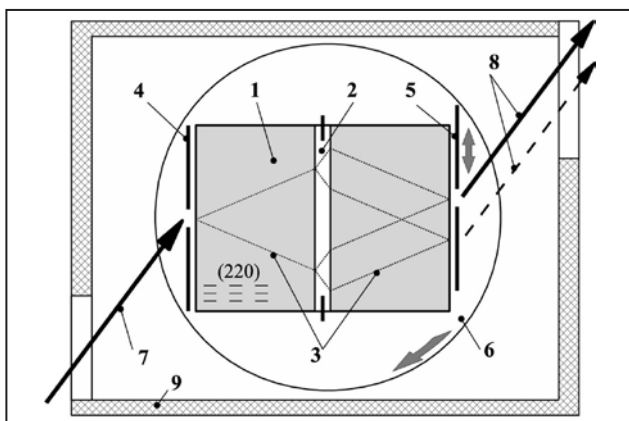


Fig. 1. Scheme of the experiment

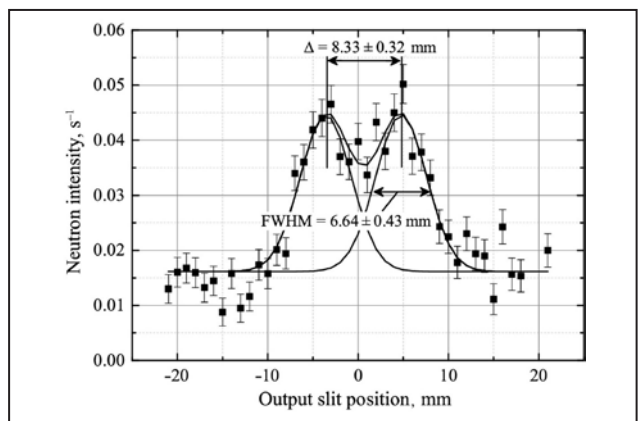


Fig. 2. Neutron beam intensity distribution along the exit face of the second crystal

1. Voronin V.V. ..., Borisov Yu.V., Braginets Yu.P., Kuznetsov I.A., Lasitsa M.V., Semenikhin S.Yu., Fedorov V.V. et al. // JETP Lett. 2015. V. 102. Iss. 7. P. 417–420.
2. Kuznetsov I.A. ..., Borisov Yu.V., Braginets Yu.P., Fedorov V.V., Lasitsa M.V., Semenikhin S.Yu. ..., Voronin V.V. // J. Phys.: Conf. Ser. 2016. V. 746. P. 012049.

Luminosity class of neutron reflectometers

N.K. Pleshanov

Neutron Research Division of NRC “Kurchatov Institute” – PNPI

The relationship between resolution and intensity in neutron reflectometry has been considered in the greatest detail. The issue is vital both for optimization of measurements at any neutron reflectometer and for designing neutron reflectometers. The luminosity \mathcal{L} was defined as the neutron flux incident onto the sample surface for the measurements made with a given momentum transfer q_0 and a resolution Δq_0 , i.e., for the first time it was coupled with the resolution in the momentum transfer. Thus, similar expressions have been obtained for the flux of monochromatic and white beams. Namely, in measurements with a monochromatic beam with q and Δq the flux:

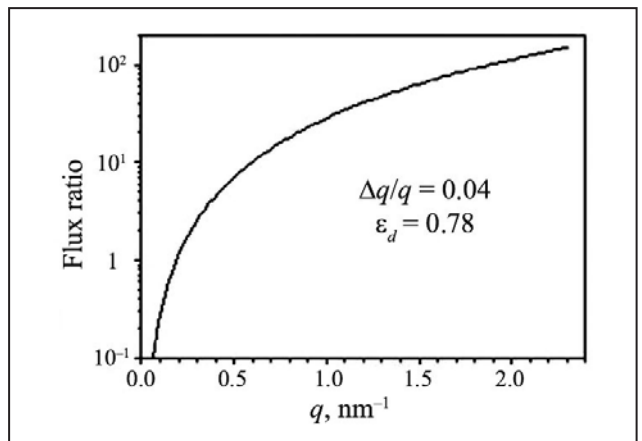
$$\Phi = \varepsilon_g \varepsilon_d \frac{q_0}{q} \left(\frac{\Delta q}{\Delta q_0} \right)^3 \mathcal{L},$$

where $\varepsilon_g = 2(d_1/d_2 + d_2/d_1)^{-1}$ is the factor that defines the flux decrease when the widths of the first and the second collimation diaphragms deviate from the optimum relation $d_1 = d_2$ (for a given divergence $\Delta\theta$); $\varepsilon_d = (3\sqrt{3}/2)\kappa(1 + \kappa^2)^{-3/2}$ is the factor that defines the flux decrease when the ratio $\kappa = (\Delta\lambda/\lambda)(\Delta\theta/\theta)^{-1}$ deviates from its optimum value with $\Delta\theta/\theta = \sqrt{2}\Delta\lambda/\lambda$ for a given resolution Δq .

The formulas allow finding the intensities for different measurement conditions and serve as a good illustration of the suggested approach to the problem of relationship of intensity and resolution in neutron reflectometry. Defining the luminosity for unified parameters (suggested values are $q_0 = 1 \text{ nm}^{-1}$, $\Delta q_0 = 0.01 \text{ nm}^{-1}$), one obtains the reference luminosity, or the luminosity class $C_R = \log_{10} \mathcal{L}$. The luminosity class characterizes

(each operation mode of) the instrument by one number and can be used to classify operating reflectometers and optimize designed reflectometers.

The potential of the new approach has been demonstrated by applying it to the neutron reflectometer NR-4M (NRC “Kurchatov Institute” – PNPI). It has been shown that due to optimization of measurements with monochromatic beams, the fluxes increase up to two orders of magnitude at large q (Fig.) practically without worsening the resolution. Due to optimization of measurements with white beams, the fluxes increase up to an order of magnitude at large q , the resolution being even improved. The luminosity class of the reflectometer NR-4M was found for its four operation modes: 2.1 (monochromatic non-polarized beam), 1.9 (monochromatic polarized beam), 1.5 (white non-polarized beam), 1.1 (white polarized beam).



The ratio of the flux with diaphragms slit widths varying so that $\Delta q/q = 0.04$ and $\varepsilon_d = 0.78$ to the flux obtained with fixed slit widths 0.2 mm as a function of q

1. Pleshanov N.K. // J. Surf. Invest.: X-ray, Synchrotron Neutron Tech. 2016. No. 8. P. 20–32.
2. Pleshanov N.K. // Nucl. Instrum. Meth. A. 2016. V. 820. P. 146–155.
3. Pleshanov N.K. // Nucl. Instrum. Meth. A. 2016. V. 834. P. 197–204.

Instrumental and radiochemical neutron activation analysis of the quartz adularia veins from the deposit Milogradovka

A.I. Egorov, Yu.E. Loginov, I.A. Mitropolsky, I.S. Okunev, T.M. Tyukavina,
G.I. Shulyak, V.G. Zinovyev – Neutron Research Division
P.A. Sushkov – Department of Reactor Physics and Engineering
NRC “Kurchatov Institute” – PNPI

Instrumental and radiochemical neutron activation techniques have been developed for the analysis of samples of quartz-adularia veins from the epithermal gold-silver deposit Milogradovka (the Far East, Primorye). The optimal separation conditions of the Pt, Au, Ir, Re, Ag from non-noble metals have been determined in the chromatographic system Purolite A400 MB in the Cl^- form – 0.2 M HCl chromatographic system.

The Purolite A400 MB is a strong base anion exchange resin supplied in the hydroxide form, which has a polystyrene-divinylbenzene cross-linked copolymer matrix of the high exchange capacity up to 1.3 eq/l (in the Cl^- form). The sorption kinetics curves of the $[\text{PtCl}_4]^{2-}$, $[\text{PtCl}_6]^{2-}$, $[\text{AuCl}_4]^-$, $[\text{ReO}_4]^-$ anion complexes on the A400 MB in the OH^- and Cl^- form are compared with model in Fig. 1.

The optimum height of the adsorbent layer was found by the radionuclide distribution profile

along the column length. The ratios of radioactivity A_1 on the high L to the analyte radioactivity A_0 were measured in the A400 MB in the Cl^- form – 0.2 M HCl system. Distribution profiles of the Re, Pt, Ir, Au and Ag along the column length L are given in Fig. 2. The radionuclides were completely retained in the first 2–5 cm of the column. The 10-cm resin layer was used to perform the measurements.

The gamma-ray spectra of the samples analyzed and the reference samples were measured with the coaxial p -type HPGe-detector of 20% relative efficiency and energy resolution of 1.7 keV at the 1332.5 keV line of ^{60}Co . The input count rate of the detector was about 5 times smaller, and the “signal-to-background” ratio was 82 times better with gamma radiation of the sample, past the ion-exchange chromatographic separation, compared with the spectrum of the unseparated sample. The measured Au, Pt, Re, Ag and Ir concentrations in the samples from the quartz-adularia veins

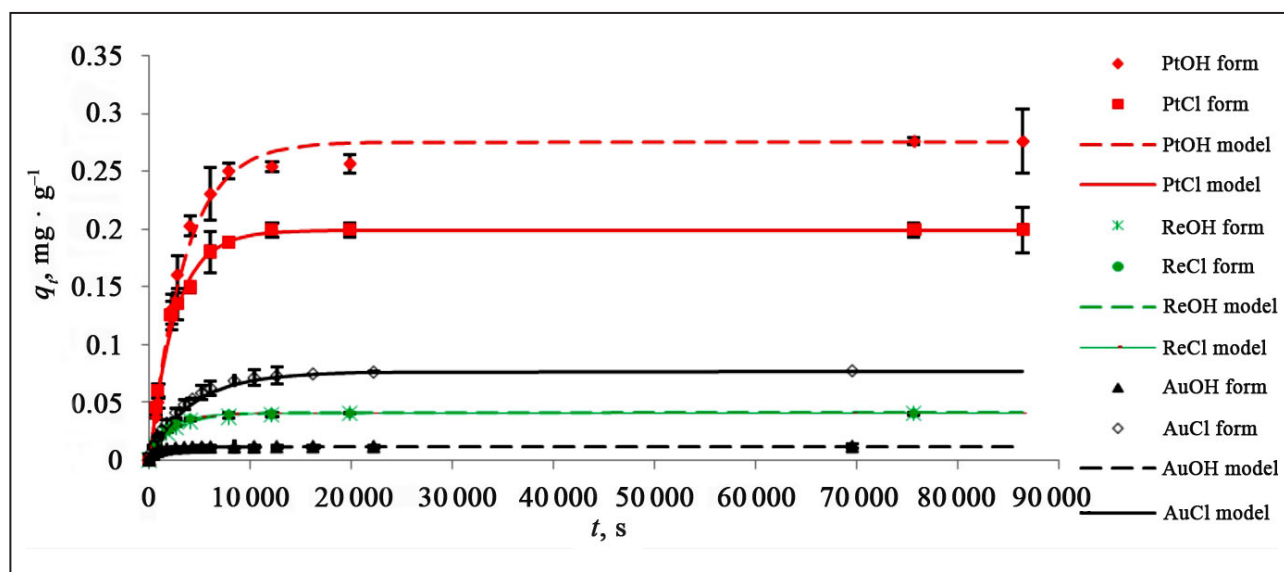


Fig. 1. The sorption kinetics curves of the anion complexes on the A400 MB in the OH^- and Cl^- form

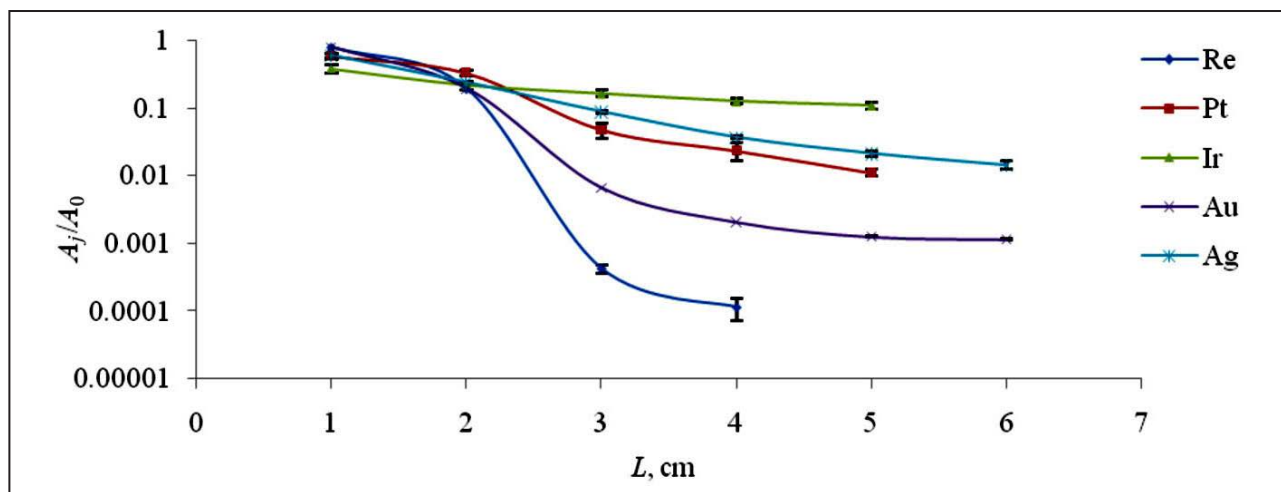


Fig. 2. Distribution of the Re, Pt, Ir, Au and Ag along the column length L in the A400 MB system

Table. The Au, Pt, Re, Ag and Ir concentrations (% wt) in the samples from the quartz-adularia veins of the deposit Milogradovka

Sample	Au	Pt	Re	Ag	Ir
582 28-12	$6.8(8) \cdot 10^{-5}$	$4.6(4) \cdot 10^{-4}$	$7(2) \cdot 10^{-7}$	$3.9(2) \cdot 10^{-3}$	$5.2(3) \cdot 10^{-5}$
583 15-12	$2.3(4) \cdot 10^{-6}$	$1.0(1) \cdot 10^{-3}$	$1.3(4) \cdot 10^{-6}$	$2.4(2) \cdot 10^{-4}$	$1.3(8) \cdot 10^{-4}$
583 16-12	$2.8(6) \cdot 10^{-6}$	$4.2(3) \cdot 10^{-4}$	$6(2) \cdot 10^{-7}$	$1.7(1) \cdot 10^{-4}$	$7.4(3) \cdot 10^{-5}$
583 66-13	$3.2(3) \cdot 10^{-4}$	$4.5(3) \cdot 10^{-4}$	$1.3(1) \cdot 10^{-6}$	$1.6(1) \cdot 10^{-2}$	$8(2) \cdot 10^{-5}$
583 80-13	$8.7(9) \cdot 10^{-4}$	$1.1(1) \cdot 10^{-3}$	$2.8(3) \cdot 10^{-6}$	$4.0(2) \cdot 10^{-2}$	$2.5(8) \cdot 10^{-4}$

of the gold-silver deposit Milogradovka are presented in the table.

The determination limits of Au, Pt, Re, Ir and Ag for the given radiochemical technique equal $3 \cdot 10^{-9}$; $2 \cdot 10^{-8}$; $8 \cdot 10^{-8}$; $7 \cdot 10^{-7}$ and $1 \cdot 10^{-8}\%$ respectively at the measurement uncertainties of 3–25%. The combination of instrumental and radiochemical neutron activation techniques al-

lowed extending the number of determinable elements to 40 with determination limits of $n \cdot (10^{-4} - 10^{-10})\%$ in mass at the measurement uncertainties of 3–25% in mass. The principal result of the study is confirmation of the platinum mineralization in the quartz-adularia veins from the gold-silver epithermal deposit Milogradovka.

Spin structure of quasi- two-dimensional frustrated magnet $\text{Li}_3\text{Ni}_2\text{SbO}_6$ with a magnetic “honeycomb”-type lattice

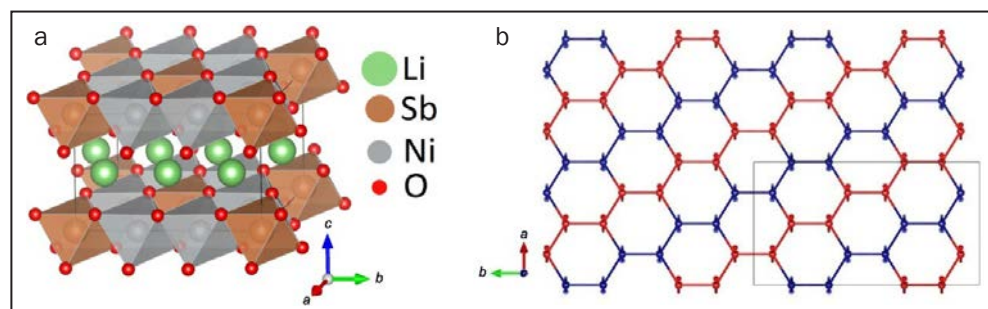
A.N. Korshunov, A.I. Kurbakov, A.L. Malyshev, S.Yu. Podchezertsev
Neutron Research Division of NRC “Kurchatov Institute” – PNPI

Quasi-two-dimensional magnetism is one of the most enthralling topics of modern solid-state physics. Reduced dimension gives rise to plenty of new phenomena. One of the most intriguing case for 2D lattices is a hexagonal net of magnetic ions in a layer. Magnetic spin ordering, coordination number ($z = 3$) – the minimal possible for 2D lattices, frustrated interactions between the nearest and the second and third neighboring spins as well as quantum fluctuations lead to a large variety of a possible ground states. This work is devoted to the experimental study of the crystal structure and the establishment of the ground quantum state in a low-dimensional magnet with layered superstructure of “honeycomb”-type cationic layers $\text{Li}_3\text{Ni}_2\text{SbO}_6$ using neutron and synchrotron powder diffraction.

The synchrotron experiment revealed a slight peak splitting that allowed identifying a true space group to be $C2/m$; additional diffuse scattering indicating the presence of stacking faults was also detected. The crystal structure of the compound is based on structural motives of the edge-sharing oxygen octahedral layers. The ordered mixed layers consisting of magnetic Ni^{2+} and non-magnetic Sb^{5+} cations inside oxygen octahedra alternate with Li layers (Fig. a.). It was defined that the order within the layer is almost perfect: no sub-

stitution between Ni and Sb positions is observed. The values of Ni-O-Ni bond angles close to 90° show the presence of weak ferromagnetic inlayer interactions according to Goodenough–Kanamori rules; slightly distorted O-Ni-O angles indicate a trigonal crystal field presence at Ni sites.

Low-temperature neutron powder diffraction revealed appearance of addition peaks associated with magnetic scattering below $T_N = 15$ K. Non-trivial quantum ground state namely antiferromagnetic zigzag-type with the propagation vector $\mathbf{k} = (1/2, 1/2, 0)$ is established experimentally for the first time (Fig. b): zig-zag ferromagnetic chains coupled with each other antiferromagnetically in ab -plane. At the same time spins inclined along crystallographic c direction at TN undergo a tilt with the temperature decrease, aligning perpendicular to the honeycomb (001) layer at $T = 1.5$ K with a total tilt angle 15.6° . Such behavior indicates the presence of non-negligible exchange interaction between “honeycomb” layers that has not been taken into account anywhere before. It is shown that diffraction data correlate perfectly with results of measurements of a temperature dependence of the magnetic susceptibility, specific heat, high frequency electron spin resonance and theoretical calculations.



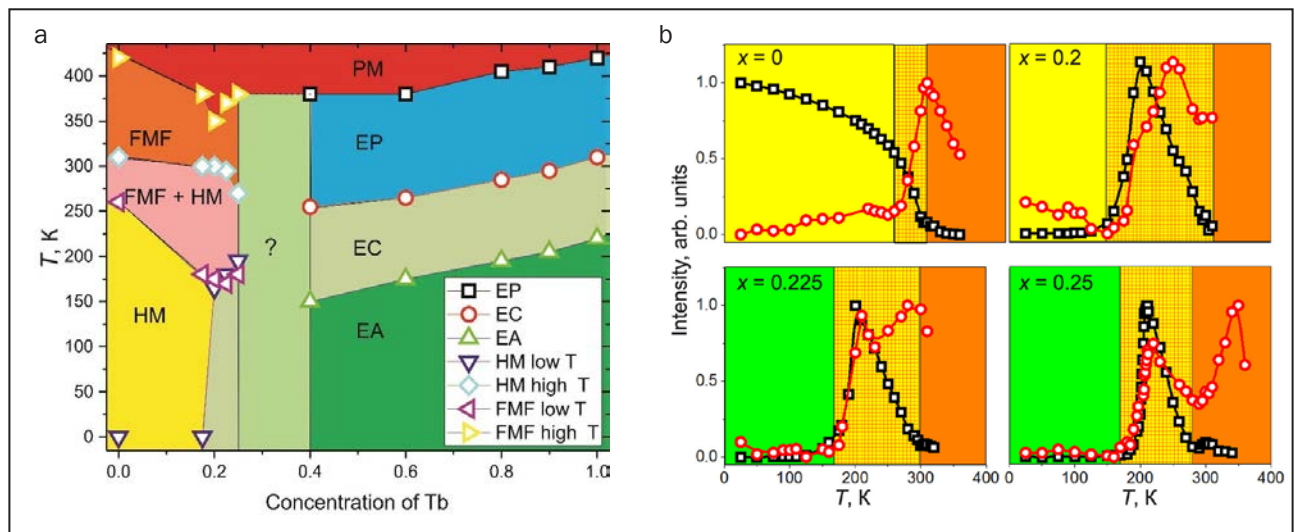
Crystal (a) and magnetic (b) structure of $\text{Li}_3\text{Ni}_2\text{SbO}_6$. The magnetic unit cell (rectangle) is doubled along the a and b crystallographic axes in comparison to the crystallographic one. The opposite directions of the spins are marked in different colors

Magnetic phase diagram of $Y_{1-x}Tb_xMn_6Sn_6$ ($x = 0; 0.175; 0.2; 0.225; 0.25$) compounds

A.A. Bykov, Yu.O. Chetverikov, S.V. Grigoriev, E.V. Moskvina, A.N. Pirogov – Neutron Research Division of NRC “Kurchatov Institute” – PNPI
S.V. Grigoriev, E.V. Moskvina – Saint Petersburg State University
A.N. Pirogov – Mikheev Institute of Metal Physics, Ural Federal University

Over the last years, researchers have focused their attention on compounds, which possess a natural magnetic layered structure. A number of studies have been devoted to the RMn_6Sn_6 compounds with layered crystal structure, where R – rare earth ion. The $Y_{1-x}Tb_xMn_6Sn_6$ compounds ($x = 0; 0.175; 0.2; 0.225; 0.25$) were studied by small angle neutron scattering (SANS) and paramagnetic neutron spin echo. The YMn_6Sn_6 compound is found to be a helimagnet in the whole temperature range below $T_N = 310$ K. Close to T_N an additional peak of

a Lorenz shape was observed at $Q = 0$. The peak is thought to have originated from the ferromagnetic fluctuations of the magnetic Mn moment in the ab -plane of the hexagonal crystal structure. Compounds, in which Y is replaced by Tb, change their magnetic order with the increase of temperature: from easy cone ferromagnetic phase at low T through the helicoidal phase to the ferromagnetic fluctuation close to T_N . Temperature-concentration phase diagram of $Y_{1-x}Tb_xMn_6Sn_6$ is built on the basis of the obtained data.



Температурно-концентрационная магнитная фазовая диаграмма (а); температурная зависимость интегральных интенсивностей брэгговского и центрального пиков для различных концентраций Tb (б). Цветом отмечены различные магнитные состояния: желтым – геликомагнитная фаза; зеленым – ферримагнитная легкая плоскость; оранжевым – ферромагнитные флуктуации (смесь геликомагнитной фазы и фаза ферромагнитных флуктуаций заштрихованы)

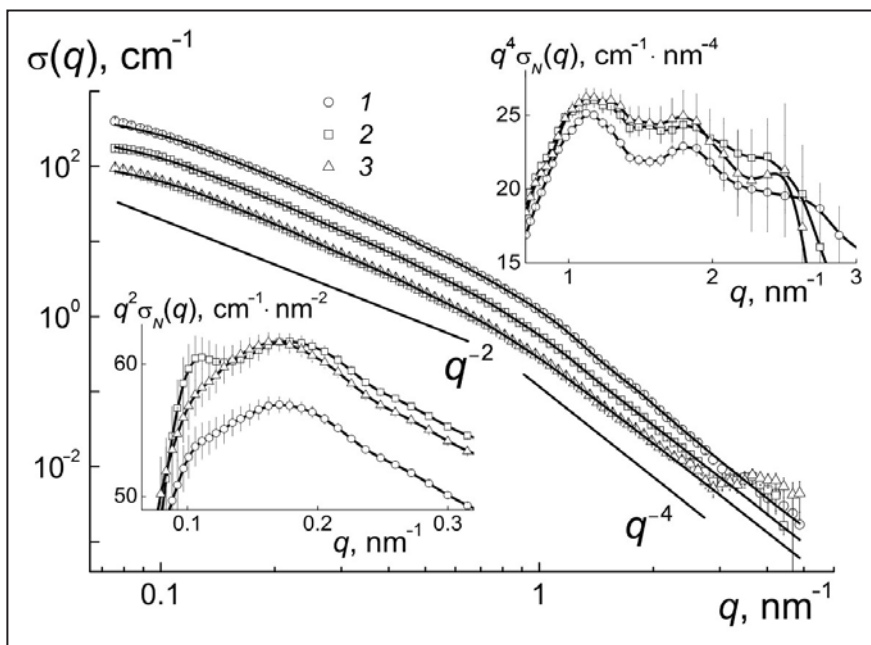
1. Bykov A.A., Chetverikov Yu.O. ..., Grigor'ev S.V. // JETP Lett. 2015. V. 101. P. 699.
2. Bykov A.A., Chetverikov Yu.O., Moskvina E.V. ..., Grigor'ev S.V. // J. Magn. Magn. Mater. 2017. V. 424. P. 347–351.

Multilevel structure of diamond hydrogels by neutron scattering

Yu.V. Kulvelis, V.T. Lebedev – Neutron Research Division of NRC “Kurchatov Institute” – PNPI
 A.I. Kuklin – Joint Institute for Nuclear Research
 A.Ya. Vul – Ioffe Institute of RAS

Neutron scattering data analysis in direct and reciprocal space (Fig.) has allowed decoding the structure of diamond hydrogels synthesized for the first time (Ioffe Institute, RAS) as the systems having three levels of structural organization at the scales from ones to tens of nanometers. It has been established that the formation of short range order in such a system is realized subsequently through the bonding of charged particles (diameter ~ 5 nm) in the first coordination sphere and the association of these fragments into the aggregate joint to form the chains linked into

the network (scale ~ 40 nm). The formation of gel was detected via a giant increase of system's viscosity. Neutron experiments demonstrated the conservation of original gel local structure by four-fold dilution below the critical point ($C^* \sim 4.2\%$ wt.). This unusual phenomenon can be explained by a formation of “microgel” when continuous gel is broken into submicron domains dispersed in water. This transformation confirms a key role of electrostatic attraction between non-spherical diamond crystals in the stabilization of gel structure.



Samples' cross sections $\sigma(q)$ for the diamond contents 5.05; 2.25; 1.13% wt. (1–3) vs. momentum transfer.

Characteristic slopes for q -dependencies of cross sections are shown.

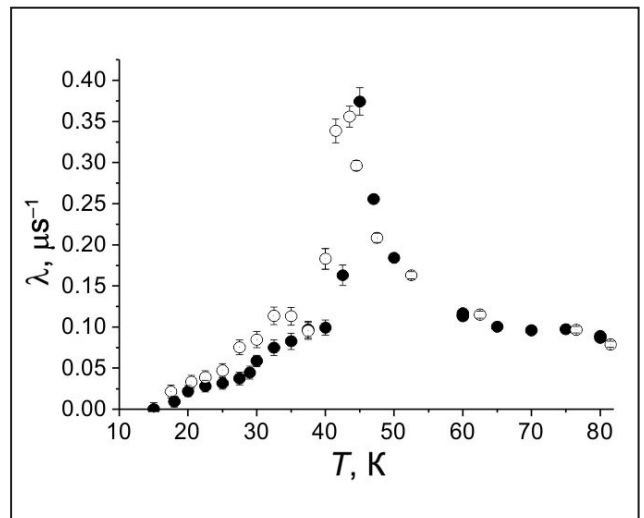
The inserts (left, right) illustrate the normalized data in Porod and Kratky presentations, which display the maxima characterizing the network scale and chain-like association of particles

μ SR study of $\text{Eu}_{0.8}\text{Ce}_{0.2}\text{Mn}_2\text{O}_5$ and EuMn_2O_5 multiferroics

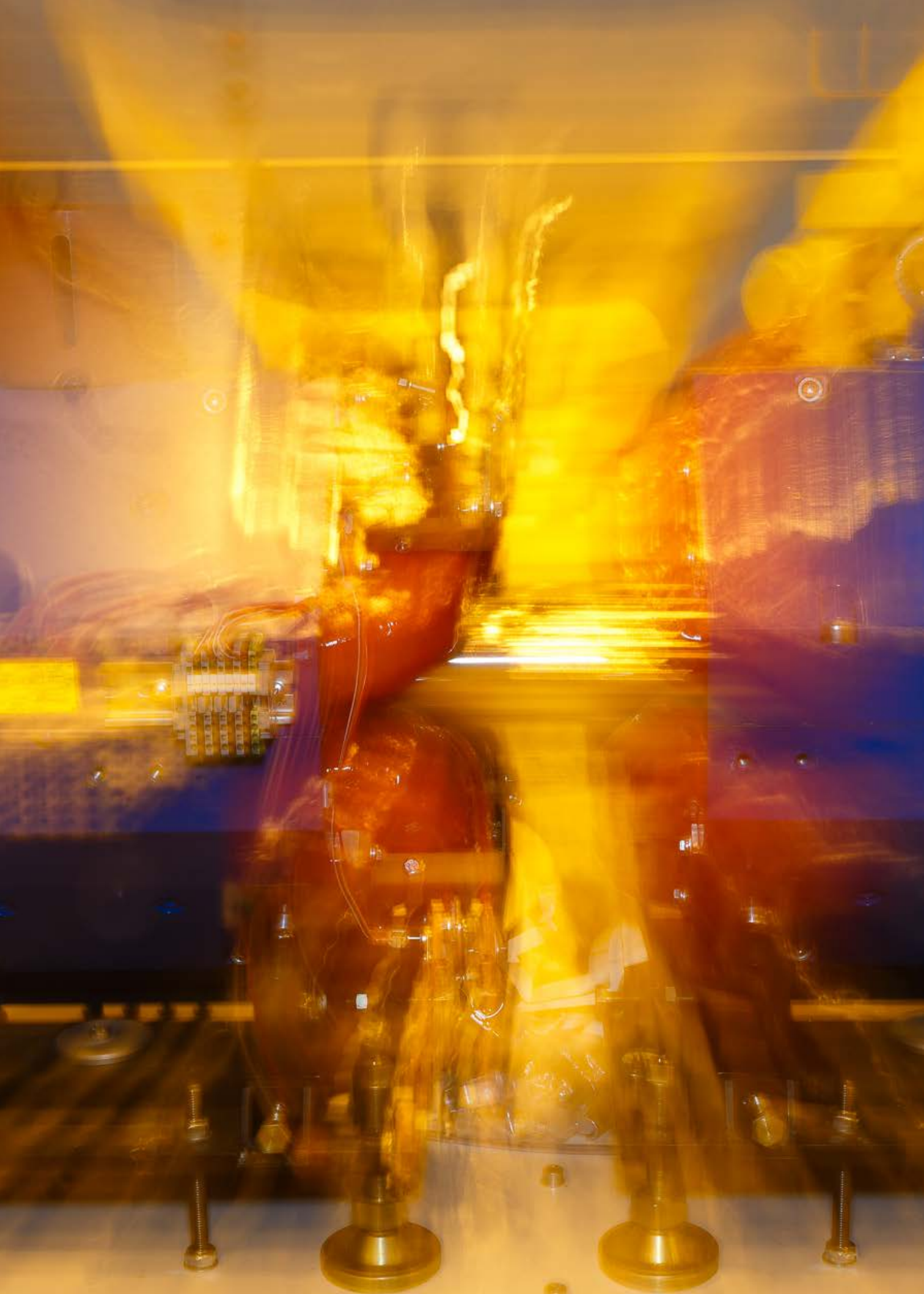
*D.S. Andrievskii, S.G. Barsov, A.L. Getalov, E.N. Komarov, S.A. Kotov, G.V. Shcherbakov, S.I. Vorob'ev – High Energy Physics Division of NRC “Kurchatov Institute” – PNPI
E.I. Golovenchits, V.A. Sanina – Ioffe Institute of RAS
A.Yu. Mishchenko – National Research Nuclear University MEPhI*

A comparative μ SR study of ceramic samples of the EuMn_2O_5 and $\text{Eu}_{0.8}\text{Ce}_{0.2}\text{Mn}_2\text{O}_5$ multiferroics is performed in the temperature range from 15 to 300 K. It is found that the Ce doping of the EuMn_2O_5 sample slightly reduces the temperature of the magnetic phase transition from $T_N = 45$ K for the EuMn_2O_5 sample to $T_N = 42.5$ K for the $\text{Eu}_{0.8}\text{Ce}_{0.2}\text{Mn}_2\text{O}_5$ sample (Fig.). Below the temperature T_N for both samples, there are two types of localization of a thermalized muon with different temperature dependences of the precession frequency of the magnetic moment of the muon in an internal magnetic field. The higher frequency in both samples refers to the initial antiferromagnetic matrix. The behavior of this frequency in $\text{Eu}_{0.8}\text{Ce}_{0.2}\text{Mn}_2\text{O}_5$ follows the Curie-Weiss law with the exponent $\beta = 0.29 \pm 0.02$, which differs from the value $\beta = 0.39$ standard for 3D Heisenberg magnetics and is observed in EuMn_2O_5 , because of the strong frustration of the doped sample. The temperature-independent low frequency is due to the presence of Mn^{3+} - Mn^{4+} ferromagnetic pairs located along the b axis of the antiferromagnetic matrix and in the regions of phase separation, which contain such ion pairs and eg electrons recharging them. In both samples, polarization losses are the same (about 20%) and are associated with the formation of

Mn^{4+} - Mn^{4+} + Mu complexes near Mn^{3+} - Mn^{4+} ferromagnetic pairs. In the temperature interval from 25 to 45 K, the separation of the $\text{Eu}_{0.8}\text{Ce}_{0.2}\text{Mn}_2\text{O}_5$ structure into two fractions where the relaxation rates of polarization of muons differ by an order of magnitude is revealed. This effect is due to a change in the state of regions of phase separation (1D superlattices) at the indicated temperatures. Such effect in EuMn_2O_5 is significantly weaker.



Temperature dependence of the relaxation rate of the polarization of muons stopped in the (open circles) $\text{Eu}_{0.8}\text{Ce}_{0.2}\text{Mn}_2\text{O}_5$ and (closed circles) EuMn_2O_5 samples



Research Based on the Use of Protons and Ions. Neutrino Physics

- 68 Combined ATLAS and CMS analysis on production and decays of Higgs boson and constrains of its coupling constants at Large Hadron Collider energies 7 and 8 TeV
- 70 Indication on BFKL-evolution manifestation in dijet azimuthal decorrelations with wide rapidity separation in CMS at Large Hadron Collider energy 7 TeV
- 72 Measurement of the angular coefficients in Z-boson events using electron and muon pairs from data taken at $\sqrt{s} = 8$ TeV with the ATLAS detector
- 74 The search for high mass resonances in the ATLAS experiment
- 75 Investigation of exotic hadrons at the LHCb experiment
- 76 Evidence for the CP -violation in decays of baryons
- 77 Anomalous yield of charmonium in peripheral lead-lead collisions at the Large Hadron Collider
- 78 Thermal photon emission in ultrarelativistic gold-gold collisions in the PHENIX at Relativistic Heavy Ion Collider
- 79 Decay energy for “astrophysical” nuclide ^{123}Te
- 81 Laser resonance ionization scheme development for tellurium and germanium
- 82 Investigation of the shape coexisting phenomena in the light thallium isotopes by laser spectroscopy
- 84 Beta-delayed fission and alpha decay of ^{196}At
- 85 Search for narrow resonances in πp elastic scattering from the EPECUR experiment
- 86 The structure effects in polarization and cross section in inelastic $A(p, p')X$ reaction with the ^{12}C and ^{40}Ca nuclei at 1 GeV
- 87 Investigation of fragmentation ($Z = 2$) of relativistic nuclei ^{16}O and ^{208}Pb
- 88 Search for low-energy neutrino and antineutrino signals of Borexino correlated with gamma-ray bursts
- 89 The first results of dark matter search with low-radioactivity argon in DarkSide-50 detector
- 90 Recovery method of gas discharge detectors at appearance of the malter effect

Combined ATLAS and CMS analysis on production and decays of Higgs boson and constrains of its coupling constants at Large Hadron Collider energies 7 and 8 TeV

ATLAS Collaboration

A.E. Basalaev, A.E. Ezhilov, O.L. Fedin, V.T. Grachev, M.P. Levchenko, V.P. Maleev, I.G. Naryshkin, V.A. Schegelsky, V.M. Solovyev

CMS Collaboration

L.A. Chtchipounov, V.L. Golovtsov, Yu.M. Ivanov, V.T. Kim, E.V. Kuznetsova, V.A. Murzin, V.A. Oreshkin, V.V. Sulimov, A.A. Vorobyev – High Energy Physics Division of NRC “Kurchatov Institute” – PNPI

CMS and ATLAS experiments, the most ambitious projects in contemporary high energy physics, demonstrated in RUN 1 unique capabilities of extending the human knowledge in field of fundamental elementary particle physics. Until now the main result of the two major experiments is the discovery of the Higgs-boson made in 2012. In the Standard Model (SM), the Higgs-boson is the quantum of the fundamental scalar vacuum field responsible for spontaneous electroweak symmetry breaking and origin of mass.

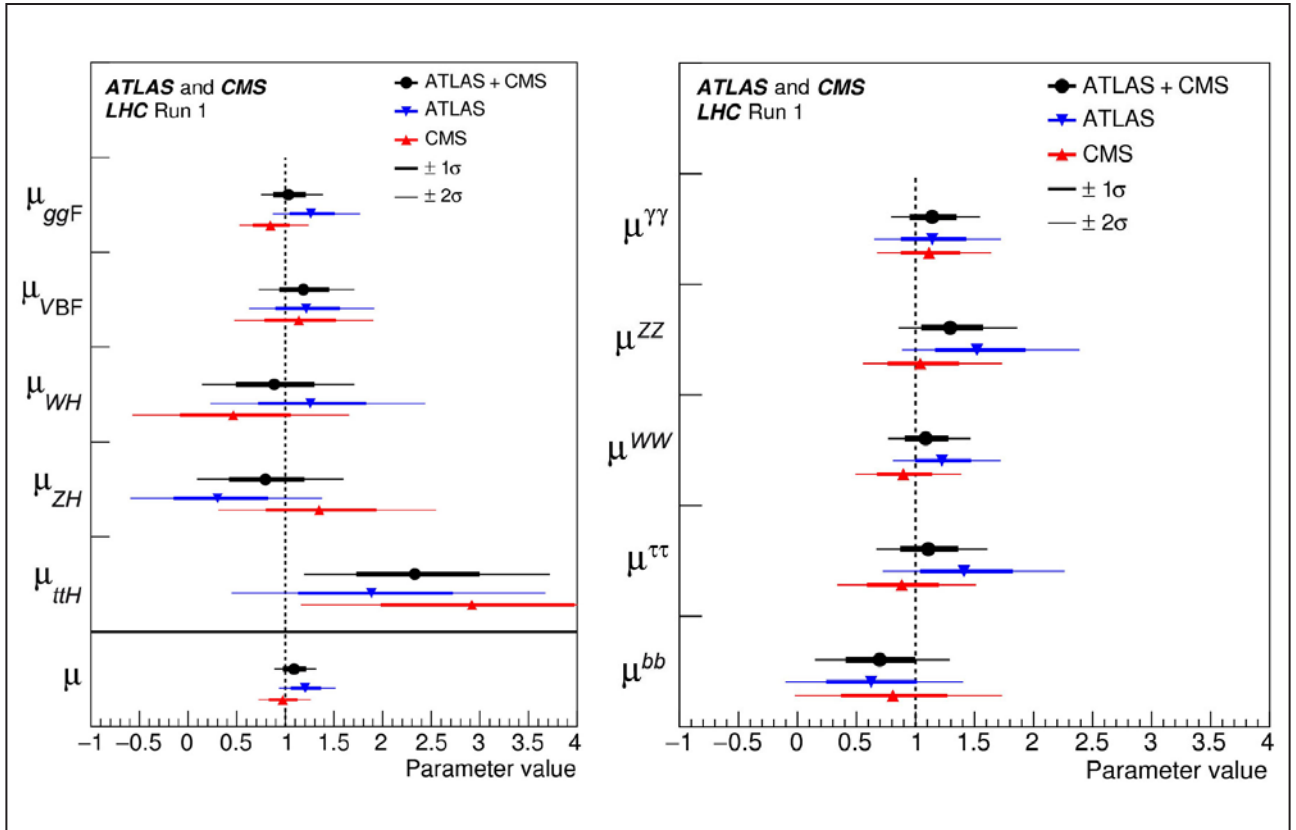
NRC “Kurchatov Institute” – PNPI team made substantial contributions to the construction and maintenance of the CMS endcap Muon system (the EMU system) and the ATLAS inner tracker (the TRT system), which in their turn played an important role in the discovery of the Higgs-boson and determination of its properties.

In 2016, the CMS and ATLAS collaborations presented the results of combined measurements of the Higgs boson production and decay rates, as well as constraints on its couplings to vector bosons and fermions based on the data recorded in 2011 and 2012. The combination is based on the analysis of five production processes, namely gluon fusion, vector boson fusion, and associated production with a W or a Z boson or a pair of top quarks, and of the six decay modes $H \rightarrow ZZ$, WW , $\gamma\gamma$, $\tau\tau$, bb , and $\mu\mu$. All results are received

assuming a value of 125.09 GeV for the Higgs boson mass, the result of the combined Higgs boson mass measurement by the two experiments. The combined analysis is sensitive to the couplings of the Higgs boson to the weak vector bosons and to the heavier fermions (top quarks, b quarks, τ leptons, and – marginally – muons). The analysis is also sensitive to the effective couplings of the Higgs boson to the photon and the gluon. At the LHC, only products of cross sections and branching fractions are measured, so the width of the Higgs boson cannot be probed without assumptions beyond the main one used for all measurements presented here, namely that the Higgs boson production and decay kinematics are close to those predicted by the SM.

In general, the combined analysis presented in this paper provides a significant improvement with respect to the individual combinations published by each experiment separately. The precision of the results improves in most cases by a factor of approximately 1/2, as one would expect for the combination of two largely uncorrelated measurements based on similar-size data samples.

Figure 1 shows the best fit results for the production signal strengths (*left*) and for the decay signal strengths (*right*) for the combination of ATLAS and CMS data. The combined signal yield



Best fit results for the production signal strengths (left) and for the decay signal strengths (right) for the combination of ATLAS and CMS data. Also shown are the results from each experiment. The error bars indicate the 1σ (thick lines) and 2σ (thin lines) intervals. The measurements of the global signal strength μ are also shown

relative to the SM prediction is measured to be 1.09 ± 0.11 . The combined measurements lead to observed significances for the vector boson fusion production process and for the $H \rightarrow \tau\tau$ decay of 5.4 and 5.5 standard deviations, respectively.

In conclusion, the finalized data of Run 1 on production and decays of Higgs boson and constraints of its coupling constants within available uncertainties are consistent with the SM predictions.

Indication on BFKL-evolution manifestation in dijet azimuthal decorrelations with wide rapidity separation in CMS at Large Hadron Collider energy 7 TeV

CMS Collaboration

*L.A. Chtchipounov, V.L. Golovtsov, Yu.M. Ivanov, V.T. Kim, E.V. Kuznetsova,
V.A. Murzin, V.A. Oreshkin, V.V. Sulimov, A.A. Vorobyev –
High Energy Physics Division of NRC “Kurchatov Institute” – PNPI*

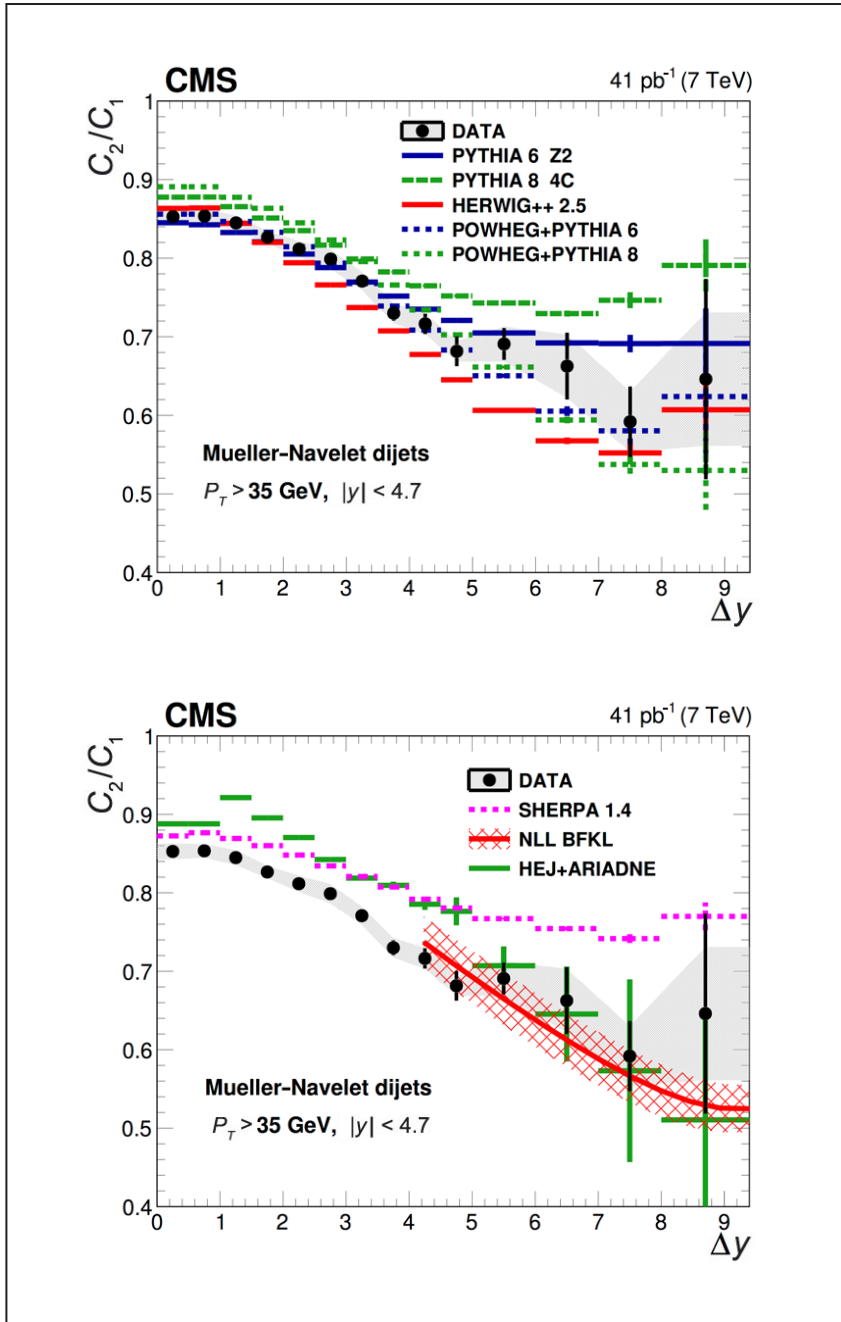
An ultimate goal of Compact Muon Solenoid (CMS) experiment at Large Hadron Collider (LHC) is to find new physics beyond the Standard Model (SM) and define the limits of its validity. To reach this goal, CMS measurements is steadily improving the precision of measured SM parameters and testing SM properties at new energy frontiers. There are two major kinematic regimes at high energy collisions. One, hard scattering regime ($\sqrt{s} \sim k_T \gg \Lambda_{\text{QCD}}$), which is describing by Gribov–Lipatov–Altarelli–Parisi–Dokshitzer (GLAPD) evolution equations of perturbative Quantum Chromodynamics (QCD), is well tested, and it is broadly used for SM predictions. The another one, semi-hard regime ($\sqrt{s} \gg k_T \gg \Lambda_{\text{QCD}}$), which should become dominant at high-energy QCD asymptotics, is governing by Balitsky–Fadin–Kuraev–Lipatov (BFKL) evolution equation.

In perturbative QCD parton-parton scattering at leading order in the strong coupling α_s produces two outgoing partons, which are back-to-back in the azimuthal plane. The partons manifest themselves as a collimated stream of hadrons, which are the observable jets. A deviation from the back-to-back configuration occurs due to parton showers initiated by the initial and final partons in the scattering process. The corresponding asymptotic high-energy region, which is described by BFKL-evolution equation, might be approximated experimentally in pp collisions by requiring jets of similar k_T but highly separated in rapidity. The azimu-

thel decorrelation of such jets with large rapidity separation might therefore show effects beyond the GLAPD description. Main contribution is expected from the jets with most forward and backward rapidities (Mueller–Navelet jets). In a kinematic region, where semi-hard parton interactions are important, the azimuthal angle decorrelations will increase with increasing rapidity separation $\Delta y = |y_1 - y_2|$ between the jets.

In 2016, CMS experiment presented an additional indication on asymptotic high-energy behavior of Quantum Chromodynamics (QCD) by measuring dijet azimuthal angle decorrelations with wide rapidity separation in pp -collisions at energy 7 TeV. The previous indication was observed in dijet cross section ratios with large rapidity separation between jets. The measured dijet decorrelations in Fig. 1 are consistent with BFKL-evolution manifestation in the next-to-leading logarithm approximation (NLLA) **improved by the prescription suggested in [6]** (shown as solid curve). At the same time, the various Monte Carlo event generators based on GLAPD evolution cannot describe all observable features.

To summarize, CMS obtained an indication on asymptotic BFKL-evolution manifestation in dijet azimuthal decorrelations with wide rapidity separation at LHC energy 7 TeV. Future measurements at higher energies are needed to established the new asymptotic behavior of SM.



Ratio of averaged cosines for single and double angles in dijet azimuthal plane as a function of rapidity separation between jets. The measured cosine ratio is consistent with BFKL predictions (solid curve) in NLLA [5] improved by prescription [6], while the various Monte Carlo event generators based on GLAPD evolution cannot describe all observable features

Measurement of the angular coefficients in Z-boson events using electron and muon pairs from data taken at $\sqrt{s} = 8$ TeV with the ATLAS detector

ATLAS Collaboration

V.T. Grachev, A. E. Ezhilov, O. L. Fedin, M. P. Levchenko, V.P. Maleev,
Y. G. Naryshkin, V. A. Schegelsky, V.M. Solovyev –
High Energy Physics Division of NRC “Kurchatov Institute” – PNPI

The angular distributions of charged lepton pairs produced in hadron-hadron collisions via the Drell-Yan neutral current process provide a portal to precise measurements of the production dynamics through spin correlation effects between the initial-state partons and the final-state leptons mediated by a spin-1 intermediate state, predominantly the Z-boson.

The full five-dimensional differential cross-section describing the kinematics of the two Born-level leptons from the Z-boson decay can be decomposed as a sum of nine harmonic polynomials, which depend on $\cos\theta$ and φ , multiplied by corresponding helicity cross-sections that depend on the Z-boson transverse momentum (p_T^Z), rapidity (y^Z), and invariant mass (m^2). The dimensionless angular coefficients $A_{0-7}(p_T^Z, y^Z, m^2)$ represent ratios of helicity cross-sections with respect to the unpolarized one.

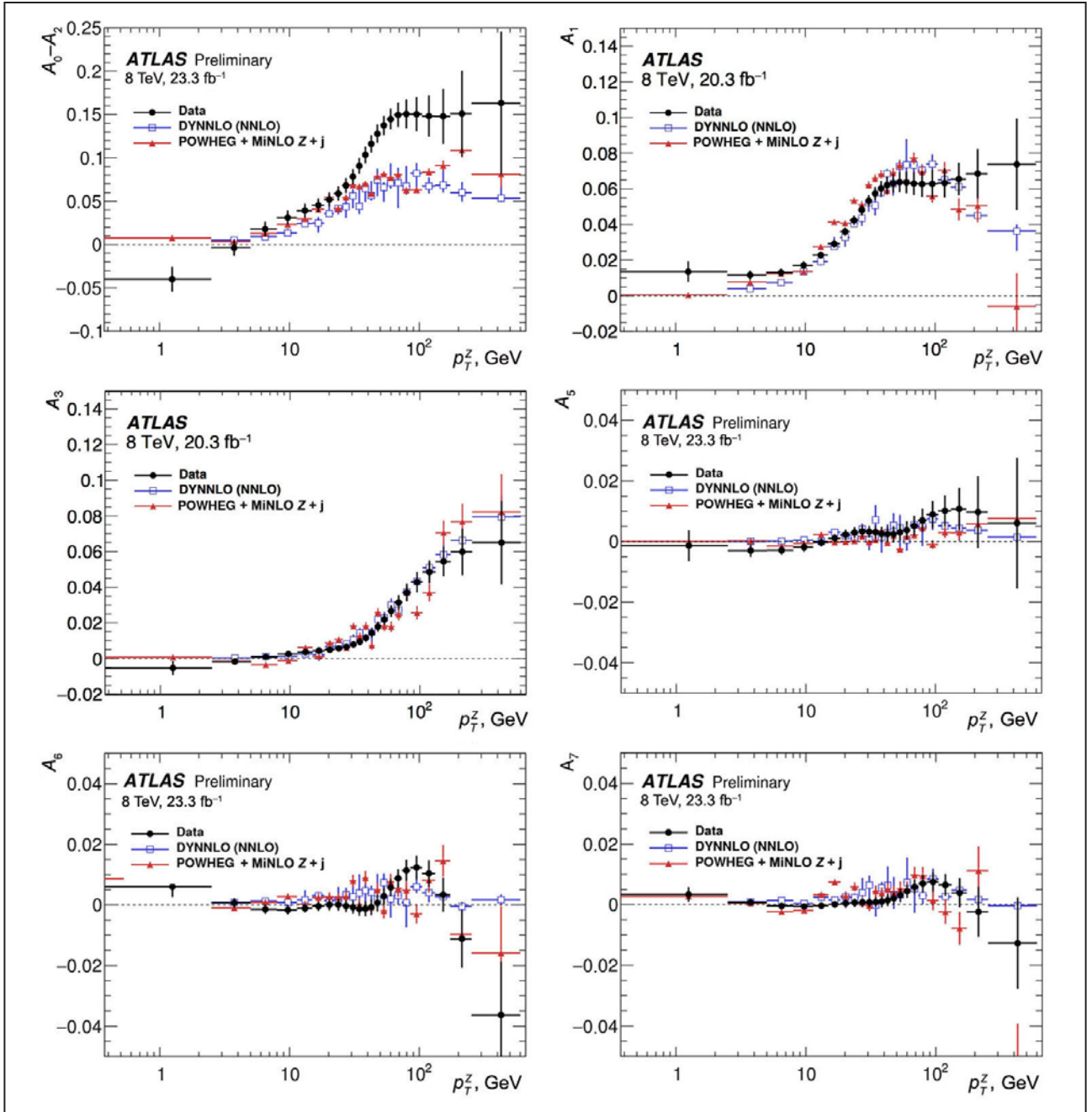
The measurement of the complete set of angular coefficients A_{0-7} were done using 20.3 fb^{-1} of pp-collisions at $\sqrt{s} = 8$ TeV collected by the ATLAS detector. Over most of the phase space, the measurements that are obtained from samples of electron and muon pairs covering respectively the ranges $0 < |y^Z| < 3.5$ and $0 < |y^Z| < 2.5$ are limited only by statistical uncertainties in the data. These uncertainties are small and range from 0.002 at low p_T^Z to 0.008 at $p_T^Z = 150$ GeV. The experi-

mental systematic uncertainties are much smaller in almost all cases. The theory systematic uncertainties are minimized through the template-building procedure, so that the PDF uncertainties, which are the dominant source of theoretical uncertainties, are below 0.004 in all cases.

The measurements are compared to the most precise fixed-order calculations currently available ($O(\alpha_s^2)$) and to theoretical predictions embedded in Monte Carlo generators. These comparisons are precise enough to probe QCD corrections beyond the formal accuracy of these calculations and to provide discrimination between different parton-shower models.

The results of measurements of angular coefficients show a significant deviation observed for A_0 – A_2 (Lam-Tung relation) from fixed-order prediction (Fig.), indicating that higher-order QCD corrections are required to describe the data. Evidence at the 3σ level is found for non-zero $A_{5,6,7}$ coefficients (Fig.), consistent with the expectations from DYNNLO at $O(\alpha_s^2)$.

The measurements of the A_i coefficients, in particular through the correlation of the angular distributions with the lepton transverse momentum distributions, are an important ingredient to the next steps in precision measurements of electroweak parameters at the LHC, both for the effective weak mixing angle $\sin^2\theta_W$ and for the W-boson mass.



Distributions of the angular coefficients $A_0 - A_2$ (top left) and angular coefficients A_1 (top right), A_3 (left center), A_5 (right center), A_6 (bottom left) and A_7 (bottom right) as a function of p_T^z

1. ATLAS Collaboration // JHEP. 2016. V. 8. P. 159.
2. Ezhilov A., Fedin O. // PoS.DIS2016. P. 121.

The search for high mass resonances in the ATLAS experiment

ATLAS Collaboration

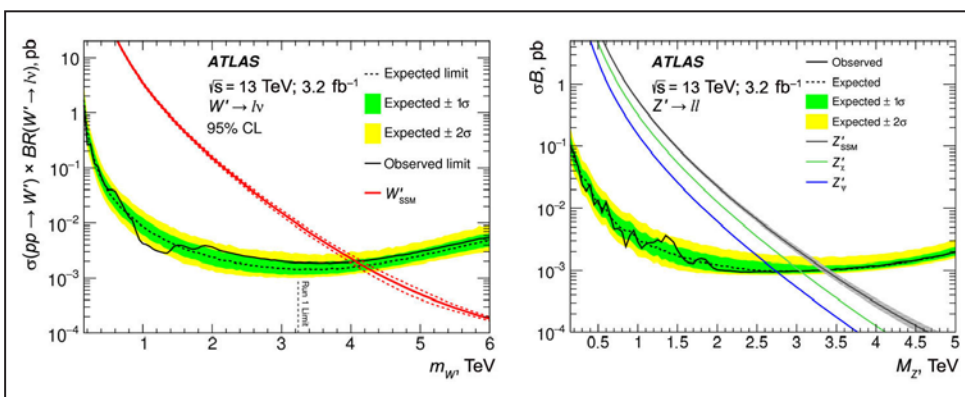
V.T. Grachev, A.E. Ezhilov, O.L. Fedin, M.P. Levchenko, V.P. Maleev,
Y.G. Naryshkin, V.A. Schegelsky, V.M. Solovyev –
High Energy Physics Division of NRC “Kurchatov Institute” – PNPI

In 2015 the Large Hadron Collider (LHC) resumed its work after a two-year technical stop (TS). The TS was caused by the necessity of modernization of the accelerator complex and work on increasing energy of the proton-proton collisions. The energy of the proton-proton collisions at a center-of-mass is 13 TeV after the TS.

ATLAS experiment continued to search for heavy (with masses of the order of 1 TeV) resonances, which are bosons, i. e. particles with integer spins. A class of models designed to solve the problems of the Standard Model (SM), such as the existence of dark matter, the problem of gauge hierarchy, etc., contains additional gauge bosons, commonly referred as Z' (for a neutral gauge boson) or W' (for a charged gauge boson). The Hadron Physics Laboratory of the High Energy Physics Division of NRC “Kurchatov Institute” – PNPI participated in this search.

The search was carried out in the $W' \rightarrow l\nu$ and $Z' \rightarrow ll$ channels, where l is an electron or a muon. No significant discrepancy between data and SM

predictions was found in 2015 dataset corresponding to an integrated luminosity of 3.2 fb⁻¹. In the absence of the detected signal from the heavy boson decay, the upper limits on cross-sections for the production of new bosons times branching ratio of the lepton decay channel ($\sigma \times B$) are set at 95% CL as functions of their masses. It was done for a few models. The Sequential Standard Model (SSM) has been chosen as the benchmark model for the search. In this model, the couplings of the W' and Z' to fermions are assumed to be identical to the couplings of the Z -bosons and the W -boson of the SM. Results of the search for Z' bosons are also interpreted in the context of the GUT-inspired models based on E₆ gauge group, which includes two neutral gauge bosons Z'_{ψ} and Z'_{χ} . The Figure presents the expected and observed limits for the combination of the electron and muon channels. Masses below 4.07 and 3.36 TeV for the SSM W' and Z' bosons, and masses below 2.74 and 3.05 TeV for Z'_{ψ} and Z'_{χ} bosons respectively are excluded at 95% CL.



Expected (dashed black line) and observed (solid black line) 95% CL upper limits on cross-section times branching ratio ($\sigma \times B$) in the combined (electron plus muon) channel, along with predicted $\sigma \times B$ for W' (left) and Z' (right) production

Investigation of exotic hadrons at the LHCb experiment

LHCb Collaboration

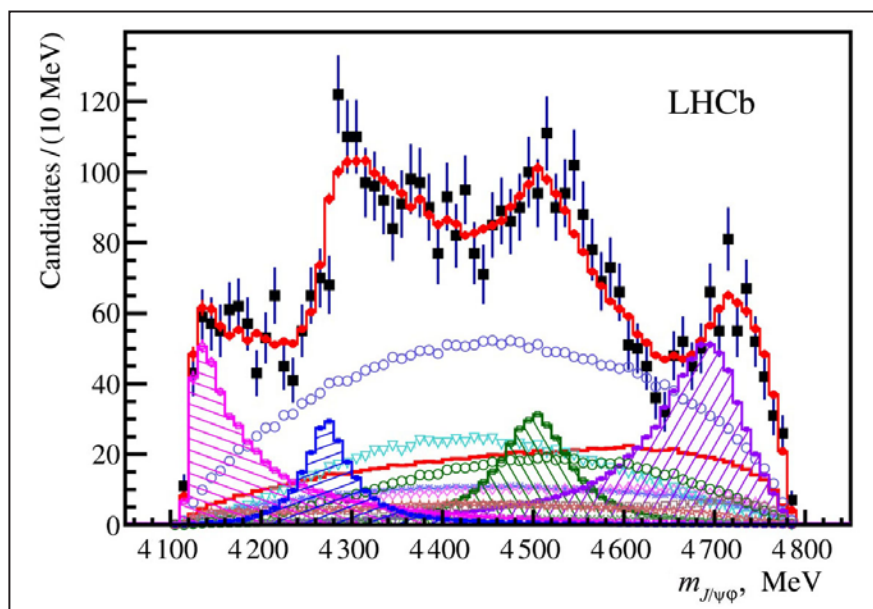
G.D. Alkhazov, N.F. Bondar, A.A. Dzyuba, O.E. Maev,

N.R. Sagidova, Yu.A. Shcheglov, A.A. Vorobyev –

High Energy Physics Division of NRC “Kurchatov Institute” – PNPI

Investigation of exotic hadron states – tetraquarks and pentaquarks – is one of research areas of the LHCb experiment at the Large Hadron Collider (LHC). The discovery of pentaquarks, particles which consist of four quarks and one anti-quark, was one of the main achievements of LHCb in 2015. Two exotic states manifest themselves in the decay $\Lambda_b^0 \rightarrow J/\psi p K^-$. In 2016, LHCb announced an evidence for these states in another Λ_b^0 decay channel: $\Lambda_b^0 \rightarrow J/\psi p \pi^-$. The statistical significance for the evidence is slightly larger than three standard deviations. The relatively small value of the significance can be explained by suppression of this decay channel with the $|V_{cd}|$ element of the Cabibbo–Kobayashi–Maskawa matrix.

Also, in 2016 new results on the amplitude analysis of $B^+ \rightarrow J/\psi \phi K^+$ decays were announced by the LHCb collaboration. Four new heavy exotic states are required to describe the angular and mass distributions of the products of the B^+ mesons decays. The statistical significance of each new exotic state is larger than five standard deviations. The contributions of these states into the $J/\psi \phi$ invariant mass spectrum are presented in the Figure. The corresponding quantum numbers of the discovered states have been determined with the statistical significance larger than four standard deviations.



The invariant mass distribution of the $\phi/J/\psi$ system. The black points correspond to the experimental data. The red points show the result of the full amplitude analysis for the $B^+ \rightarrow J/\psi \phi K^+$ decay. The contributions from the exotic states are demonstrated by shaded histograms

1. LHCb Collaboration // Phys. Rev. Lett. 2016. V. 117. P. 082002.
2. LHCb Collaboration // Phys. Rev. Lett. 2016. V. 117. P. 082003.
3. LHCb Collaboration // Phys. Rev. Lett. 2017. V. 118. P. 022003.
4. LHCb Collaboration // Phys. Rev. D. 2017. V. 95. P. 012002.

Evidence for the CP -violation in decays of baryons

LHCb Collaboration

G.D. Alkhazov, N.F. Bondar, A.A. Dzyuba, O.E. Maev,

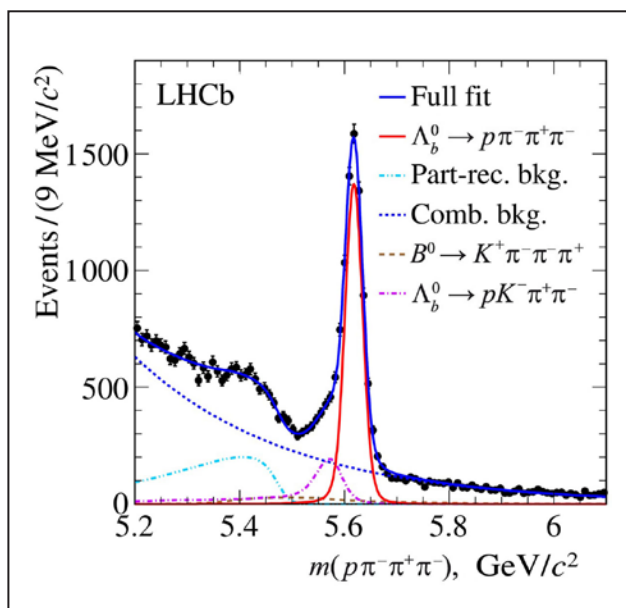
N.R. Sagidova, Yu.A. Shcheglov, A.A. Vorobyev –

High Energy Physics Division of NRC “Kurchatov Institute” – PNPI

One of the goals of the LHCb experiment is studies of the CP invariance violation in various processes. As it was shown for the first time by Andrey Sakharov, the CP invariance violation accounts for the baryon asymmetry of the Universe. In the Standard Model (SM), the effects of the CP violation are predicted and observed in the decays of the particles which contain s - or b -quarks. These effects are explained by the complex phase for some elements of the quark mixing (Cabibbo–Kobayashi–Maskawa) matrix. So far, the CP violation was observed only in decays of the K and B mesons.

In 2016, the LHCb experiment presented the data analysis devoted to the decay of the beauty hyperon $\Lambda_b^0 \rightarrow p\pi^-\pi^+\pi^-$ and demonstrated for the first time an evidence for the CP violation

in the baryon sector. During the LHC RUN I, in which the LHCb experiment has collected an experimental data set corresponding to the integrated luminosity of 3 fb^{-1} , 6646 ± 105 candidates for the $\Lambda_b^0 \rightarrow p\pi^-\pi^+\pi^-$ decay were selected (Fig.). Two observables ($a_p^{T\text{-odd}}$ and $a_{CP}^{T\text{-odd}}$), which have to be consistent with zero in case of the parity (P)- and CP -conservation, were determined for different parts of the phase space for the decay of interest. Two variants of the phase space partitioning have been studied in the presented analysis. For both types of partitioning there were places in the phase space with the significant deviation of $a_p^{T\text{-odd}}$ and $a_{CP}^{T\text{-odd}}$ from zero values. The statistical significance for the first evidence of the CP violation in the baryon decay consists in 3.3 standard deviations.



Invariant mass distribution for $p\pi^-\pi^+\pi^-$ system. Points demonstrate the data obtained by LHCb. Red solid curve corresponds to the contribution of Λ_b^0 decay of interest; dashed, dotted and dash-dotted lines correspond to different background sources, blue solid line corresponds to the full model

Anomalous yield of charmonium in peripheral lead-lead collisions at the Large Hadron Collider

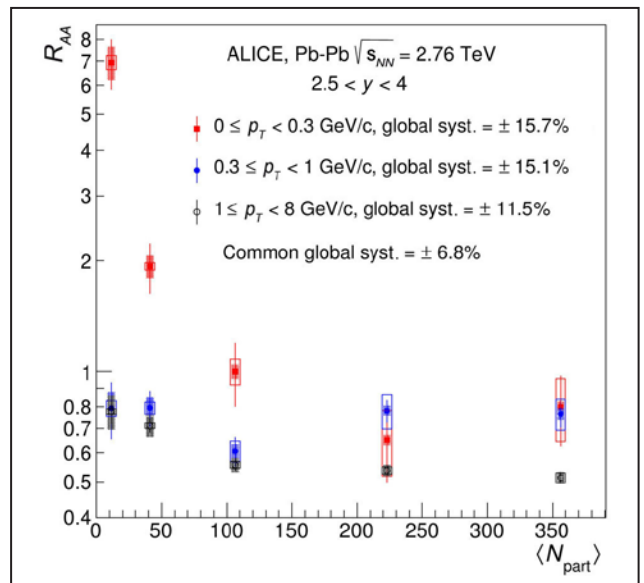
ALICE Collaboration

V.V. Ivanov, A.V. Khanzadeev, E. L. Kryshen, M.V. Malaev, V.N. Nikulin, V.G. Riabov, Yu.G. Riabov, V.M. Samsonov, M.B. Zhalov – High Energy Physics Division of NRC “Kurchatov Institute” – PNPI

Quarkonium (J/ψ , $\psi(2s)$, Υ) production in ultra-relativistic heavy ion collisions is one of the key probes of a medium created in the interaction zone. To date, bulk of the inclusive $J/\psi \rightarrow \mu^+\mu^-$ data in PbPb collisions has been accumulated in the rapidity range $-4 < y < -2.5$ with the muon spectrometer of the ALICE detector. The NRC “Kurchatov Institute” – PNPI team contributed significantly to design of this spectrometer, its successful operation, data assembly and analysis. Probably the most intriguing result which has been obtained analyzing the data from muon spectrometer is the large excess of J/ψ with very small $p_T < 0.3$ GeV/c in the events of PbPb peripheral collisions with small multiplicity. To characterize this effect the inclusive J/ψ nuclear modification factor R_{AA} , defined by the ratio of the charmonium yield in nucleus-nucleus collision to that in nucleon-nucleon one scaled by the number of binary inelastic NN collisions N_{coll} in nucleus-nucleus interaction geometry, is shown in Fig.

Centrality is expressed in terms of the number of nucleons N_{part} participating in the nucleus-nucleus collision. The measurements have been made for three intervals of the J/ψ transverse momentum: $p_T < 0.3$ GeV/c, $0.3 < p_T < 1$ GeV/c and $1 < p_T < 8$ GeV/c. For central collisions ($N_{part} > 200$) yield of J/ψ in AA collisions is suppressed $R_{AA} \sim 0.5-0.8$ and rather weakly depends on p_T . Together with observation of strong hadronic elliptic flows and jet quenching in such events this is considered as clear evidence of Quark-Gluon Plasma formation. Small excess of events

with low $p_T < 1$ GeV/c at $N_{part} > 300$ is treated as revealing of regeneration mechanism of J/ψ formation in kinematics of the Large Hadron Collider (LHC). Looking at the region of peripheral collisions ($N_{part} < 50$) one finds large excess of J/ψ with small $p_T < 0.3$ GeV/c both comparing to the yield with larger transverse momenta and to the yield in NN collisions scaled by corresponding N_{coll} . So far, production of J/ψ in strong interaction processes failed to explain such significant effect and the only reasonable suggestion is possible contribution of the coherent charmonium photoproduction on heavy fragments of interacting nuclei.



The J/ψ nuclear modification factor in inclusive J/ψ production in PbPb collisions at the LHC

Thermal photon emission in ultrarelativistic gold-gold collisions in the PHENIX at Relativistic Heavy Ion Collider

PHENIX Collaboration

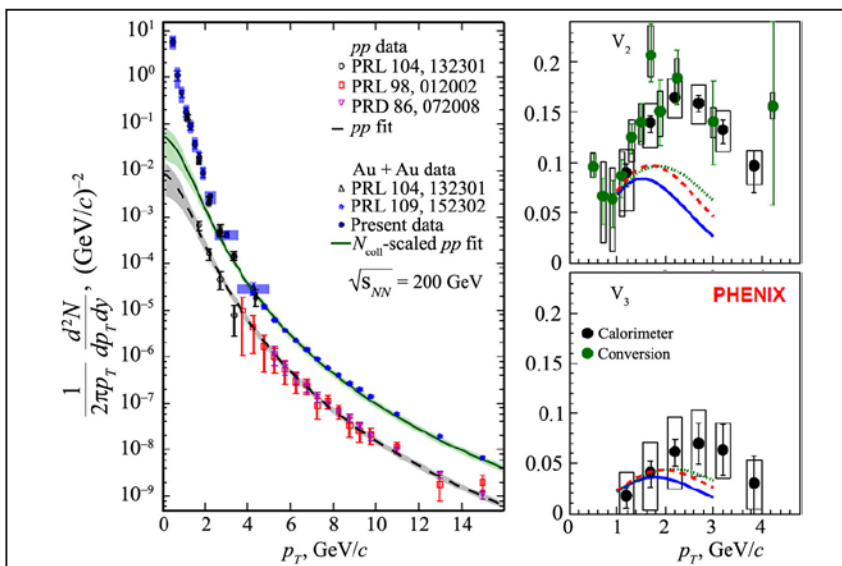
V.V. Baublis, D.A. Ivanischev, A.V. Khanzadeev, B.G. Komkov,
D.O. Kotov, L.M. Kochenda, V.G. Riabov, Yu.G. Riabov, V.M. Samsonov –
High Energy Physics Division of NRC “Kurchatov Institute” – PNPI

One of the most impressive results published by PHENIX Collaboration in 2016 is the measurement of the yield and anisotropic flows of direct photons in the central gold-gold collisions at the Relativistic Heavy Ion Collider (RHIC). Photons were detected through their conversion into e^+e^- pairs by the central tracking system of the PHENIX detector which was designed with significant contribution of NRC “Kurchatov Institute” – PNPI.

Spectra of direct photons in proton-proton (black and red points approximated by black dash line) and gold-gold collisions measured in the wide range of the photon transverse momenta from 0 to 15 GeV/c are shown in the Figure (left panel).

The green line demonstrates what spectrum of direct photons in AuAu interaction can be expected basing on their yield in pp collisions scaled by the number of binary inelastic NN collisions in the corresponding geometry of AuAu interaction. Strong excess of soft photons seen at $p_T < 2$ GeV/c is well described by exponential

function specific for the thermal radiation from hot equilibrated medium. The effective temperature $T_{\text{eff}} \sim 240$ MeV, extracted from the data fit, is much higher than critical temperature of hadron-parton phase transition ~ 175 MeV. This observation suggests fast thermalization of partonic medium created in the interaction zone of colliding nuclei and radiation of direct photons at the early stage of reaction. Fourier analysis of the measured spectrum of direct photons in gold-gold collisions revealed significant azimuthal anisotropy. Elliptic and triangular flows extracted from the data are shown in the Figure (right panel). Up to now, calculations in different theoretical models (blue, red and green curves) failed to describe the data. Progress in theoretical models and new measurements of the direct photon yield in ultrarelativistic heavy ion collisions will result in improving of our understanding of the space-time evolution of medium created in the central zone of ion interaction.



Spectrum and collective flows of direct photons measured by PHENIX in gold-gold collisions at RHIC

Decay energy for “astrophysical” nuclide ^{123}Te

SHIPTRAP Collaboration

S.A. Eliseev, P.E. Filianin, Yu.N. Novikov –

High Energy Physics Division of NRC “Kurchatov Institute” – PNPI

An investigation of modes of some astrophysical processes is based on the abundances of very long-lived nuclides with half-lives comparable with the age of the Universe. However, in stellar conditions, the life times of some of these nuclides can be very different from the earth values. There are two reasons for that: In hot stellar conditions besides the ground states also nuclear excited states in nuclides can be populated. These excited states can undergo beta-transitions, resulting in a considerable decrease of the effective lifetime. The second factor concerns the decay of these states in highly ionized atoms that influences the transition probabilities, which are especially large for small transmission energies. These energies can be measured precisely and, which is of importance, reliably only in a Penning trap.

Such a type of experiments was started at the SHIPTRAP-facility at GSI (Darmstadt) some time ago and one result for ^{187}Re has already been published recently. In 2016 we published the result of the decay energy measurement for the beta-decay of ^{123}Te . This nuclide can be synthesized only during the s-process, therefore the knowledge of

its “stellar” features is of paramount importance for a description of this process itself.

The first excited state of ^{123}Te with the 159 keV excitation energy is populated at a typical process temperature of $4 \cdot 10^8$ K with a probability of 2% with respect to the ground state (Fig. 1). Meanwhile, due to the opening of an allowed electron capture transition channel the effective half-life becomes superior over the ground state transition for many orders of magnitude (see Fig. 2).

The determination of the decay energy Q of ^{123}Te has been done via a measurement of the mass difference with the daughter nuclide ^{123}Sb . The measurements of the resonance frequencies, which are in a direct connection to the masses, have been implemented with utilization of a new phase imaging method. The result between the neutral ground state transition $Q = 51.912(67)$ keV was used to obtain the picture of the temperature dependence of the effective half-life of ^{123}Te which showed dramatic, up to 14 orders of magnitude, enhancement in comparison to the earth conditions.

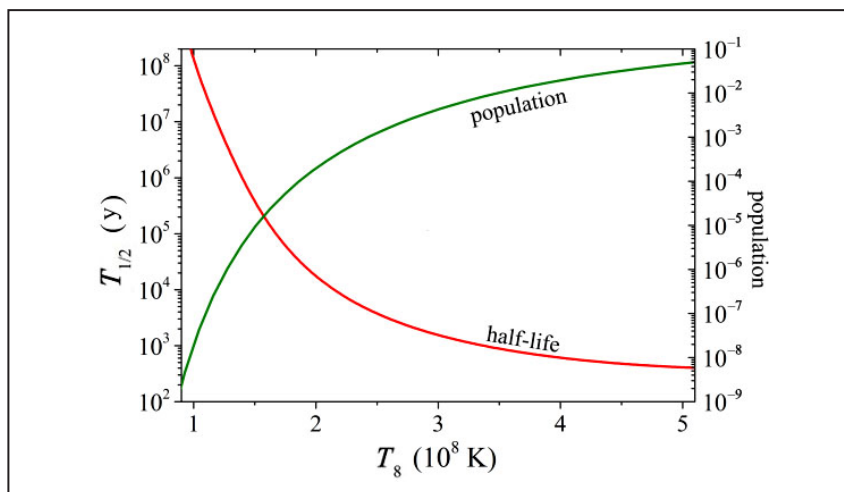


Fig. 1. The dependence of the population of the excited state of ^{123}Te with the 159 keV excitation energy (*right scale*) and effective half-life of ^{123}Te (*left scale*) depending on the temperature

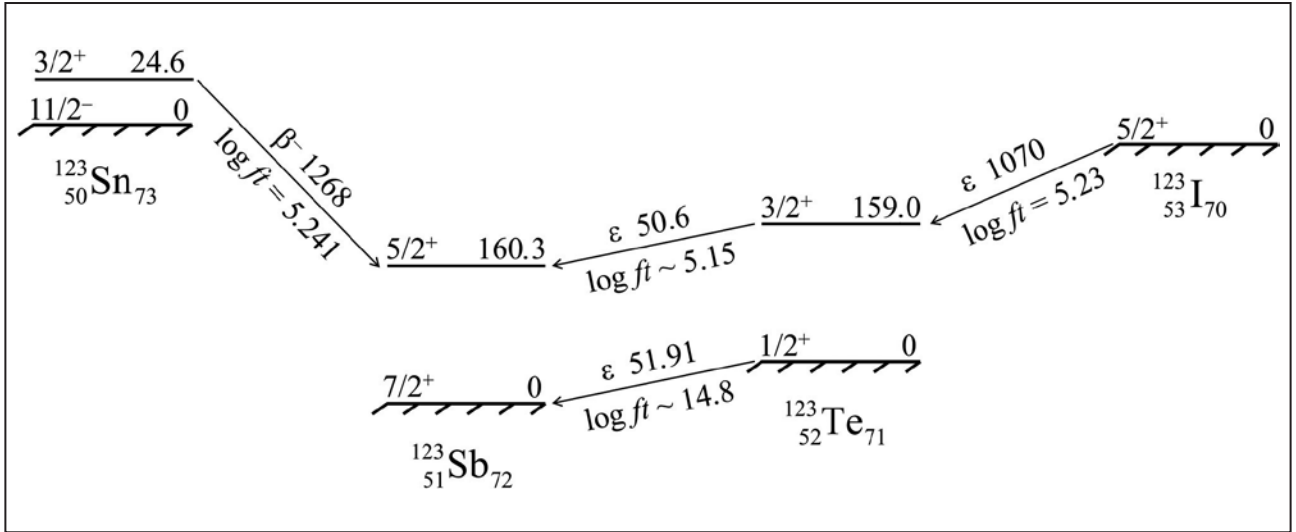


Fig. 2. The scheme of the decay for the isobaric nuclides with the mass number $A = 123$ in “stellar” conditions when excited states with the energy 159 keV undergo beta-transitions with a probability that is 10 orders of magnitude greater than the ground state transition (in earth conditions)

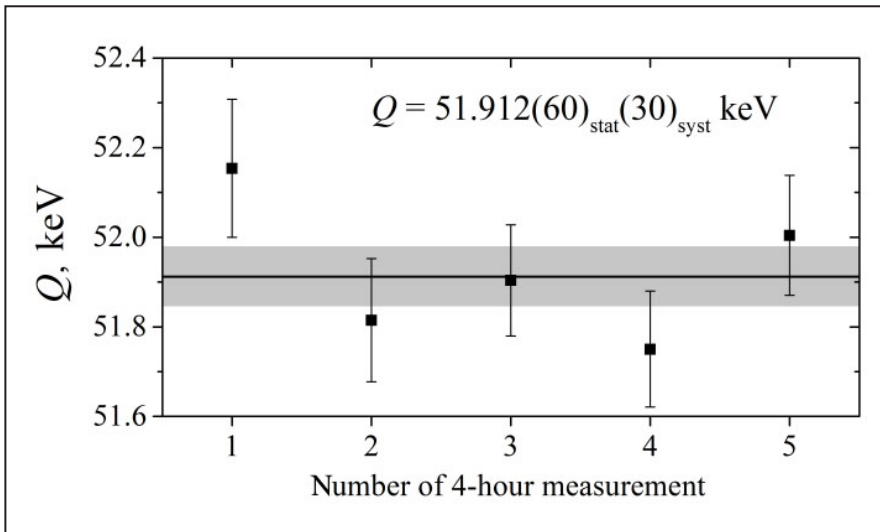


Fig. 3. The values of the decay energy of ^{123}Te obtained for separate measurement cycles

1. Filianin P. ..., Eliseev S., Novikov Yu. et al. // Phys. Lett. B. 2016. V. 758. P. 407–411.
 2. Takahashi K. ..., Novikov Yu.N. // Astroph. J. 2016. V. 819. P. 118.

Laser resonance ionization scheme development for tellurium and germanium

D.V. Fedorov
 High Energy Physics Division of NRC “Kurchatov Institute” – PNPI

Beams of ionized ^{116}Te and ^{118}Te are required for the Coulomb excitation experiment investigating change of shell-structure in the region near $Z = 50$. Earlier, tellurium beams at ISOLDE (CERN) have been produced using arc discharge ion sources, which do not offer the element selective capabilities. A laser ion source could provide the isobar-clean ion beam of tellurium. Search for an efficient scheme of laser ionization of Te has been carried out in 2016 (Fig. 1).

Laser ionized germanium beams are required for the study of the β^+/EC decay of ^{64}Ge and ^{66}Ge by total absorption spectroscopy. This is of importance for investigation of the rp -process development, responsible for nucleosynthesis in the as-

trophysical events. The experiments on the efficient laser resonance ionization scheme for germanium atoms have been carried out at RILIS facility. In Fig. 2 the most efficient of the tested germanium ionization schemes is presented.

An efficiency measurement has been performed for this scheme using a calibrated mass marker of germanium. During the sample evaporation, the laser ion signal was measured on a Faraday cup located after the mass-separator magnet. A ratio of the ion current integrated over the measurement time to the amount of atoms in mass marker gives the ionization efficiency value of 2%.

The work was performed in collaboration with colleagues from Switzerland, the UK and Germany.

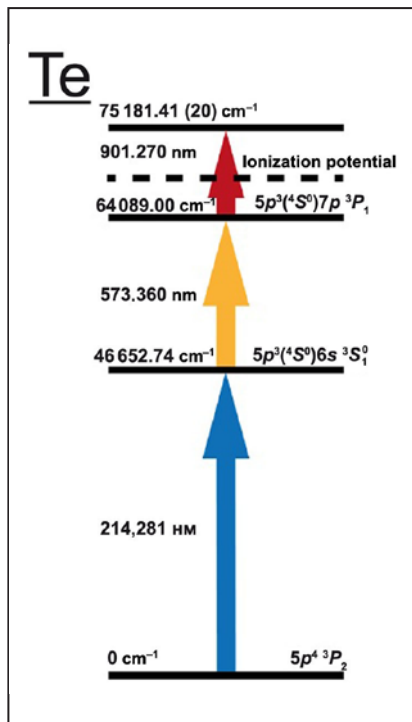


Fig. 1. The optimal tellurium RILIS scheme using autoionizing resonance

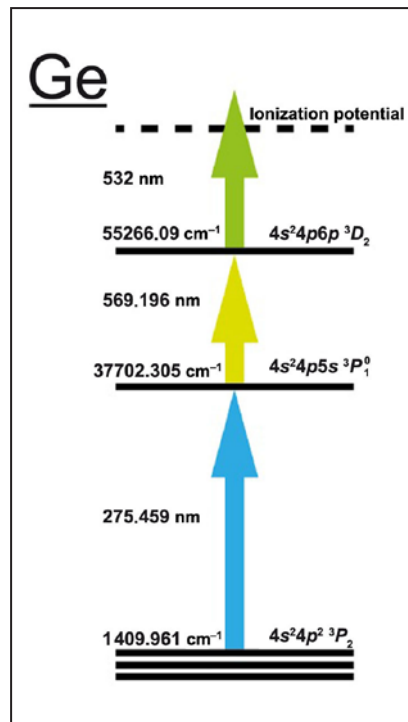


Fig. 2. The most efficient of the tested germanium ionization schemes

Investigation of the shape coexisting phenomena in the light thallium isotopes by laser spectroscopy

A.E. Barzakh, D.V. Fedorov, P.L. Molkanov, M.D. Seliverstov
High Energy Physics Division of NRC "Kurchatov Institute" – PNPI

Hyperfine structure (hfs) parameters and isotope shifts have been measured for the neutron-deficient thallium isotopes ($A = 179-184$) using the 276.9 nm atomic transition. The measurements were performed at ISOLDE (CERN) using the in-source resonance-ionization spectroscopy technique and Windmill setup for photoion current monitoring. From the analysis of the hfs, spins for $^{179, 181, 183}\text{Tl}^g$ were determined to be $I = 1/2$. Magnetic moments and changes in the nuclear mean-square charge radii have been deduced. A detailed analysis of the hyperfine structure patterns produced by different α and γ lines following the decay of ^{182}Tl confirms the existence of a low-spin isomer in ^{182}Tl . Magnetic moments of $^{179, 181, 183}\text{Tl}^g$ ($I = 1/2$) and $^{183}\text{Tl}^m$ [$I = (9/2)$] follow the respective parabolic and linear trends for the heavier Tl nuclei with the same spins (Fig. 1). The application of the additivity relation

for magnetic moments of the odd-odd Tl nuclei enables us to confirm leading configuration assignments and spins: $[\pi 3s_{1/2} \times \nu 1h_{9/2}]_{4-}$ for ^{180}Tl and $^{182}\text{Tl}^m$; $[\pi 3s_{1/2} \times \nu 1i_{13/2}]_{7+}$ for $^{182}\text{Tl}^m$ and $^{184}\text{Tl}^m$; $[\pi 1h_{9/2} \times \nu 1i_{13/2}]_{10-}$ for $^{184}\text{Tl}^m$. The charge radii of the $^{179-184}\text{Tl}$ ground states follow the trend previously observed for isotonic (spherical) lead nuclei (Fig. 2). A significant difference in charge radii for ground and isomeric (intruder, $9/2^-$, and 10^-) states of $^{183, 184}\text{Tl}$ is observed (Fig. 2, 3). The greater charge radii for the isomers suggest a larger deformation of these isomers compared to the ground states. The unexpected increase in the isomer shift for ^{183}Tl (Fig. 3) points to a possible prolate-oblate mixture.

The α decay of $^{182, 184}\text{Tl}$ was studied at the ISOLDE facility. The α decay of the three long-lived states in ^{184}Tl , (10^-), (7^+) and (2^-), has been disentangled and for the first time, α -decay branches

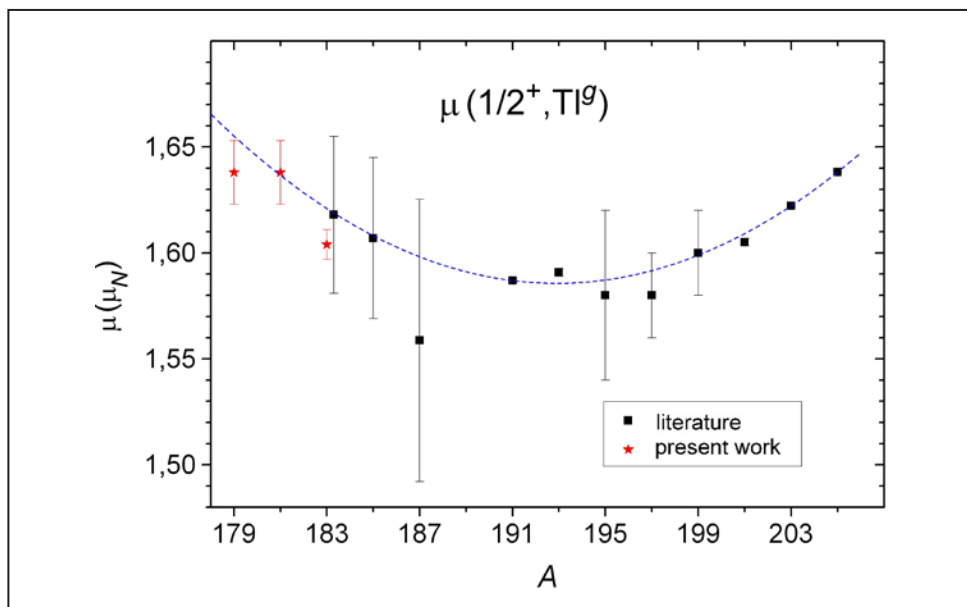


Fig. 1. Isotopic dependence of the magnetic moments of thallium ground states ($I = 1/2$)

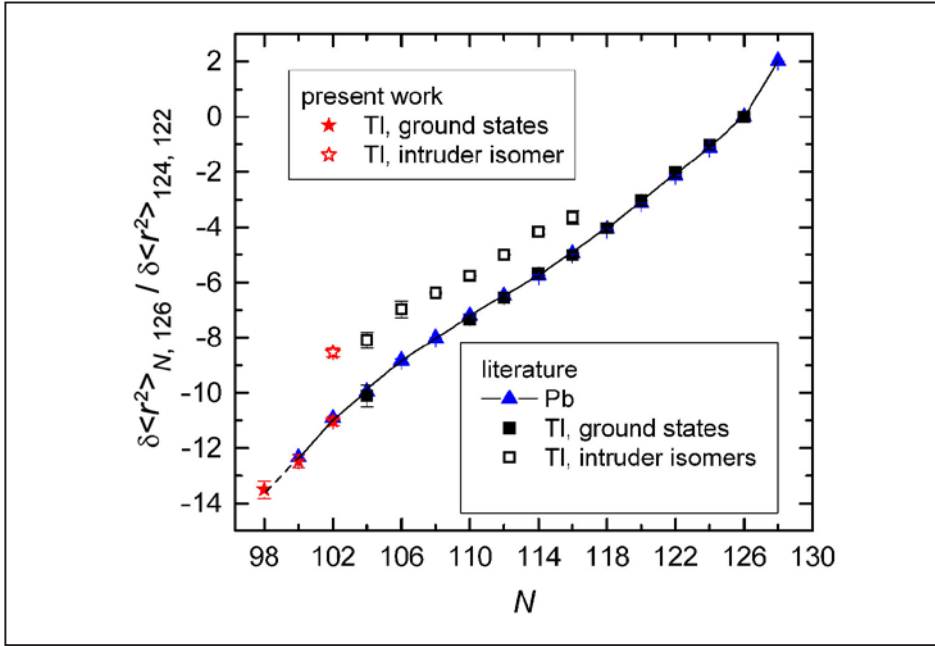


Fig. 2. Relative changes in $\delta \langle r^2 \rangle$ for the even-neutron thallium and lead nuclei

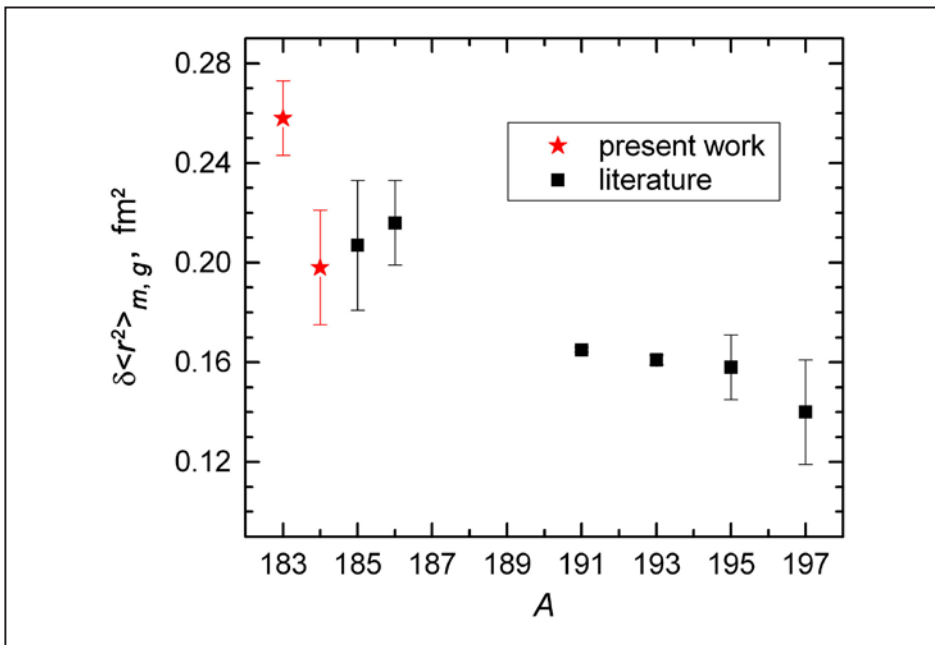


Fig. 3. Isomer shift between intruder and normal states for Tl isotopes. Only statistical errors are shown

for the (10^-) and (7^+) states were identified. New α -decay lines were identified also for ^{182}Tl . Only the ^{184}Tl (10^-) state is α decaying unhindered to a state in ^{180}Au , all other α -decay channels observed in this study are hindered, indicating a dif-

ferent underlying structure of the mother and daughter isotopes.

The work was done in collaboration with scientists from Japan, the UK, Belgium, Switzerland, Germany, France and Slovakia.

1. Beveren C. van ..., Barzakh A.E. ..., Fedorov D.V. et al. // J. Phys. G: Nucl. Part. Phys. 2016. V. 43. P. 025102.
2. Barzakh A.E. ..., Fedorov D.V. ..., Molkanov P.L. ..., Seliverstov M.D. et al. // Phys. Rev. C. 2017. V. 95. P. 014324.

Beta-delayed fission and alpha decay of ^{196}At

A.E. Barzakh, D.V. Fedorov, M.D. Seliverstov
High Energy Physics Division of NRC "Kurchatov Institute" – PNPI

We investigated the α -decay fine-structure and β -delayed fission (βDF) of the neutron-deficient isotope ^{196}At produced by using the laser ionization and mass-separation techniques at ISOLDE (CERN). By exploiting the purity of the ^{196}At sample due to the high selectivity of the laser system and a sensitive detection system, which also included HPGe detectors, new and significantly improved data were collected. In particular, several new excited states in the daughter ^{192}Bi were identified and multiplicities of γ rays from their decay were deduced (Fig. 1), which could be helpful for further in-beam studies of this isotope.

The systematics of the βDF in the astatine chain was extended to ^{196}At and includes now three βDF isotopes $^{192}, ^{194}, ^{196}\text{At}$. A mixture of symmetric and asymmetric fission-fragment mass distributions (multimodal fission) of the daughter isotope ^{196}Po (populated by β decay of ^{196}At) was deduced based on the measured fission-fragment energies (Fig. 2). This work extends the previous studies of the multimodal fission phenomenon

in the transactinides to the very neutron-deficient nuclei in the lead region. A βDF probability $P_{\beta\text{DF}}(^{196}\text{At}) = 9(1) \cdot 10^{-5}$ was determined.

The work was done in collaboration with scientists from Japan, the UK, Belgium, Slovakia, Switzerland, France and Germany.

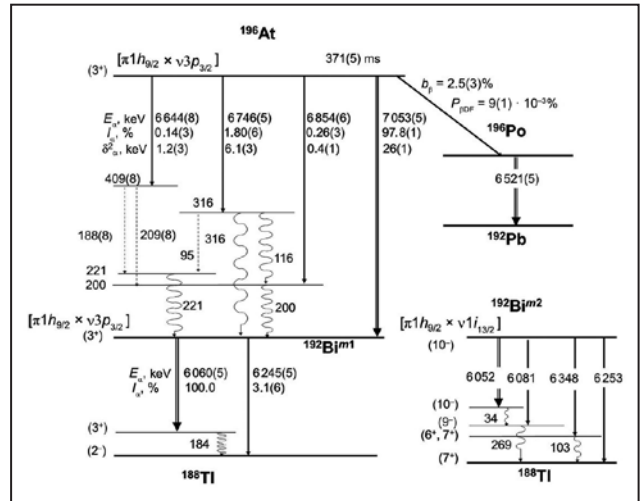


Fig. 1. Decay scheme of ^{196}At deduced in this work

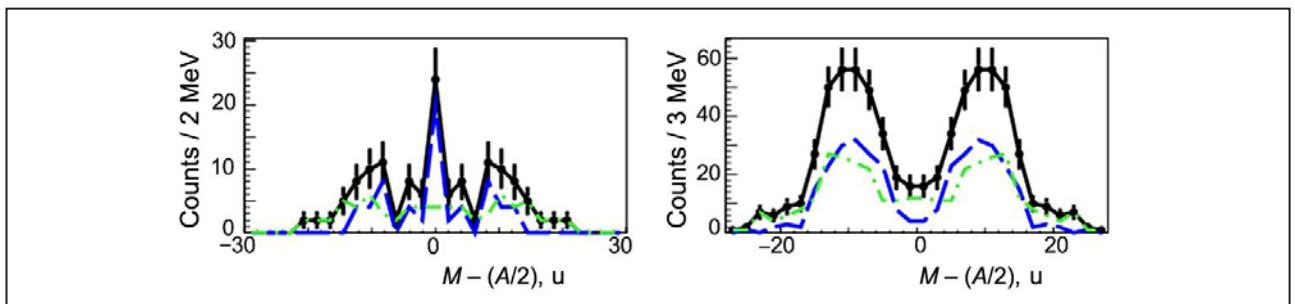


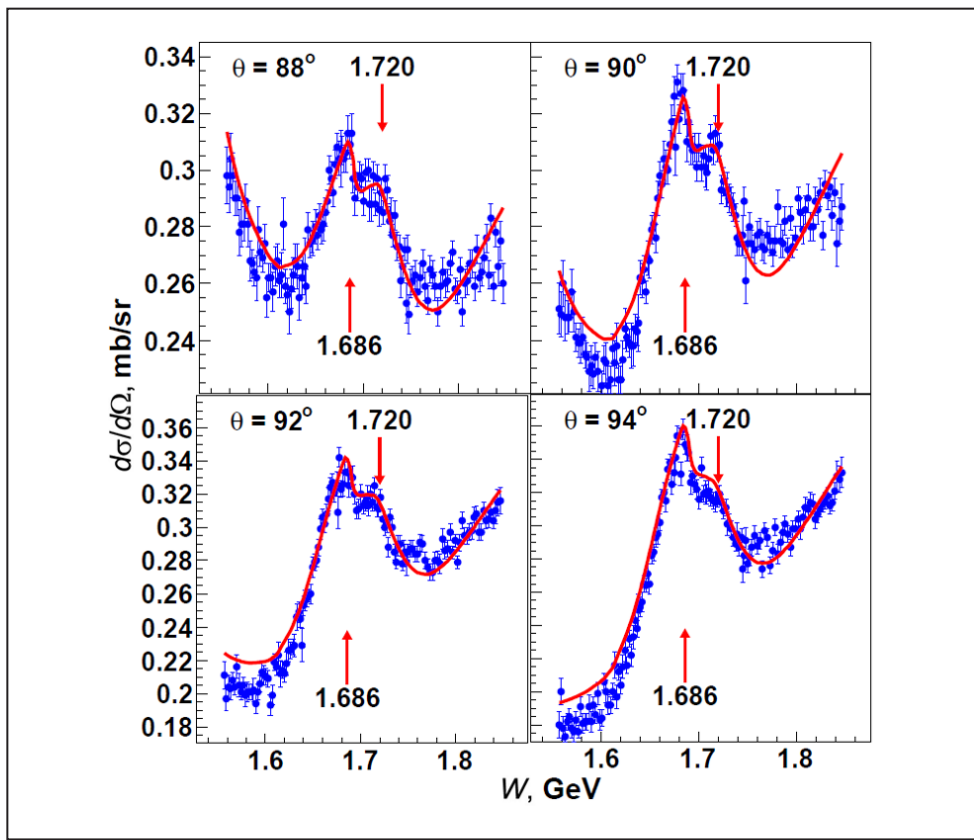
Fig. 2. Comparison of βDF data for ^{196}At (left panel, present work) and for ^{180}Tl (right panel, literature). The fission-fragment mass distributions are shown. The mass distributions shown by the black lines are for all observed events, while those shown by the dot-dashed green line and the dashed blue line correspond to events with the total kinetic energy (TKE) values below and above the most probable TKE values, respectively

Search for narrow resonances in πp elastic scattering from the EPECUR experiment

A.B. Gridnev, Ye.A. Filimonov, N.G. Kozlenko, V.S. Kozlov, A.G. Krivshich, V.A. Kuznetsov, D.V. Novinsky, V.V. Sumachev, V.I. Taranov, V.Yu. Trautman
 High Energy Physics Division of NRC “Kurchatov Institute” – PNPI

The analysis of high-precision πp elastic cross section data from the EPECUR Collaboration based on the multichannel K -matrix approach is presented. In total, about 10 000 new data points have been included in analysis. The sharp structures seen in these data are studied in terms of both opening thresholds and new resonance contributions. The results are shown in Figure. Some prominent features are found to be due to the opening $K\Sigma$ channel. However, a complete description of the data is improved with the addition of two

narrow resonant structures at $W \approx 1.686$ and $W \approx 1.720$ GeV. These structures are interpreted as manifestations of S_{11} and P_{11} resonances. Both resonances have the small widths and the small couplings to the elastic πN channel. This is in agreement with the predicted properties of the non-strange pentaquark state. We consider the $P_{11}(1724)$ resonance which has the nucleon quantum numbers to be the best candidate for the non-strange member of an exotic antidecuplet.



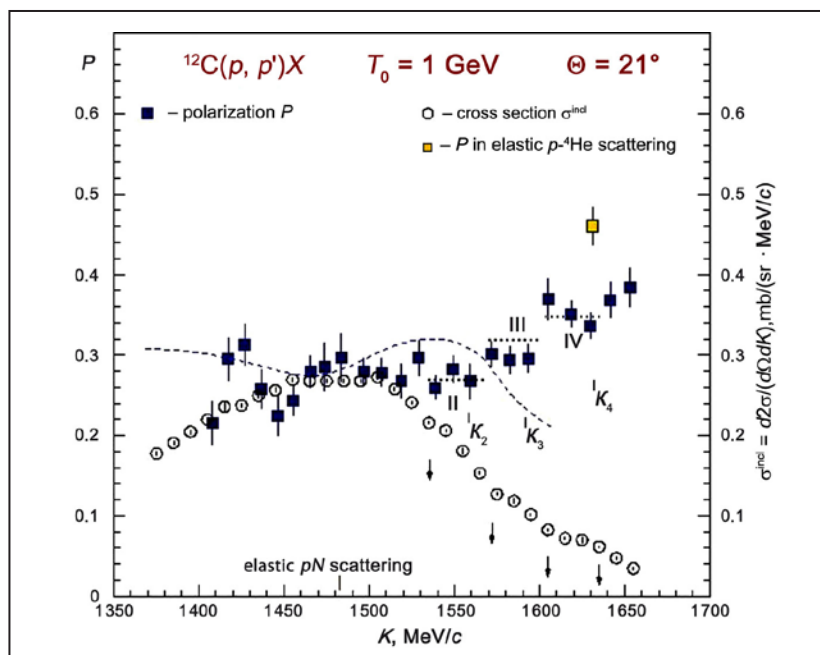
Differential πp elastic scattering. Red solid line gives the present calculation with added resonances

The structure effects in polarization and cross section in inelastic $A(p, p')X$ reaction with the ^{12}C and ^{40}Ca nuclei at 1 GeV

G.M. Amalsky, V.A. Andreev, G.E. Gavrilov, A.A. Izotov, A.Yu. Kisselev, N.G. Kozlenko, P.V. Kravchenko, M.P. Levchenko, O.V. Miklukho, D.V. Novinskiy, A.N. Prokofiev, A.V. Shvedchikov, S.I. Trush, A.A. Zhdanov
High Energy Physics Division of NRC "Kurchatov Institute" – PNPI

The structure effects in the polarization and cross section of the inclusive $A(p, p')X$ reaction with nuclei (Figure – scattering off the ^{12}C nucleus) were for the first time observed [1]. The dotted line segments correspond the momentum intervals II, III, and IV where the polarization doesn't depend practically on the secondary proton momentum (K). An averaged value of the polarization increases from the interval II to interval IV. The onset of each momentum interval is close to momentum (marked in Fig. by arrow) which corresponds to a slowing down of the cross section drop. The observed behaviour of polarization and cross section in the momentum ranges II, III, and IV can be related to proton quasi-elastic scattering off nucleon associations (correlations) which consist of two, three, and four nucleons, re-

spectively. A contribution from the scattering off the uncorrelated nuclear nucleons is strongly suppressed in the intervals III and IV, since these nucleons have a momentum upwards of the Fermi momentum ($K_F \sim 250$ MeV/c). K_2 , K_3 , and K_4 correspond to the final proton momenta in quasi-elastic scattering off the ^2H , ^3He (^3H), and ^4He – like immovable nucleon clusters. In these calculations the masses of real light nuclei were used as the nucleon correlation masses. The residual nuclei (X) in the reactions were assumed to be in a ground state. A width of the momentum intervals mentioned above is determined by a motion of the correlations. Note that a high momentum range, just following the momentum interval IV, possibly corresponds to quasi-elastic scattering off the residual nuclei X of the reactions considered above.



Dashed curve corresponds to polarization P calculated in the framework of a spin-dependent Distorted Wave Impulse Approximation taking into account a modification of the nucleon spinor in nuclear medium. Reaction kinematics: at $K > 1480$ MeV/c the four-momentum Q transferred to a nucleus is practically constant and equal to 600 MeV/c ($Q > 2K_F$)

Investigation of fragmentation ($Z = 2$) of relativistic nuclei ^{16}O and ^{208}Pb

E.A. Kotikov

Knowledge Transfer Division of NRC "Kurchatov Institute" – PNPI

For investigation of fragmentation ($Z = 2$) of relativistic nuclei the angular distributions of double charged fragments of a nucleus ^{16}O with the momentum 4.5A GeV/c and ^{208}Pb with the momentum 160A GeV/c are used during their interaction with photoemulsion nuclei. The primary measurements of oxygen and lead were made in High Energy Physics Division. In this work the events with two and more double charged fragments of a primary nucleus are reviewed separately.

The results of the approximation of experimental distribution of paired angles in events with two, three, and four double charged fragments of a nucleus ^{16}O by normal probability distribution using the software program Origin Pro 7.0 is shown in the Table.

According to the statistical model $\sigma(\varphi_{ij})$ equals 14.45 mrad, which does not correspond to the obtained experimental results. Therefore, not in a single group of the investigated events the statistical model of nuclei fragmentation describes the momentum distribution of double charged fragments in a fragmentation of a ^{16}O nucleus.

In the search for events (with 2–4 α particles) the "pure" events of a type $^{16}\text{O} \rightarrow \alpha + ^{12}\text{C}$, $^{16}\text{O} \rightarrow \text{Li} + \text{B}$ and $^{16}\text{O} \rightarrow p + \text{N}$ were also observed. The excited states of Li, B, ^{12}C and N can contribute to the double charged fragments under consideration.

The visual observation of the ^{16}O nuclei fragmentation with four double charges fragments suggests that ^{16}O nucleus itself can represent one of: ($p + \text{N}$), ($\text{Li} + \text{B}$), ($\text{Be} + \text{Be}$) и ($\text{He} + \text{C}$) virtual

cluster structures in a dynamic state. The observed ensembles of the ^{16}O nucleus clusters emerge as a result of the electromagnetic effect of a target nucleus (virtual γ quantum) and the nuclear interaction inside ^{16}O .

The obtained values $\sigma(\varphi_{ij})$ in all groups of events differ significantly (with respect to the measurement value) from those (520 μrad) expected from the statistical model. Therefore, not in a single group of the investigated events the statistical model of nuclei fragmentation describes the momentum distribution of double charged fragments in a fragmentation of a ^{208}Pb nucleus.

This work has yielded the result that is an alternative to a common belief that fragmentation of relativistic nuclei in a wide range of masses and energy conforms to the statistical model. The work also suggests that entire and minute investigation of fragmentation of relativistic nuclei can impart information about their structure frame. This being said, the investigation has to begin from lightest nuclei moving to heavier ones step by step.

Table. Parameters of approximating functions

$\sigma(\varphi_{ij}) = 9.3 \pm 0.5 \text{ mrad}$	$\chi^2 = 0.95$	(2 α)
$\sigma(\varphi_{ij}) = 9.5 \pm 0.5 \text{ mrad}$	$\chi^2 = 0.94$	(3 α)
$\sigma(\varphi_{ij}) = 6.1 \pm 0.5 \text{ mrad}$	$\chi^2 = 0.86$	(4 α)

Search for low-energy neutrino and antineutrino signals of Borexino correlated with gamma-ray bursts

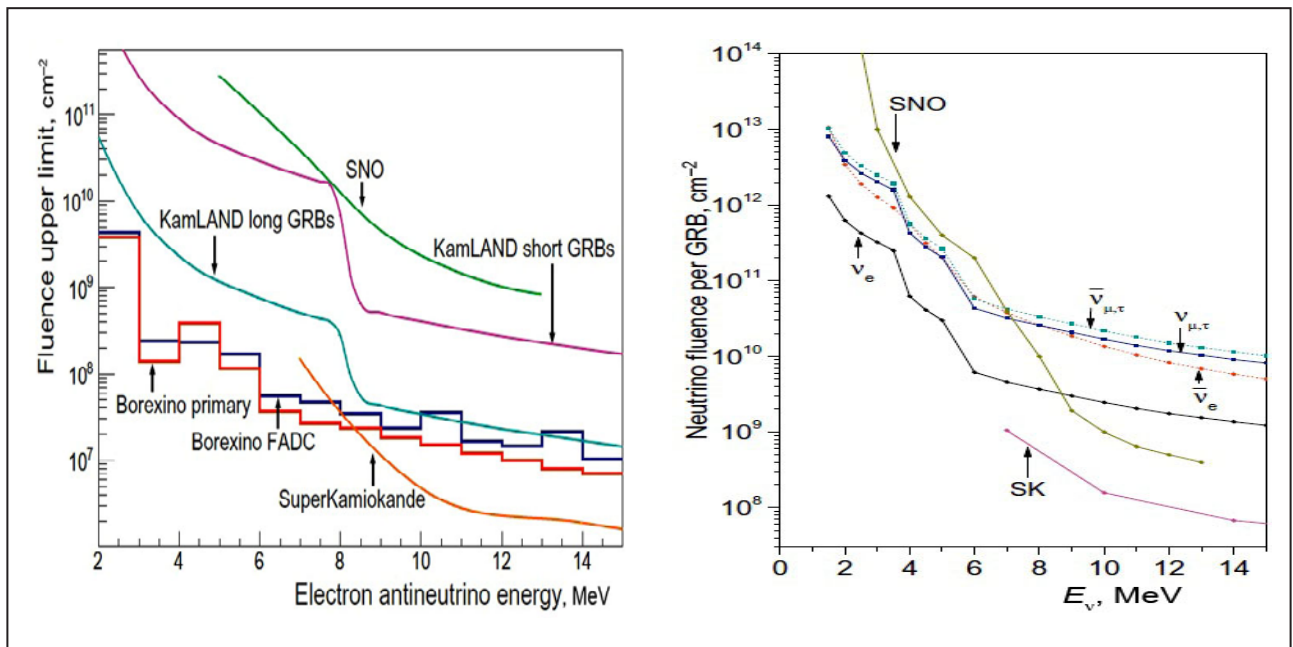
BOREXINO Collaboration

A.V. Derbin, I.S. Drachnev, V.N. Muratova, D.A. Semenov, E.V. Unzhakov – Neutron Research Division of NRC “Kurchatov Institute” – PNPI

Gamma-ray burst (GRB) is a large-scale explosive energy emission of the cosmic nature observed in distant galaxies in the hard part of the electromagnetic spectrum. The duration of a typical GRB is a few seconds. The Borexino Collaboration analyzed correlations of Borexino detector data collected in the period from December 2007 to November 2015 with 2350 GRBs. Employees of NRC “Kurchatov Institute” – PNPI proposed to search for correlations not only with the events of inverse beta decay for electron antineutrinos,

but also with the events of neutrino-electron scattering for all neutrino flavors. No statistically significant correlations have been found. The most stringent upper limits on the fluence in neutrinos and antineutrinos associated with a GRB have been obtained for energies below 7-8 MeV (Fig.).

The results were obtained with active participation of Russian researchers from NRC “Kurchatov Institute” – PNPI, NRC “Kurchatov Institute”, JINR and INP MSU. The work is supported by RFBR grants No. 15-02-02117 and No. 16-29-13014.



On the left: fluence upper limits for electron antineutrinos from GRBs versus antineutrino energy. Borexino results are shown in comparison with results from Super-Kamiokande, SNO, and KamLAND.

On the right: Borexino 90% C.L. fluence upper limits obtained through neutrino-electron elastic scattering for ν_e , $\bar{\nu}_e$, $\nu_{\mu,\tau}$, and $\bar{\nu}_{\mu,\tau}$. The limits obtained for ν_e by SNO and Super-Kamiokande are also shown

The first results of dark matter search with low-radioactivity argon in DarkSide-50 detector

DarkSide Collaboration

A.V. Derbin, V.N. Muratova, D.A. Semenov, E.V. Unzhakov – Neutron Research Division of NRC “Kurchatov Institute” – PNPI

The DarkSide-50 experiment searches for dark matter in the form of weakly interacting massive particles (WIMPs), whose collisions with argon nuclei would produce nuclear recoils with recoil energy of tens of keV. These argon nuclei can be registered by the detector (Fig. 1). NRC “Kurchatov Institute” – PNPI participates in the DarkSide Collaboration since its inception in 2010. DarkSide-50 is a two-phase liquid-argon TPC with 46 kg mass. In 2016, an underground argon with the content of radioactive ^{39}Ar isotope contamination 1 400 times less than the atmospheric argon

was used in the detector for the very first time ever. As a result of new measurement that lasted for 71 days, the most stringent limits on the spin-independent cross sections and masses of massive weakly interacting particles have been obtained for argon-based detectors (Fig. 2).

The results were obtained with active participation of Russian researchers from NRC “Kurchatov Institute” – PNPI, NRC “Kurchatov Institute”, JINR and INP MSU. The work is supported by RFBR grants No. 15-02-02117 and No. 16-29-13014.

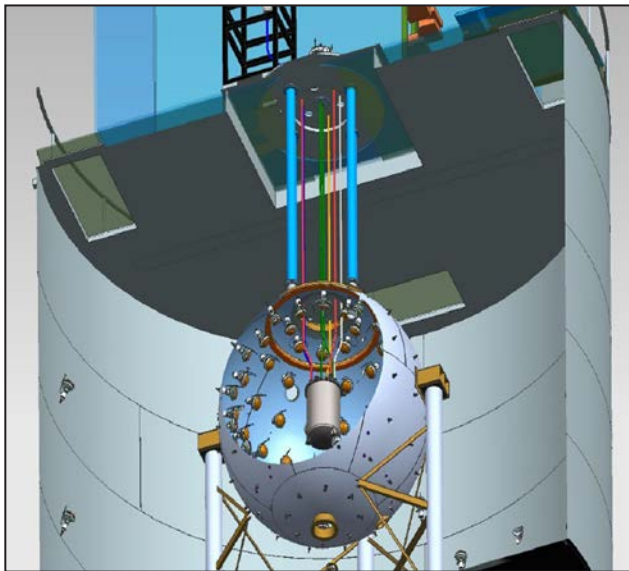


Fig. 1. DarkSide-50 scheme. The central detector is inside a steel sphere filled with the scintillator with the addition of boron to absorb neutrons. The entire structure is placed inside a water tank for suppression of external gamma activity

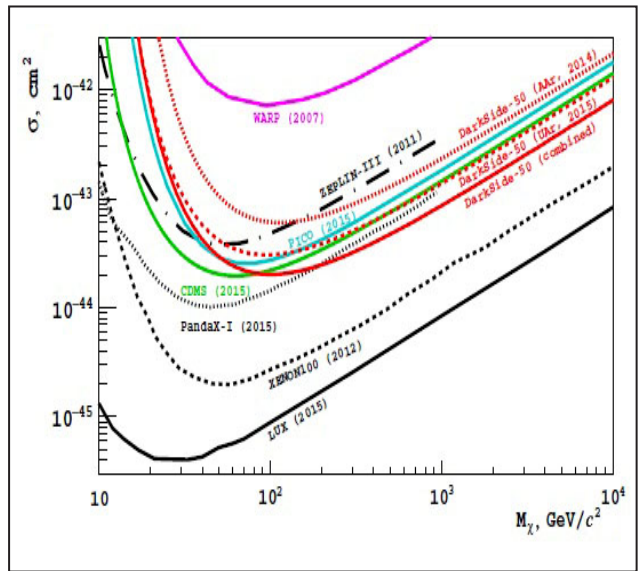


Fig. 2. Spin-independent WIMP-nucleon cross section 90% C.L. exclusion plots for the DarkSide-50 (red lines). There are also results from LUX and XENON100 that obtained more stringent limits with liquid Xe-detectors

1. DarkSide Collaboration // Phys. Lett. B. 2015. V. 743. P. 456.
 2. DarkSide Collaboration // Phys. Rev. D. 2016 V. 93. P. 081101.

Recovery method of gas discharge detectors at appearance of the malter effect

G.E. Gavrilov, O.E. Maev, D.A. Maisuzenko, S.A. Nasybulin
High Energy Physics Division of NRC "Kurchatov Institute" – PNPI

The problem of aging of the gas discharge particle detectors still remains relevant to modern physical facilities, including experiments at the Large Hadrons Collider (LHC). This work is devoted to the development of an anti-Malter effect (ME) method, which is one of the most common types of cathode aging, leading to the emergence of zones of the spontaneous self-sustaining current in the detector.

Today when working on the LHC beam a significant number of multiwire proportional chambers (MWPC) of the LHCb muon detector demonstrate recurrent appearance of Malter currents. This leads to the distortion of the output data, to the accumulation of the huge local doses in the detector and to the alarm resets of high-voltage power supply sources.

Usually the emergence of the ME is associated with the zone growing on the cathode surface, which consists of high resistive silicon-compound film that is charged by positive ions and stimulates the secondary electron emission in the MWPC. To suppress the ME, the working gas mixture is added to water vapor, or various alcohols, which stop the polymerization and remove the charge from the film. However, these additives do not eliminate but only quench Malter currents, and during the work a permanent use of the modified gas mixture is needed. As a result, there is a risk of chemical interaction of the additives with MWPC structural materials. Therefore, given methods of ME extinguishing cannot be applied to all proportional chambers.

Then in the LHCb experiment the proportional chambers are recovered from ME with long-term training at high Malter current in the working gas mixture of 55% Ar + 40% CO₂ + 5% CF₄. The recovery procedure of the Malter current zone can vary from one to several weeks. To accelerate and improve the efficiency of the recovery a new the method based on training in the working mixture supplemented with 2% oxygen has been developed. The method was tested at four MWPCs dismounted from the LHCb muon detector due to the high Malter currents. ME suppression procedure consisted in localization of the self-sustaining current ignition zones by scanning of the chamber with β -source ⁹⁰Sr and then in training of these zones at high Malter current under ⁹⁰Sr electron irradiation. As a result, the removal of the ME took just 4–6 hours.

Figure 1 shows the Malter currents during the training procedure by the working gas mixture (—◊—) and by the new mixture with addition of 2% oxygen (—○—). The growth of the ME ignition voltage during MWPC workout without adding oxygen and with 2% oxygen in the gas mixture is demonstrated in Fig. 2.

The results of the LHCb chambers recovery have the long-term character: all MWPC recovered by the new method are successfully working on the LHC beam. It is evident that the use of the MWPC recovery method presented above can be widely applied to the detectors in other experiments.

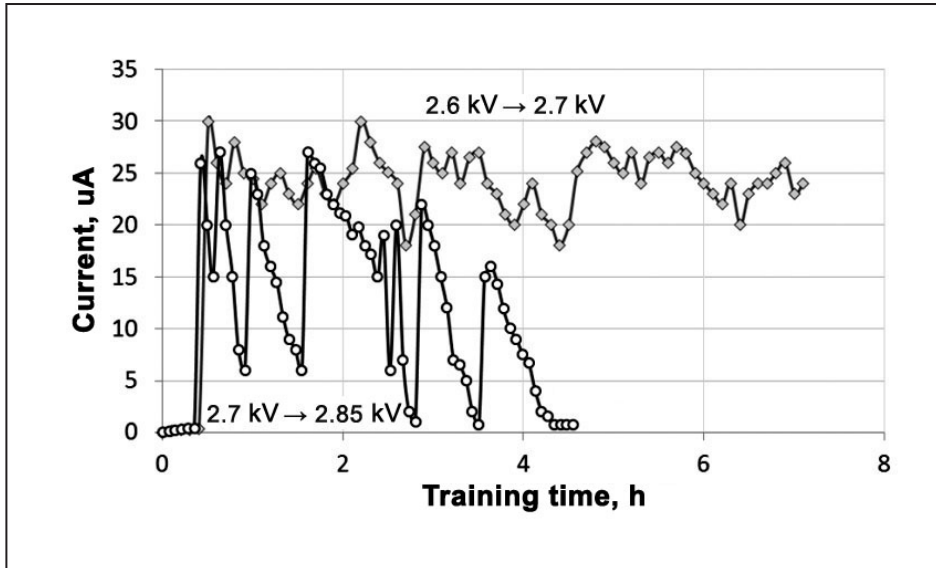


Fig. 1. Maltor currents during the training:
 —◇— by working gas mixture 55% Ar + 40% CO₂ + 5% CF₄;
 —○— by working gas mixture with 2% oxygen

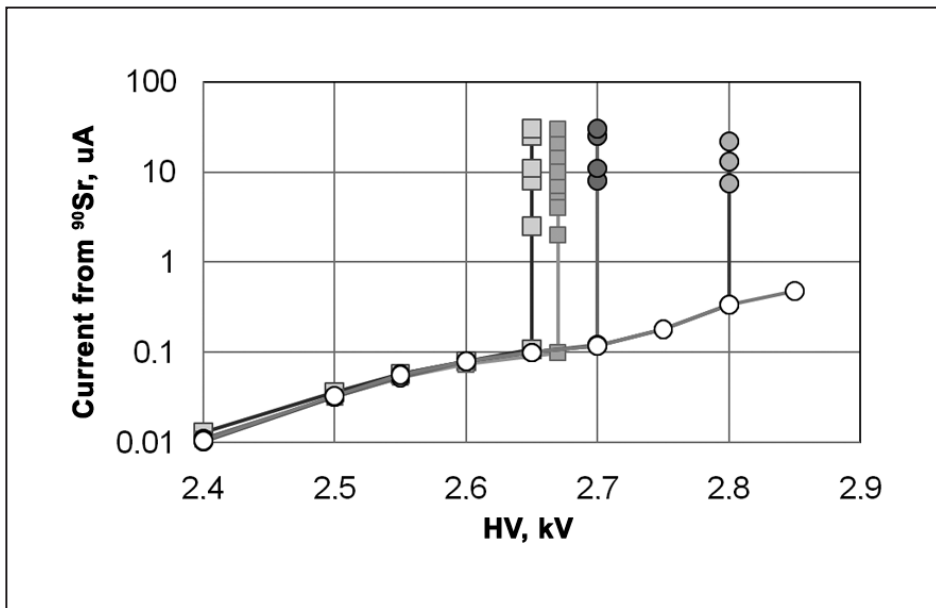
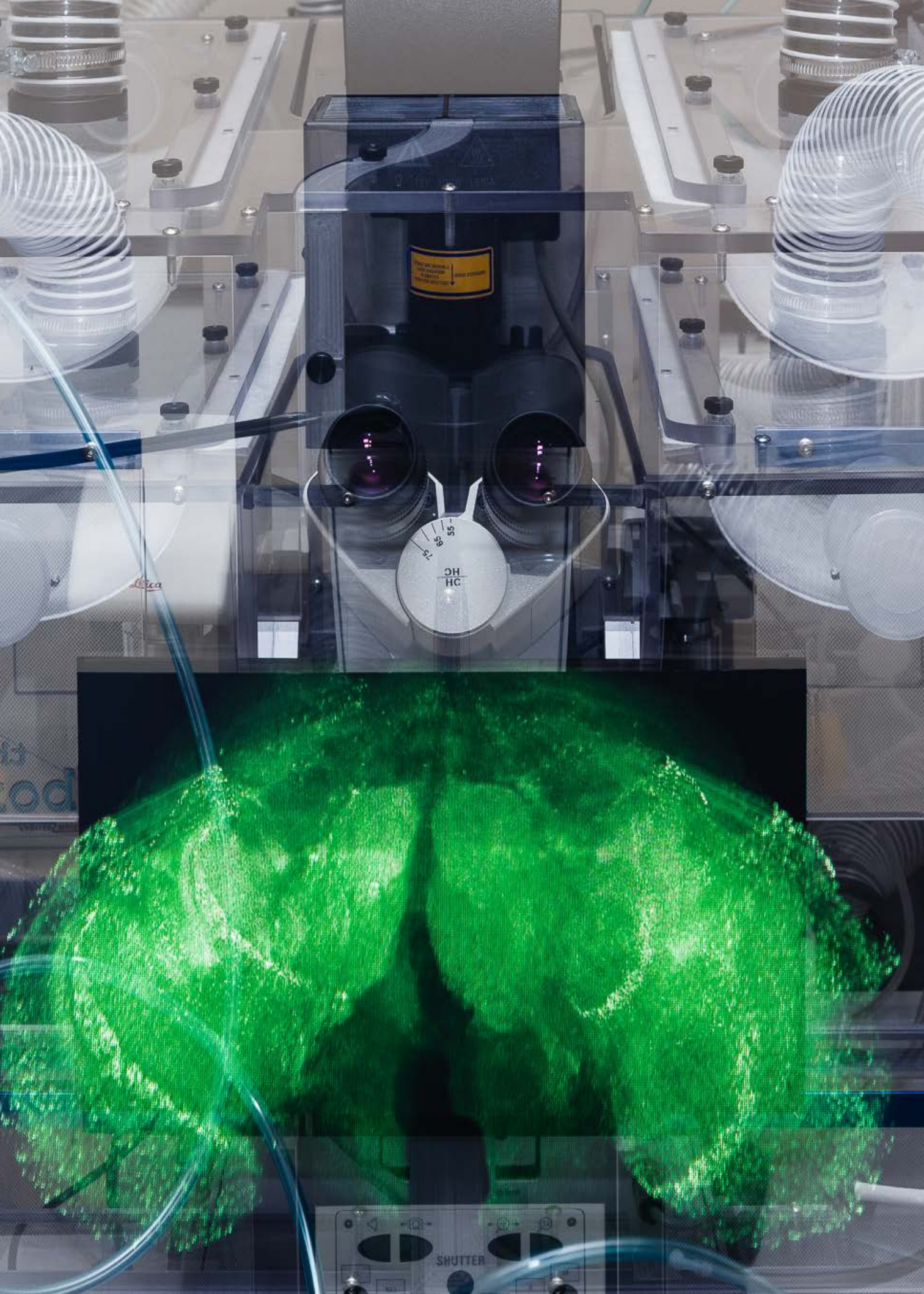


Fig. 2. Dependences of the ⁹⁰Sr ionization current on high voltage (HV) during training in the working gas mixture: ● at the beginning, ■ in 7 h and during training with the addition of 2% oxygen: □ in 2 h, ○ in 4 h, ○ in 6 h



Molecular and Radiation Biophysics

- 94 Partially assembled nucleosome structures at atomic detail: molecular dynamics model and experimental data interpretation
- 96 Characterization of a new α -L-fucosidase isolated from *Fusarium proliferatum* LE1 that is regioselective to α -(1 \rightarrow 4)-L-fucosidic linkage in the hydrolysis of α -L-fucobiosides
- 97 DNA metabolism in balance: rapid loss of a RecA-based hyperrec phenotype
- 98 The structural disorder of oligomers of intrinsically disordered brain proteins BASP1 and GAP-43
- 99 Detection of experimental myocardium infarction in rats by MRI using heat shock protein 70 conjugated superparamagnetic iron oxide nanoparticle
- 100 Microbiology of the subglacial Antarctic Lake Vostok: borehole-frozen lake water
- 101 Proteomic profiling of high-grade glioblastoma using virtual-experimental 2DE
- 102 A role for tuned levels of nucleosome remodeler subunit ACF1 during *Drosophila* oogenesis

Partially assembled nucleosome structures at atomic detail: molecular dynamics model and experimental data interpretation

A.V. Ilatovskiy, V.V. Isaev-Ivanov, A.Yu. Konev, D.V. Lebedev, G.N. Rychkov, A.V. Shvetsov – Molecular and Radiation Biophysics Division of NRC “Kurchatov Institute” – PNPI
 A.V. Ilatovskiy – Skaggs School of Pharmacy and Pharmaceutical Sciences
 I.B. Nazarov – Institute of Cytology RAS
 A.V. Onufriev – Virginia Polytechnic Institute and State University

For the first time, we built full-atom models of partially assembled nucleosome structures (PANS) (Figure 1: the disome (a), the tetrasome (b) and the hexasome (c)), that are believed to be important for key biological processes related to processing and maintenance of genetic information carried by the DNA. Structural characteristics of PANS were compared with the core nucleosome particle – the octasome (d). Potential DNA accessibility for nuclear factors in PANS were revealed (Figure 1, top left). We have also illustrated utility of the atomistic models of subnucleosomal states for *in vitro*

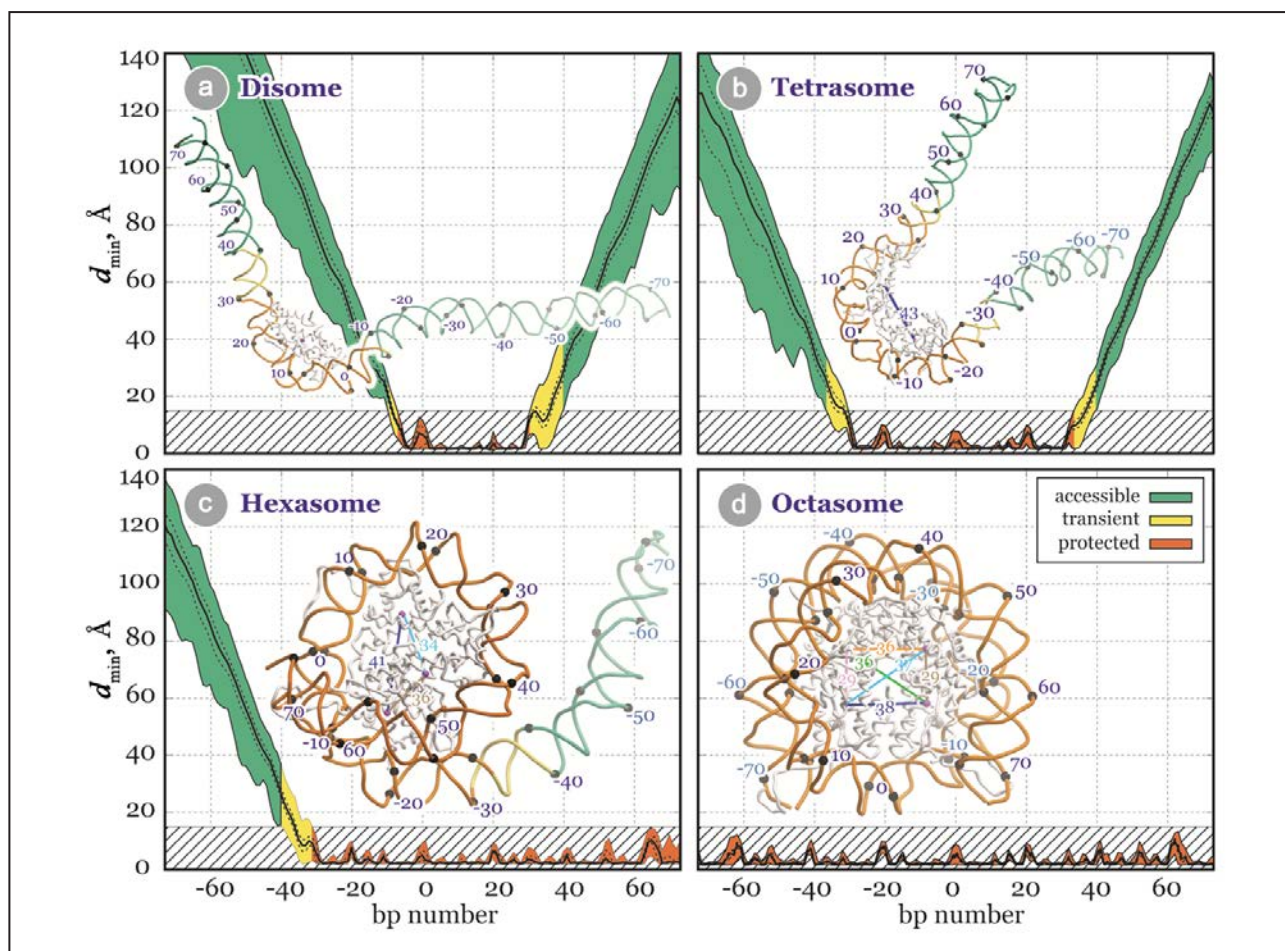


Fig. 1. Nucleosome particles: the disome (a), the tetrasome (b), the hexasome (c) and the octasome (d). Full-atom models of PANS and computational data on protected DNA lengths

studies, including interpretation of AFM (Figure 1, bottom), FRET, and SAXS experiments. Further, we suggested an alternative interpretation of a recent genome-wide study of DNA protection in active chromatin of fruit fly, leading to a conclusion that the three PANS are present in actively transcrib-

ing regions in a substantial amount. The presence of PANS may not only be a consequence, but also a prerequisite for fast transcription *in vivo*. The results of the study were published in the special issue of Biophysical Journal devoted to chromatin biophysics.

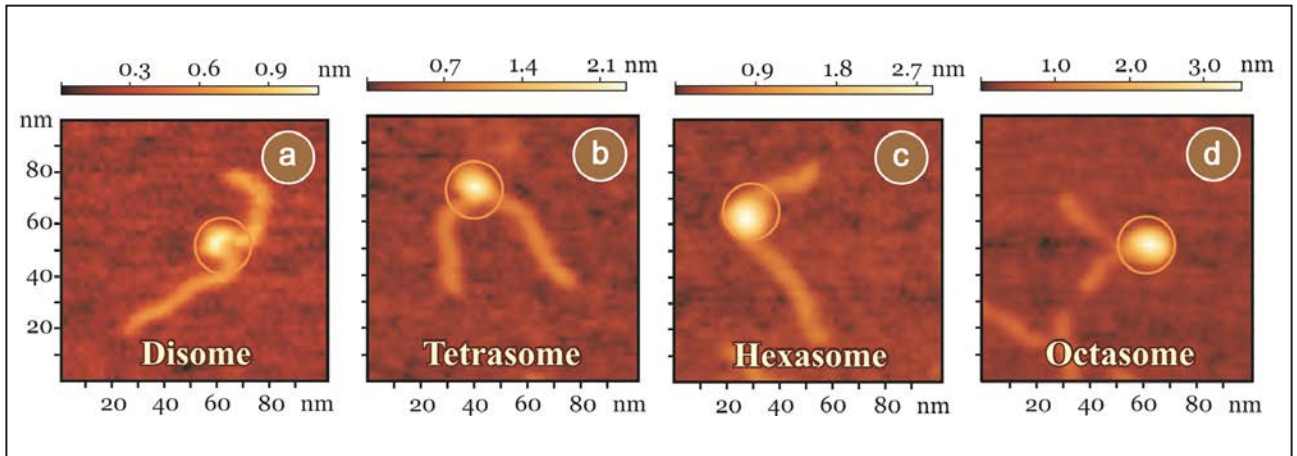


Fig. 2. Representative images of PANS observed in AFM experiment: the disome (a), the tetrasome (b), the hexasome (c) and the octasome (d)



Fig. 3. The graphical review of the work published at the cover of Biophysical Journal (2017, No. 112(3)) – the nucleosome particles are arranged to form the abbreviation “PANS”

Characterization of a new α -L-fucosidase isolated from *Fusarium proliferatum* LE1 that is regioselective to α -(1 \rightarrow 4)-L-fucosidic linkage in the hydrolysis of α -L-fucobiosides

K.S. Bobrov, E.V. Eneyskaya, D.R. Ivanen, A.A. Kulminskaya,
S.N. Naryzhny, K.A. Shabalin, S.V. Shvetsova –
Molecular and Radiation Biophysics Division of NRC “Kurchatov Institute” – PNPI
A.A. Kulminskaya, K.A. Shabalin, S.V. Shvetsova –
Peter the Great St. Petersburg Polytechnic University
V.B. Krylov, N.E. Nifantiev, N.E. Ustyuzhanina – N.D. Zelinsky Institute of Organic Chemistry RAS
S.N. Naryzhny, V.G. Zgoda – V.N. Orekhovich Research Institute of Biomedical Chemistry of RAMS

Here, we report the biochemical characterization of a novel α -L-fucosidase with broad substrate specificity (FpFucA) isolated from the mycelial fungus *Fusarium proliferatum* LE1. Highly purified α -L-fucosidase was obtained from several chromatographic steps after growth in the presence of L-fucose. The purified α -L-fucosidase appeared to be a monomeric protein with an isoelectric point of $pI = 5.21 \pm 0.05$ and molecular mass of 67 ± 1 kDa. The enzyme is sufficiently stable in a wide pH range of 4.5–6.0 demonstrating the optimum pH at 5.5. The optimal value of the temperature in the hydrolysis of a synthetic substrate pNPFuc is equal to 45 °C, but after incubating the enzyme for 20 minutes at this temperature, the activity was reduced by half. Enzyme is able to hydrolyze the synthetic substrate p-nitrophenyl α -L-fucopyranoside (pNPFuc), with $K_m = 1.1 \pm 0.1$ mM and $k_{cat} = 39.8 \pm 1.8$ s⁻¹. L-fucose, 1-deoxyfuconojirimycin and tris(hydroxymethyl)aminomethane inhibited pNPFuc hydrolysis, with inhibition constants of 0.2 ± 0.05 mM, 7.1 ± 0.05 nM, and 12.2 ± 0.1 mM, respectively. The analysis of the divalent metal ions influence on the enzyme activity shows a significant inhibitory effect of Hg²⁺, which may indicate the presence of sulfhydryl groups in the catalytic site respon-

sible for enzyme activity. We assumed that the enzyme belongs to subfamily A of the GH29 family (CAZy database) based on its ability to hydrolyze practically all fucose containing oligosaccharides used in the study and the phylogenetic analysis. Among pNP- α / β -glucosides enzyme FpFucA was specific only for pNPFuc. A set of fucose-containing substrates including specifically synthesized difucosides with “pure” L-fucosidic linkage as well as natural fucooligosaccharides (Le^x, Le^d, L-Fuc- α -OPr, L-Fuc- α -(1 \rightarrow 4)-D-GlcNAc-PAA and 6-O- α -L-Fuc-N,N'-diacetyl-chitobiose) was used to determine the substrate specificity. We found that this enzyme was a unique α -L-fucosidase that preferentially hydrolyzes the α -(1 \rightarrow 4)-L-fucosidic linkage present in α -L-fucobiosides with different types of linkages. As a retaining glycosidase, FpFucA is capable of catalyzing the transglycosylation reaction with alcohols (methanol, ethanol, and 1-propanol) and pNP-containing monosaccharides as acceptors. These features make the enzyme an important tool that can be used in the various modifications of valuable fucose-containing compounds.

Part of the research was supported by the Russian Science Foundation (RSF) grant No. 16-14-00109.

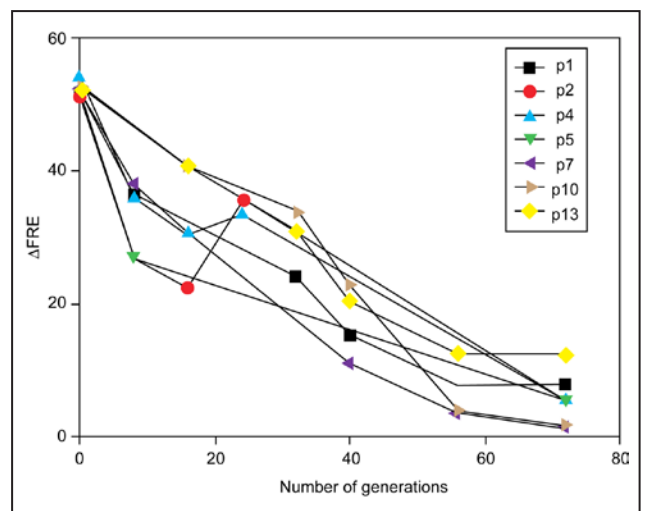
1. Shvetsova S.V., Zhurishkina E.V., Bobrov K.S., Ronzhina N.L., Lapina I.M., Ivanen D.R. ..., Kulminskaya A.A. // J. Basic Microbiol. 2015. V. 55. No. 4. P. 471–479.
2. Shvetsova S.V., Shabalin K.A., Bobrov K.S., Ivanen D.R. ..., Krylov V.B. ..., Naryzhny S.N. ..., Eneyskaya E.V., Kulminskaya A.A. // Biochimie. 2017. V. 132. P. 54–65: doi: 10.1016/j.biochi.2016.10.014.

DNA metabolism in balance: rapid loss of a RecA-based hyperrec phenotype

V.A. Lanzov, D.M. Baitin, I.V. Bakhlanova, A.V. Dudkina –
Molecular and Radiation Biophysics Division of NRC “Kurchatov Institute” – PNPI
M.M. Cox, E.A. Wood – University of Wisconsin–Madison

The RecA recombinase of *Escherichia coli* has not evolved to optimally promote DNA pairing and strand exchange, the key processes of recombinational DNA repair. Instead, the recombinase function of RecA protein represents an evolutionary compromise between necessary levels of recombinational DNA repair and the potentially deleterious consequences of RecA functionality. A RecA variant, RecA D112R, promotes conjugational recombination at substantially enhanced levels. We demonstrated that the frequency of recombination exchanges (FRE) is increased over fiftyfold when RecA D112R replaces the wild type RecA protein in *E. coli*. Cells expressing RecA D112R thus exhibit a hyperrec phenotype. However, expression of the D112R RecA protein in *E. coli* results in a reduction in cell growth rates. This report documents the consequences of the substantial selective pressure associated with the RecA-mediated hyperrec phenotype. With continuous growth, the deleterious effects of RecA D112R, along with the observed enhancements in conjugational recombination, are lost over the course of 70 cell generations (Fig.). The suppression reflects a decline in RecA D112R expression, associated primarily with a deletion in the gene promoter or chromosomal mutations that decrease plasmid copy number. The deleterious effects of RecA D112R on cell growth can also be negated by over-expression of the RecX protein. The effects of the RecX proteins

in vivo parallel the effects of the same proteins on RecA D112R filaments *in vitro*. The only known function of RecX protein is the removal of RecA protein from the DNA. The capacity of RecX to eliminate the growth deficiency in cells expressing RecA D112R implies that this RecA variant simply binds to chromosomal DNA too persistently. The results indicate that the toxicity of RecA D112R is due to its persistent binding to duplex genomic DNA, creating barriers for other processes in DNA metabolism. A substantial selective pressure is generated to suppress the resulting barrier to growth.



Loss of hyperrec phenotype in cells expressing RecA D112R upon continuous culture

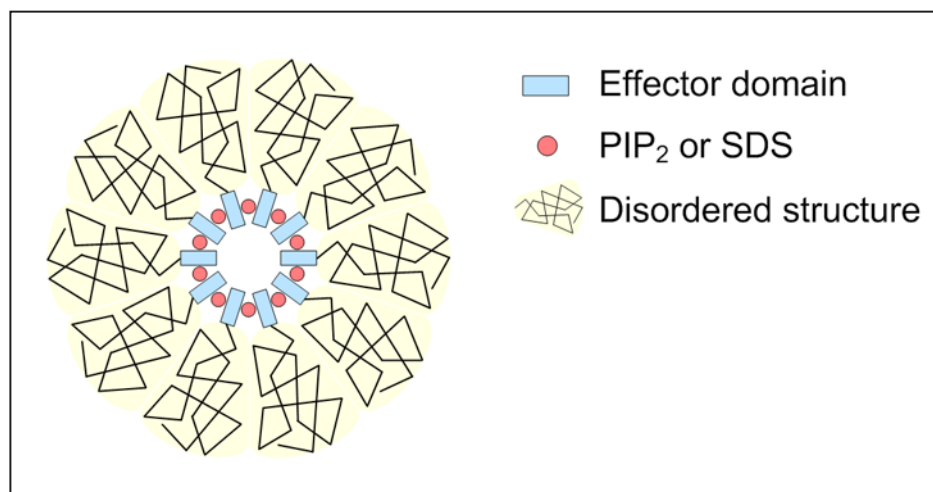
The structural disorder of oligomers of intrinsically disordered brain proteins BASP1 and GAP-43

O.S. Forsova, V.V. Zakharov

Molecular and Radiation Biophysics Division of NRC “Kurchatov Institute” – PNPI

BASP1 and GAP-43 are presynaptic membrane proteins participating in axon guidance, neuroregeneration and synaptic plasticity. They are presumed to sequester phosphatidylinositol-4,5-diphosphate (PIP₂) in lipid rafts. Previously we have shown that the proteins form heterogeneously-sized oligomers in the presence of anionic phospholipids or sodium dodecyl sulfate (SDS) at submicellar concentration. BASP1 and GAP-43 are intrinsically disordered proteins (IDPs). In light of this, we investigated the structure of their oligomers. Using partial cross-linking of the oligomers with glutaraldehyde, the aggregation numbers of BASP1 and GAP-43 were estimated as 10–14 and 6–7 monomer subunits respectively. The cross-linking pattern indicated that the subunits are circularly arranged. The circular dichroism (CD) spectra of the monomers were characteristic of coil-like IDPs showing unordered structure with a high population of polyproline-II

conformation. The oligomerization was accompanied by a minor CD spectral change attributable to formation of a small amount of α -helix. The number of residues in α -helical conformation was estimated as 13 in BASP1 and 18 in GAP-43. However, the overall structure of the oligomers remained disordered. It was confirmed by measuring the hydrodynamic dimensions of the oligomers using size-exclusion chromatography and polyacrylamide gradient gel electrophoresis, and by assaying their sensitivity to proteolytic digestion. Based on the obtained results we have suggested the model of “the electrostatic core”, describing the structure of BASP1 and GAP-43 oligomers (Fig.). According to the model, the short basic effector domains, which are presumably tethered together via molecules of PIP₂ or SDS, form the α -helical core of the complex, while the bulk of the protein molecules preserve the disordered structure.



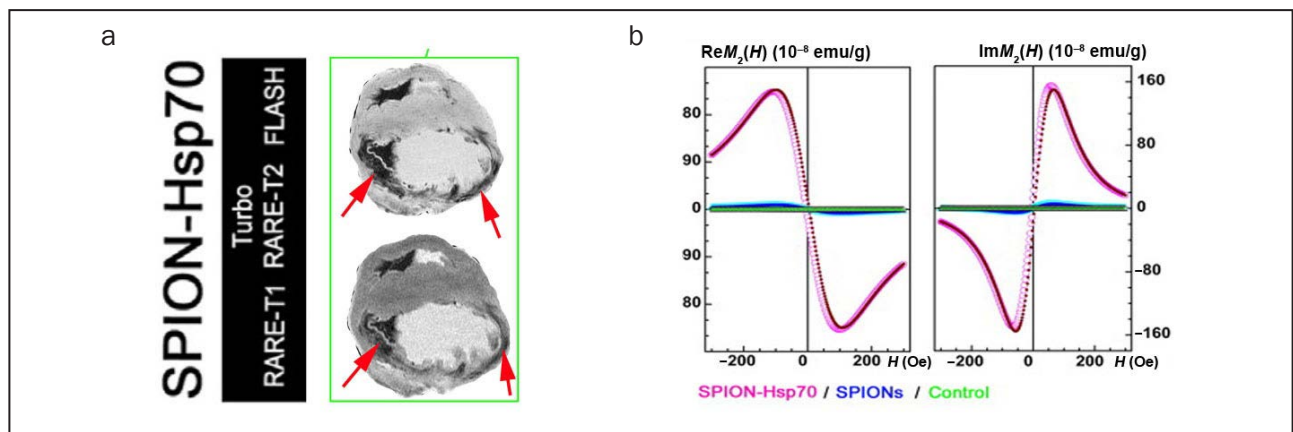
The model of “the electrostatic core”, describing the structure of BASP1 and GAP-43 oligomers

Detection of experimental myocardium infarction in rats by MRI using heat shock protein 70 conjugated superparamagnetic iron oxide nanoparticle

V.A. Ryzhov – Molecular and Radiation Biophysics Division of NRC “Kurchatov Institute” – PNPI
 G. Multhoff, M. A. Shevtsov – Technische Universität München
 Ya.Yu. Marchenko, B.P. Nikolaev, L.Yu. Yakovleva –
 Research Institute of Highly Pure Biopreparations
 A.V. Dobrodumov – Institute of Macromolecular Compounds of RAS
 I.V. Guzova, B.A. Margulis – Institute of Cytology of RAS
 E. Pitkin – University of Pennsylvania
 A.L. Mikhrina – Sechenov Institute of Evolutionary Physiology and Biochemistry of RAS

It is known that magnetic nanoparticles (MNP) based on iron oxides (SPIONs) may be used as a promising T_2 -negative contrast agent for diagnostics of myocardial infarction by magnetic resonance imaging (MRI). Furthermore, it is a well-established fact that CD40, which is a specific receptor for stress-inducible 72 kDa heat shock protein Hsp70, is well expressed on cardiac myocytes. So, the functionalization of the SPION surface with Hsp70 as biological ligand can increase the specificity of infarction targeting, providing its MRI diagnostics in detail. The assessment of this assumption, together with the study of Hsp70-SPION conjugate biodistribution were the main goals of this work.

Measurements of the second harmonic of non-linear response to a weak *ac* magnetic field (NLR- M_2) in *dc* field *H* parallel to it, indicated a 30-fold increase in Hsp70-SPION uptake in infarction zones of rats as compared to SPIONs (Fig. b). This provided the essential increase of their contrast in MRI (Fig. a). Biodistribution analysis using NLR- M_2 data showed that retention of the magnetic conjugates in the infarction zones is 5 times larger than in liver and at least 10 times higher than in other organs and tissues. This shows the possibility of targeted drug delivery to the infarction zone by Hsp70-SPION conjugate. The necessary drug may be placed, for example, into dextran shell of SPIONs.



T_2 -weighted and FLASH (gradient echo) MR scans of heart for rats treated by Hsp70-SPION (a). The infarction regions with accumulated MNPs are seen as hypotensive zones on MR images (indicated by red arrows). Panels b (left, right) present the biodistribution of MNPs in heart tissue of control rats and animals treated with SPIONs and Hsp70-SPION particles from NLR- M_2 data

Microbiology of the subglacial Antarctic Lake Vostok: borehole-frozen lake water

S.A. Bulat, M.V. Doronin, D.S. Karlov, M.O. Khilchenko –
Molecular and Radiation Biophysics Division of NRC “Kurchatov Institute” – PNPI
D. Marie – Station biologique de Roscoff, National Centre for Scientific Research (CNRS) (France)

The objective was to discover whether microbes (and in which forms) thrive in the subglacial Antarctic Lake Vostok, buried beneath a 4-kilometer polar glacial sheet. The molecular-microbiological analysis of the only available samples of lake water, which came up into the borehole following two lake drilling sessions and got frozen afterwards, has given the first results (1). The earlier obtained data on the microbial content of the natural lake water ice (dubbed accretion ice) were used for the comparison. Amongst the findings of that time, an unknown unidentified (92% similarity with closest taxa in Genbank) bacterium AF532061 was discovered. The present-day DNA analysis (sequencing of 16S rRNA genes followed by phylogenetic inferences) of borehole-frozen water samples, which were all contaminated with the microbiologically dirty kerosene-based drill fluid in a various ratio, has resulted in revealing

yet another unknown (unidentified and unclassified) (< 86% similarity with closest taxa) bacterium w123-10. It has successfully passed all possible control tests for contamination and showed a rather far relatedness with the above-mentioned unidentified bacterium AF532061 originated from the accretion lake ice. Thus, these two bacteria both representing populations may represent unknown microbial communities thriving in the lake water body under the ice ceiling in the uppermost water horizons. Such a suggestion requires to be confirmed by collecting unfrozen lake water samples as clean as possible. The given discovery proved to be possible due to the use of certified clean room facilities and the on-site constructed Contaminant Library that at present embraces 300 bacterial contaminant phlotypes. The Library is used to test all the findings.



The 'drill-bit' frozen water sampling in a field. The drill fluid outflow is obvious

Proteomic profiling of high-grade glioblastoma using virtual-experimental 2DE

*N.V. Belyakova, M. V. Filatov, O.A. Kleyst,
O.K. Legina, S.N. Naryzhny, R.A. Pantina, N.L. Ronzhina –
Molecular and Radiation Biophysics Division of NRC “Kurchatov Institute” – PNPI
M.A. Maynskova, S.N. Naryzhny, S.E. Novikova, V.G. Zgoda –
V.N. Orekhovich Research Institute of Biomedical Chemistry of RAMS*

Identification and quantitative analysis of different proteoforms (protein species) presented in a cell line generated from high grade glioblastoma were performed using two-dimensional electrophoresis (2DE), mass spectrometry (ESI LC-MS/MS), and immunodetection. A 2DE protein map containing an extensive data set comprising 937 spots with 1542 unique protein identifications (proteoforms) of 600 genes was obtained (Fig. 1). Additionally, another set of experiments was performed, where 16012 proteoforms coded by 4050 genes were identified by MS/MS according to their position in 96 gel sections (pixels) (Fig. 2). Special attention

has been paid to the proteins that are the potential biomarkers of glioblastoma. The list of these biomarkers was compiled from literature. Next, we generated the graphs with theoretical and experimental information about proteoforms coded by the same gene. Such a virtual-experimental representation allowed better visualization of the state of these gene products. Many proteins, potential biomarkers of glioblastoma as well, are characterized by high numbers of protein species. We assume that these species could be a potential source of highly specific biomarkers of glioblastoma.

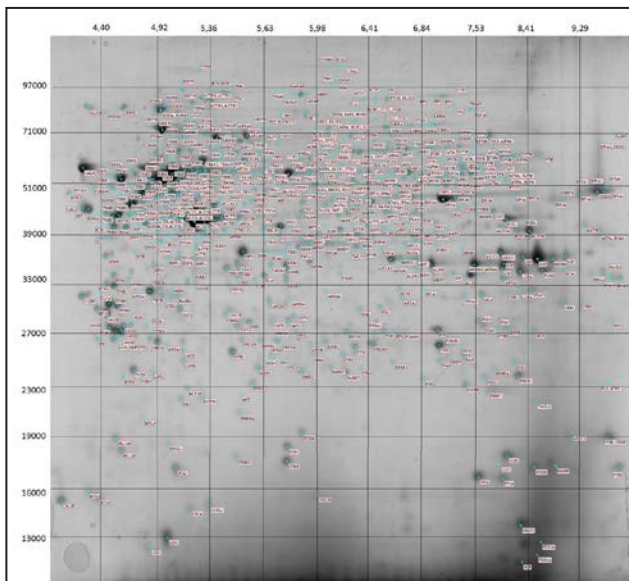


Fig. 1. 2DE, identifications of proteoforms, located in spots (spot-picking approach)

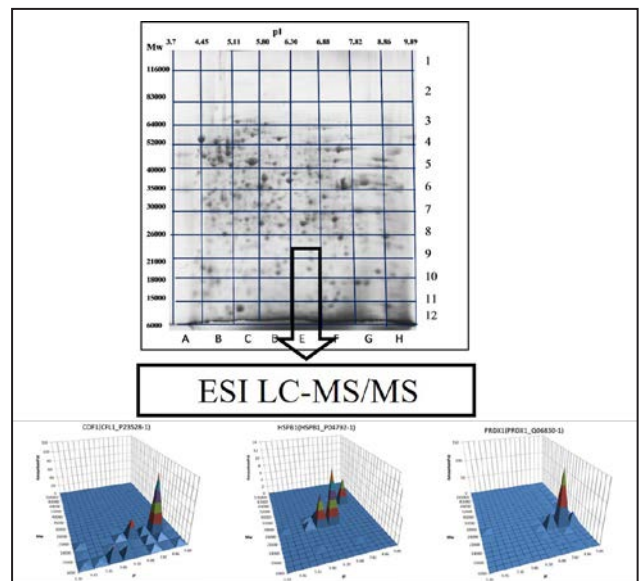


Fig. 2. Identification of proteoforms located in selected sections (pixel-picking approach)

1. Naryzhny S.N. ..., Ronzhina N.L., Kleyst O.A. et al. // J. Proteome Res. 2016. V. 15. P. 525–530.
2. Naryzhny S.N. ..., Ronzhina N.L. et al. // Electrophoresis. 2016. V. 37. P. 302–309.
3. Naryzhny S.N. ..., Ronzhina N.L. et al. // J. Proteom. Bioinf. 2016. V. 9. Iss. 6. P. 158–165.

A role for tuned levels of nucleosome remodeler subunit ACF1 during *Drosophila* oogenesis

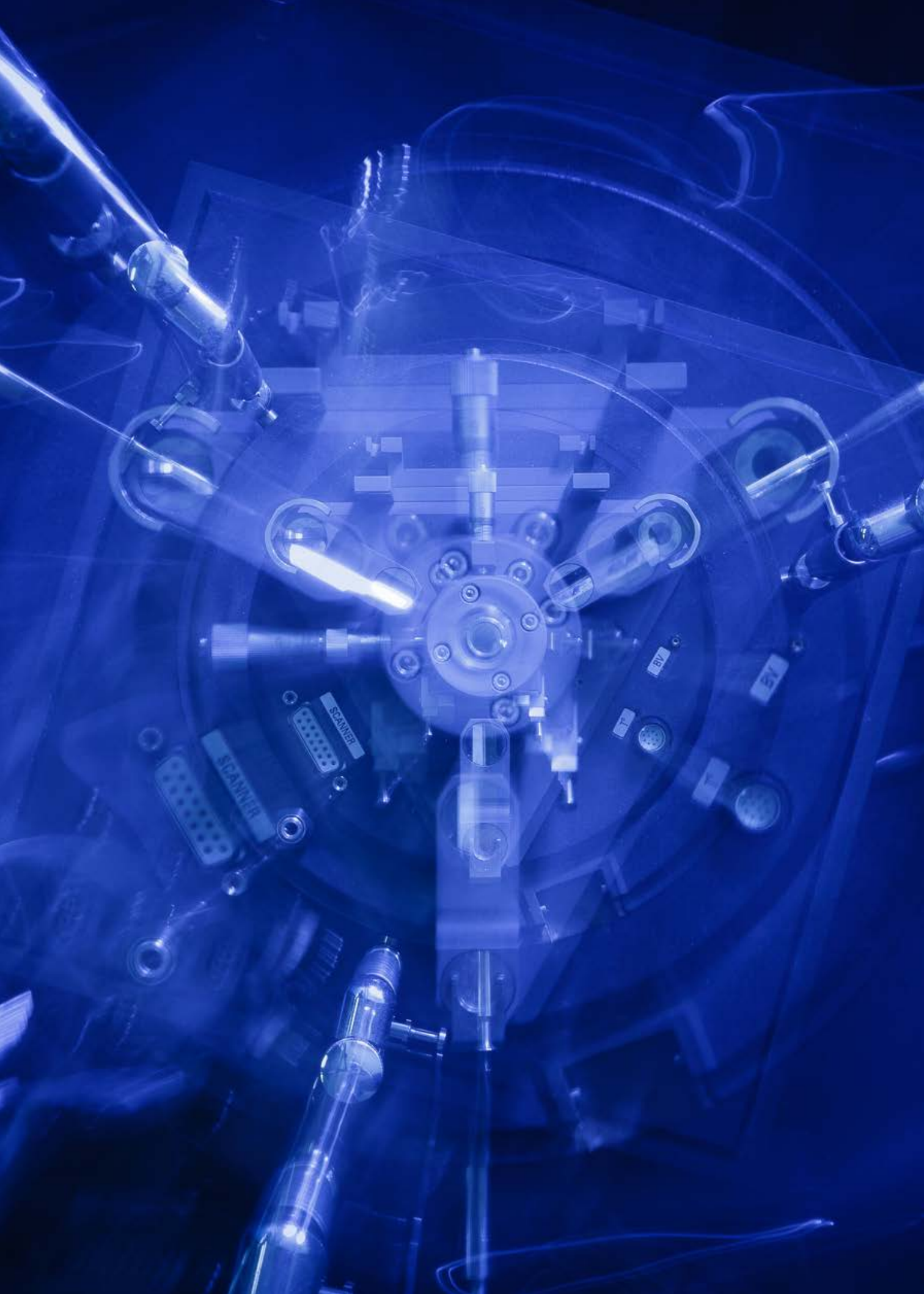
*A.Yu. Konev – Molecular and Radiation Biophysics Division of NRC “Kurchatov Institute” – PNPI
 P.B. Becker, K. Börner, D. Jain, N. Steffen, S. Vengadasalam –
 Biomedical Center and Center for Integrated Protein Science Munich (CIPSM),
 Ludwig-Maximilian University of Munich
 B. Suter, P. Vazquez-Pianzola – Institute of Cell Biology – University of Bern
 D.V. Fyodorov – Albert Einstein College of Medicine
 P. Tomancak – The Max Planck Institute of Molecular Cell Biology and Genetics (MPI-CBG)*

The Chromatin Accessibility Complex (CHRAC) consists of the ATPase ISWI, the large ACF1 subunit and a pair of small histone-like proteins, CHRAC-14/16. CHRAC is a prototypical nucleosome sliding factor that mobilizes nucleosomes to improve the regularity and integrity of the chromatin fiber. This may facilitate the formation of repressive chromatin. Expression of the signature subunit ACF1 is restricted during embryonic development, but remains high in primordial germ cells. Therefore, we explored roles for ACF1 during *Drosophila* oogenesis. ACF1 is expressed in somatic and germline cells, with notable enrichment in germline stem cells and oocytes. The asymmetrical localization of ACF1 to these cells depends on the transport of the *Acf1* mRNA by the Bicaudal-D/Egalitarian complex. Loss of ACF1 function in the novel *Acf1(7)* allele leads to defective egg chambers and their elimination through apoptosis. In addition, we find a variety of unusual 16-cell cyst packaging phenotypes in the previously known *Acf1(1)* allele, with a striking prevalence of egg chambers with two functional oocytes at opposite poles. Surprisingly, we found that the *Acf1(1)* deletion—despite disruption of the *Acf1* reading frame—expresses low levels of a PHD-bromodomain module from the C-terminus of ACF1 that becomes enriched in oocytes. Expression of this module from the *Acf1* genomic locus leads to packaging defects in the absence of functional ACF1, suggesting competitive interactions with unknown target molecules. Remarkably, a two-fold overexpression of CHRAC (ACF1 and

CHRAC-16) leads to increased apoptosis and packaging defects. Evidently, finely tuned CHRAC levels are required for proper oogenesis.



Cover of the journal "Developmental Biology".
Egg chamber of *Acf1*¹ with two oocytes at opposite poles



Nuclear Medicine (Isotope Production, Beam Therapy, Nano- and Biotechnologies for Medical Purposes)

- 106 Effect of low doses of radiation ^{169}Yb on proliferation and cell death in human cells in culture
- 107 Oligomeric α -synuclein and glucocerebrosidase activity levels in *GBA*-associated Parkinson's disease
- 109 New production method for ^{82}Sr and the other medical radionuclides

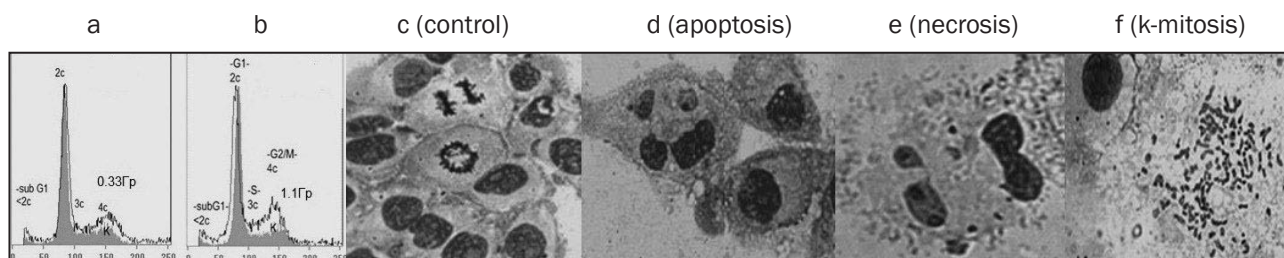
Effect of low doses of radiation ^{169}Yb on proliferation and cell death in human cells in culture

*N.Ya. Giliano, L.V. Konevega, L.A. Noskin, S.I. Stepanov, E.V. Zhurishkina – Molecular and Radiation Biophysics Division of NRC “Kurchatov Institute” – PNPI
S.V. Akulinichev, S.A. Chaushanskii, V.I. Derzhiev, I.A. Yakovlev – Institute for Nuclear Research of RAS*

Due to its radiation properties, ^{169}Yb is a radionuclide with great potential for the use in cancer brachytherapy. We studied ytterbium sources developed by LLC “Delis” and the Institute for Nuclear Research RAS (patent No. 131302-RU). These sources are composed of a dense ceramic core of enriched ytterbia in a hermetic titanium container.

In this work, the effect of sources of ^{169}Yb on the proliferation, progression of the cell cycle, apoptotic death and the level of chromosome aberrations in carcinoma (HeLa G63) and endothelial (ECV304) human cells in culture was studied. It has been shown that exposure of cells to ^{169}Yb – with doses 0.33–1.2 Gy leads to cell blocking in G2/M phases of the cell cycle. We found that the blocking of the progression of cells is dose dependent and becomes irreversible, resulting in repopulation changes. The ^{169}Yb radiation also inhibited

the growth of cells in a dose dependent manner (Fig. a, b). Morphological analysis of the cells identified an apoptotic form of cellular death (d), not only and not so much in irradiated cells, as in their descendants. In the latter case we also recorded an abnormal mitosis (f), a damage of the mitotic apparatus of cell division. Necrotic form of cellular death (e) was registered only after prolonged exposure of ytterbium irradiation. Observation of the irradiation effects for several cellular generations indicates that low doses of radiation induced systemic changes of cellular metabolism, which was accompanied by activation of mechanism of “checkpoint” control and apoptosis. The observed manifestation of the damaging effect late after the irradiation by ytterbium sources may significantly contribute to the total effect of treatment, which is important in clinical practice.



Cytometric (a and b) and morphological (c–f) analysis of the cell population before and after the exposure of cells HeLa ^{169}Yb -sources

- Giliano N.Ya., Konevega L.V., Stepanov S.I., Zhurishkina E.V., Noskin L.A. // Pathogenesis. 2015. V. 13. No. 4. P. 57–61.
- Giliano N.Ya., Zhurishkina E.V., Konevega L.V., Stepanov S.I. et al. Эффективность гено- и цитотоксического действия γ -излучения иттербия-169 на клетки человека в культуре // Радиц. биол. Радиоэкол. 2017. In press.

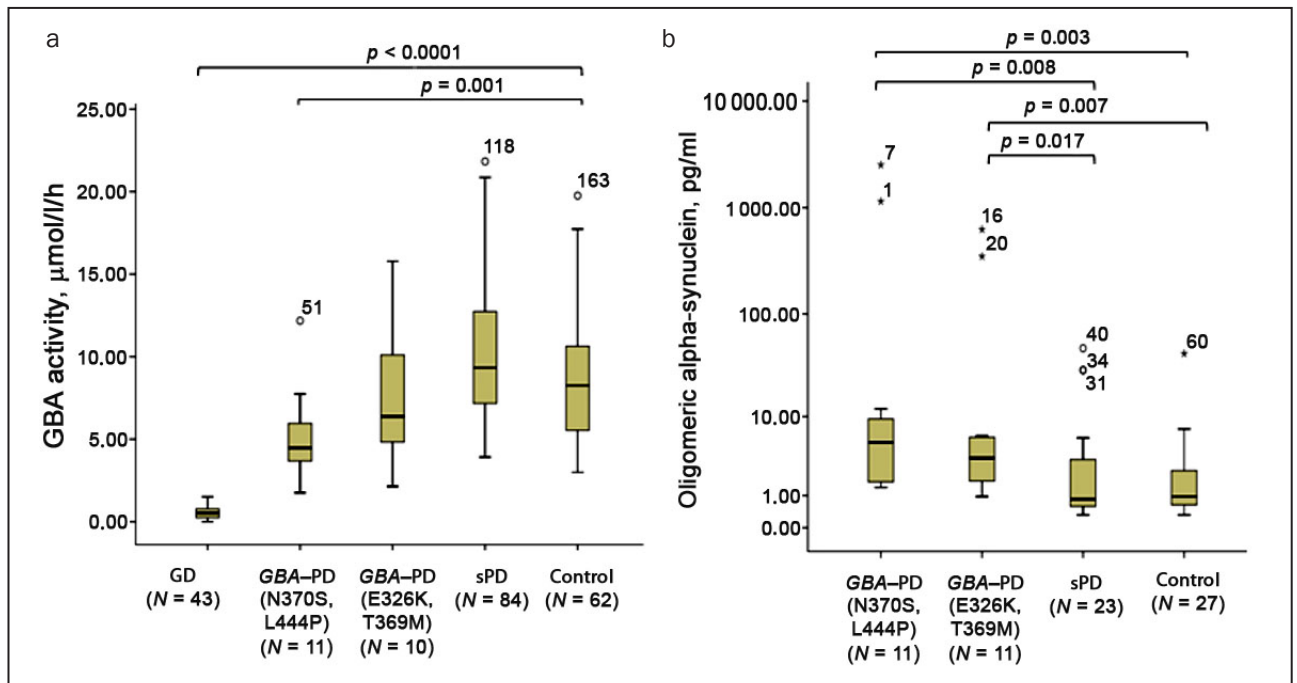
Oligomeric α -synuclein and glucocerebrosidase activity levels in *GBA*-associated Parkinson’s disease

P.A. Andoskin, A.K. Emelyanov, L.A. Garaeva, A.E. Kopytova, D.G. Kulabukhova, A.O. Lavrinova, M. A. Nikolaev, S.N. Pchelina, K.A. Senkevich, T.S. Usenko – Molecular and Radiation Biophysics Division of NRC “Kurchatov Institute” – PNPI E.Yu. Zakharova – Medical Genetics Research Center

In 2014–2015 we have demonstrated the increased levels of blood oligomeric alpha-synuclein in patients with Gaucher disease (GD), caused by mutations in the gene encoding glucocerebrosidase 1 (*GBA*). We have also reported an inverse correlation between plasma oligomeric alpha-synuclein levels and leukocyte *GBA* activity in patients with GD. *GBA* mutations have been identified as the most common known genetic risk factor for the development of Parkinson’s disease PD, however the molecular basis of high PD risk in *GBA* mutation carriers remains unknown. Besides the most common *GBA* mutations (N370S, L444P), several *GBA* polymorphic variants (E326K, T369M) that did not

lead to GD in homozygous state have been associated with increased risk of PD development have been described. We suggested that altered *GBA* activity in *GBA*-PD patients could be accompanied by an increase in alpha-synuclein oligomerization.

GBA enzymatic activity and plasma oligomeric alpha-synuclein levels were assessed in sPD patients ($N = 84$), in *GBA*-PD patients ($N = 22$) and controls ($N = 62$) by LC-MS/MS and ELISA (Human Alpha-Synuclein PATHO ELISA kit (Analytik Jena, Germany)) methods accordingly. *GBA*-PD patients showed lower *GBA* enzymatic activity compared to controls ($p = 0.001$) and to sPD ($p = 0.0001$). At the same time plasma oligomeric



GBA activity in DBS of GD patient, PD patients with N370S, L444P *GBA* mutations, PD patients with E326K, T369M *GBA* polymorphic variants, sPD patients and controls (a). Oligomeric alpha-synuclein levels in blood plasma from PD patients with N370S, L444P *GBA* mutation, PD patients with E326K, T369M *GBA* polymorphic variants, sPD patients and controls (b). Data for oligomeric alpha-synuclein levels are shown on the logarithmic scale

Таблица. Активность глюкоцереброзидазы и уровень олигомерного альфа-синуклеина крови у носителей мутаций и полиморфных вариантов в гене *GBA*

Обследованные группы пациентов с БП	Активность GBA (медиана, минимум – максимум), мкмоль/л/ч	N	P (по сравнению с сБП)	Уровень олигомерного альфа-синуклеина минимум – максимум), пкг/мл	N	P (по сравнению с сБП)
Носители мутаций L444P, N370S	4.47 (1.76–12.78)	11	< 0.0001	5.3 (1.38–2 518.81)	11	0.008
Носители полиморфных вариантов E326K, T369M	6.38 (2.14–15.78)	10	0.05	3.50 (0.95–623.22)	11	0.017
Пациенты с отсутствием мутаций в гене <i>GBA</i> (сБП)	9.33 (3.91–21.83)	84	–	0.85 (0.32–47.12)	23	–

alpha-synuclein levels were increased in GBA–PD group compared to SPD and controls ($p = 0.002$ and $p < 0.0001$, respectively) (Fig.). The most significant GBA activity reduction was detected in carriers of GBA mutation (L444P, N370S) as compared to controls ($p = 0.001$) and to SPD ($p < 0.0001$). However, in PD carriers of GBA polymorphic variants (E326K, T369M) associated with PD but not with GD, GBA enzymatic activity was also reduced at the level of statistical significance ($p = 0.053$ compared SPD).

Thus, we showed that GBA–PD is characterized by a decrease in GBA activity and an increase in plasma oligomeric alpha-synuclein levels. Our results support the notion that enzyme-enhancing therapies could have merit for the treatment of at least GBA–PD.

The work was supported by Russian Foundation for Basic Research (RFBR) No. 16-04-00764, No. 16-54-76009 (ERA.Net RUS Plus Group of Funding Parties ID230).

1. Nuzhnyi E., Emelyanov A., Boukina T., Usenko T., Yakimovskii A. ..., Pchelina S. // *Mov. Disord.* 2015. V. 30. Iss. 7. P. 989–991.
2. Pchelina S., Emelyanov A. ..., Andoskin P. ..., Nikolaev M. ..., Usenko T., Kulabukhova D., Lavrinova A., Kopytova A., Garaeva L. et al. // *Neurosci. Lett.* 2017. V. 636. P. 70–76.

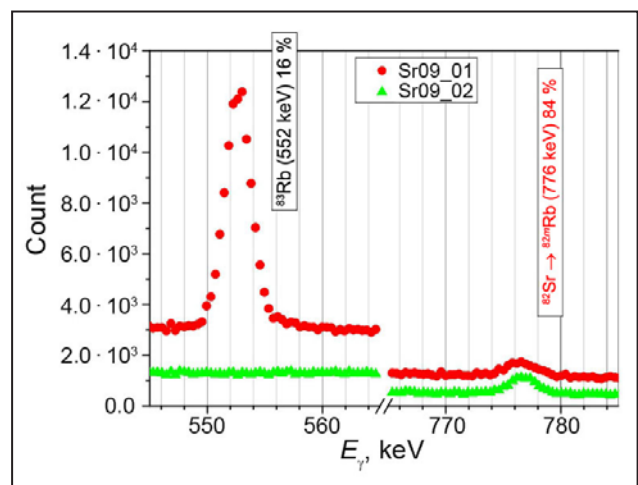
New production method for ^{82}Sr and the other medical radionuclides

A.E. Barzakh, L.Kh. Batist, D.V. Fedorov, V.S. Ivanov, A.S. Krotov,
P.L. Molkanov, F.V. Moroz, S.Yu. Orlov, V.N. Panteleev, Yu.M. Volkov
High Energy Physics Division of NRC "Kurchatov Institute" – PNPI

Recently at NRC "Kurchatov Institute" – PNPI the cyclotron C-80 with the planned parameters of the beam energy 40–80 MeV and intensity up to 200 μA has been launched. The C-80 parameters allow producing the broad nomenclature of radioisotopes and pharmaceuticals which are very promising for diagnostics and therapy. The radioisotope complex RIC-80 (Radioactive Isotopes at cyclotron C-80), which is presently constructed at the beam of C-80, offers the opportunity of obtaining sources of a high activity practically for the whole list of radionuclides produced at accelerators. An essential peculiarity of the RIC-80 is the use an on-line mass-separator connected to one of the target stations, that will allow the production of separated radionuclides of high purity. The unique parameters of the RIC-80 will give the possibility to produce a broad range of radioisotopes. They include ^{68}Ge , ^{82}Sr , ^{111}In , ^{123}I , ^{124}I , ^{223}Ra , ^{224}Ra and nuclides, which are at present considered to be the promising candidates for diagnostics and therapy: ^{64}Cu , ^{67}Cu , ^{67}Ga , ^{77}Br and ^{81}Rb . The production of radionuclides that decay with emission of positrons, allowing their use for PET (Positron Emission Tomography), is very important for diagnostics of different diseases. Isotope-generator ^{82}Sr which is utilized for PET diagnostics of heart and brain diseases is the one of the most needed radionuclides for PET diagnostics in the world. For production of the radioisotope ^{82}Sr a new method of a high temperature separation of produced radionuclides and irradiated target has been developed. The general idea of the method is the usage of the evaporation speed difference of the target material and produced radioactive species. This

method of complete target material evaporation into a specially constructed separated volume, when the required nuclides do not escape from the target vessel appeared to be very effective. In the case of separation of strontium radioisotopes from RbCl or metallic rubidium target material, the efficiency of ^{82}Sr production was 90%. In Figure the gamma-spectra demonstrating the process of separation of the irradiated target material and produced ^{82}Sr are presented.

The new presented method of a high temperature separation of the target material and produced radionuclides is rather universal and can be used for production of other medical radioisotopes. The promising results have been obtained when separating ^{67}Cu (radionuclide for therapy) from zinc target material.



The spectrum of the vessel with the irradiated RbCl after the heating at a temperature 500 °C (upper part). The spectrum after one hour vessel heating at a temperature (900–1000) °C (lower part)



Nuclear Reactor and Accelerator Physics

- 112** Burnable neutron poison for modernized fuel assemblies of PIK reactor
- 114** Determination of platinum amount in catalysts by neutron activation method
- 115** The operating experience of heavy water reactor PIK reflector from 2010 to 2016
- 117** The specification of postulated initiating events for safety analysis of PIK reactor
- 118** Fuel charging control during PIK reactor energy start-up

Burnable neutron poison for modernized fuel assemblies of PIK reactor

S.R. Fridman, K.A. Konoplev, I.M. Kosolapov, A.S. Zakharov –
 Department of Reactor Physics and Technology
 A.S. Poltavsky – Department of Nuclear and Radiation Safety
 M.S. Onegin – Theoretical Physics Division
 S.L. Smolsky – Deputy Director for Exploitation of Nuclear Installations
 NRC “Kurchatov Institute” – PNPI

The concept of the operational set of PIK-2 fuel assemblies (FA) stipulates 20% increase of fuel load as it was realized at SM reactor and the installation of burnable poison rods (BPR) with the purpose of increasing the duration of a reactor cycle. PIK and SM fuel elements fabrication should be unified. The PIK fuel element differs from the SM one only in height of an active fuel layer. The FA set consists of 12 hexagonal and 6 square FAs. The square FAs can be delivered in a standard version or with a cavity for placing the irradiated surveillance specimens or additional BPR blocks (Fig. 1).

The designed semi-cylindrical BPRs are destined to replace the steel displacers. The reactivity worth of this BPR version is limited. In view of increase of fuel loading some options of refueling cannot be realized.

The concept of PIK-2 fuel assemblies allows the installation of BPR instead of the part of fuel elements. In 2016 some design and organizational decisions were considered to provide more efficient refueling and loading of surveillance specimens. It is useful to install the cruciform BPR with low useless reactivity loss due to the reduced water displacement effect instead of selected fuel elements (FE) (Fig. 2). This option increases BPR efficiency and provides reduced non-uniformity of power distribution in the reactor core. Another variant is the installation of BPR of any shape in FA cavities (channels) that allows increasing their reactivity worth. The optimization of water-uranium ratio makes it possible to reduce FE quantity in the reactor core without an evident reduction of the reactor cycle duration.

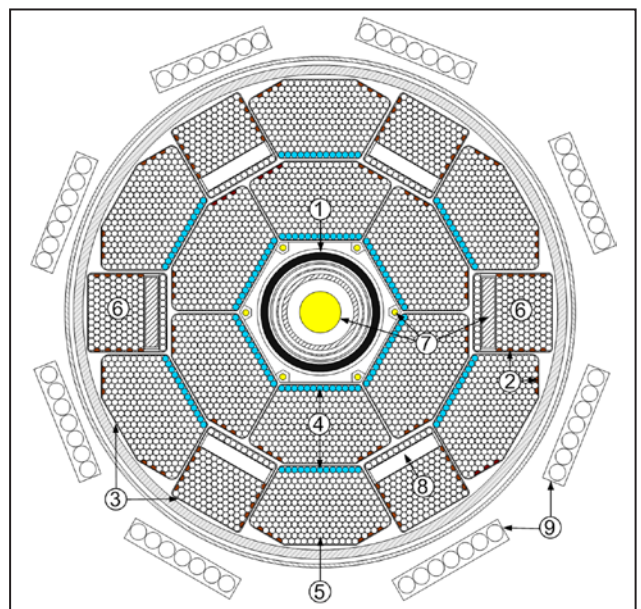


Fig. 1. The scheme of PIK reactor core with additional cavities: 1 – hafnium absorbing shutters; 2 – burnable poison rods $Gd_2O_3 + ZrO_2$; 3 – zirconium casings of FA; 4 – fuel elements with the reduced fuel content (0.48 of nominal value); 5 – fuel elements with the nominal fuel content; 6 – fuel assemblies with the surveillance specimens; 7 – irradiated samples; 8 – additional cavities for irradiated samples or BPR; 9 – reflector control rods

The possibility to use PIK-2 FAs in the reactor PIK has been confirmed. The maximum reactor cycle duration can be increased from 30 to ≈ 38 days with due account for the reactivity loss due to the irradiation of surveillance specimens (Fig. 3).

It is necessary to develop the hexagonal FA version with additional BPR not only to increase the reactor cycle but also to equalize the power distribution and to provide new possibilities for irradiation of materials in a reactor core. The FA produc-

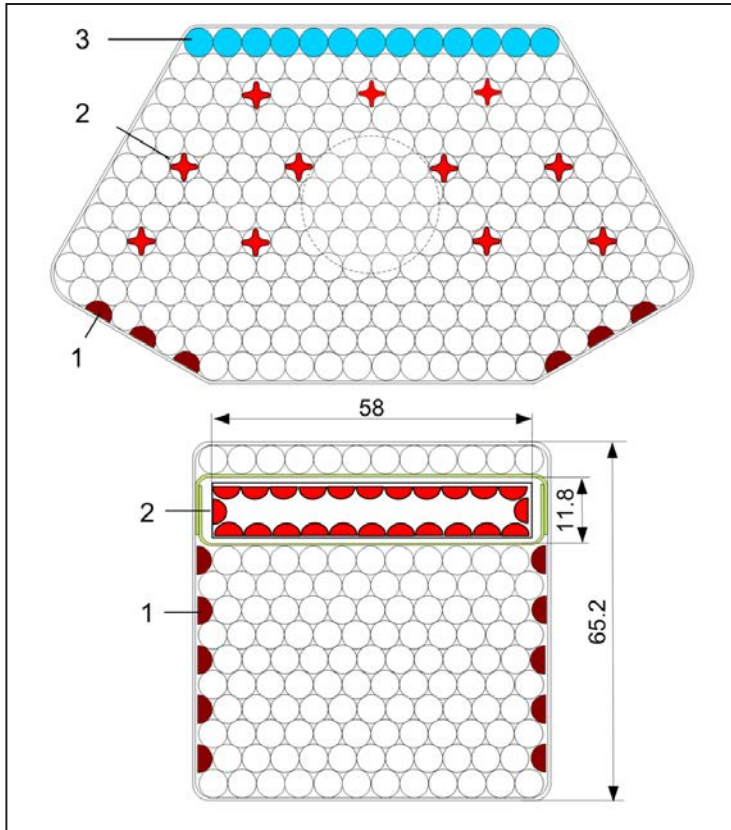


Fig. 2. BPR arrangement pattern:
 1 - standard BPR; 2 - additional BPR;
 3 - fuel profiling zone

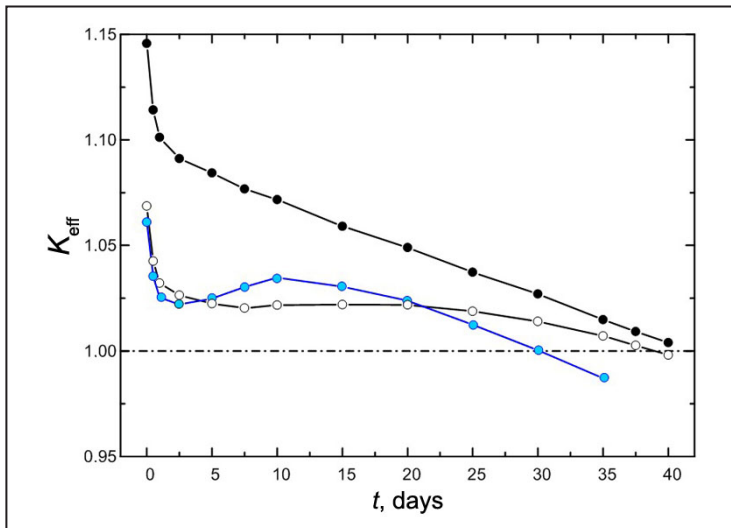


Fig. 3. Change in K_{eff} under burn-up of a core with combined installation of 132 cruciform and 140 standard semi-cylinder BPRs:
 1 - FE without gadolinium 8.57 g ^{235}U ;
 2 - FE 8.57 g ^{235}U , BPR 1.4 g Gd;
 3 - FE 7.14 g ^{235}U ; BPR 0.7 g Gd

tion with new BPR versions is not changed essentially; the needed FE quantity will be a little reduced.

The future improvement of reactor parameters is connected with the use of a modern fuel com-

position. New BPR variants are suitable for different refueling schemes including full core reloading and its variants can be used in case of use of new FEs with a low-absorbing matrix.

Determination of platinum amount in catalysts by neutron activation method

*I.A. Alekseev, S.A. Panasenko, P.A. Sushkov – Department of Reactor Physics and Technology
V.G. Zinovyev – Neutron Research Division
NRC “Kurchatov Institute” – PNPI*

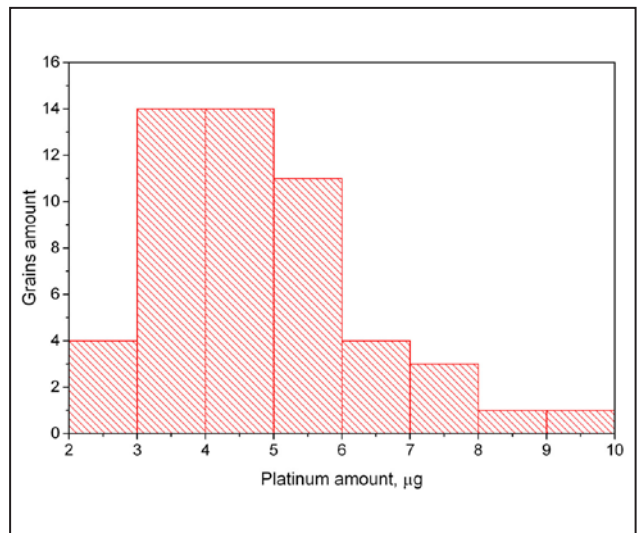
To remove a radioactive isotope of hydrogen – tritium that is produced in the heavy-water moderator of the PIK reactor, a method of counter-flow isotopic exchange between water and hydrogen in columns filled with packing and platinum hydrophobic catalyst, combined with electrolysis, will be used.

One can use the mass-exchange coefficient divided by the amount of platinum to compare the platinum use efficiency in catalysts of isotopic exchange.

Since the data provided by the catalyst manufacturer was insufficient and undetailed, it was decided to develop the method of platinum amount measurement by neutron activation analysis at WWR-M reactor for RCTU catalysts, which are supposed to be used at the tritium removal unit of the PIK reactor.

The measurements were carried out by comparing the platinum activity in samples under study with the activity in the standard sample. The neutron irradiation of catalyst grains was done at the V-4 vertical channel of WWR-M reactor at NRC “Kurchatov institute” – PNPI. The size and brightness distribution of grains was determined additionally by analyzing the photos of grains.

As a result of measurements, it was discovered that the platinum amount in catalysts differs from the quantity that was provided by the manufacturer (0.8% wt.) and equals $1.11 \pm 0.02\%$ wt. for RCTU-SM catalyst and $1.33 \pm 0.02\%$ wt. for RCTU-3SM catalyst (Fig.). It was determined that



Platinum amount distribution of grains

there is a linear correlation with the multiple correlation coefficient equaling 0.89 between platinum amount, its volume and brightness.

The obtained results could be used to compare the platinum use efficiency in RCTU catalysts with the efficiency of foreign analogues. A developed method allows the determination of platinum amount not only for catalysts on organic substrate, but also for the other most common substrates, since atoms of chemical elements of natural isotopic abundance that comprise these substrates (aluminum, oxygen, silica and fluorine for hydrophobization) do not become radioactive after neutron irradiation.

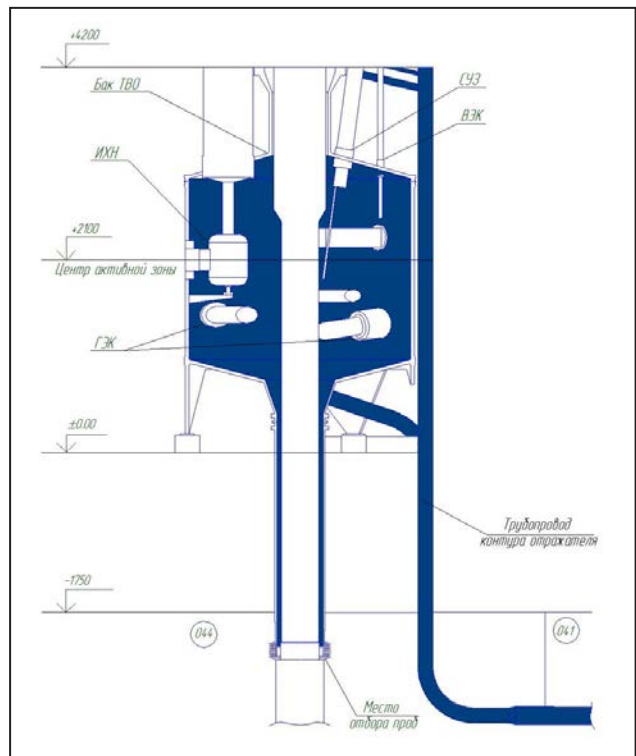
The operating experience of heavy water reactor PIK reflector from 2010 to 2016

S.D. Bondarenko, K.A. Konoplev, A.S. Zakharov – Department of Reactor Physics and Technology
 V.N. Tischenko, D.Y. Tugusheva, T.V. Voronina – Department of Nuclear and Radiation Safety
 V.P. Maschetov, G.I. Pereverza – Department of Commissioning of PIK Neutron Research Center
 NRC “Kurchatov Institute” – PNPI

The physical start-up of the PIK reactor with a capacity of 100 W was carried out on 28 February 2011. A necessary condition for neutron flux obtaining was filling the heavy water reflector (HWR) tank with highly-concentrated heavy water with the deuterium a_D content not less than 99.80%. For this reason, the filling of the HWR tank with heavy water was carried out from 12 to 25 May 2010.

According to the project, the HWR tank is filled up by means of the HWR circuit filling system. But HWR tank was cut off from the HWR circuit in the period of the physical start-up of the PIK reactor. Therefore, the filling operation was carried out according to the temporary scheme – direct decanting of heavy water from the canisters to HWR tank under nitrogen atmosphere. This scheme of the heavy water filling operation was very successful for two reasons: 1) the tank filling was done quickly – for 3 working days, much quicker than the standard scheme. The minimum number of reactor staff took part in that work. 2) the probability of heavy water isotopic dilution in such a scheme of tank filling was minimal, because the heavy water from the canisters got directly into the HWR tank, escaping working tanks and long pipelines of the filling system. As a result, the isotopic and chemical composition of heavy water in the HWR tank corresponded to the design standards. Therefore, the main task to preserve the high concentration (a_D) of deuterium in heavy water was achieved.

From the tank filling of heavy water (in 2010) until the tank draining (in 2016), the HWR tank (see Figure) was in operation, which included: 1) periodic quality control of heavy water in the tank;



Vertical cross-section of the PIK reactor. The colored areas mark the equipment filled with heavy water during the period from 2010 to 2016

2) carrying out of technological draining of heavy water from the tank.

In that period of time the equipment and piping of the HWR tank were at atmosphere pressure of 0.1 MPa, temperature of $(20 \pm 5)^\circ\text{C}$; there was no circulation of coolants, the cleaning system of heavy water was not put into operation. In fact, it was the storage of heavy water in the tank with periodic quality control and technological draining. The content of deuterium in the heavy water of HWR tank remained invariable ($99.856 \pm 0.005\%$) during the entire period of operation and the vo-

lume activity of tritium decreased in accordance with the tritium half-life. This being said, it is possible to claim that the HWR tank was hermetically tight and the quality of the nitrogen that was used to maintain the pressure in the tank was high. However, the chemical quality of heavy water for 2010–2016 became significantly worse. Almost all the indicators grew several times, the content of corrosion products in 2016 exceeded the norms established by Regulation standards. The reasons of heavy water contamination were: 1) corrosion processes; 2) insufficient washing of HWR tank before filling. Therefore, the commissioning of the cleaning system of heavy water at the stage of preparation for power start-up of PIK reactor is highly necessary.

Heavy water draining out of HWR tank of the PIK reactor was performed during the period from 15 March to 28 April 2016. All the heavy water drained from HWR tank was registered.

The loss of heavy water during the operation time of HWR tank including filling, quality control of

heavy water, technological draining, the complete heavy water draining out of HWR tank and tank drying did not exceed the established norms and equaled 0.46% of the total.

However, there was a dilution of heavy water from 99.86 to 99.58% (for the deuterium content) during the heavy water draining from the HWR tank. It is most likely that the reason for this dilution was the draining of water with high content of protium and impurities from “dead zones” of HWR tank such as: 1) control seal lines and blowing gap lines; 2) cavities of control rod; 3) gaps between the horizontal channels and the HWR tank. The heavy water dilution showed that it is necessary to improve the drying procedure of the HWR tank. Considering the quality of the heavy water in cans it is necessary to make its isotope and chemical cleaning before the following filling of the HWR tank.

The authors are grateful to the staff of the PIK reactor, who participated in the work.

1. *Voronina T.V., Pereverza G.I.* The Operating Experience of Heavy Water Reactor PIK Reflector from 2010 to 2016. Technical Report, Inv. No. 16RY-11 Department of Nuclear and Radiation Safety. Gatchina, 2016. 63 p.
2. *Bondarenko S.D., Voronina T.V., Zakharov A.S., Konoplyov K.A., Pereverza G.I., Tischenko V.N., Tugusheva D.Yu.* The Operating Experience of Heavy Water Reactor PIK Reflector from 2010 to 2016. // Mat. of VIII Scientific and Technical Conf. “Problems and Prospects for the Development of Chemical and Radiochemical Control in Nuclear Power Engineering” (Atomenergoanalytics-2017). 2017. Preparing for Printing.

The specification of postulated initiating events for safety analysis of PIK reactor

*S.R. Fridman, A.S. Zakharov – Department of Reactor Physics and Technology
A.V. Korotynsky, A.S. Poltavsky – Department of Nuclear and Radiation Safety
S.L. Smolsky – Deputy Director for Exploitation of Nuclear Installations
NRC “Kurchatov Institute” – PNPI*

In the framework of the PIK reactor power start-up preparation, the specialists of the Cooperation that consists of NRC “Kurchatov Institute”, NRC “Kurchatov Institute” – PNPI, JSC “NIKIET”, JSC “Atomtechenoergo” and JSC “Alliance-Gamma” have developed base documents for safety analysis of PIK: “The Statement of Work under preparation of Safety Analysis Report of PIK reactor” and “The Specification of postulated initiating events for safety analysis of possible accidents at PIK reactor”.

The developed Statement of Works determines the scope of works, authority and responsibility of participants, and general requirements to the analysis of possible design and beyond design-basis accidents in accordance with requirements of regulations NP-049-03 under preparation of corresponding sections for “Safety Analysis Report of PIK reactor”.

The developed Specification sets up the compliance of postulated initiating events stated in the Safety Analysis Report with the requirements of NP-049-03 as well as other federal rules and regulations in the atomic energy use: NP-061-05, NP-033-11, NP-009-04.

The Specification includes the following sections involving all postulated initiation events, which can potentially result in abnormal conditions of the reactor:

- Initiating events resulting in insertion of excess reactivity;

- Initiating events resulting in heat removal failure;
- Pressure change in reactor primary circuit;
- Degradation of heat removal by a secondary circuit (auxiliary circuit and recycling water supply circuit);
- Failure in nuclear fuel handling;
- Initiating events of design accidents for fuel storage systems;
- Natural phenomena and man-caused events;
- Initiating events for design analysis of beyond design-basis accidents.

The developed Specification takes into account specific design features, neutronic and technical characteristics of the PIK reactor during the transient analysis. In total 85 postulated initiating events have been considered. The preliminary calculations show that part of initiating events requires clarification of accident scenarios, additional organizing and engineering decisions to reduce radiological consequences: leakage of maximum diameter pipelines, insertion of positive reactivity, and loss of off-site power with subsequent additional failures.

This Specification will be used as the basis for design analysis in design maintenance of high-priority works for commissioning support of the PIK reactor facility and safety substantiation under the first power program and commissioning with stage-by-stage increase of reactor power and its experimental possibilities.

Fuel charging control during PIK reactor energy start-up

S.R. Fridman, V.P. Stulov, A.S. Zakharov. – Department of Reactor Physics and Technology
 A.A. Lankovich, G.T. Potapenko – Department of Commissioning of PIK Neutron Research Center
 NRC “Kurchatov Institute” – PNPI

The data obtained from standard detectors of control and protection system (CPS) and additional start-up channels during the reactor loading in 2011 under the first criticality program were analyzed in order to prepare the PIK reactor equipment for energy start-up. The data analysis has been carried out in cooperation with the chief reactor designer JSC “NIKIET”. The experiments with tests of standard control channel at a full-scale critical facility (Fig. 1) were used as well. The proposals which provide a more reliable registration of the change of core states during fuel charging were developed.

Neutronic calculations were performed using the precision code MCU-KS with a library MDBKS50, which represents the evolution of programs MCU-RFFI/A and MCU-REA. The sub-module FIMTOEN was applied for simulation of neutron interaction in the region of neutron thermalization. The reactor simulation model includes the simulated channels of the control and protection system (CPS) (Fig. 2, 3).

The calculated simulation of the first criticality program in 2011 showed that the acceptable level of neutron flux and signal flow will be obtained after charging of seven fuel assemblies (FA). The needed level is defined as the level exceeding the certificate sensitivity of a standard detector. The calculation results correspond to the actual ones. At the first stage, the additional start-up channel equipment beside of sub-criticality control should be used at the critical experiments for data processing and calculation of reactor characteristics at the lowest possible power level. The various configurations of the reactor core, arrangements of detectors and types of external neutron sources have been considered.

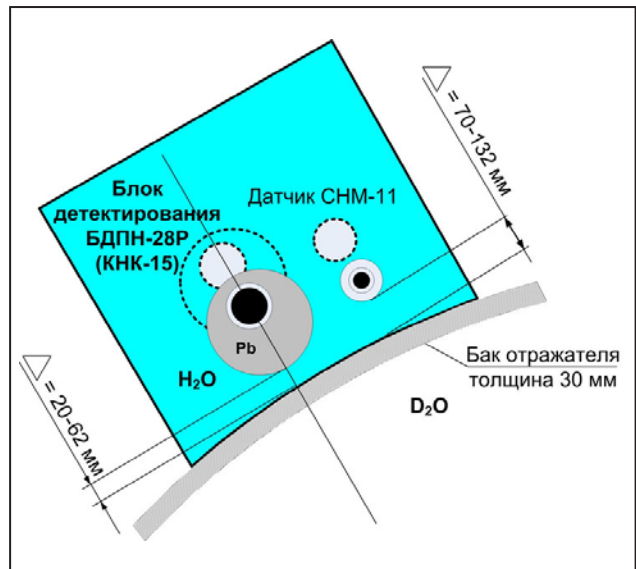


Fig. 1. The placement of detector blocks with an adjustable water clearance in the mockup iron-water protection tank at a critical facility

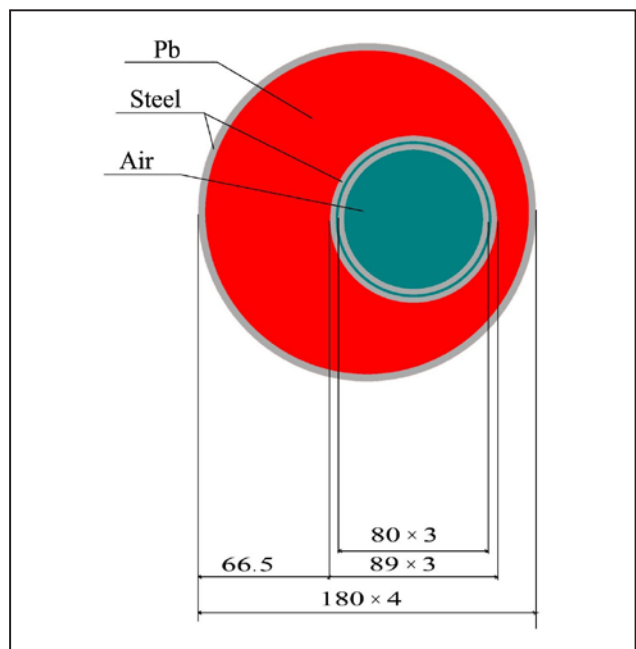


Fig. 2. CPS channel in the reactor simulation model

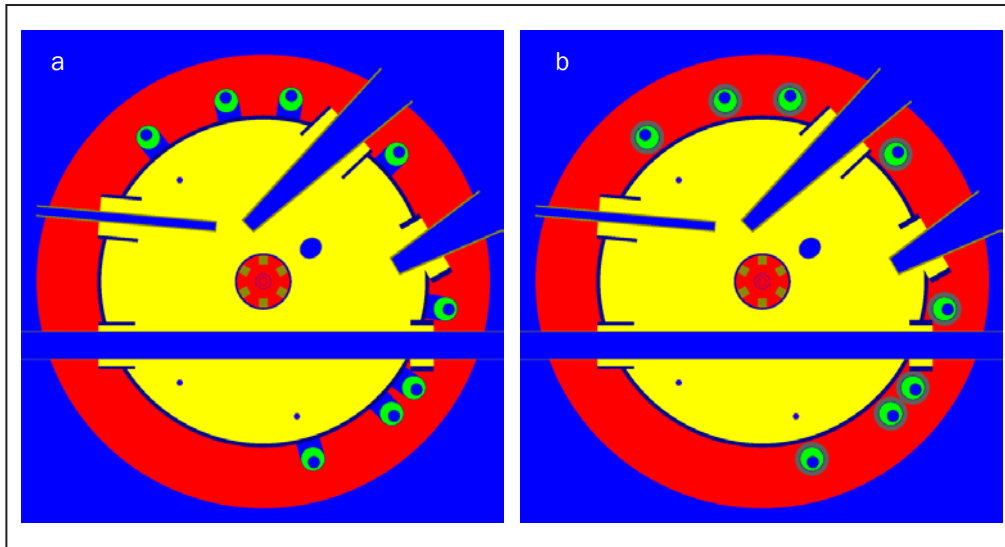


Fig. 3. The placement of detector blocks in CPS channels with displacers in the reactor simulation model: irregular-shaped displacer (a); ring-shaped displacer (b)

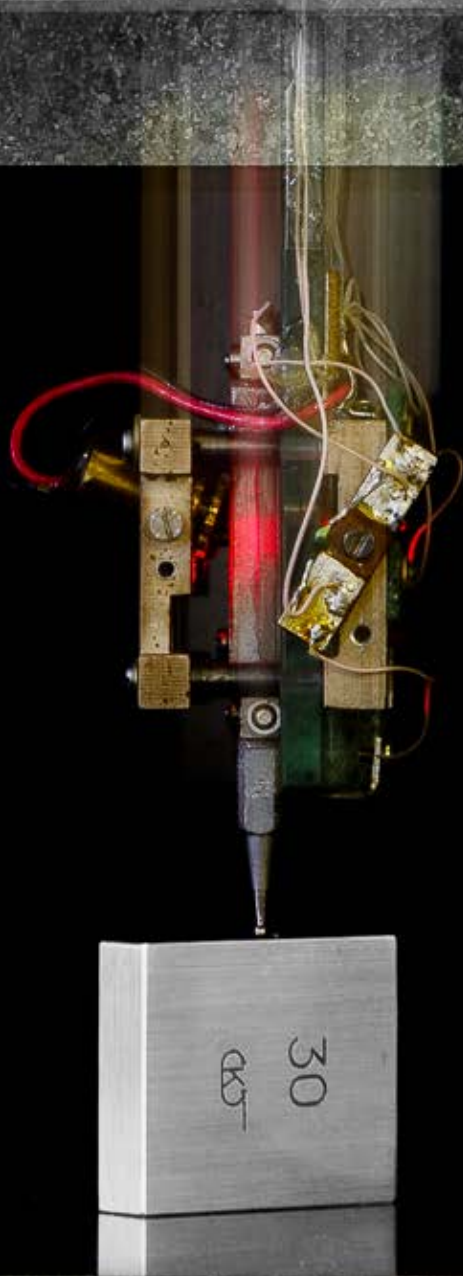
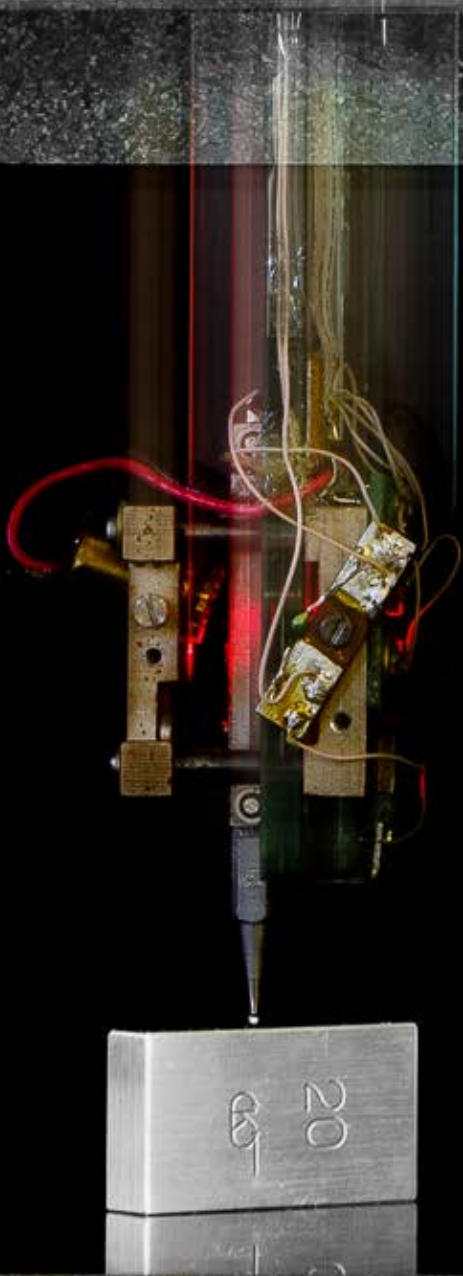
Table. Change of counting rate for standard detector at the first stages of fuel loading

Variant	Effect
Replacement of plutonium-beryllium neutron source of $4.5 \cdot 10^7 \text{ s}^{-1}$ intensity to californium source of $1.0 \cdot 10^9 \text{ s}^{-1}$ intensity	$\times 10.0$
Displacement of water from a core by aluminum displacers	$\times 2.2$
Movement of detector channels closer to HWR tank (minimal gap 10 mm)	$\times 3.9$
Full water displacing between HWR tank and lead shielding of detectors	$\times 10$
Installation of annular displacer (aluminum alloy AD1) of 3.5 cm thickness around of detector lead shielding	$\times 3.6$
Replacement of steel claddings to zirconium/aluminum ones for lead shielding and detectors	$\times 3.6/3.4$
Installation of detectors into HWR tank	> 100
Use more sensitive detectors	5–10

The physical analysis of neutron transmission from a neutron source in the core to detectors takes into account four significant stages: 1) neutron transmission in the reactor core volume; 2) neutron transmission in a heavy-water reflector (HWR); 3) neutron transmission in HWR casing and a gap between HWR and lead shielding of detectors; 4) neutron transmission in the lead shielding and channel cover of detectors. The Table presents conceptual actions for the increase of standard detector units during loading of first fuel portions. The required effect can be obtained by combination of several actions.

The simplest way for improvement of statistics of detector counting is the temporary installation of reserve standard detectors based on ionization chambers KNK-15 into inclined experimental channels of HWR. At a later stage, these channels must be handed over for free use.

The received results are necessary for designing the equipment for the refueling monitoring system. The detectors of this system are different from the instrumentation of the first reactor start-up, since they have low sensitivity to gamma radiation from irradiated FAs and they must be installed behind the reflector.



Applied Research and Developments

- 122 Investigation of conditions for scientific research in the ice borehole of Lake Vostok in Antarctica
- 124 Two-section ionization chambers for monitoring of variable energy proton beams
- 125 3D coordinate nano measuring machine “3D NANO CMM”
- 127 Universal proton and neutron center for radiation resistance of avionic, space electronics and other applications at the 1 GeV synchrocyclotron in NRC “Kurchatov Institute” – PNPI

Investigation of conditions for scientific research in the ice borehole of Lake Vostok in Antarctica

V.F. Ezhov, A.A. Zakharov – Knowledge Transfer Division
 S.A. Bulat – Molecular and Radiation Biophysics Division
 Yu.O. Chetverikov, V.A. Solovej – Neutron Research Division
 NRC “Kurchatov Institute” – PNPI

The first unsealing of subglacier Lake Vostok in Antarctica was performed on 5 February 2012, however the scientific research of the lake has not started to date. The drilling fluid loaded in a borehole comprises aviation kerosene TS-1 and freon R-141b. The temperature in the borehole gradually increases from -55°C on the surface to the water freezing point of -2.7°C at the depth of 3 769 meters. Freon R-141b remains liquid at low temperatures. It is used as a densifier for the drilling fluid to maintain the hydrostatic pressure in the borehole, which is a bit lower than the pressure inside the lake. While unsealing Lake Vostok with a drilling tool the water goes upward into the borehole due to a pressure difference between the pressure inside the lake and the drilling fluid hydrostatic pressure.

In the process of the recurrent drilling of frozen water in the borehole a white plug was discovered inside the borehole. A drilling tool has extracted 10.5-meter-long core containing R-141b clathrate hydrates. The clathrate hydrates are formed when water contacts the drilling fluid containing freon R-141b. The clathrate plug in the borehole hinders the immersion of scientific instruments into the lake and it can cause the pollution of lake water.

Several experiments were carried out at NRC “Kurchatov Institute” – PNPI to study the formation of R-141b clathrate hydrates. Three types of clathrate macrostructures were discovered (Fig. 1).

To prevent the contact of drilling fluid with water in the borehole a hydrophobic silicone (polymethylsiloxane) fluid can be used as a buffer layer. Fluid levels in the borehole are shown in Fig. 2. Ecologically inert silicone fluid is loaded in the borehole before drilling of the last meter of ice remaining until reaching the lake (Fig. 2a). The height of the buffer layer of silicone fluid, which is located under the drilling fluid shall not be less than 45 meters.

The compensation of the lake pressure is produced by the column of fluids in the borehole in such a way that the rise of water would be approximately 10 meters when the lake is unsealed. Levels of different fluids in the borehole after unsealing of the lake are shown in Fig. 2b.

There is an additional 43-meters rise of the water level in the borehole when removing the carrying cable with a drill tool (Fig. 2c). The overall water level in the borehole reaches 53 meters. Water washes the borehole walls, where silicone fluid was located, not the drilling fluid. In turn, when the

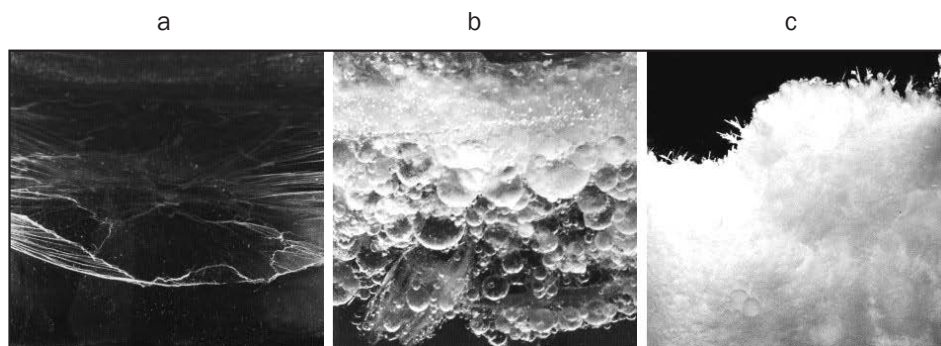


Fig. 1. R-141b clathrate hydrate macrostructure: crystal film between water and R-141b (a); clathrate hydrate structure in water (b); clathrate hydrate structure in a volume with R-141b (c)

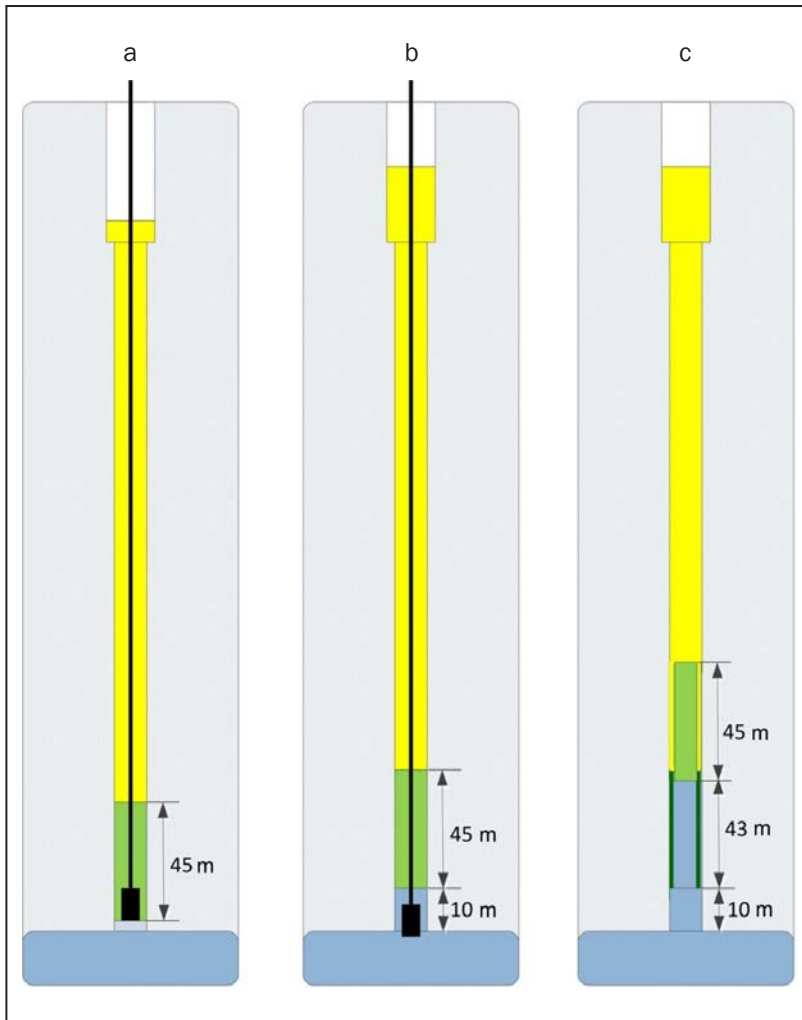


Fig. 2. Fluid levels in the borehole: before the lake unsealing with 45 meter buffer layer of silicone fluid (a); after unsealing and the 10-meters rise of water in the borehole (b); after extracting the equipment from the borehole followed by additional 43-meters rise of water (c)

column of silicone fluid rises 43 meters, it washes the surface, where the drilling fluid was located. The drilling fluid remaining on the walls of the borehole, dissolves in the silicone fluid.

Laboratory experiments have demonstrated that when the drilling fluid contacts the water, the formation and growth of clathrate hydrates are not observed, if the drilling fluid contains more than 20% of silicone fluid.

In the first stage of scientific research, the lake water risen to the borehole will be investigated. After the extraction of the carrying cable with a drilling

tool, the scientific instruments are immersed sequentially in the borehole. The change of fluid levels in the borehole during these immersions is shown in Fig. 2b and Fig. 2c.

Experiments at NRC “Kurchatov Institute” – PNPI provided the opportunity to study the processes of formation of R-141b clathrate hydrates and justify the need for the use of the hydrophobic silicone fluid, which allows to avoid the formation of a clathrate plug in the borehole and carry out an environmentally friendly delivery of scientific equipment to the lake water.

Two-section ionization chambers for monitoring of variable energy proton beams

*D.A. Amerkanov, G.I. Gorkin, E.M. Ivanov, N.A. Ivanov, E.A. Kotikov,
Zh.S. Lebedeva, O.V. Lobanov, V.V. Pashuk
Knowledge Transfer Division of NRC "Kurchatov Institute" – PNPI*

The absolute program-controlled proton monitor working in real time is used in studies of radiation resistance of electronics at the NRC "Kurchatov Institute" – PNPI synchrocyclotron with proton energies 64–1000 MeV. It is a two-section ionization chamber (TSIC), filled with air at atmosphere pressure, with various interelectrode distances in each section. TSIC of various modifications with apertures of 10 cm and 20 cm were designed and manufactured. For shielding from external radiation, they were placed in case made of duralumin. The signal and high voltage electrodes are made of aluminum foil with a thickness of 10 μm and soldered on panels made of one-sided foil Teflon plate with a thickness of 1.5 mm using the self-developed technology at Radiation Physics Laboratory. Interelectrode distances was chosen to be 2.1 cm and 4.2 cm. Aperture electrodes are made of duralumin with the thickness of 0.2 mm.

The background contribution to ionization of the sensitive area of TSIC due to δ -electrons emitted from Al-foil electrode irradiated by protons, was estimated. The coefficients that determine the contribution of δ -electrons from the electrodes to the total ionization for the three modifications of the TSIC (6, 10 and 20 cm) were calculated using the program complex Geant4. The maximum contribution was 6% at the energy of 60 MeV and a minimum contribution of 4% at the energy of 1000 MeV.

The testing of cameras with the aperture electrodes 10 cm and 20 cm in diameter was carried out at the proton beam of energy 1000 MeV. The proton beam was formed by a collimator with a diameter of 20 mm. Control of the constancy of the proton flux was carried out by a large ionization chamber placed in the main hall of the accelerator. Studies have shown that the response of the cameras to the impact of protons with the same flux is identical in both central and peripheral areas of the cameras (range up to 5%).

Algorithm to calculate the number of protons corresponding to any given region of the beam cross section was proven experimentally using "photos" of different energy proton beam. To this end, the photographic image was processed using standard software (MathCad, Origin, etc.) to find the distribution of the blackening and consequently, of the distribution of the proton flux density.

Simultaneously with the TSIC-based monitor, the proton fluxes were measured by method of induced activity of carbon and polyethylene foils with a diameter of 3 cm. Using the proposed method, the proton fluxes were calculated within the same region. Taking into account measurement errors, the measurement results are practically the same in the energy range of protons 64–1000 MeV.

3D coordinate nano measuring machine “3D NANO CMM”

V.V. Dobyryn, O.G. Ermolenko, S.N. Khanov, L.A. Konstantinov, V.E. Kormin, Yu.M. Lavrov, R.P. Sinelshchikova, V.G. Tolchin, B.G. Turukhano, N. Turukhano, N.A. Schipunova, E.A. Vilkov
 Knowledge Transfer Division of NRC “Kurchatov Institute” – PNPI

3D coordinate nano measuring machine (3D NANO CMM) contains nano-encoders of linear movements with a high precision measuring element in the form of a metrological holographic diffraction grating (HDG), which is designed for high-precision measurement of linear movements and the definition of a real-time geometry of complex products, processing and storage of measurement results while working with automated systems (Fig. 1).

A study of the volumetric accuracy of the machine (obtained value $\pm 1.6 \mu\text{m}$) is demonstrated in Fig. 2. Figure 3 shows the measurement of toroidal mirrors by 3D NANO CMM. First, four angles were measured, and then the automatic machine was turned on, and the picture was printed out.

To implement the synchronous movement of two heads within the accuracy of a few tens of nanometers on the Y-axis, the hysteresis delay of the right side of the bridge with respect to its left-hand part will be observed. With the purpose of correcting this phenomenon, in addition to the encoder Y_1 , the second encoder – Y_2 with

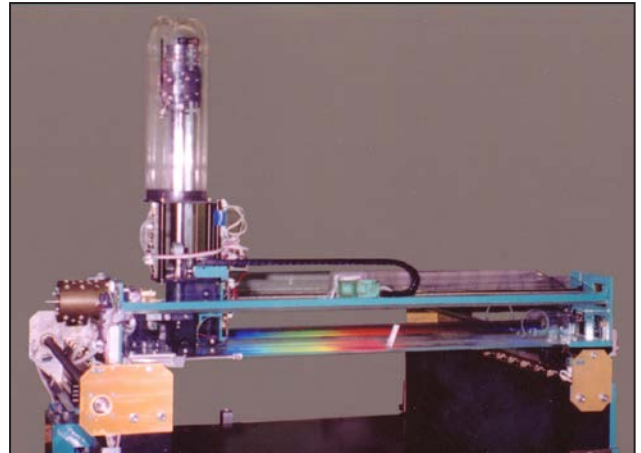


Fig. 1. 3D NANO CMM

its own measuring grating and the head is installed on the Y-axis. The calculation of the final value of the Y-axis is performed under software control and represents a position function of the X-axis corresponding to the axis of vertical holographic lengthmeter measuring the Z-axis. Thus, the values of Y_1 and Y_2 counted by measuring encoders Y_1 and Y_2 allow us to find the true value of the coordinate Y:

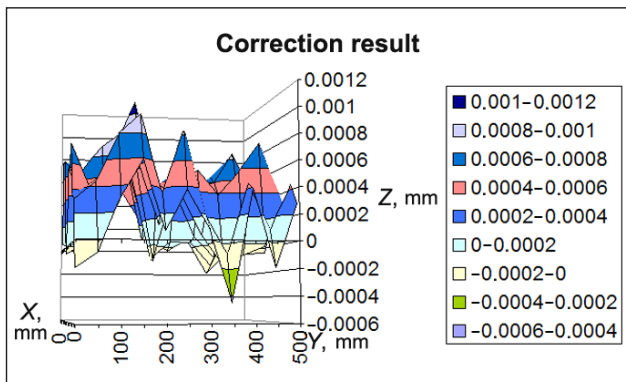


Fig. 2. Corrections of 3D NANO CMM

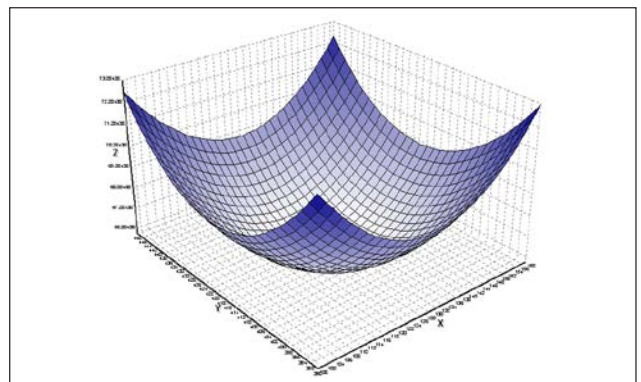


Fig. 3. Scan picture of toroidal mirror with the help of 3D NANO CMM

$$Y = 1/L [(L - X)Y_1 + XY_2],$$

where L – the total length on the X-axis.

The introduction of the fourth coordinate Y_2 shifts the measuring machine into the “nano” category.

The second design feature of the 3D NANO CMM is that the lengthmeter with a touch sensor (TS) combines the principles of operation of an encoder of linear movements along the Z-axis with a TS (since TS is made in the form of an encoder of linear movements on the basis of the diffraction gratings). Moreover, it has the same HDGZ measuring grid and the same guide for the sensor along the Z-axis and TS.

Main features of 3D NANO CMM are:

- the use of four ultraprecision nanomeasuring linear holographic sensors (UNLS);
- availability of internal autonomous high-precision guides;
- the use of lightweight and hard glass bridges that serve for fixing of the measuring system – the X- and Z-axes. Considerable weight of a diabase bridge, usually used in 3D-CMM by various

companies as an accurate guide of the X-axis, leads to an increase in deformation, the inertia of the system and, as consequence, to reduction of the precision of the measuring machine;

- installation of two sensors Y_1 and Y_2 on the Y-axis simultaneously.

Technical specification of 3D NANO CMM are shown in the Table.

As a result, owing to the use of UNLS, the coordinate measuring machine with nanoresolution and a record precision was created for the first time.

Table. Technical specification of 3D NANO CMM

Dimensions, mm	550 × 550 × 200
Volumetric accuracy, μm	±1,6
Resolution, nm	10
Communication interface	CAN-USB
Environment temperature, °C	20 ± 2

Universal proton and neutron center for radiation resistance of avionic, space electronics and other applications at the 1 GeV synchrocyclotron in NRC “Kurchatov Institute” – PNPI

D.A. Amerkanov, S.A. Artamonov, E.M. Ivanov, J.S. Lebedeva, G.F. Mikheev, G.A. Riabov – Knowledge Transfer Division

*O.A. Shcherbakov, A.S. Vorobyev – Neutron Research Division
NRC “Kurchatov Institute” – PNPI*

*V.S. Anashin, L.R. Bakirov, P.A. Chubunov, A.E. Koziukov –
Institute of Space Device Engineering*

The report presents a short description of the proton (IS SC-1000 and IS OP-1000) and neutron (ISNP/GNEIS) test facilities developed at NRC “Kurchatov Institute” – PNPI in collaboration with the Branch of JSC “United Rocket and Space Corporation” – “Institute of Space Device Engineering”, a Head Organization of the ROS-COSMOS Interagency Testing Center. A unique conjunction of proton beams with variable energy 60–1000 MeV and atmospheric-like neutron beam with broad energy range (1–1000 MeV) enable to perform complex testing of the semiconductor electronic devices at the SC-1000 within a single testing cycle.

Proton test facilities

At present, two of three proton beam lines of the SC-1000 are used for radiation testing of electronics. The IS SC-1000 test facility has fixed proton energy of 1000 MeV and is located on the P2 beam line. At the IS OP-1000 facility located on the P3 beam line, proton energy can be varied from 1000 MeV down to 60 MeV by means of a system of copper degrader (absorber) of variable thickness from 73 mm (at 900 MeV) to 530 mm (at ~ 60 MeV). A scheme of the proton beams and irradiation workstations placed in the experimental room, as well as a photo

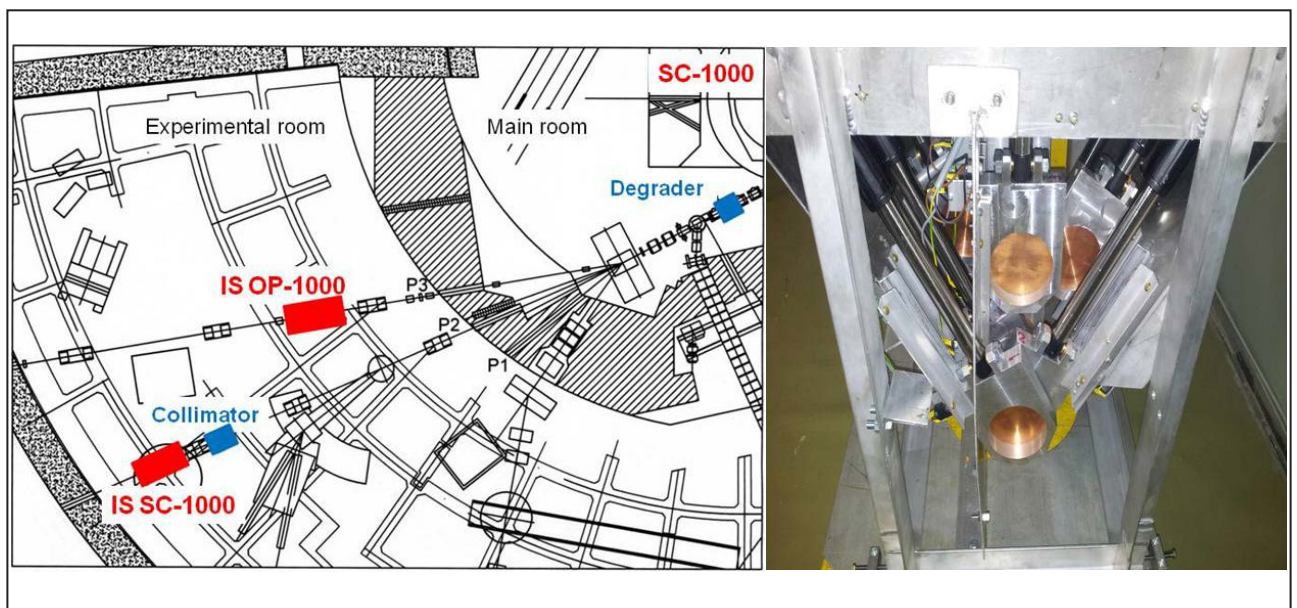


Fig. 1. Scheme of the proton beam lines: P2 – protons with the energy of 1000 MeV; P3 – protons with variable energy of ~ 60–1000 MeV (left). Device for remote variation of the absorber length and the proton energy (right)

Table. Parameters of the proton test facilities

Parameter	IS SC -1000	IS OP - 1000
Irradiation conditions	Atmosphere	Atmosphere
Particle	Protons	Protons
Energy, MeV	1000	60-1000
Flux, $\text{cm}^{-2} \cdot \text{s}^{-1}$	10^5 - 10^8	10^5 - 10^8
Irradiation area, mm	$\varnothing \geq 25$	$\varnothing \geq 25$
Uniformity, %	≤ 10	≤ 10
Status	In operation (1998)	In operation (2015)

of the degrader system located in the SC-1000 main room are shown in Fig. 1. The parameters of both proton test facilities are given in Table.

Parameters of the proton beam at the outlet of copper absorber of variable thickness have been evaluated by means of the Geant-4 code calculation. Beam diagnostics is carried out using a set of standard tools which includes: 1) thin scintillator – screen coupled with a CCD-sensor for rapid evaluation of the beam profile image; 2) 2D-moving Se-stripe-type beam profile meter; 3) double-section ionization chamber for “on-line” control of the proton intensity (fluence); 4) Al-foil activation technique in conjunction with a high-resolution HPG-detector as absolute “off-line” monitor of proton fluency.

Neutron test facility

The ISNP/GNEIS test facility has been in operation since 2010 at the neutron TOF-spectrometer GNEIS. Its main feature is a spallation source with neutron spectrum resembling that of terrestrial neutrons in the energy range of 1–1000 MeV. The water-cooled lead target located inside the accelerator vacuum chamber (Fig. 2) produces short 10 ns pulses of fast neutrons with a repetition rate of 45–50 Hz and average intensity up to $3 \cdot 10^{14} \text{ cm}^{-2} \cdot \text{s}^{-1}$. The ISNP/GNEIS test facility is located inside the GNEIS building on the neu-

tron beam No. 5, which has the following parameters: neutron energy range: 1–1000 MeV; neutron flux: $4 \cdot 10^5 \text{ cm}^{-2} \cdot \text{s}^{-1}$ (at 36 m flight path); beam diameter: 50–100 mm (at 36 m flight path); uniformity of the beam profile plateau: $\pm 10\%$.

The neutron flux of $4 \cdot 10^5 \text{ cm}^{-2} \cdot \text{s}^{-1}$ is an integral over neutron spectrum in the energy range 1–1000 MeV. It corresponds to the maximum value of 3 μA of the internal average proton beam current. The neutron flux and shape of the neutron spectrum are measured using FIC (neutron monitor) and TOF-technique (Fig. 4). The FIC is a fast parallel-plate ionization chamber which contains two targets of ^{235}U and ^{238}U . The neutron fission cross sections of these nuclei are recommended standards in the energy range 1–200 MeV. The neutron beam profile is measured by means of MWPC – the 2-coordinate position sensitive multiwire proportional counter used for registration of fission fragments from the ^{235}U target deposited on the MWPC’s cathode. The neutron spectrum $F_{\text{ISNP}}(E)$ is shown in Fig. 2 together with the JEDEC standard terrestrial neutron spectrum from JESD89A referenced to New York City and multiplied by scaling factor $7 \cdot 10^7$, as well as the neutron spectra of leading test facilities. Both the shape of the neutron flux and neutron intensity demonstrates that the ISNP/GNEIS is successfully competing with the other first-grade test facilities with the atmospheric – like neutron spectrum. The SC-1000 possesses a potential of the neutron intensity growth. A new irradiation station located at a distance of 5-6 m from the neutron-production target operated on the extracted proton beam enables to increase neutron flux at least 10 times at the DUT position. Simultaneously, an irradiation of the bulky equipment will be possible.

A versatile complex of test facilities has been developed at the SC-1000 accelerator of NRC “Kurchatov Institute” – PNPI. At present, a growing number of Russian research organizations specialized in radiation testing of the electronics conduct their research on the proton and neutron beams under direct agreements with the NRC “Kurchatov Institute” – PNPI or with the Branch of JSC “URSC” – “ISDE”.

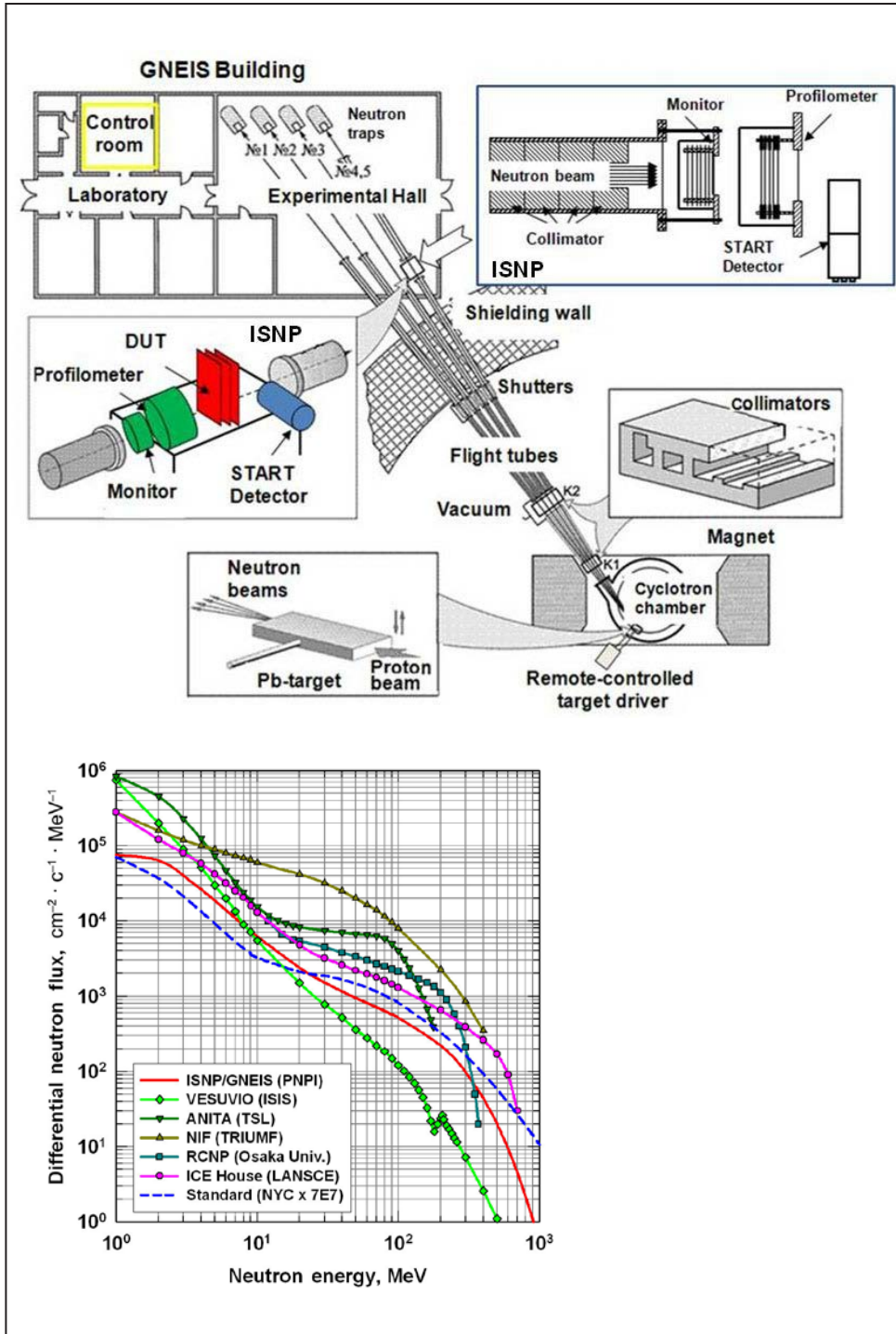


Fig. 2: General layout of the neutron time-of-flight spectrometer GNEIS and ISNP test facility (up). Neutron spectrum $F_{\text{ISNP}}(E)$ of the ISNP/GNEIS facility in comparison with standard terrestrial neutron spectrum and spectra of other world-class test facilities (down)



Basic Installations

- 132** Status of the 1 000 MeV synchrocyclotron in 2016
- 133** Isochronous cyclotron C-80. Status and prospects

Status of the 1 000 MeV synchrocyclotron in 2016

S.A. Artamonov, E.M. Ivanov, G.F. Mikheev
 Knowledge Transfer Division of NRC "Kurchatov Institute" – PNPI

The synchrocyclotron SC-1000 for a proton energy of 1 000 MeV with intensity of the extracted beam of $1 \mu\text{A}$ is the basic installation of the NRC "Kurchatov Institute" – PNPI since 1970. It is widely used for fundamental research in the field of particle physics, structure of atomic nuclei (including nuclei far from stability) and mechanisms of nuclear reactions in them, solid state physics, as well as in applied studies on radiological tests and nuclear medicine studies.

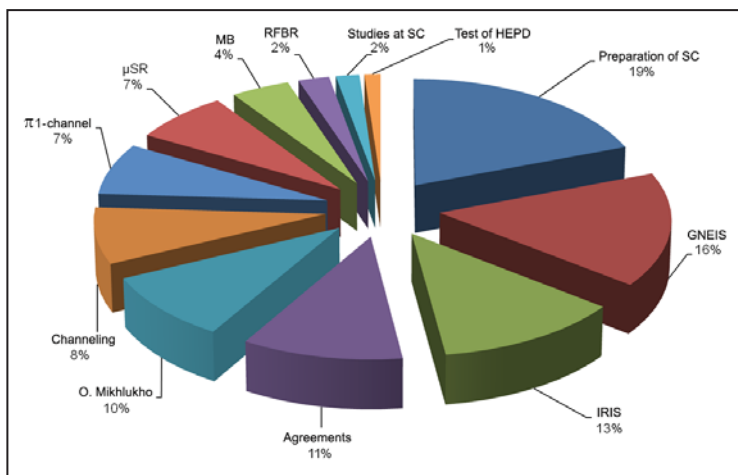
In 2016, the accelerator was in operation for 3 225 hours in total. The diagram shows the distribution of SC-1000 operating time in various areas of research on its beams.

Furthermore, this year marked the creation of a universal center for tests of radiation resistance of the electronics used in space, aviation and other application areas. The center includes two test stands to work at a proton beam with an energy of 1 000 MeV, and at proton beams

of variable energy $\sim 60, 100, 200, 300, 400, 500, 600, 700, 800, 900, 1\,000$ MeV, as well as the test stand at a neutron beam of an atmosphere-like range. A series of contractual projects with third parties has been successfully executed on the basis of the created center.

In collaboration with the staff of the Russian Institute for Power Radiobuilding (RIPR), the investigation was carried out to determine the feasibility of the replacement of obsolete electrical machines of SC-1000 with their modern and highly compact analogs. The results of the research showed that the development of power supplies for the magnetic elements of the synchrocyclotron is possible.

Together with Molecular and Radiation Biophysics Division (MRBD), we started the development of methods of diagnosis and treatment of oncology diseases using irradiation of laboratory rodents with a modified proton beam.



Directions of work carried out on beams of synchrocyclotron SC-1000

1. Amerkanov D.A., Artamonov S.A., Ivanov E.M., Lebedeva J.S., Mikheev G.F., Riabov G.A., Shcherbakov O.A., Vorobyev A.S. et al. // Proc. of XXV Russ. Part. Accel. Conf. (RuPAC-2016). 2016. P. 105–107.
2. Synchrocyclotron Focusing Device: the Patent for the Utility Model No. 165907 / E.M. Ivanov, G.F. Mikheev; Priority of 16.02.2016.

Isochronous cyclotron C-80. Status and prospects

D.A. Amerkanov, S.A. Artamonov, V.P. Gres, E.M. Ivanov, G.F. Mikheev, I.A. Petrov, A.S. Pokrovsky, G.A. Ryabov, V.A. Tonkikh, V.I. Yurchenko
 Knowledge Transfer Division of NRC “Kurchatov Institute” – PNPI

On 8 November 2016 in NRC “Kurchatov Institute” – PNPI the isochronous cyclotron C-80 for the acceleration of negative ions of hydrogen with the energy of the extracted proton beam ranging 40–80 MeV was brought to its design parameters for the first time (Fig.).

The creation of a cyclotron C-80 opens tempting opportunities for the start of production of radioisotopes at a totally new level both in terms of production growth and in terms of expansion of the assortment of the produced radioisotopes. Practically all requirements of the medical institutions of the north-west of the Russian Federation which are engaged in introduction of new radiopharmaceuticals into medical practice will be satisfied in this respect. At the same time, this project provides for a strategic opportunity of not only producing the isotopes, but also preparing the isotope-based radiopharmaceuticals.

The variable energy of an accelerated beam combined with its high intensity allows the pro-

duction of high-quality radioactive isotopes and radiopharmaceuticals that cannot be produced at commercial cyclotrons, in particular generator isotopes of ^{82}Sr и ^{68}Ge . The project provides the possibility of isotope separation by means of a magnetic separator.

The use of a mass-separator for electromagnetic separation of the produced radionuclides will ensure the production of a wide range of ultra-pure radionuclides (better than $1 \cdot 10^{-4}$) for the diagnosis and therapy.

The high energy of the proton beam will allow the creation of an ophthalmology center for radiation therapy of eye cancer disease. It will be the first center of this kind in Russia and CIS countries. Such technology of treatment of eye cancer diseases is highly effective, it is widely used abroad and it is in demand in the medical community. The center will be used by clinics of St. Petersburg and Leningrad region.



Isochronous cyclotron.
 Top level (left). Paths to target stations. Lower level (right)

1. Artamonov S.A., Chernov A.N., Ivanov E.M., Riabov G.A., Tonkikh V.A. // Proc. of XXV Russ. Part. Accel. Conf. (RuPAC-2016). 2016. P 176–178. <http://accelconf.web.cern.ch/AccelConf/rupac2016/>
2. Amerkanov D.A., Artamonov S.A., Ivanov E.M., Riabov G.F., Yurchenko V.I. et al. // Proc. of XXV Russ. Part. Accel. Conf. (RuPAC-2016). 2016. P. 179–181. <http://accelconf.web.cern.ch/AccelConf/rupac2016/>



Management and Research

136 Awards. Prizes

138 Seminars

141 Conferences

Awards. Prizes

NRC “Kurchatov Institute” – PNPI is an actively functioning institute which keeps pace with the current scientific trends. Numerous prizes and grants of its employees attest to this statement.



Winners of 2016 Kurchatov prize

According to the results of 2016 Kurchatov prize, an active participation in this competition has become a good tradition among the employees of the Institute. It is notable that the competition participants are represented not only by the leading and young scientists and engineers, but also by students. For this purpose, the Regulations of the competition contain special terms and conditions for their application. This year, 11 scientific works of the Institute employees were recognized as the best ones.

In the area of scientific research:

- “10 years of neutrino research in Borexino experiment” – A.V. Derbin, V.N. Muratova, (E.A. Litvinovich, I.N. Machulin, M.D. Skorokhvatov – NRC “Kurchatov Institute”);
- “Study of delayed fission and nuclear shape coexistence by methods of resonant ionization in a laser ion source” – A.E. Barzakh, D.V. Fedorov, M.D. Seliverstov, P.L. Molkanov, V.N. Panteleev;
- “Penning traps for high-precision measurements of the mass of nuclides for a wide range of problems of the fundamental physics” – S.A. Eliseev.

The following young employees of NRC “Kurchatov Institute” – PNPI got the 2016 Kurchatov prize in the nomination for the best work among young staff scientists and R&D engineers:

- “Development of theoretical methods of calculation of the electronic structure of molecules and crystals for experiments in physics beyond the standard model” – L.V. Skripnikov;
- “Defects in helical magnets with the Dzyaloshinskii-Moriya Interaction” – O.I. Utyosov, A.V. Sizanov;
- “High-order oligomers of intrinsically disordered brain proteins BASP1 and GAP-43 preserve the structural disorder” – O.S. Forsova.

Five students who conducted their research in NRC “Kurchatov Institute” – PNPI were awarded the 2016 Kurchatov prizes in the category “Best student works”:

- “The development and commissioning of the bunched beam current measurement system at the COSY accelerator” – L.D. Eltsov;

- “Diffraction studies of the crystal structure of layered honeycomb oxides” – S.Yu. Podchezertsev;
- “Channeling and volume reflection of 1 GeV protons in bent silicon crystals” – M.V. Malkov;
- “Low-energy nuclear isomerism” – N.S. Martynova;
- “The study of the structure of carbon nanotubes” – A.N. Matveeva.

The winners of a competition for the prize named after academician A.P. Alexandrov

Young researchers of NRC “Kurchatov Institute” – PNPI became the winners in the category for young scientists of an annual competition of scientific works – 2016 Alexandrov prize of NRC “Kurchatov Institute”:

- “Development of gas-discharge neutron detectors for experimental set-ups for condensed matter physics and fundamental physics” – D.S. Ilyin;
- “Launch of a full-scale model of UCN source. Analysis of the results” – V.A. Lyamkin.

The administration of Leningrad Oblast continued to support 11 papers of NRC “Kurchatov Institute” – PNPI researchers, who were formerly awarded the scientific scholarships of the governor of Leningrad Oblast: two employees were awarded a personal scholarship of the governor of Leningrad Oblast in the category “Young scientist”, and 9 employees in the category “Leading scientists”.



In 2016 the head of the laboratory of Human Molecular Genetics of Molecular and Radiation Biophysics Division of NRC “Kurchatov Institute” – PNPI Sofia N. Pchelina got the prize of the governor of Leningrad oblast for efforts in development of science and technology and achievements in fundamental research in the category “Natural and technical sciences” for her work “Genetic and biochemical markers of Parkinson’s disease”.

The scholarships in honor of distinguished scientists S.E. Bresler, V.N. Gribov, G.M. Drabkin, V.M. Lobashev, whose scientific activity was connected with the Institute, were established in NRC “Kurchatov Institute” – PNPI for young scientists and specialists demonstrating significant advances in research. In 2016,

four young employees of the Institute became the holders of these scholarships. Scholarships were awarded in the following nominations:

- S.E. Bresler Scholarship for works in the field of biology – O.S. Forsova;
- V.N. Gribov Scholarship for works in the field of theoretical physics – O.I. Utyosov;
- G.M. Drabkin Scholarship for works in the field of condensed matter physics – N.M. Chubova;
- V.M. Lobashev Scholarship for works in the field of nuclear physics – V.M. Samoilov.



Seminars

Schedule of seminars

All-Institute seminars:

- General seminar – once a month, on Thursdays;
- Seminar on condensed state physics – every Thursday (except the General Seminar Day);
- Seminar on biology – 1-2 times a month, on Wednesdays;
- Joint seminar of High Energy Physics Division and Theoretical Physics Division – once a month, on Thursdays.

Seminars in Divisions:

- High Energy Physics Division – every Tuesday;
- Neutron Research Division – once a month, on Wednesdays;
 - Condensed State Research Department – every Tuesday;
 - X- and γ -Ray Spectroscopy – once a quarter, on Wednesdays;
 - Neutron Research Division on atomic and molecular physics – once a quarter, on Thursdays;
- Theoretical Physics Division – on Mondays in Euler International Mathematical Institute (Saint Petersburg); on Thursdays – in NRC “Kurchatov Institute” – PNPI (Gatchina);
- Molecular and Radiation Biophysics Division (on the to-be-published articles) – 1-2 times a month, on Wednesdays;
 - Laboratory of Genetics of Eukaryotes – once a week, on Fridays;
 - Laboratory of Biophysics of Macromolecules – every two weeks, on Wednesdays;
 - Laboratory of Cell Biology – once a week, on Thursdays;
 - Laboratory of Protein Biosynthesis – every two weeks, on Fridays;
 - Laboratory of Proteomics – every two weeks, on Mondays;
 - Laboratory of Experimental and Applied Genetics – once a week, on Wednesdays;
 - Laboratory of Enzymology – every two weeks, on Tuesdays;
 - Laboratory of Molecular Genetics – once a month, on Wednesdays;
 - Laboratory of Human Molecular Genetics – once a week, on Wednesdays;
- Knowledge Transfer Division – every third Tuesday, monthly;
 - Accelerator Department – every Tuesday, monthly.

All-Institute Seminars

- 14 January.** V.A. Schegelsky (High Energy Physics Division of NRC “Kurchatov Institute” – PNPI) – “Bose-Einstein femtoscopy, proton structure and the “pomeron size”.
- 26 January.** D.Yu. Minkin (NRC “Kurchatov Institute” – PNPI) – “Particularities of use of modern missile armament”.
- 4 February.** O.A. Shcherbakov (Neutron Research Division of NRC “Kurchatov Institute” – PNPI) – “Test stand at the NRC “Kurchatov Institute” – PNPI synchrocyclotron for neutron radiation testing of electronics”.
- 11 February.** I.V. Golosovsky (Neutron Research Division of NRC “Kurchatov Institute” – PNPI) – “Magnetic structures in the CoO nanoparticles with a “wurtzite” and “zinc blende” crystalline structure existing only in the form of nanoparticles. Neutron and X-ray diffraction”.
- 24 March.** M.I. Eides, A.A. Vorobyov (Theoretical Physics Division, High Energy Physics Division of NRC “Kurchatov Institute” – PNPI) – “The proton radius puzzle: discussion of the problem and project of new elastic ep -scattering experiment”.
- 24 March.** A.O. Sorokin (Theoretical Physics Division of NRC “Kurchatov Institute” – PNPI) – “Topological defects in two-dimensional helical magnetic material and the method of non-perturbative renormalization group”.
- 7 April.** V.Yu. Petrov (Theoretical Physics Division of NRC “Kurchatov Institute” – PNPI) – “Quantum wire with an impurity as 0-dimensional field theory”.
- 14 April.** A.S. Sukhanov (Neutron Research Division of NRC “Kurchatov Institute” – PNPI) – “The measurement of spin-wave stiffness in helimagnets studied by small-angle neutron scattering”.
- 14 April.** I.M. Belyaev (NRC “Kurchatov Institute” – ITEP) – “Search for possible tetraquark state $X(5568)$ with LHCb data”.
- 28 April.** A.V. Nakin (Neutron Research Division of NRC “Kurchatov Institute” – PNPI) – “Mathematical modeling of anisotropic lattices of Josephson contacts in the inhomogeneous magnetic field”.
- 11 May.** M.G. Khrenova (Lomonosov Moscow State University) – “Supercomputer molecular modeling for interpretation and prediction of properties of protein systems”.
- 12 May.** S.I. Tutunnikov (Joint Institute for Nuclear Research) – “EXAFS-spectroscopy at Kurchatov Synchrotron Radiation Source (KSRS)”.
- 19 May.** B.N. Gikal (Flerov Laboratory of Nuclear Reactions, Joint Institute for Nuclear Research) – “The cyclotron complex of heavy ions in the FLNR JINR for research and applications (current status and development plans for the next 7 years)”.
- 23 May.** Yu. Polikanov (University of Illinois at Chicago) – “From the ribosome structure to antibiotics”.
- 26 May.** V.A. Matveev (Neutron Research Division of NRC “Kurchatov Institute” – PNPI) – “Study of titanium nano-layers by neutron and X-ray reflectometry”.
- 9 June.** Jan K. Kruger, Martine Philipp (University of the Saarland, Saarbrücken) – “The role of nonlinearities at phase transitions and glass transitions in polymers”.
- 9 June.** M.G. Ryskin and V.A. Schegelsky (Theoretical Physics Division, High Energy Physics Division of NRC “Kurchatov Institute” – PNPI) – “Two zooms in Bose-Einstein correlations. First observation of the “radiating pomeron” by ATLAS”.
- 15 June.** T.A. Isaev (Neutron Research Division of NRC “Kurchatov Institute” – PNPI) – “Prospects for studies with cold molecules in NRC “Kurchatov Institute” – PNPI”.
- 16 June.** A.A. Szhogina (Neutron Research Division of NRC “Kurchatov Institute” – PNPI) – “Structure and magnetic relaxation properties of iron-carbon endohedral complexes”.
- 16 June.** M. Strikman (Pennsylvania State University) – “Color fluctuation phenomena in high energy proton- and photon-A collisions at the LHC”.

- 23 June.** S. V. Maleev (Theoretical Physics Division of NRC “Kurchatov Institute” – PNPI) – “Interaction of spin waves in B2O (MnSi etc.) magnetic materials”.
- 30 June.** M.V. Suyasova (Neutron Research Division of NRC “Kurchatov Institute” – PNPI) – “The aggregation and self-organization mechanisms of fullerenols in aqueous solutions”.
- 6 October.** Ya.M. Beltukov (Ioffe Institute RAS) – “Random matrix theory approach to describe vibrations of granular media”.
- 13 October.** A.V. Syromyatnikov (Theoretical Physics Division of NRC “Kurchatov Institute” – PNPI) – “Spin-flop transition accompanied with changing the type of magnetic ordering”.
- 27 October.** A.Yu. Aktersky (Theoretical Physics Division of NRC “Kurchatov Institute” – PNPI) – “Low-energy singlet sector in the spin $-1/2$ J_1 - J_2 Heisenberg model on a square lattice”.
- 2 November.** D.S. Karlov (Molecular and Radiation Biophysics Division of NRC “Kurchatov Institute” – PNPI) – “A variety of bacteria in pelagic and benthic zones of freshwater Antarctic Radok lake (Amery oasis)”.
- 3 November.** A.B. Arbuzov (Joint Institute for Nuclear Research) – “Radiative corrections to elastic electron-proton scattering”.
- 10 November.** A.Yu. Goikhman (Functional Nanomaterials Research & Educational Center, Immanuel Kant Baltic Federal University) – “Mobile growth units for the in situ formation and studies of unique nanostructures and systems at megascience installations”.
- 17 November.** I.V. Golosovsky (Neutron Research Division of NRC “Kurchatov Institute” – PNPI) – “Spin waves and exchange interactions in a multiferroic $\text{NdFe}_3(\text{BO}_3)_4$. Inelastic neutron scattering”.
- 1 December.** I.A. Babintsev (Theoretical Physics Division of NRC “Kurchatov Institute” – PNPI) – “Degeneracy of eigenvalues of an operator of a Becker–Döring kinetic equation”.
- 8 December.** M.G. Ryskin, V.A. Schegelski (Theoretical Physics Division, High Energy Physics Division of NRC “Kurchatov Institute” – PNPI) – “The boiling QCD vacuum: BEC study with ATLAS LHC experiment from 900 GeV till 13 TeV”.
- 29 December.** A.V. Titov (Knowledge Transfer Division of NRC “Kurchatov Institute” – PNPI) – “Theoretical studies of molecules and solids with heavy atoms in the laboratory of quantum chemistry of NRC “Kurchatov Institute” – PNPI: development of methods and calculations”.

Conferences

NRC “Kurchatov Institute” – PNPI acts as an organizer of its own conferences, lectures and workshops in the framework of a wide range of research subject matters. The events bring together participants from the leading research centers of Russia and abroad.

In 2016 the Institute organized 13 scientific events (workshops, conferences and schools), which were attended by over 1 500 people, including more than 300 foreign representatives of the world scientific community from such countries as Germany, Sweden, the USA, Switzerland, Japan, China, the Netherlands, Italy, Belgium, Ireland, etc.











Organized events

1. Workshop «Neutron Diffraction – 2016». **18–19 February.**
2. 50th Winter School of NRC “Kurchatov Institute” – PNPI on Nuclear and Particle Physics, Theoretical Physics, Reactor Physics and Technologies, Accelerator Physics and Technologies. **29 February – 5 March.**
3. XVII Winter School on Biophysics and Molecular Biology. **29 February – 5 March.**
4. L Winter School of NRC “Kurchatov Institute” – PNPI on Condensed State Physics. **14–19 March.**
5. Fourth workgroup meeting on the project of reconstruction of instruments at the PIK reactor “PIK-GGBase”. **26–27 May.**
6. International Conference “Quarks-2016”. **29 May – 4 June.**
7. Workshop on enalastic neutron scattering “Spectrina-2016“. **23–24 June.**
8. International conference “Hadron Structure and QCD (HSQCD’2016)”. **27 June – 1 July.**
9. II Reactor PIK School for Young Scientists (Professionalism. Intellect. Carrier. “PIK-2016”). **3–8 July.**
10. International meeting of the FAIR/NuSTAR/R3B collaboration “R3B Collaboration Meeting”. **19 September – 23 September.**
11. IV Workshop on Small-Angle Neutron Scattering “MURomets-2016”. **28–30 September.**
12. Youth Scientific Forum “Open Science – 2016”. **16–18 November.**
13. V School on Polarized Neutron Physics. **15–16 December.**

In addition, in the course of 2016 the researchers of NRC “Kurchatov Institute” – PNPI participated in 130 Russian and international conferences, where they presented 350 talks.

